

---

# **Phycobiliprotein Lyases:**

## **Structure of Reconstitution Products and Mechanistic Studies**

**Jun-Ming Tu**

---



2008 MUNICH

---

# **Phycobiliprotein Lyases:**

**Structure of Reconstitution Products and Mechanistic Studies**

**Jun-Ming Tu**

---

Dissertation

zur Erlangung des Doktorgrades

der Fakultät für Biologie

der Ludwig-Maximilians-Universität

München

Submitted

by

Jun-Ming Tu

2008 MUNICH

1. Referee: Prof. Dr. Hugo Scheer
  2. Referee: Prof. Dr. Lutz Eichacker
- Date of oral defense: October 29, 2008

## Publications:

**Tu, J.M.**, Kupka, M., Böhm, S., Plöscher, M., Eichacker, L., Zhao, K.H., and Scheer, H. (2008) Intermediate binding of phycocyanobilin to the lyase, CpeS1, and transfer to apoprotein. *Photosynth. Res.* **95**:163-168.

Zhao, K. H., Su, P., Li, J., **Tu, J.M.**, Zhou, M., Bubenzer, C. and Scheer, H. (2006) Chromophore attachment to phycobiliprotein beta-subunits: phycocyanobilin: cysteine-beta84 phycobiliprotein lyase activity of CpeS-like protein from *Anabaena sp.* PCC7120. *J. Biol. Chem.* **281**: 8573-8581.

Zhao, K.H., Su, P., **Tu, J.M.**, Wang, X., Liu, H., Plöscher, M., Eichacker, L., Yang, B., Zhou, M. and Scheer, H. (2007) Phycobilin:cysteine-84 biliprotein lyase, a near-universal lyase for cysteine-84-binding sites in cyanobacterial phycobiliproteins. *Proc Natl Acad Sci USA*, **104**:14300-14305.

Zhao, K.H., Zhang, J., **Tu, J.M.**, Böhm, S., Plöscher, M., Eichacker, L., Bubenzer, C., Scheer, H., Wang, X., and Zhou, M. (2007) Lyase activities of CpcS and CpcT-like proteins from *Nostoc* PCC7120, and sequential reconstitution of binding sites of phycoerythrocyanin and phycocyanin  $\beta$ -subunits. *J. Biol. Chem.* **282**:34093-34103

# Acknowledgements

This work was performed at the laboratory of Prof. Dr. H. Scheer in the Department I of the Botanical Institute of the Ludwig-Maximilians-University in Munich, Germany and at the laboratory of Prof. Dr.K-H. Zhao in College of Environmental Science and Engineering, Huazhong University of Science and Technology in Wuhan, PR China

I am very much grateful to my supervisor Prof. Dr. H. Scheer for theoretical and practical supervision during the work. I would like to thank him for inviting me into his group, for giving me an opportunity to conduct my PhD research in his laboratory and for excellent working conditions. I would like to acknowledge him for his help, continuous support and valuable discussions throughout my PhD study. I am thankful for the advises that he gave me, for careful reading and correction of this thesis and for his helpful comments. I also appreciate a lot his optimism and never-ending enthusiasm.

I am thankful to my supervisor in PR China Prof. Dr. K-H.Zhao. Thanks for his support, care, for teaching me at the beginning of my studies in Huazhong University of Science and Technology, for introducing me into molecular biology and providing all of plasmids for this work.

My sincere thanks go to Dr. Stephan Böhm for his excellent technical help, support, patience, care and for interesting talks about life. I am grateful to him for his bright personality and for helping me to better understand people of his country

My special thanks to Dr. Zhen-Hua Cui for her help, for introducing me into the lab life, for scientific and personal support since my very first days in the lab, for nice discussions and for good time in and outside the lab.

Many thanks to Prof. Dr. Lutz Eichacker and Dr. Matthias Plöscher (LMU, Biology Department I, Munich) for the ESI-MS measurements, and to Dr. Rainer Haessner (Technical University Munich, Germany) for NMR measurements.

I would like to thank all graduate students and post-docs who used to work or are currently working in this group for their friendly and helpful collaboration, for creating a pleasant working atmosphere and for a nice time.

My dear parents, sister and my wife H-X Tong; many, many thanks for your constant and genuine love, care, encouragement, understanding, inspiration and support at each step of my life. Thank you very much!

Last but not least, I gratefully acknowledge the Chinese Scholarship Council for a doctoral scholarship.

# Abbreviations

A	absorption
a.u.	arbitrary unit
APC	allophycocyanin
ApcA	apoprotein of allophycocyanin $\alpha$ -subunit
ApcA2	apoprotein of allophycocyanin $\alpha$ -subunit
ApcD	apoprotein of allophycocyanin $\alpha$ -subunit
ApcB	apoprotein of allophycocyanin $\beta$ -subunit
ApcF	apoprotein of allophycocyanin $\beta$ -subunit
APS	ammonium persulfate
bp	base pair
BSA	bovine serum albumin
BV IXa	biliverdin IXa
CD	circular dichroism
Cpc A	apoprotein of C-Phycocyanin $\alpha$ -subunit
CpcB	apoprotein of C-Phycocyanin $\beta$ -subunit
CpcE, CpcF	subunits of Phycocyanobilin- $\alpha$ -Phycocyanin-lyase
DNA	deoxyribonucleic acid
DMSO	dimethyl sulfoxide
<i>E. coli</i>	<i>Escherichia coli</i>
EDTA	ethylenediaminetetraacetic acid
ESI-MS	electrospray ionization mass spectrometry
NR	ferredoxin NADP <sup>+</sup> oxidoreductase
hr	hour(s)
IPTG	isopropyl $\beta$ -D-thiogalactoside
k	rate constant [ $s^{-1}$ ]
kDa	kiloDalton
LB	Luria-Bertani medium
ME	2-mercaptoethanol
MHz	Megahertz
min	minute
MS	mass spectrometry
MW	molecular weight
m/z	mass per charge
nm	nanometer
NMR	nuclear magnetic resonance
NOESY	nuclear Overhauser and Exchange Spectroscopy
ORF	open reading frame
PAGE	polyacrylamide gel electrophoresis
PBS	phycobilisome
PC	phycocyanin
PCB	phycocyanobilin
PCR	polymerase chain reaction

PE	phycoerythrin
PEB	phycoerythrobilin
PEC	phycoerythrocyanin
PecA	apoprotein of phycoerythrocyanin $\alpha$ -subunit
PecB	apoprotein of phycoerythrocyanin $\beta$ -subunit
PecE and PecF	phycoviolobilin- $\alpha$ 84-cystein-lyase-isomerase subunits
PFB	phytochromobilin
PK	protein kinases
PSI	photosystem I
PSII	photosystem II
PVB	phycoviolobilin (4,5-Dihydro-mesobiliverdin)
rpm	revolutions per minute
SDS	sodium dodecyl sulfate
TBE	tris-borate-EDTA buffer
TE	Tris-EDTA
TEMED	N, N, N', N'-tetramethylethylene diamine
TFA	trifluoroacetic acid
TLC	thin layer chromatography
$t_r$	retention time
Tris	tris-(hydroxymethyl)-aminomethane
TritonX-100	alkylphenyl polyethylenglycol
WT	wild type
v/v	volume per volume
$Q_{Vis/UV}$	ratio of maximum absorption in the visible (Vis) and the ultraviolet (UV) spectral region
w/v	weight per volume

## TABLE OF CONTENTS

1: Introduction.....	1
1.1 Structures of phycobilisomes .....	1
1.2 Biosynthesis of phycobilins .....	6
1.3 Chromophore attachment.....	7
1.3.1 Spontaneous attachment.....	8
1.3.2. Autocatalytic attachment.....	9
1.3.3. E/F-type lyases.....	9
1.3.4. Cyanobacterial S/U-type lyases .....	10
1.3.5. Cyanobacterial T-Type lyases.....	11
1.4 Lyase mechanisms.....	11
1.5 Applications .....	13
1.6 Thesis plan .....	14
2: Materials and Methods.....	16
2.1 Materials .....	16
2.1.1 Organisms .....	16
2.1.2 Vectors.....	16
2.1.3 Plasmids .....	16
2.1.3 Chemicals.....	17
2.1.4 Technical devices .....	20
2.2 Methods.....	22
2.2.1 General molecular biological methods.....	22
2.2.2 Protein isolation .....	22
2.2.3 Pigment isolation.....	25
2.2.4 Phycobiliprotein reconstitution/preparation .....	27
2.2.5 Lyase CpcS (Alr0617) reaction assay .....	29
2.2.6 Chromophore adduct assay .....	29
2.2.7 Spectroscopy .....	30
2.2.8 Websites .....	31
3: Results and Discussion .....	32
3.1 Structure analysis of reconstituted holo-PecA .....	32
3.1.1 Reconstitution principle of holo-PecA.....	32
3.1.2 Expression and Purification of the holo-PecA .....	33
3.1.3 Circular Dichroism Spectroscopy .....	35
3.1.4 Photoisomerization of $\alpha$ -PEC .....	36
3.1.5 HPLC–ESI-MS analysis of chromopeptides from holo-PecA .....	37
3.1.6 NMR analysis of peptic chromopeptides from holo-PecA.....	39
3.1.7 Discussion.....	42
3.2 Structure analysis of reconstituted holo-CpcA.....	45
3.2.1 Reconstitution principle of holo-CpcA .....	45
3.2.2 Expression and Purification of the holo-CpcA.....	46
3.2.3 Circular Dichroism Spectroscopy .....	48
3.2.4 HPLC–ESI-MS analysis of chromopeptides from holo-CpcA .....	48

---

3.2.5 NMR analysis of peptic chromopeptides from holo-CpcA.....	50
3.2.6 Discussion.....	53
3.3 Structure analysis of reconstituted subunits of allophycocyanin.....	55
3.3.1 Reconstitution principle of subunits of allophycocyanin.....	55
3.3.2 Expression and Purification of the subunits of allophycocyanin.....	56
3.3.3 Circular Dichroism Spectroscopy.....	58
3.3.4 Chromophore analyses of reconstitution products.....	59
3.3.5 HPLC–ESI-MS analysis of chromopeptides from reconstituted subunits of allophycocyanin.....	61
3.3.6 NMR analysis of peptic chromopeptides from reconstituted subunits of allophycocyanin.....	63
3.3.7 Discussion.....	67
3.4 Structure analysis of reconstitution $\beta$ -subunit of C-phycoerythrin.....	71
3.4.1 Reconstitution principle of $\beta$ -subunit of C-phycoerythrin.....	71
3.4.2 Expression and Purification of the $\beta$ -subunits of C-phycoerythrin.....	72
3.4.3 Circular Dichroism Spectroscopy.....	73
3.4.4 Chromophore analyses of reconstitution products.....	74
3.4.5 HPLC–ESI-MS analysis of chromopeptides from reconstituted $\beta$ -subunits of C-phycoerythrin.....	76
3.4.6 NMR analysis of peptic chromopeptides from reconstituted $\beta$ subunits of C-phycoerythrin.....	78
3.4.7 Discussion.....	82
3.5 Structure analysis of reconstituted $\beta$ -subunits of phycoerythrin.....	85
3.5.1 Reconstitution principle of $\beta$ -subunit of phycoerythrin.....	85
3.5.2 Expression and Purification of the $\beta$ -subunits of phycoerythrin.....	85
3.5.3 Circular Dichroism Spectroscopy.....	87
3.5.4 Chromophore analyses of reconstitution products.....	88
3.5.5 HPLC–ESI-MS analysis of chromopeptides from reconstituted $\beta$ -subunits of phycoerythrin.....	90
3.5.6 NMR analysis of peptic chromopeptides from reconstituted $\beta$ -subunits of phycoerythrin.....	92
3.5.7 Discussion.....	96
3.6 Structure analysis of imidazole-bilin adducts.....	98
3.6.1 Binding of PCB to CpcS.....	98
3.6.2 Imidazole binding PCB.....	99
3.6.3 Chromophore transfer from CpcS-PCB to CpcB(C155I).....	102
3.6.4 Chromophore transfer from imidazole-bilin adducts to CpcB(C155I), CpcS or mercaptoethanol.....	103
3.6.5 HPLC–ESI-MS analysis of imidazole-bilin adducts.....	106
3.6.6 NMR analysis of imidazole-bilin adducts.....	107
3.6.7 Discussion.....	110
3.7 Structure analysis of mercaptoethanol-bilin adducts.....	113
3.7.1 Mercaptoethanol binding PCB catalyzed by CpcS.....	113
3.7.2 Spontaneous binding of mercaptoethanol to PCB.....	115

3.7.3 Structure analysis of mercaptoethanol-bilin adducts.....	117
3.7.4 Chromophore transfer from CpcS-PCB to ME .....	122
3.7.5 Chromophore transfer from bilin adducts to CpcB(C155I) .....	122
3.7.6 Discussion .....	124
3.8 Attachment of a locked chromophore, 15Za-PCB .....	127
3.8.1 Structure of 15Za-PCB.....	127
3.8.2 Absorption and extinction coefficient of 15Za-PCB .....	127
3.8.3 Chromophore binding assay.....	128
3.8.4 Denaturation of the 15Za-PCB addition products.....	130
3.8.5 Chromophore reaction with Zn <sup>2+</sup> .....	131
3.8.6 The effect of pH on chromophore spectra.....	132
3.8.7 Conclusion .....	133
3.9 Test of a protein with Heat-like repeats, DOHH, for lyase activity .....	134
4: Concluding Discussion .....	136
4.1 A multi-plasmidic expression system.....	136
4.2 A multi-step analytic system .....	137
4.3 E/F-type lyase catalyzed attachment.....	139
4.4 S (/U)-type lyase catalyzed attachment.....	139
4.5 T-type lyase catalytic attachment .....	141
4.6 Imidazole-bilin adducts.....	143
4.7 Mercaptoethanol-bilin adducts.....	144
4.8 Some interesting observations as by-products of the experiments.....	145
4.9 Future prospects .....	146
5: Summary .....	148
6: References.....	151
Curriculum Vitae .....	172

# 1: Introduction

## 1.1 Structures of phycobilisomes

Phycobilisomes (PBSs) are multimeric highly organized protein complexes that harvest light in the wavelength range from 480 to 650 nm in the “chlorophyll gap” and may constitute 50% of the soluble proteins in cyanobacterial and red algal cells. Contrary to light harvesting antennae, LHCII, of higher plants which are located within the thylakoid membrane, the PBS of cyanobacteria are peripherally associated with the outer cytoplasmic surface of the photosynthetic membranes (Glazer et al., 1983, 1985) (Fig. 1-1). PBSs are not only antenna complexes for light harvesting, but can also be used as storage materials for carbon and nitrogen (Bryant, 1987).

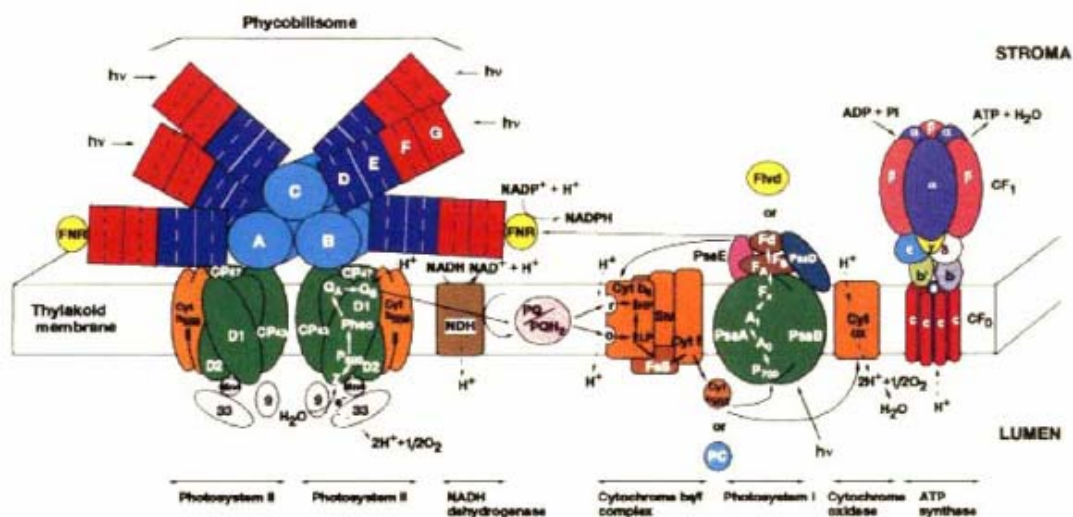


**Fig. 1-1: Major respiratory and photosynthetic electron transport components of cyanobacteria (Bryant, 1994).** A,B,C = core of allophycocyanin; D-G: rod of phycocyanin (D,E) and phycoerythrin or phycoerythrocyanin (F,G).

These PBSs are composed of two types of proteins: colored phycobiliproteins (PBPs), which absorb and transmit light energy to the photosynthetic reaction centers, and non-pigmented linker proteins, which organize the former into the PBSs and modulate their absorptions (Glazer, 1989).

The non-pigmented linker proteins are integrated into the PBS structure (Fig.1-2).

These polypeptides with molecular masses from 8 kDa to 120 kDa serve several functions in the PBSs. They help stabilizing the PBS structure, determine the positions of specific PBPs in the complex, facilitate assembly of PBP-containing substructures, modulate the absorption characteristics of the PBPs to promote unidirectional transfer of energy within the PBSs and from PBSs to chlorophylls of the photosynthetic reaction centres, and physically link the entire complex to the photosynthetic membranes (Glazer et al., 1983, 1985, 1988, 1989; Bryant, 1991; Grossman et al., 1993). Linker proteins can be divided into four groups: rod core linkers ( $L_{RC}$ ) that attach the peripheral rods to the PBS core, rod linkers like  $L_R^{10}$ ,  $L_R^{33}$ ,  $L_R^{35}$  (the superscript indicates the molecular weight) that associate phycocyanin (PC) or phycoerythrin (PE) substructures into rod segments, the small core linkers like  $L_C^8$ , that are associated with trimeric allophycocyanin (APC) at the peripheries of the core cylinders, and the core-membrane linker like  $L_{CM}^{99}$  that acts in the organisation of the PBS core, in the PBS attachment to the membrane and due to its chromophore, also as the major terminal energy emitter to PSII (Glazer, 1989; Capuano et al., 1991; Sidler, 1994). The latter one was suggested to couple PBSs to the membrane via a domain called the PB-loop, but deletion mutagenesis of this domain that has been proposed to be a transmembrane domain, did not show any changes in the association of PBSs with thylakoid membranes in the mutant strain (Ajilani and Vernotte, 1998; Piven, 2006). Most of the linker proteins are colorless, but at least two of them also carry covalently bound chromophores, namely, the aforementioned core-membrane linker  $L_{cm}$  (= PCB-ApcE), and the  $\gamma$ -subunits of class II and some class I phycoerythrins (PEs) (Scheer and Zhao, 2008).

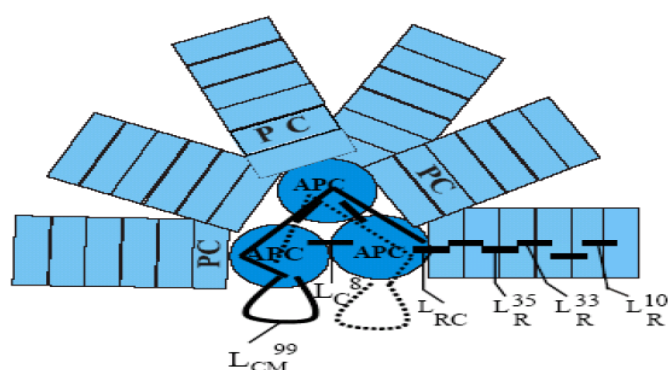


**Fig. 1-2: Schematic structure of PBSs of *Synechocystis* sp. PCC 6803.** PC – phycocyanin, APC – allophycocyanin,  $L_{CM}$ – core -membrane linker,  $L_C$ –core linker,  $L_{RC}$ – rod corelinker,  $L_R$ – rod linker (Piven, 2006)

PBPs are categorized into three types according to their absorption maximum in the visible range (Table 1-1), those of high energy (PE or phycoerythrocyanin (PEC)), intermediate energy (PC), and low energy (APC) (Tab.1-1). Energy will flow from highest- to lowest-energy pigments and this is how the PBSs are organized (Fig. 1-1). The details of PBS structure are quite variable. However, a common theme is that the PBS has a central “core” composed of APCs and specific linker polypeptides that is situated in proximity to the thylakoid membrane and photosystem II, where chlorophyll a is located. Radiating out from the core are a number of “rod” elements composed of PCs (and often also PEs and other PBPs) together with their associated linker polypeptides. The entire assemblage typically has a molecular mass in the range from 7 to 15 MDa. Cyanobacterial PBSs are typically hemidiscoidal in overall form, with diameters in the range of 32–70 nm (Grossman 1993). In hemidiscoidal PBSs, there are generally six rods, and three cylinders in their core.

Cyanobacterial and red-algal biliproteins are generally trimers of an  $\alpha/\beta$  -heterodimer.  $\alpha$  and  $\beta$  subunits are closely related proteins, carrying 1–4 covalently bound chromophores, the phycobilins (Fig. 1-3).

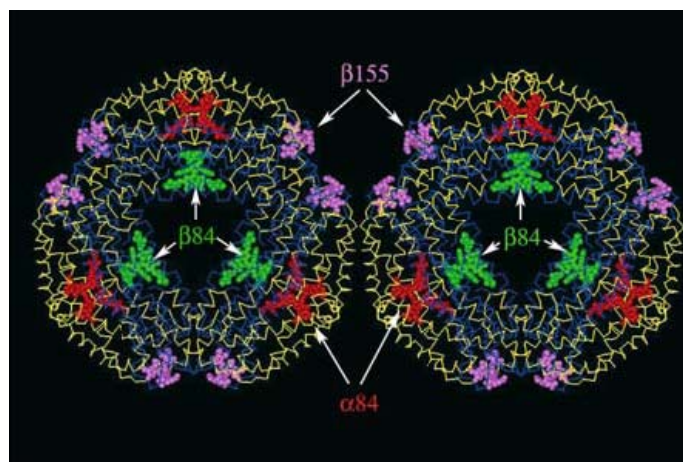


**Fig. 1-3: Levels of PBS association as seen in the crystallographic unit cell of Tv-PC620.** The  $\alpha$  and  $\beta$  subunits are shown in  $C_a$  traces for simplicity (yellow and blue, respectively). Application of crystallographic symmetry reconstructs a number of physiologically important aggregation states: the  $(\alpha\beta)_3$  trimer (the top of each ring), the  $(\alpha\beta)_6$  hexamer disk (the bottom trimer is directly below the top trimer and is thus superimposed). Notice that the three PCB cofactors are separated spatially:  $\alpha 84$  PCBs (red) are buried in the  $(\alpha\beta)$  interface of the trimer,  $\beta 84$  PCBs (green) are all located within the trimer and hexamer disk and probably associate with linker proteins and  $\beta 155$  PCBs (pink) are all located on the circumferential surface of the disks and may help in energy transfer between disks and between rods (Adir, 2005).

**Table 1-1: The visible absorption maxima of various phycobiliproteins (after Coyler et al., 2005)**

Phycobiliprotein	Maxima of visible absorption [nm]	Color
Phycoerythrin (PE)	540-570	orange-red
Phycoerythrocyanin (PEC)	570-590	purple
Phycocyanin (PC)	610-620	blue
Allophycocyanin (APC)	650-655	blue-green

**Table 1-2: Phycobilin binding sites and types of various phycobiliproteins**

Biliproteins	Binding sites of bilins					
	$\alpha$ -75	$\alpha$ -84*	$\alpha$ -140	$\beta$ -50/60	$\beta$ -84*	$\beta$ -155
Allophycocyanin		PCB			PCB	
C-Phycocyanin		PCB			PCB	PCB
Phycoerythrocyanin		PVB			PCB	PCB
R-Phycocyanin		PEB			PCB	PEB
R-Phycocyanin <sup>a</sup>		PUB			PCB	PEB
Phycocyanin (WH8501)		PUB			PCB	PCB
C-Phycoerythrin		PEB	PEB	PEB	PEB	PEB
CU-Phycoerythrin <sup>b</sup>		PEB	PUB	PUB	PEB	PEB
CU-Phycoerythrin <sup>c</sup>	PUB	PEB	PEB	PUB	PEB	PEB

After Frank et al. 1978; Sidler et al. 1981; Füglistaller et al. 1983; Klotz et al. 1985; Sidler et al. 1986; Ong et al. 1987; Swanson et al. 1991

\* Consensus numbering; a) *Synechococcus* sp. WH8102 (unpublished); b) *Synechococcus* sp. WH8103 PE(I); c) *Synechococcus* sp. WH8020 PE(II) (Boehm, 2006)

Individual PBP subunits carry 1-4 chromophores. The binding sites and types of bilins associated with the subunits of various PBPs are summarized in Table 1-2.

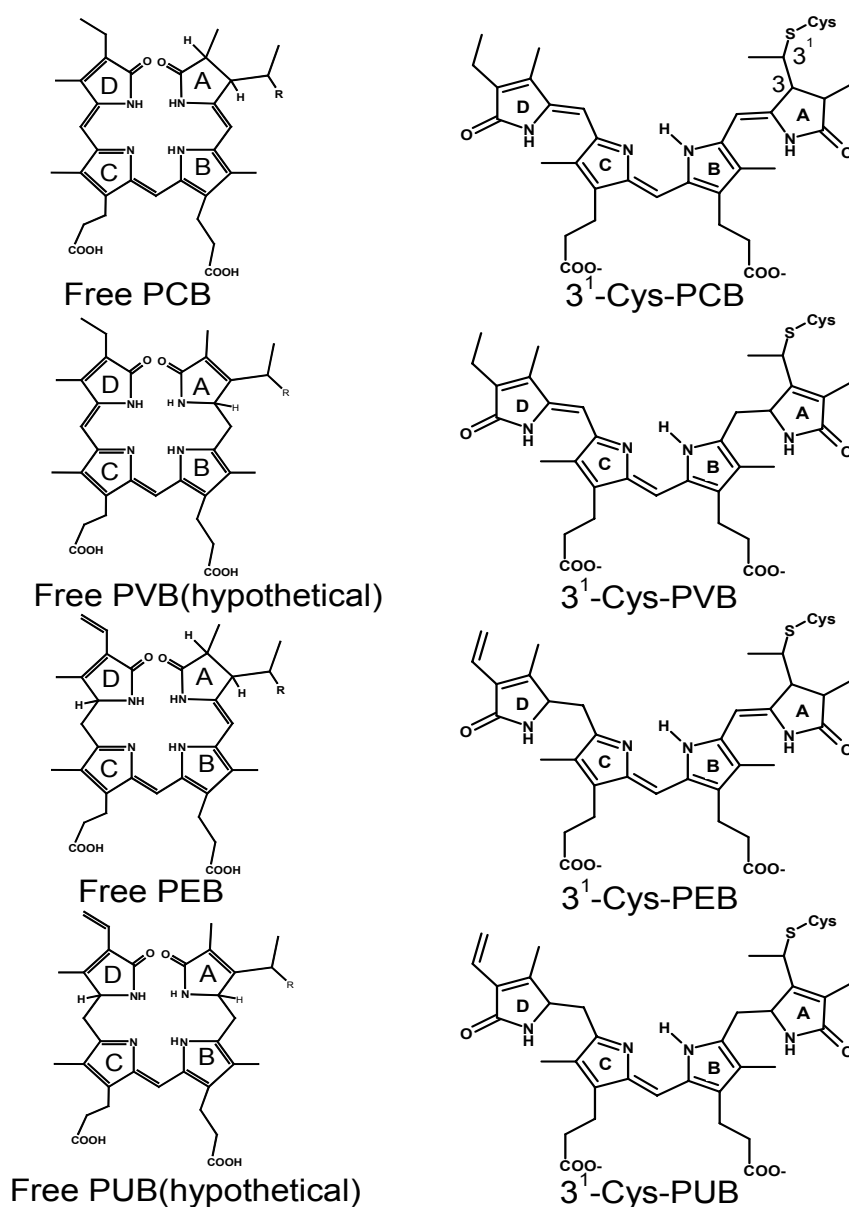


**Fig. 1-4: Structures of free and protein-bound bilins.** Structures of PCB, PVB (not known as free chromophore), PEB, PUB(not known as free chromophore) in their free forms (left) and bound at C-3<sup>1</sup> to the apoprotein via cysteine thioether bond. Free chromophores prefer a cyclic-helical conformation, bound ones have extended conformations in the native biliproteins (Boehm et al, 2007).

With the number of binding sites increasing from APC to PC and PEC and further to PEs (and also cryptophyte biliproteins that are not organized in phycobilisomes (Sidler, 1994)), the  $\alpha$ - and  $\beta$ -subunits of phycobiliproteins carry at least one linear tetrapyrrole chromophore (bilin) called phycocyanobilin (PCB), phycoviolobilin (PVB),

phycoerythrobilin (PEB) or phycourobilin (PUB) which is covalently attached to cysteines of the apoprotein via a thioether bond to C-3<sup>1</sup> on ring A (Fig. 1-4) and in some cases by an additional thioether bond to C-18<sup>1</sup> on ring D (Sidler, 1994).

## 1.2 Biosynthesis of phycobilins

Bilin is the collective generic name for linear tetrapyrroles. The major bilins in nature are biliverdin (BV), bilirubin (BR), PCB, PEB and phytychromobilin (PΦB), they are all derived from heme. The biosynthesis is summarized in Fig1-5.

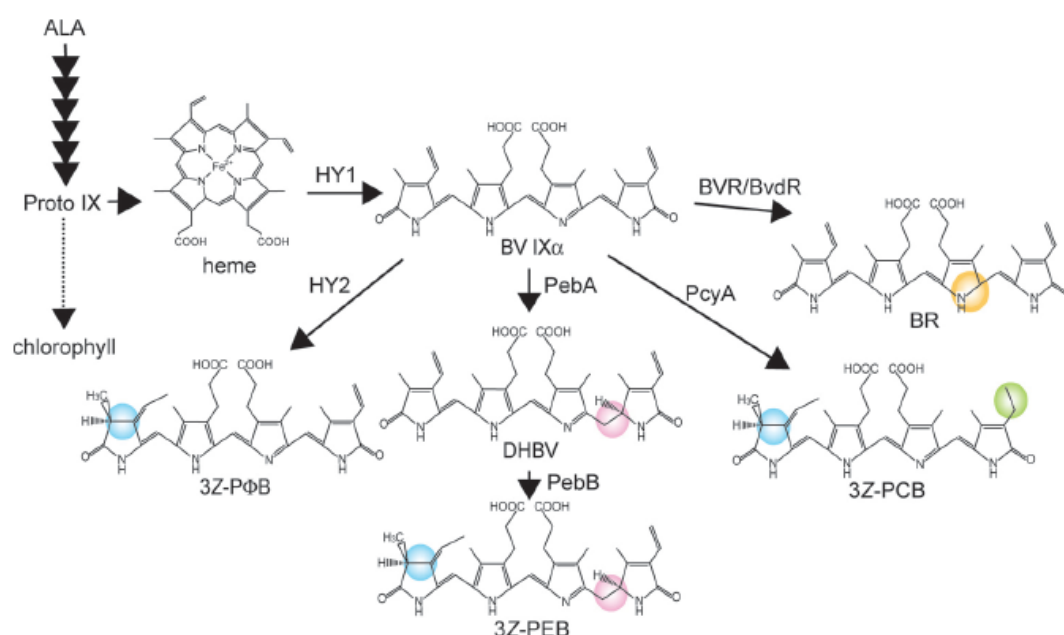


**Fig. 1-5: Chemical structures and biosynthetic pathways of chlorophylls, heme and bilins.** BV is synthesized from 5-aminolevulinic acid (ALA) via heme. BV is further reduced to produce PΦB in plants, PEB and PCB in cyanobacterial and algae and BR in animals by the action of different bilin reductase. Note that no obvious sequence similarity was detected between BV reductases (BVR and bvdR) and other ferredoxin-dependent bilin reductases (HY2, PcyA, PebA and PebB) (Kohchi et al., 2005).

Heme, which contains iron, is synthesized from protoheme IX by ferrochelatase. Heme is an essential prosthetic group in many reduction/oxidation processes. Heme is cleaved to BV IXα by heme oxygenase; this is a degradation process in animals but for photosynthetic organisms this step is a biosynthetic process (Muramoto et al. 1999). Further reduced bilins are synthesized from BV IXα by the action of different ferredoxin- dependent bilin reductases (FDBRs) (Kohchi et al. 2001; Frankenberg et al.

2003; Dammeij et al., 2008), a new family of radical enzymes.

The reduction to phycocyanobilin is catalyzed by the FDBR phycocyanobilin:ferredoxin oxidoreductase, PcyA, that carries out two reductions, at ring A and the 18-vinyl group (Frankenberg et al., 2003). PΦB reductase (Hy2) catalyzes only reduction of ring A, leading to PΦB, the typical chromophore of plant phytochromes (Kohchi et al., 2001; Gambetta et al., 2001), while a dedicated reductase catalyzing only reduction of the 18-vinyl group would yield mesobiliverdin (MBV), one of the chromophores of cryptophyte biliproteins.

The biosynthesis of PEB requires two subsequent two-electron reductions, each step being catalyzed by one FDBR. The first reaction in PEB biosynthesis is the reduction of the  $\Delta^{15,16}$ -double bond of BV IX $\alpha$  by 15,16-dihydrobiliverdin:ferredoxin oxidoreductase (PebA). This reaction shortens the conjugated  $\pi$ -electron system, thereby blue-shifting the absorption maxima of the linear tetrapyrrole. The second FDBR, PEB:ferredoxin oxidoreductase (PebB), then reduces the A-ring 2,3,3<sup>1</sup>,3<sup>2</sup>-diene structure of 15,16-dihydrobiliverdin to yield PEB (Dammeyer et al., 2006). A single subunit reductase that carries out both steps has been characterized (Dammeyer et al., 2008).

### 1.3 Chromophore attachment

The final step in phycobiliprotein biosynthesis is the covalent chromophore attachment to the apoprotein. Heterodimeric lyases (CpcE/CpcF and PecE/pecF) that catalyzes the covalent attachment of PCB to cysteine- $\alpha$ C84 of CPC, and of PVB to cysteine- $\alpha$ 84 of PEC, respectively, were characterized before the beginning of this thesis. During, and in part in this thesis, the S/U-type and T-type lyase were characterized by Zhao et al. (2006a, 2007a,b) and Shen et al. (2006, 2008a). Currently, there are five characterized modes of chromophore attachment (Tab. 1-3).

**Table 1-3: Modes of chromophore attachment in biliproteins**

<b>Mode</b>	<b>Biliprotein</b>
1. Spontaneous attachment	Most biliproteins in the absence of lyase (Arciero et al., 1988; Fairchild and Glazer, 1994a; Schluchter and Glazer, 1999; Zhao et al., 2007a, b; Scheer and Zhao, 2008; Boehm et al., 2007)
2. Autocatalytic attachment	Phytochromes (Wu and Lagarias, 2000; Zhao et al., 2004; Bhoo et al., 1997; Lamparter, 2004; Wagner et al., 2005)  L <sub>CM</sub> (=PCB-ApcE) (Zhao et al., 2005)
3. Catalyzed by E/F-type lyases	PCB-CpcA (Zhou et al., 1992; Tooley et al., 2001) PVB-PecA (Zhao et al., 2000; Tooley et al., 2002)
4. Catalyzed by cyanobacterial S/U-type lyases	CpcB-C84-PCB (Shen et al., 2004; Zhao et al., 2006a; Shen et al., 2008; Saunée et al., 2008) PecB-C84-PCB (Zhao et al., 2006a) CpeA-C84-PEB, CpeB-C84-PEB (Zhao et al., 2007a) ApcA,B,D,F-PCB (Zhao et al., 2007a; Saunée et al., 2008)
5. Catalyzed by cyanobacterial T-Type lyases	CpcB-C155-PCB (Shen et al., 2006; Zhao et al., 2007b) PecB-C155-PCB (Zhao et al., 2007b)

### 1.3.1 Spontaneous attachment

Most apoproteins can bind phycobilins (PCB, PEB) spontaneously in vitro. This process is very frequently observed, but is of low fidelity and generally leads to product mixtures containing oxidation products and incorrect stereochemistry of the adduct (Arciero et al., 1988; Fairchild and Glazer, 1994a; Schluchter and Glazer, 1999; Boehm et al., 2007). Spontaneous attachment is a considerable problem in binding studies, especially in vitro, because it interferes with lyase assays and is not easily distinguished from truly autocatalytic lyase activities (Schluchter and Bryant, 2002; Zhao et al., 2007; Böhm et al., 2007).

Scheer and Zhao (2008) analyzed important clues for understanding and distinguishing correct chromophore binding and spontaneous binding. Firstly, many, if not all, apoproteins can form thioether bonds with suitable chromophores. Secondly, the bonds are formed with the correct cysteines, namely, only those located at the native binding sites, indicating site-specific interactions of the chromophores with the binding pockets. This is further emphasized by the non-covalent, yet (largely) functional binding of chromophores in mutants that lack the chromophore binding cysteine residue (Lamparter and Michael, 2005; Gindt et al., 1992; Shen et al., 2008), or the non-covalent binding of modified chromophores (Inomata et al., 2006).

### 1.3.2. Autocatalytic attachment

Autocatalytic attachment has been reported for ApcA from two cyanobacteria, including *Anabaena* PCC7120 (Hu et al., 2006; Zhao et al., 2007). In our view, the product differed distinctly in its absorption, fluorescence and circular dichroism from isolated native  $\alpha$ -APC, this is therefore an incorrect attachment, spontaneous rather than a true autocatalytic attachment. Currently, autocatalytic binding in phycobiliproteins has only been found for ApcE that could be reconstituted with PCB to give native-like  $L_{CM}$ . (Zhao et al., 2005), and for the various phytochromes (Wu and Lagarias, 2000). Both the chromophore carrying and the lyase domains reside in the N-terminal region of this large protein. Phytochromes have two alternative binding sites; both are chromophorylated autocatalytically. The autocatalytic chromophore attachment in phytochromes requires the co-action of domains that are near the two alternative binding sites (Zhao et al., 2004; Bhoo et al., 1997; Lamparter et al., 2004).

### 1.3.3. E/F-type lyases

Up to date, two E/F-type lyases (CpcE/CpcF and PecE/PecF) have been studied. A heterodimeric lyase (CpcE/F) from *Synechococcus* PCC 7002 (Zhou et al., 1992) is the first phycobiliprotein lyase that was identified by an *in vitro* assay. Tooley et al. (2001) also proved this conclusion by heterologous *in vivo* reconstitution in *E. coli*. CpcE/F is required for correct binding of PCB to Cys- $\alpha$ 84, and catalyzes both the forward (binding) and the reverse (releasing) reaction (Fairchild et al., 1992). It also catalyzes the addition of PEB to apo- $\alpha$ -CPC (CpcA), but with reduced affinity and

kinetics compared to PCB (Fairchild and Glazer, 1994b).

The heterodimeric lyase/isomerase (PecE/PecF) catalyzes both the covalent attachment of PCB at Cys- $\alpha$ 84 of PecA and the concurrent isomerization of the molecule to PVB. This conclusion was reached by *in vitro* and *in vivo* reconstitution by Tooley et al. (2002, *in vivo*), Zhao et al. (2000, *in vitro*) and Storf et al. (2001, *in vitro*). The data indicate high protein specificity combined with a high site-specificity for the E/F-type lyases.

Zhao et al. (2002) studied the cofactor requirements and enzyme kinetics of the novel, dual-action enzyme, the isomerizing phycoviolobilin phycoviolobilin:phycoerythrocyanin-Cys $\alpha$ 84 lyase (PVB:PEC-lyase) from *M. laminosus*, which catalyses both the covalent attachment of phycocyanobilin to PecA, the apo- $\alpha$ -subunit of phycoerythrocyanin, and its isomerization to phycoviolobilin. A mechanism has been proposed by Boehm et al. (2007). A similar reaction sequence would generate bound PUB from free PEB, lyases for this process have been proposed by Six et al. (2007).

#### 1.3.4. Cyanobacterial S/U-type lyases

Shen et al. (2004) presented first evidence for new types of lyases in *Synechococcus* PCC7002 at a meeting. One of them, *cpcS*, has very high sequence similarity to *cpeS* in *Fremyella diplosiphon*, this gene is located on an operon (*cpeCDEST*) that was sequenced, and related to the biogenesis of phycoerythrin (Cobley et al., 2002).

The possible function of CpcS has been rapidly characterized thereafter. *In vitro* and in *E. coli*, it can catalyses chromophore attachment to all binding sites of APCs, to  $\beta$ 84 of CPCs and PECs, and even to some binding sites ( $\alpha$ 84 and  $\beta$ 84) of CPEs (Zhao et al., 2007a; Zhao et al., 2006a; Saunée et al., 2008; Shen et al., 2008). These data indicated that S-type lyases are near-universal lyases for cysteine-84 binding sites in cyanobacterial phycobiliproteins. Notable exceptions are chromophore attachments to  $\alpha$ 84 of CPC, PEC that were catalyzed by E/F type lyases (see section 1.3.3).

CpcS from *Anabaena* PCC 7120 (Zhao et al., 2006a; Zhao et al., 2007a) and CpcS from *Synechococcus* PCC 7002 (Shen et al., 2008; Saunée et al., 2008), the two

CpcS-type lyases studied so far seem to belong to two subtypes: CpcS from *Anabaena* PCC 7120 acts as a monomeric, single subunit lyase. By contrast, CpcS from another organism, *Synechococcus* PCC 7002, is inactive on its own, and requires CpcU as a second subunit for activity. This functional heterogeneity is reflected by the phylogenetic classification of the two subtypes into different groups (III and I, respectively) of the complex S/U protein family (Shen et al., 2008).

### 1.3.5. Cyanobacterial T-type lyases

*Synechococcus* PCC7002 has yet another gene, *cpcT*, that is homologous to *cpeT* on the *Fremyella* operon (Cobley et al., 2002); it codes for a third type (T-type) of lyase. CpcT catalyzes the regiospecific PCB addition at Cys-155 of CpcB from *Synechococcus* PCC7002 (Shen et al., 2006), and to Cys-155 of both  $\beta$ -CPC and  $\beta$ -PEC in *Anabaena* PCC 7120 and *M. laminosus* (Zhao et al., 2007b). Since CpcB and PecB are relatively closely related, these data indicate moderate protein specificity combined with a high site-specificity for the T-type lyases.

Taking these findings together, in phycobilisome-containing cyanobacteria devoid of PE, three lyases have been identified that are capable of attaching all phycobiliprotein chromophores: CpcS(/U) attach PCB to Cys- $\beta$ 84 of PC and PEC, CpcT attach PCB to Cys- $\beta$ 155 of PC and PEC, CpcE/F and PecE/F catalyze attachment to Cys- $\alpha$ 84 of PC and of PEC, respectively, and CpcS also attaches PCB to Cys- $\alpha$ 84 and Cys- $\beta$ 84 of APCs. Together with the autocatalytic chromophore attachment to ApcE, this would allow for complete chromophorylation of the respective phycobilisomes. Note, however, that there is presently only very little known on the sequence and the regulation of the attachments.

## 1.4 Lyase mechanisms

Currently, there are very few mechanistic studies on biliprotein lyases published, and they have focused on CpcE/F from *Synechococcus* PCC 7002 (Fairchild and Glazer, 1994b; Schluchter and Glazer, 1999), on CpcE/F and PecE/F from *Mastigocladus laminosus* and *Anabaena* PCC7120 (Böhm et al., 2007), and on CpcS1 from *Anabaena* PCC7120 (this thesis, Tu et al., 2008) that has been classified as an S-type

lyase of group III (Shen et al., 2008). Most of this work has been published during the time that this thesis has been prepared.

CpcS1 from *Anabaena* PCC7120 is a relatively simple system. It is active as a monomer, and does not require cofactors (Zhao et al., 2007a; Zhao et al., 2006a). Tu et al. (2008) have shown that CpeS1 can bind PCB, as assayed by Ni<sup>2+</sup> chelating affinity chromatography. Binding is rapid, and the chromophore is bound in an extended conformation similar to that in phycobiliproteins, but it is only poorly fluorescent. Upon addition of apo-biliproteins, the chromophore is transferred to the latter much more slowly (~1 h), indicating that chromophorylated CpeS1 is an intermediate in the enzymatic reaction.

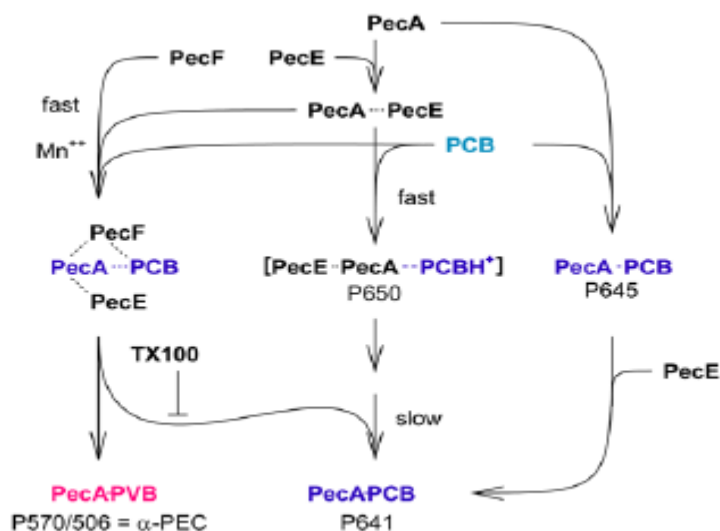


**Fig. 1-6: Reaction scheme of the isomerizing E/F-type lyases (Scheer and Zhao, 2008)**

Non-covalent chromophore binding is indicated by broken lines, covalent binding by solid lines and coloration of both the chromophore and the protein. Intermediates (Pxxx) are named according to their absorption maxima at xxx nm.

The reaction catalyzed by the E/F-type lyases is more complex (Fig 1-6). The first reaction step is addition of a fraction of the PCB (PCB\*) immediately available for binding to CpcE/F and subsequent transfer to apo- $\alpha$ -PC (CpcA) from *Anabaena* PCC7120. The second, slower rate would depend on the rate of isomerization of the bulk of the PCB to PCB\*(Fairchild et al., 1992). PCB addition to the apoprotein by the E-subunit is slow, but is accelerated if a complex of the protein substrate with the

E-subunit is formed prior to chromophore addition, indicating that protein-protein interactions are rate limiting. These studies (Böhm et al., 2007) with the E-subunit also provided the first experimental evidence for a chaperone-like function that had previously been discussed for lyases (Schluchter and Glazer, 1999). PecE can transform a low absorption, low fluorescence spontaneous addition product, P645, to a product P641 that has the high absorption and high fluorescence typical for native biliproteins: P641 is the same product that is formed from PecA and PCB in the presence of the E-subunit. Both lyase subunits are required for chromophore attachment. The reaction has been studied in some detail with the isomerizing lyase, PecE/F from *Anabaena* PCC 7120. The F-subunit alone is inactive, but carries the isomerase activity for which a motif has been identified (Zhao et al., 2005); the E-subunit alone catalyzes only the PCB attachment without isomerization (Scheer and Zhao, 2008).

## 1.5 Applications

The first “application” of lyase-based reconstitution systems is studies on biliprotein function. Tooley et al. 2001 first attempted to use complete biosynthesis of holo-CpcA from heme in *E. coli*. The lyases, for the first time, make it possible to modify the chromophore and protein separately, then linking them covalently by the use of the appropriate lyase(s). This reconstitution system consists of 1) the apoprotein, 2) the phycobilin biosynthesis enzyme, and 3) the lyase(s) (Tooley and Glazer, 2002; Tooley et al., 2001; Saunée et al., 2008; Zhao et al., 2006a, 2007a, 2007b).

The second emerging application in basic research is studies on protein folding, where covalently bound chromophores in a native system are desirable to avoid artifacts. In particular, fluorescence has been proposed as an indicator for the protein dynamics, and absorption and Vis-CD as indicators for the tertiary structure (Kupka and Scheer, 2008; Ma et al., 2007).

The third application is the use of PVB-containing  $\alpha$ -PEC-(fusion)-proteins as a light switch. The native protein environment enables the PVB chromophore to be switched between two states with different absorption and vastly different fluorescence characteristics: the 15Z-isomer is highly fluorescent, the 15E-isomer is practically

non-fluorescent (Zhao et al., 1995). Alone or in combination with acceptor proteins, this might allow for use in new high-resolution light microscopy techniques (Walter et al., 2008).

The fourth application is as fluorescence label. Phycobiliprotein properties (high molar extinction coefficients, high fluorescence quantum yields, large Stokes shifts, high oligomer stability and relatively high photostability) make them potentially powerful and highly sensitive fluorescent reagents. They can serve as labels for antibodies, receptors and other biological molecules in a fluorescence-activated cell sorter and be used in immunolabelling experiments and fluorescence microscopy or diagnostics (Spolaore, et al., 2006). In addition, because of the high molar absorptivity of these proteins at visible wavelengths, they are convenient markers in such applications as gel electrophoresis, isoelectric focusing and gel exclusion chromatography.

A final commercial application is as natural pigments. The primary potential of these molecules seems to be as natural dyes, but an increasing number of investigations have indicated health-promoting properties and a range of pharmaceutical applications. The most important current application of phycocyanin is as colorant in food (chewing gums, dairy products, ice sherbets, jellies etc) and cosmetics such as lipsticks and eyeliners in Japan, Thailand and China, replacing current synthetic pigments (Becker, 2004; Rommàn, et al., 2002). They are also potential therapeutic agents in oxidative stress-induced diseases, and some authors have suggested that biliproteins might also be effective in photodynamic therapy (He et al., 1996).

## 1.6 Thesis plan

This thesis is concerned with four different aspects of chromophore attachment to phycobiliproteins.

1) The final step in phycobiliprotein biosynthesis is the covalent chromophore attachment to the apoprotein. *In vitro*, spontaneous chromophore additions are generally of low fidelity, therefore lyases were suggested that catalyze the chromophore binding. However, at the beginning of my thesis such lyases were known only for a single binding site, cysteine- $\alpha$ 84 of PC and PEC, the E/F type lyases. The first goal was therefore to find and characterize phycobilin lyases which can attach

phycobilin to other binding sites and other phycobiliproteins. This was triggered by a meeting report (Shen 2004) that indicated a new class of lyases. While the groups of Bryant and Schluchter worked mainly with *Synechococcus* PCC7002 that contains only PCB chromophores, this work focused on *Anabaena* PCC7120 that has PCB and PVB chromophores, and whose genome is available in the databases (<http://www.ncbi.nlm.nih.gov/entrez/viewer.fcgi?db=nucleotide&val=BA000019>)

2) Tooley et al. (2001) successfully biosynthesized  $\alpha$ -PC in *E. coli* by using a multi-plasmidic expression system. It is more advantageous than reconstitution *in vitro*. Such a system seemed attractive, too, for searching and investigating new lyases, we therefore wanted to establish a multi-plasmidic expression system in *E. coli*.

3) Currently, a variety of separation, purification and analytic methods are used to analyze phycobiliproteins. Each method has a different application spectrum and limitations, and can only explain some characters of phycobiliproteins. To fully characterize the phycobiliproteins, a standardized multi-step protocol for separation, purification and determination methods should be established. Since only few reconstituted phycobiliproteins were fully characterized before the beginning of this thesis, this analytical protocol should be applied to phycobiliproteins that were reconstituted in *E. coli* both by the known E/F-type and the new lyases.

4) Even with the E/F-type lyases, there were very few mechanistic studies published. A better characterization of the mechanism of new lyases will be done, using kinetic studies, comparison of spontaneous and catalyzed attachment, and model studies with modified substrate.

## 2: Materials and Methods

### 2.1 Materials

#### 2.1.1 Organisms

*E. coli* strain:

BL21(DE3) (Studier *et al.* 1986)

Cyanobacterium strain:

*Fischerella* sp. PCC7603 (*Mastigocladus laminosus*);

*Anabaena* sp. PCC 7120 (*Nostoc* sp. PCC7120);

*Calothrix* sp. PCC 7601;

*Spirulina platensis* (Spary dried, Bonn, Germany)

#### 2.1.2 Vectors

pBluescript II KS (Stratagene, San Diego);

pET30a (Novagen, Germany);

Duet vectors (Novagen, Germany)

#### 2.1.3 Plasmids

All plasmids were a generous gift of Prof. Kai-Hong Zhao (Huazhong University of Science and Technology, China). They include three types: 1) lyase plasmids: pCDFDuet-*cpcS*, pET-*cpcS*, pETDuet-*cpcT*, pCOLADuet-*cpcE-cpcF*, pCOLADuet-*pecE*, pCDFDuet-*pecF*; 2) PCB biosynthetic plasmid: pACYCDuet-*ho1-pcyA*; 3) apoprotein plasmids: pETDuet-*pecA*, pETDuet-*cpcA*, pET-*apcA1*, pET-*apcB*, pET-*apcA2*, pET-*apcD*, pET-*apcF*, pET-*cpcB*, pET-*cpcB(C155I)*, pET-*cpcB(C84S)*, pET-*pecB*, pET-*pecB(C155I)*, pET-*pecB(C84A)*. The CPC and PEC genes come from *M. laminosus*, the other genes come from *Anabaena* PCC 7120.

### 2.1.3 Chemicals

Generally, bidistilled water is used as well as chemicals of the highest obtainable degree of purity unless indicated otherwise.

#### 2.1.3.1 Buffers and solutions

The following table lists frequently used buffers and solutions (Table 2-1).

**Table 2-1: list of frequently used buffers and solutions**

Name	Composition
Coomassie-blue staining	Staining Solution: 0.15% (w/v) Coomassie Brilliant Blue G-250 (Serva) 40 % (v/v) Methanol 10 % (v/v) Acetic acid Destain Solution: 10 % (v/v) Methanol 10 % (v/v) Acetic acid
Di-potassium phosphate buffer (DPP-buffer)	50 mM $K_2HPO_4$ 0.5 M NaCl pH 7.2
Fluka solution	Fluka advanced protein assay (Sigma-Aldrich) in 1:5 dilution with water
IPTG	100 mM IPTG (Roth) in aqueous solution
TB-Medium	1.2 % (w/v) Tryptone 2.4 % (w/v) Yeast extract 0.4% (v/v) Glycerol 17mM $KH_2PO_4$ 72mM $K_2HPO_4$
LB-Medium	1 % (w/v) Tryptone 0.5 % (w/v) Yeast extract 1 % (w/v) NaCl pH 7.2 Sterilized by autoclaving for 20 min
RB- Medium	1 % (w/v) Tryptone

	0.5 % (w/v) Yeast extract 0.5 % (w/v) NaCl 0.2 % (w/v) Glucose pH ranging from 6.8 to 7.5 Sterilized by autoclaving for 20 min
SDS-7 Marker	Dalton Mark VII-L, MW range 14-70 kDa, Sigma
SDS-PAGE loading buffer	625 mM Tris/HCl 1 M pH 6.8 2 % (w/v) SDS 10 % (v/v) Glycerine 0.003 % (w/v) Bromphenol blue 5 % (v/v) 2-Mercaptoethanol
SDS-PAGE running buffer	25 mM Tris/HCl pH 8.3 192 mM Glycin 0.1 % (w/v) SDS
SDS-Gel Stacking Gel 15% (for two chambers [8.3 x 7 x 0.075 cm])	1 ml Tris/HCl 3 M, pH 8.8 4 ml 30% Acrylamide/Bisacrylamide (35.7:1) 2.9 ml H <sub>2</sub> O 80 µl 10% SDS 40 µl 10% APS 4 µl TEMED
Separating Gel 5% (for two chambers [8.3 x 7 x 0.075 cm])	0.5 ml Tris/HCl 1 M, pH 6.8 0.65 ml 30% Acrylamide/Bisacrylamide (35.7:1) 2.8 ml H <sub>2</sub> O 40 µl SDS 20 µl APS 4 µl TEMED
Coomassie-blue staining solution	0.15% (w/v) Coomassie Brilliant Blue G-250 (Serva) 40 % (v/v) Methanol 10 % (v/v) Acetic acid
Coomassie-blue destaining solution	10 % (v/v) Methanol 10 % (v/v) Acetic acid
Zinc solution	1.5 M Zinc acetate
FPLC-buffer	K <sub>2</sub> HPO <sub>4</sub> 50 mM NaCl 150 mM pH 7.0

Ni <sup>2+</sup> -solution	50 mM NiSO <sub>4</sub> in aqueous solution
Starting buffer for the Ni <sup>2+</sup> -chelating chromatography	20 mM K <sub>2</sub> HPO <sub>4</sub> , pH 7.0, 1 M NaCl
Washing buffer for the Ni <sup>2+</sup> -chelating chromatography	20 mM K <sub>2</sub> HPO <sub>4</sub> pH 7.0 1 M NaCl 50 to 100 mM Imidazole
Elution buffer for the Ni <sup>2+</sup> -chelating chromatography	20 mM K <sub>2</sub> HPO <sub>4</sub> pH 7.0 1 M NaCl 500 to 1000 mM Imidazole
EDTA buffer for the Ni <sup>2+</sup> -chelating chromatography	20 mM K <sub>2</sub> HPO <sub>4</sub> pH 7.0 500 mM NaCl 50 mM EDTA
Reconstitution buffer for CpcS	K <sub>2</sub> HPO <sub>4</sub> and KH <sub>2</sub> PO <sub>4</sub> 500 mM NaCl 100 mM pH 7.5
Reconstitution buffer for PecA	K <sub>2</sub> HPO <sub>4</sub> 50 mM NaCl 500 mM MnCl <sub>2</sub> 3 mM 2-Mercaptoethanol 1 mM Triton X-100 0,85% (v/v) Glycerin 10% (v/v) pH 7.0
Start buffer for Sep-Pak C18 column	0.1% (v/v)TFA
Elution solvent for Sep-Pak C18 column	Methanol
Start buffer for Bio-gel P-6 DG column	Dilute HCl pH 2
Elution buffer for Bio-gel P-6 DG column	30%(v/v) acetic acid in dilute HCl pH 2

### 2.1.3.2 Antibiotics

Antibiotic concentrations and related vectors are shown in Table 2-2

**Table 2-2: Antibiotics and their used concentrations**

Antibiotics	Company	Vectors	Concentration ( $\mu\text{g/ml}$ )( <i>E. coli</i> )	
			Single Plasmid	Multiple Plasmid
Ampicillin	Roth	pBluescript; pETDuet	140	100
Chloramycetin	Sigma-Aldrich	pACYCDuet	17	10
Kanamycin	Sigma-Aldrich	pET30, pCOLADuet	30	20
Streptomycin	Sigma-Aldrich	pCDFDuet	25	15

### 2.1.4 Technical devices

#### Centrifuges

Refrigerated centrifuge:

Centricon H-401 (Kontron, Eching)

Sorvall RC-5B (Thermo, Waltham, MA, USA)

Rotor: F9S (Piramoon, Santa Clara, CA, USA)

Refrigerated benchtop centrifuges:

Sigma 3K18 C (Braun, Melsungen), Rotoren: 12154, 12155

Biofuge fresco (Kendro, Hanau)

#### Electrophoresis

Mini Protean III Dual Slab Cell (Bio-Rad, Munich Germany)

Constant Voltage Power Supply 1000/500 (Bio-Rad, Munich Germany)

#### UV/VIS-Spectrometer

UV-2401 PC Spectrometer (Shimadzu, Japan)

Lambda 25 Spectrometer (Perkin Elmer, USA)

#### Fluorescence Spectrometer

LS 55 Luminescence Spectrometer (Perkin Elmer, USA)

**CD-Spectrometer**

J-810 Spectropolarimeter (Jasco, Tokyo, Japan)

**NMR-Spectrometer**

DMX 750 Spectrometer (Bruker, Karlsruhe)

**Mass Spectrometer**

Micromass Q-ToF Premier (Waters Micromass Technologies, Manchester, UK)

Medium Nano-ES spray capillaries No. ES380 (Proxeon Biosystems, Denmark)

**Chromatography for peptide purification**

PD-10 (Sephadex G-25)-column (Amersham Biosciences, USA)

Sep-Pak C18 (Waters, USA)

Bio-gel P-6 DG (Bio-Rad, Munich Germany)

**Vacuum concentrator**

Eppendorf Concentrator 5301 (Eppendorf, Germany)

**Fast Performance Liquid Chromatography**

Series controller LKB GP-10, Pump P-50 (Pharmacia, Sweden)

Superdex 200 prep grade column 16/60 (Pharmacia, Sweden)

TIDAS UV/Vis Spectrometer and detector (J&M, Germany)

Software: Spectacle 1.55 (Lab Control, Germany)

**High Performance Liquid Chromatography**

Series controller 600 E multisolvent delivery system (Waters, USA)

TIDAS UV/Vis Spectrometer and detector (J&M, Germany)

Zorbax 300SB-C18 column (Agilent Technologies, USA)

Software: Spectacle 1.55 (Lab Control, Germany)

**Documentation**

Fluorescent gels: CCD KP 161 (Hitachi, GB)

Protein gels: hp scanjet 7400 c, reflection mode (HP, USA)

### **Others**

Column matrix: Chelating Sepharose™ (Amersham Biosciences, USA) (affinity chromatography)

Cold light source: Intralux 150 H universal (Volpi, USA )

Dialysis tubing: Servapor dialysis tubing 16mm (Serva, Germany)

Pump: Minipuls 2 (Gilson, Netherland)

Rotary evaporator: Rotavapor-R (Büchi, Germany)

Sonifier: Sonifier W-450 (Branson Ultraschall, Germany)

Shaker: Orbit Environ Shaker (Lab-Line, USA)

### **Data analysis**

Software employed for advanced data processing and visualization includes:

Data transfer: Spectacle 1.55 (Lab Control, Germany)

General analysis: Origin 7.0 (Microcal Software, USA), Microsoft Excel 2003 (Microcal Software, USA), Adobe Photoshop 6.0 (Adobe Photoshop, USA)

Kinetic analysis: SPECFIT/32 (Spectrum Software Associates, USA)

Analysis of NMR spectra: MestReC (Mestrelab Research SL, Spain)

Word processing: Microsoft Word 2003 (Microcal Software, USA)

## **2.2 Methods**

### **2.2.1 General molecular biological methods**

General molecular biological methods such as growing conditions of bacteria, restriction endonuclease digestion, DNA ligation, agarose gel electrophoresis, transformation of *E. coli* and recombinant DNA procedures were carried out according to standard procedures as described in Sambrook et al., (1989). Plasmid DNA isolation, PCR and gel purification were prepared using Qiagen plasmid mini kits 12125 (Hilden, Germany) according to manufacturer's protocols.

### **2.2.2 Protein isolation**

For convenient preparation of proteins, a heterologous system was established by Zhao et al. (2002), using the expression vector pET-30a (Novagen, Schwalbach) with intrinsic kanamycin-resistance and D-galactose-inducible promoter. Additionally, His<sub>6</sub>-tagged derivatives were constructed to allow for easy purification of the gene products.

### **2.2.2.1 Protein expression in *Escherichia coli***

The pET-based plasmids were used to transform *E. coli* BL21(DE3). Cells were grown in Luria-Bertani (LB) medium containing kanamycin (see Table 2-2 for antibiotic concentrations) at 37 °C for genes from *M. laminosus* or at 20 °C for genes from *Anabaena* sp. PCC 7120. For expression of untagged proteins, which is available with the Duet vectors (Novagen, Germany), kanamycin has to be substituted by other antibiotics in different final concentrations (see Table 2-2).

Once the cultures have reached the exponential growth phase (after 4-5 hr, A<sub>600</sub> = 0.5–0.7), expression of the foreign gene is induced with IPTG (1mM). Cells were collected by centrifugation (7000 xg, 15min) 5 hr after induction (for genes from *M. laminosus*) or after 6 hr (for genes from *Anabaena* sp.), then washed twice with doubly distilled water and stored at -20 °C until use.

### **2.2.2.2 Protein purification**

Cell pellets were resuspended in ice-cold start buffer and disrupted by sonication (30 min at 150 W, duty cycle 40%). The suspension was centrifuged at 12,000 xg for 30 min at 4 °C. The crude protein-enriched supernatant was stored at 4 °C until use.

### **Ni<sup>2+</sup>-affinity chromatography**

Subsequently, the supernatant was purified via Ni<sup>2+</sup>-affinity chromatography on chelating Sepharose (Amersham Biosciences). The His<sub>6</sub>-tag coordinates the bivalent cation and is adsorbed to the column, while the major fraction of the bacterial proteins has generally no or little affinity for the column material. 30 ml of the supernatant were applied to a Ni<sup>2+</sup>-chelating column (60 x 20 mm) equilibrated with start buffer (see Tab. 2-1 for all solutions and buffers), and then were washed with start buffer and elution buffer. The following washing steps increase in stringency to enhance the purification

process. To finally elute the product fraction, high imidazole concentration (0.5-1M) is applied, which is a strong chelator of  $\text{Ni}^{2+}$  ions, thus displacing the histidines and releasing them from the stationary phase.

After collection, the protein fractions were dialyzed twice against the initial buffer and kept at  $-20\text{ }^{\circ}\text{C}$  until use.

For regeneration of the column, EDTA buffer is used to strip off  $\text{Ni}^{2+}$  and protein remainders. After excessive rinsing with water,  $\text{Ni}^{2+}$ -solution is applied to recharge the column. Consecutive equilibration with starting buffer prepares the column for application of another protein sample. In case the EDTA buffer is not sufficient to clean the column (when a “dirt veil” is still visible after the rinsing step), a washing step with 0.5 M NaOH can be included for improved cleaning. If not in use, the column is stored in 20% ethanol.

### **Fast Performance Liquid Chromatography**

Samples (6 ml) in Tris buffer (1 M, pH 6.0) were concentrated to an overall volume of 1 ml using centrifugal filter devices (Amicon Ultra-15, Millipore, USA). They were then applied to the gel column, Superdex 200-16/60 preparative grade (Amersham Biosciences, flow rate 0.75 ml/min) equilibrated with Tris buffer (1 M, pH 6.0). The eluant was monitored with a diode array detector (Tidas, Diode-Array-Photometer, J&M, Germany; 280–800 nm, measurement interval 5 s). Fractions were collected and analyzed by SDS-PAGE according to Laemmli (1970) using 15% stacking and 5% separating gels (Boehm, 2006).

#### **2.2.2.3 Protein analysis**

After dialysis, the solutions are retrieved, transferred to Falcon tubes, and their protein contents were evaluated employing two methods:

##### **Sodium dodecyl sulphate polyacrylamide (SDS-PAGE) gels**

50  $\mu\text{l}$  of the protein solution are mixed with 50  $\mu\text{l}$  SDS-PAGE loading buffer and boiled for 5 minutes. 10-20  $\mu\text{l}$  of the sample are applied to a two step SDS-PAGE gel (see table 2-1) and run for 30 min of 50 V, followed by 75 min of 150 V. The gel is developed by overnight incubation in staining solution, and subsequently excess dyes removed by destaining solution, until the desired degree of contrast is achieved.

Chromophorylated protein species are identified by Zn<sup>2+</sup>-induced fluorescence prior to Coomassie staining: after soaking the gels in 1 M Zn<sup>2+</sup> acetate solution for 15 min, UV-light (360 nm) induced fluorescence can be observed (Berkelman and Lagarias, 1986).

### **Protein assay**

Protein concentrations were determined by protein assay kits from Fluka advance (Seelze, Germany). 10 µl of the protein solution are mixed with 300 µl FLUKA solution and 690 µl distilled water, and incubated for several minutes. Absorption of the protein sample is measured at 590 nm and the concentration in mg/ml deduced by comparison to an albumin standard. For protein solutions in the expected concentration range of 5-10 mg/ml, as in this case, a 1:10 dilution with distilled water proved to give convenient absorption values. Comparing this value with the corresponding lanes on the SDS-PAGE and taking into account the contamination with co-purified *E. coli* proteins, a rough estimate of the concentration of the products is possible. Since the molar masses for the proteins are known, the concentration in mg/ml can be converted to µmol/ml. 1 L expression medium usually yields 10 ml protein solution (5-10 mg/ml in concentration as determined by the FLUKA Protein assay) which are equivalent to 4-6 µmol protein.

#### **2.2.2.4 Concentration of proteins**

In case the volume of a protein solution needs to be reduced to increase its relative protein concentration, it is transferred to a centrifuge filter (Biomax 10K 15 ml, Millipore) and centrifuged (4 °C, 7 000 xg) until the desired volume reduction is achieved.

#### **2.2.2.5 Protein storage**

The protein solutions are stable at room temperature down to 4°C for approximately 2 days. Long-term storage is possible at -20 °C but accompanied by loss of specific enzyme activity.

### **2.2.3 Pigment isolation**

Pigments are light-sensitive and prone to oxidation. All work that involves pigments is

therefore performed under green protective light or at least dim light. During phycocyanobilin (PCB) extraction, when the pigment-containing solutions are heated, argon is employed as protective gas to prevent excessive exposure to oxygen, thereby reducing the formation of oxidation- and breakdown products.

### **2.2.3.1 Pigment extraction from *Spirulina platensis***

Spray-dried cells of *Spirulina platensis* are methanolized and free pigment is extracted with chloroform. Crude pigment is obtained after solvent evaporation. The detailed procedure has been described previously (Storf et al., 2001).

### **2.2.3.2 Phycocyanobilin purification**

Chromatography of the PCB crude extract on a reversed phase column separates pure PCB from its breakdown products, derivatives, and remainders of other pigments. Stationary phase: Silica gel RP 8 (23-63  $\mu\text{m}$ ) 60 Å (ICN, Eschwege); mobile phase: 40% 2-Propanol, 60% 50 mM KPP buffer pH 2.1 (v/v) (degassed). Pressure is applied to increase the flow; the column is run under protective light conditions. The dark blue fraction is collected, and the solvent evaporated. For details see Storf et al. (2001).

### **2.2.3.3 Phycocyanobilin analysis**

The pigment thus obtained is redissolved in methanol. 5  $\mu\text{l}$  are diluted in 1 ml methanol, acidified with concentrated HCl (2% v/v), and a spectrum is recorded in the range from 300-800 nm. From the known extinction coefficient  $\epsilon_{690} = 37\,900\ \text{M}^{-1}\text{cm}^{-1}$  (Cole et al., 1967) of PCB in acidic methanol, the concentration of the pigment solution can be deduced. The position of the red maximum indicates the degree of pigment purity: Pure PCB peaks at 690 nm, while contamination with breakdown products or derivatives causes a blue shift. For reconstitution assays, PCB is dissolved in DMSO instead of methanol.

### **2.2.3.4 Phycocyanobilin storage**

The pigment is dissolved in little methanol, aliquots are transferred to small vials, and

the solvent is evaporated with a gentle stream of argon. The vials are closed tightly and can be stored for extended times at -20 °C under argon atmosphere.

## 2.2.4 Phycobiliprotein reconstitution/preparation

For convenient preparation of the phycobiliproteins, a multiple-plasmid expression system was established by Zhao et al. (2006a) using the expression vector Duet (Novagen, Germany).

### 2.2.4.1 Phycobiliprotein expression

One of the apo-phycobiliprotein plasmids, one of lyase plasmids and pACYCDuet-ho1-*pcyA* were transformed together into BL21 (DE3) cells to produce phycobiliprotein. Cells were grown at 37 °C in LB-medium under the respective antibiotic selections. When the cell density reached  $A_{600}=0.5-0.7$ , IPTG (1 mM) was added, cultivation continued for 12 hr at 20 °C in darkness. Cells were then collected by centrifugation (7000  $\times g$ , 15min), washed twice with doubly distilled water, and stored at -20 °C until use.

### 2.2.4.2 Biliprotein purification

see 2.2.2.2

### 2.2.4.3 Biliprotein extinction coefficient

The extinction coefficients of the reconstituted and biosynthesized chromobiliproteins were determined based on the extinction coefficient of PCB in CPC in 8 M acidic urea (pH=1,5) ( $\epsilon_{660}=35,500 \text{ M}^{-1}\text{cm}^{-1}$ ) (Glazer and Fang ,1973); and PVB in  $\alpha$ -PEC in 8 M acidic urea ( $\epsilon_{590}=38,600 \text{ M}^{-1}\text{cm}^{-1}$ ) (Bishop et al. , 1987).

### 2.2.4.4 Biliprotein fluorescence yields

Fluorescence yields  $\Phi_F$  of the reconstituted and biosynthesized chromobiliprotein were determined in KPP buffer (20mM, pH 7.2), using the known fluorescence

quantum yield ( $\Phi_F = 0.27$ ) of CPC from *Anabaena* sp. PCC 7120 (Cai et al., 2001) as standard.

#### 2.2.4.5 Chromoprotein digestion method

Reconstituted or biosynthesized chromoproteins were purified by  $\text{Ni}^{2+}$  chromatography (see 2.2.4.2) and dialyzed against KPP (20mM, pH 7.2). For pepsin digestions, the desired chromoprotein solution was acidified with HCl to pH 1.5, and pepsin was added to the chromoprotein (1:1, w/w). For trypsin digestions, the dialyzed chromoproteins (10  $\mu\text{M}$ ) were digested with trypsin (40  $\mu\text{M}$ ) in KPB (100 mM, pH 7.0). In both cases, the mixture was incubated for 3 hr or 4hr at 37 °C, and then fractionated on Bio-Gel P-6 DG (Bio-Rad) equilibrated with dilute HCl (pH 2.5). Colorless peptides and salts were eluted with the same solvent, and the adsorbed chromopeptides were eluted with acetic acid (30%, v/v) in dilute HCl (pH 2.5). The collected samples were desalted and concentrated by Sep-Pak C18 (Waters, USA), then eluted with 100% methanol to small vials, and the solvent is evaporated with a gentle stream of argon until the desired volume. The vials are closed tightly and can be stored for extended times at -20 °C under argon atmosphere until use.

#### 2.2.4.6 Semipreparative HPLC

The enzyme digested samples were fractionated by repeated HPLC. The collected samples were dried with a Vacuum concentrator (45 °C), and stored at -20 °C until use.

The first preparative program

Solvent: A: KPP (100 mM, pH 2.1)    B: acetonitrile

Gradient:

time (min)	0	2	22	25	45
A:B	80:20	80:20	60:40	80:20	80:20

Flow rate: 1.0 ml/min

The second preparative program:

Solvent: A: formic acid (0.1%, pH 2.0) B: acetonitrile containing 0.1% formic acid

Gradient:

time (min)	0	2	32	35	55
A:B	80:20	80:20	60:40	80:20	80:20

Flow rate: 1.0 ml/min

All solvents applied to the column are degassed and filtered through a sterile 0.22  $\mu\text{m}$ -membrane. When preparations are finished, the column is equilibrated with acetonitrile for half hour for better preservation.

### 2.2.5 Lyase CpcS (Alr0617) reaction assay

Chromophore reconstitution with apo-phycobiliproteins was assayed as described before (Zhao et al. 2006a, 2007), using the following standard reaction conditions: potassium phosphate buffer (KPB, 500 mM, pH 7.5) containing NaCl (100–150 mM), CpcS (10–30  $\mu\text{M}$ ), and apo-phycobiliprotein (10–30  $\mu\text{M}$ ). PCB (final concentration = 5–10  $\mu\text{M}$ ) was added to the proteins as a concentrated dimethylsulfoxide solution, the final concentration of dimethylsulfoxide did not exceed 1% (v/v). The mixtures were incubated at 35 °C for 0.5–4 hrs in darkness.

### 2.2.6 Chromophore adduct assay

#### 2.2.6.1 Reconstitution system

PCB and 15Za-PCB were reconstituted with imidazole (50 - 500 mM ) or ME (10-600mM), and/or CpcS (10 - 50  $\mu\text{M}$ ) by incubation in KPP (500 mM, pH 7.5) for 30min-2hr.

DOHH was incubated with PecA, PCB or/and PecE, or/and PecF in holo-PecA reconstitution system.

### **2.2.6.2 Product purification and digestion methods**

See 2.2.2.2 , 2.2.4.5 and 2.2.4.6

### **2.2.6.3 Analytical methods**

The chromophore adducts were analyzed spectroscopically (absorption, fluorescence, circular dichroism) and by SDS-PAGE using Zn<sup>2+</sup> staining (see 2.2.2.3). The HPLC products were analyzed mass spectrometry and NMR spectrometry.

### **2.2.6.4 Transfer assay**

The purified chromophore adduct was mixed with the respective apo-phycoobiliprotein (10–30 μM) and lyase (10-30 μM), and the reaction followed at 35 or 20°C for 1–3 hr by absorption and/or fluorescence spectroscopy.

## **2.2.7 Spectroscopy**

### **2.2.7.1 UV/Vis spectroscopy**

UV visible absorption spectra at room temperature were measured on Shimadzu UV-2401PC or Perkin-Elmer Lambda 25 spectrophotometer using 1 cm or 1 mm path length cuvettes. Formation of the photochromic PVB-PecA (i.e. α-PEC) in the lyase reaction was monitored by the absorption at 570 nm and by double-difference spectroscopy of the reversible photoreaction of the PVB chromophore, as previously described (Zhao et al. 1995).

### **2. 2.7.2 Fluorescence spectroscopy**

The fluorescence spectra of chromoproteins were recorded by a LS 55 Luminescence Spectrometer (Perkin Elmer, USA) using 1 cm path length cuvette at room temperature. Excitations were scanned from 300- 850 nm with the emission wavelength set to the desired wavelength in the range 500 - 660 nm.

### **2.2.7.3 Electrospray ionisation mass spectroscopy (ESI-MS)**

The isolated colored products were dissolved in spray solution (65 % methanol, 35 % water, 0.1 % formic acid ), and analyzed by mass spectrometry in positive ion mode using a Micromass Q-ToF Premier mass spectrometer (WatersMicromass Technologies, Manchester, U.K.) with a nano-ESI source. Work was done in collaboration with Dr. M. Plöscher and Prof. Dr. L. A. Eichacker (Munich University, Germany).

### **2.2.7.4 Circular dichroism (CD) spectroscopy**

Circular dichroism measurements were performed with a J-810 CD spectropolarimeter (JASCO Corp., Japan) in 1 mm (for far-UV region) or 1 cm (for visible light region) rectangular Quartz cuvettes at 22 °C.

### **2.2.7.5 Nuclear magnetic resonance (NMR) spectroscopy**

The isolated colored products were dissolved in 0.1% TFA/D<sub>2</sub>O, and transferred with thinly drawn-out Pasteur pipettes to 2 mm diameter NMR microtubes. NMR spectra were measured in collaboration with Dr. R. Haessner (Munich Technical University, Germany) at 281 K (Bruker DMX601 operating at 600.14 MHz).

## **2.2.8 Websites**

Protein sequences were taken from the sequences of database Swiss-Prot, TrEMBL (<http://www.expasy.org>) and of the National Centre for Biotechnology Information (NCBI) (<http://www.ncbi.nlm.nih.gov>). Sequences alignments were done by using BLAST (<http://www.expasy.org/tools/blast/>) or CLUSTAL W (<http://www.ebi.ac.uk/clustalw>).

## 3: Results and Discussion

### 3.1 Structure analysis of reconstituted holo-PecA

#### 3.1.1 Reconstitution principle of holo-PecA

Phycocyanobilin(PCB) is biosynthesized from heme by the action of two enzymes, heme oxygenase and BV-reductase. PCB is then attached to the apoprotein by a heterodimeric lyase, PecE/PecF, that concomitantly isomerizes the chromophore to phycoviolobilin(PVB) (Zhao et al. 2000; Storf et al. 2001). Using endogenous heme as substrate, Tooley et al.(2002) introduced five genes into *E. coli* to produce holo-HT-PecA from *Anabaena* PCC7120 with optical spectroscopic properties characteristic of the native holo subunit. Besides the genes for the apoprotein (*pecA*) and the lyase (*pecE/F*), these included the two respective genes for PCB synthesis, viz. *ho1* and *pcyA*, from the same organism (Fig.3-1).

It is known that *in vitro* tests of lyase function are hampered by the spontaneous and faulty addition of chromophores. Since there was evidence that this activity is suppressed in the *E. coli* system, a multi-plasmidic system was established in our lab, too, to generate holo-biliproteins in *E. coli*. This also served a more thorough analysis of the products, including mass, NMR and CD spectroscopy.

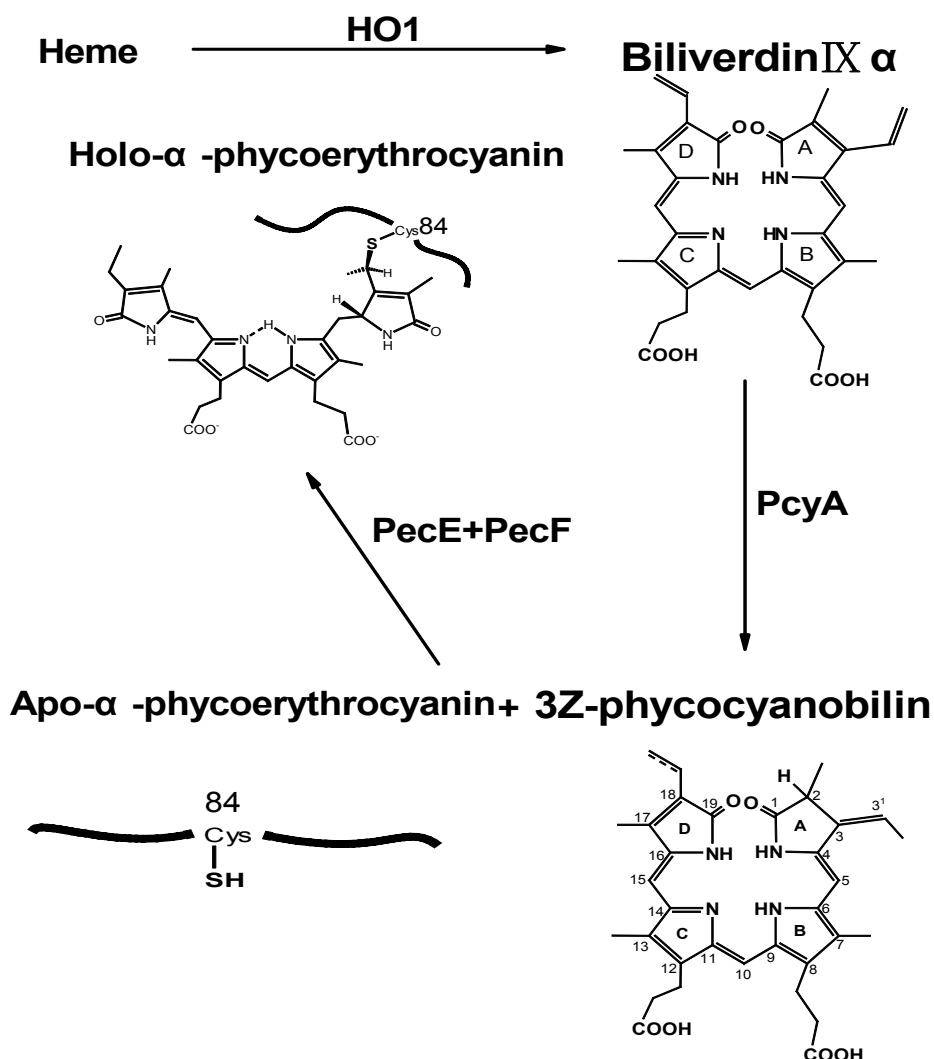
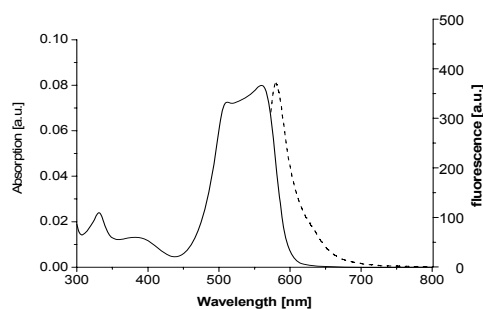


FIG. 3-1: Biosynthetic pathway of PCB from heme and its addition to the phycoerythrocyanin apo- $\alpha$  subunit and isomerization to PVB.

### 3.1.2 Expression and Purification of the holo-PecA

Expressing the pETDuet-*pecA*, pCOLADuet-*pecE*, pCDFDuet-*pecF* and pACYCDuet-*ho1-pcyA* plasmids in the strain *E. coli* strain BL21(DE3), upon induction with IPTG, the culture acquired a pronounced pink tint. The His-tagged holoprotein (holo-HT-PecA) was purified by immobilized Ni<sup>2+</sup> affinity chromatography, and its spectroscopic properties were determined with the protein fraction purified by immobilized metal affinity chromatography after dialysis against 50 mM K phosphate (pH 7.0). The absorbance spectrum of holo-HT-PecA had a  $\lambda_{\max}$  at 561 nm and the fluorescence had a  $\lambda_{\max}$  at 582 nm (Fig. 3-2). The corresponding values for *in vivo*

reconstituted holo-PecA from *Anabaena* PCC7120 are 561 nm and 582 nm (Tooley and Glazer, 2002). The spectrum corresponded closely to that of the native holo-PecA obtained from *Anabaena* PCC7120 (Bryant et al., 1976).



**FIG.3-2. Spectroscopic properties of *Anabaena* PCC7120 holo-PecA expressed in *E. coli*.** Shown are the absorption (solid) ( $\lambda_{\text{max}} = 561$  nm) and fluorescence emission spectra (dashed) ( $\lambda_{\text{max}} = 582$  nm for holo-PecA purified from *E. coli* by affinity chromatography).

Analysis of Coomassie brilliant blue-stained gels after SDS-PAGE of the purified protein showed that there were three distinct bands (Fig. 3-3, lane A), band 1 at ~28 kDa, band 2 at ~20 kDa, and band 3 at ~19 kDa. The sizes of these bands are compatible with those calculated for PecE, holo-HTPecA, and PecF, respectively. This result is like that of Tooley et al. (2002). Upon exposure to  $\text{Zn}^{2+}$  (Berkelman et al., 1986) and UV illumination, only band 2 was fluorescent, indicating that it contained covalently attached bilin (Fig.3-3, lane a).

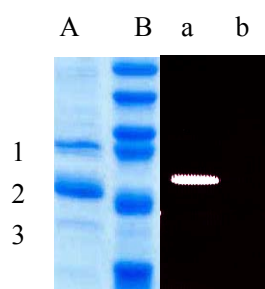


**FIG. 3-3: SDS-PAGE analysis of *Anabaena* PCC7120 His-tagged proteins expressed and purified by affinity chromatography.** Proteins were visualized by Coomassie brilliant blue staining (left panel) and by the UV excited fluorescence of bilin-bearing polypeptides in the presence of  $\text{Zn}^{2+}$  (right panel). Lanes A, a:PecE, HT-PecA, and PecF (bands 1, 2, and 3, respectively) expressed in *E. coli* strain; lanes B, b: molecular mass standards (from the top, 45, 36, 29, 24, 20 and 14 kDa).

The extinction coefficient  $\epsilon_{563}=99000 \text{ M}^{-1}\text{cm}^{-1}$  of *in vivo* reconstituted holo-PecA was similar to that for native Z-PecA, obtained from *Anabaena* PCC7120 ( $\epsilon_{568}=96000 \text{ M}^{-1}\text{cm}^{-1}$ ) (Siebzehnriibl, 1990), and higher than for holo-HT-PecA produced *in vitro* by the addition of PCB to a mixture of HT-PecA, PecE, and PecF in 100 mM phosphate buffer at pH 7.0 ( $\epsilon_{567}=77000 \text{ M}^{-1}\text{cm}^{-1}$ ) (Storf et al.,2001). A fluorescence yield  $\Phi_F = 0.22$  of *in vivo* reconstituted holo-PecA was measured.

### 3.1.3 Circular Dichroism Spectroscopy

The CD spectrum of biosynthesized holo-PecA was similar to that of native  $\alpha$ -PEC from *M. lamosus* (Parbel et al.1997; Wiegand et al. 2002), that is, with a strong positive Vis band at 563nm (Parbel: 563nm; Wiegand: 566nm) and a negative near-UV band at 330nm (Parbel: 330nm; Wiegand: 329nm) (Fig.3-4), these signals are typical for  $\alpha$ -PEC in the Z-configuration. The far-UV CD spectrum is typical for  $\alpha$ -helical proteins.

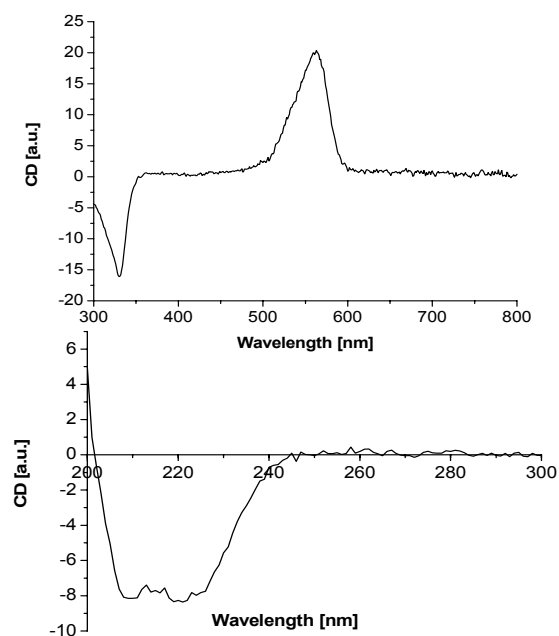


**FIG. 3-4: CD spectroscopy of reconstituted holo-PecA**

Vis- CD (top) and far-UV CD spectrum (bottom) of *Anabaena* PCC7120 holo-PecA reconstituted *in E. coli* purified by immobilized  $\text{Ni}^{2+}$  affinity chromatography.

### 3.1.4 Photoisomerization of $\alpha$ -PEC

Its responsiveness to light of certain wavelengths makes  $\alpha$ -PEC, the youngest member of the phycobilin protein family (Apt et al., 1995), unique among the phycobiliprotein subunits. The isolated PEC  $\alpha$ -subunit is photoreversibly photochromic (Björn, 1979), reminiscent of plant phytochromes, but with sensitivity to orange/green instead of red/far-red irradiation (Kufer and Björn, 1989). Light of appropriate energy content leads to the spectral changes in  $\alpha$ -PEC illustrated below.

After irradiation with 570 nm light, the band at 565 nm decreases and a new absorption band arises at 505 nm. This effect is fully reversible when the sample is irradiated with 500 nm light. Subtraction of the 500 nm spectrum from the 570 nm spectrum gives a difference spectrum with a characteristic shape for a band shift related to the photoisomerization event, as seen in Fig. 3-5 A and B.

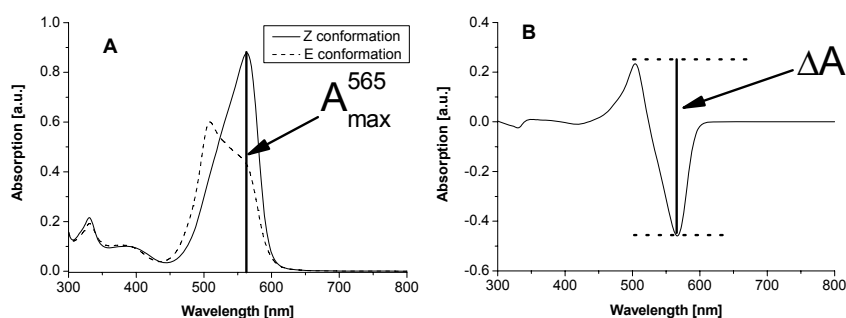


**FIG. 3-5: Photoisomerization of  $\alpha$ -PEC**

A: Absorption spectra of  $\alpha$ -PEC (of *Anabaena* sp. PCC 7120, *in vivo* reconstituted and affinity purified) after irradiation with 500 nm light (solid line) and 570 nm light (dotted line).

B: Difference spectrum (570 *minus* 500 nm) of the same sample with the characteristic maximum at ~500 nm and minimum at ~570 nm

The photoactivity of reconstituted holo-PecA from *Anabaena* PCC7120 ( $\Delta A A = 79\%$ ) is smaller than that of native holo-PecA ( $\Delta A A = 101\%$ ) from *Mastigocladus laminosus* (Zhao et al., 1995). This may be due to slightly different spectra of the two species.

The molecular changes induced by irradiation with 570/500nm light are divers. In the chromophore, it has been assigned to a E/Z-isomerization of the  $\Delta 15,16$  double bond between the C and D pyrrole rings (Zhao et al., 1995; Schmidt et al., 2006; Duerring et al. 1990; see Fig.3-6), in which the E-isomer has a strongly twisted conformation at this position.

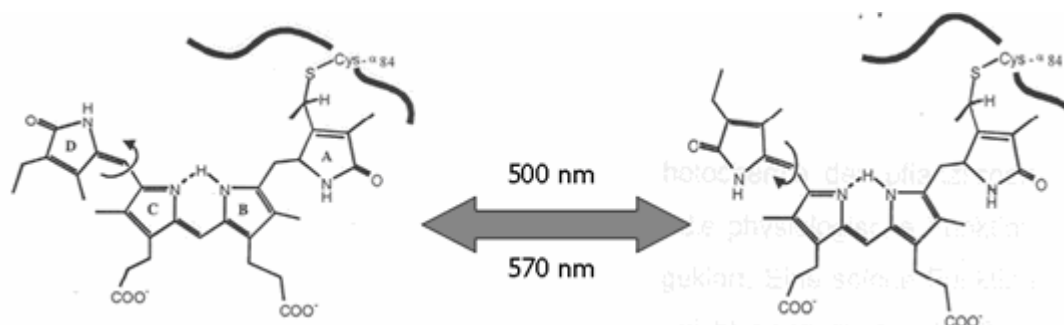


**FIG. 3-6: E-Z isomerization of PVB in the PEC  $\alpha$ -subunit**

left: *E*-constitution of PVB as induced by 570 nm light, right: *Z*-constitution of PVB as induced by 500 nm light

In the dark, either of these states is quite stable. The 500 nm absorbing *E*-form shows little fluorescence, it is higher in energy, but transfer to other biliproteins occurs efficiently only from the fluorescent *Z*-form absorbing at 570 nm (Storf, 2003).

In native  $\alpha$ -PEC, PVB is predominantly present in the 15*Z* configuration, and the SH groups are reduced (Parbel et al., 1997). However, the presence of a distinct shoulder near 565 nm in the *E*-spectrum and of a less defined shoulder near 505 nm in the *Z*-spectrum (compare FIG. 3-5) give evidence that the transformation is incomplete, due to band overlap. This is true for the reconstituted as well as the native sample.

### 3.1.5 HPLC–ESI-MS analysis of chromopeptides from holo-PecA

RP-HPLC separation of trypsin digest (Fig.3-7, top) on a C18 column gave two main colored components. Component 1 ( $t_r=13.3$  min) had an absorption maximum at 592 nm that is typical for a PVB-containing peptide, component 2 ( $t_r=28.4$  min) corresponds to free PCB according to its retention time and the absorption maximum at 686 nm (Fig.3-7). The fraction with retention time 13.3 min was used for MS.

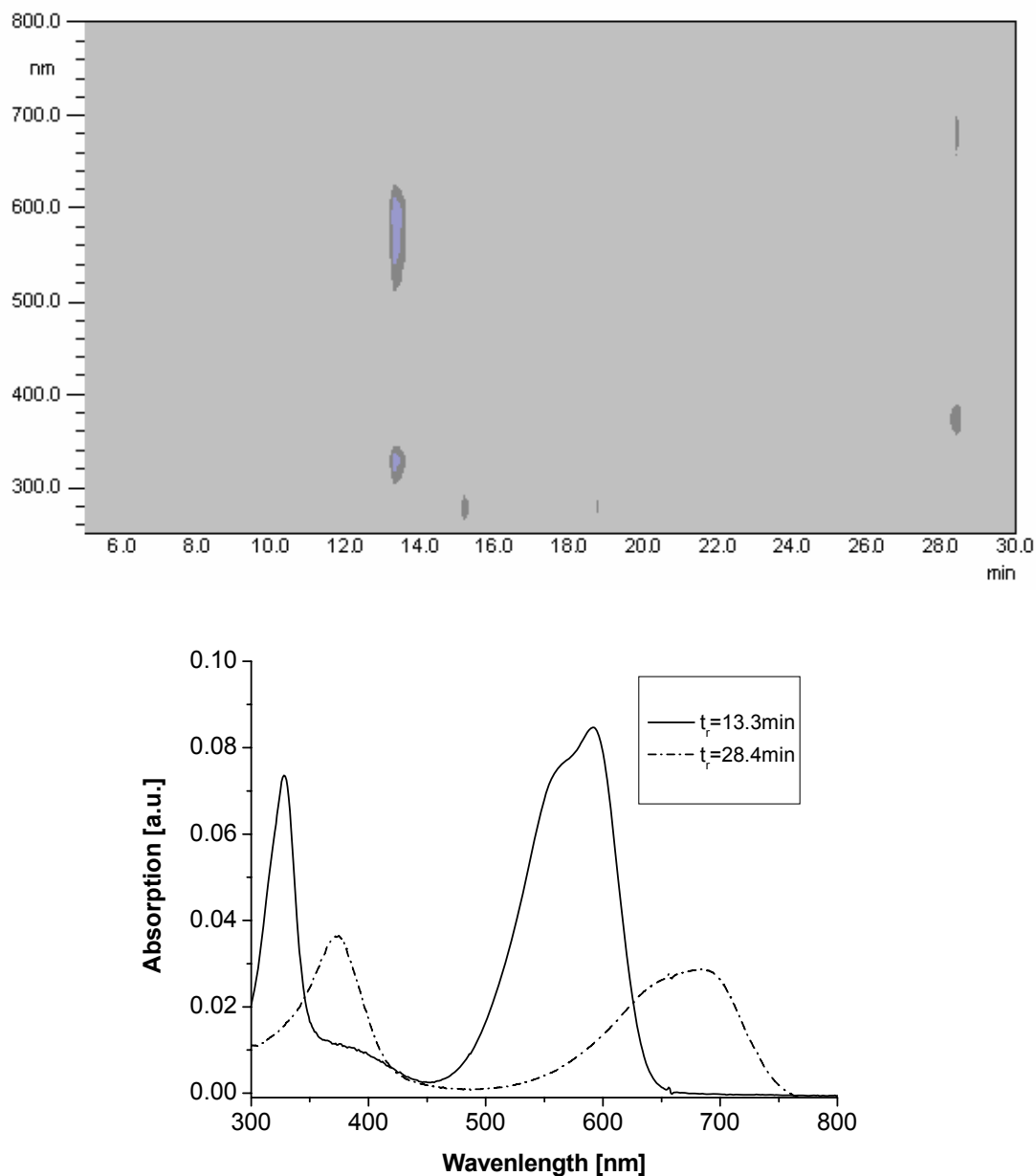


**FIG. 3-7: HPLC and absorption of the chromopeptide obtained from tryptic digestion of the reconstituted holo-PecA.** HPLC was eluted using a gradient (80:20 to 60:40) of formic acid (0.1%, pH 2) and acetonitrile containing 0.1% formic acid.

The sequence of the chromophore-containing peptide was deduced from sequence around the chromophore-binding sites in holo-PecA from *Anabaena* PCC7120. PVB is bound to cysteine residues 84 of the alpha subunit. (<http://www.ncbi.nlm.nih.gov/entrez/viewer.fcgi?db=protein&id=17129869>). There is excellent agreement between the measured peptide  $M_r$  values and peptide  $M_r$  values calculated from sequences of alpha subunits of holo-PEC from *Anabaena* PCC7120 (Table 3-1). Sequences of these peptides could be found when MS-MS capabilities of the instrument are

employed. That will make this method comparable in performance to amino acid sequencing of chromophore-containing peptides (Klotz and Glazer, 1985). The chromopeptide sequence C(PCB)VR confirms covalent chromophore binding to Cys-84 of the holo-PecA apo-protein.

**. Table 3-1 Mass of chromopeptide(component 1) from tryptic digestion of holo-PecA**

chromopeptides	Chromopeptide sequence		Peptide mass	
			Calc.	Expt.
PecA-PVB	C(PVB)VR	$[M+2H]^{2+}$	481.38	481.34

In the case of pepsin digestion, separations were equally efficient (Fig.3-8). Trypsin cuts amino-acid chains on the C terminus of lysine and arginine. Pepsin is relatively non-specific but preferentially cleaves the peptide bonds of hydrophobic amino acids. Triply charged ions found on peptides from trypsin digest originate from positive charges on the N terminus of the peptide, the N terminus of arginine, and the positively charged chromophore. Doubly charged ions from pepsin digest originate from the positively charged peptide N terminus and the positively charged chromophore (Isailovic et al. 2004). However, mass spectroscopy of tryptic chromopeptides was consistently better than that of peptic chromopeptides, therefore always tryptic digests were used for MS. By contrast, NMR spectra turned out to be consistently more reliable and cleaner with peptic peptides, possibly because the chromophore is more stable under acidic than at neutral conditions. So I choose tryptic chromopeptides to measure MS and peptic chromopeptides to measure NMR.

### 3.1.6 NMR analysis of peptic chromopeptides from holo-PecA

RP-HPLC separation of pepsin digest (Fig.3-8) was achieved on a C18 column. Chromopeptides having retention times of 3.0 and 6.6 min show absorption maxima 589 nm and 591nm, respectively (inset of Fig.3-8), and correspond to PVB-containing peptides. The fraction with retention time 3.0 min was used for NMR spectroscopy.

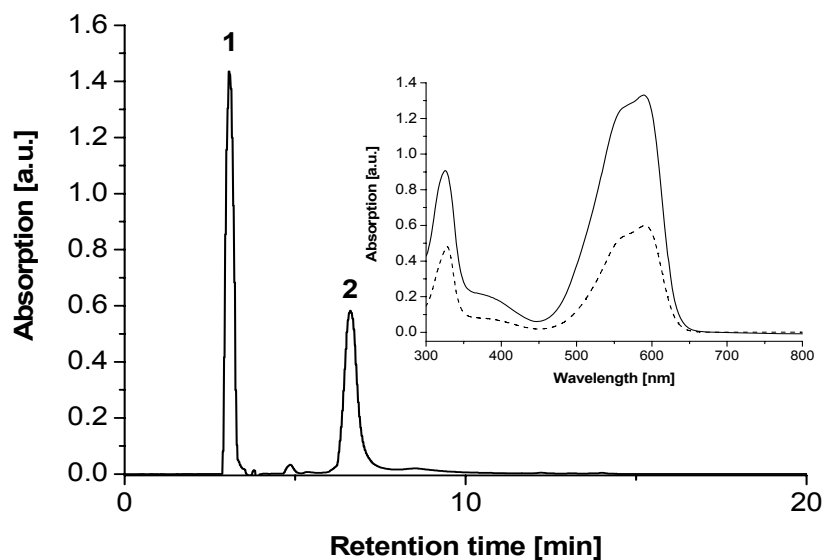


**FIG. 3-8: HPLC ( $\lambda_{\text{detect}}=590\text{nm}$ ) and absorption spectra (insert) of the chromopeptides obtained from peptic digestion of the reconstituted holo-PecA.** HPLC conditions as in Fig. 3-7. Absorption spectra of peak 1 (solid line,  $\lambda_{\text{max}}=589\text{ nm}$ ) and of the peak 2 (dashed line  $\lambda_{\text{max}}=591\text{ nm}$ ).

The  $^1\text{H}$  NMR spectra of chromopeptide ( $t_r=3.0$ ) from holo-PecA of *Anabaena* PCC 7120, *in vivo* reconstituted and pepsin digested, were measured. All assignments are made by using the A-ring linkage numbering scheme (see Fig 3-1) and are given in Table 3-2. The full 1-D  $^1\text{H}$  NMR spectrum is shown in Fig. 3-9.

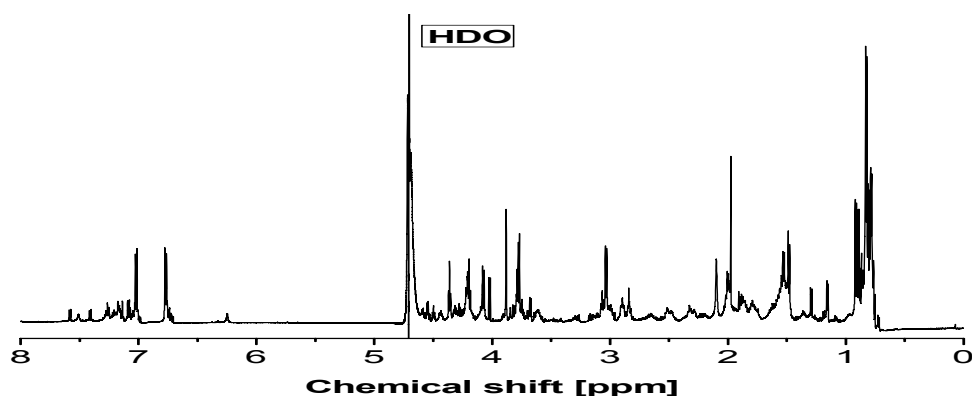


**FIG. 3-9: 1-D  $^1\text{H}$ -NMR spectrum of PecA chromopeptide in 10 mM TFA/ $\text{D}_2\text{O}$  at 25°C**

**Table 3-2:  $^1\text{H}$  NMR(600-MHz) Assignments for peptide SKC(PVB)VR of reconstituted PecA-PVB (10mM TFA/D<sub>2</sub>O)**

Chemical shift	Multiplicity (J <sub>H-H</sub> , [Hz])	Number of H's	Assignment
7.51	s	1	10-H
6.25	s	1	15-H
4.55	dd (5.94,6.79)	1	4-H
4.07	m	1	3'-H
3.67	d (5.66)	1	5-H
3.03	d (7.00)	4	8,12-CH <sub>2</sub> CH <sub>2</sub> COOH
2.84	m	4	8,12-CH <sub>2</sub> CH <sub>2</sub> COOH
2.48	m	1	5-H
2.32	m	2	18- CH <sub>2</sub> CH <sub>3</sub>
2.09	s	12	2,7,13,17-CH <sub>3</sub>
2.00	s		
1.98	s		
1.29	d ( 6.98)	3	3'- CH <sub>3</sub>
0.91	m	3	18- CH <sub>2</sub> CH <sub>3</sub>
4.49	m	1	Cys $\alpha$ - CH
3.07	m	2	Cys $\beta$ - CH <sub>2</sub>
4.19	d ( 6.96)	1	Val $\alpha$ - CH
1.90	m	1	Val $\beta$ - CH
0.83	d ( 6.41)	6	Val $\gamma$ - CH <sub>3</sub>
4.21	d ( 9.05)	1	Arg $\alpha$ - CH
1.53	m	4	Arg $\beta,\gamma$ - CH <sub>2</sub>
2.90	m	2	Arg $\delta$ - CH <sub>2</sub>
4.41	m	1	Ser $\alpha$ - CH
3.78	m	2	Ser $\beta$ - CH <sub>2</sub>
4.36	t (5.57)	1	Lys $\alpha$ - CH
1.48	d (7.13)	4	Lys $\beta,\gamma$ - CH <sub>2</sub>

Analyzing the downfield region of the spectrum, one observes the two vinylic 10-H and 15-H resonances at 7.51 and 6.25 ppm, respectively. These peaks correspond well to the 10-H and 15-H singlets previously observed in A-ring-linked peptide  $\alpha$ -1 PXB from *M. laminosus* (Bishop et al., 1987). Noticeably absent, however, is a downfield vinylic resonance corresponding to 5-H. The  $\beta$ -1 PCB chromopeptide of C-phycoyanin exhibits this proton as a singlet at 5.94 ppm (Lagarias et al., 1979). PVB lacks the methine bridge between rings A and B, therefore, shows no such resonance, the lack of the respective signal is taken as proof of saturation between the A and B rings. Because the mass spectral data prove the isomeric relationships of PVB and PCB, this double bond must exist elsewhere on the PVB-tetrapyrrole moiety.

Previous studies showed that the PEB and PUB chromophores have an exocyclic vinyl group attached at C-18 (Klotz et al., 1985; Nagy et al., 1985), typically manifested as a downfield pattern in the  $^1\text{H}$  NMR spectrum. No such group is observed in the spectrum of PVB. The only alternative position for this unsaturation is between C-2 and C-3, which is corroborated by the  $^1\text{H}$  NMR spectrum. Although only 3 vinylic methyl singlets are seen between 1.98 and 2.09 ppm, integration establishes a total of 12 protons; therefore, 4 vinylic methyl groups (C-2, C-7, C-13, and C-17) are actually present, thereby proving the presence of a double bond between C-2 and C-3.

The broad doublet of doublets at 4.55 ppm is assigned to 4-H, and coupling with the two nonequivalent 5-H protons at 3.67 and 2.48 ppm is obvious. The doublet at 1.29 ppm is assigned to  $3^1\text{-CH}_3$  and a multiplet at 4.07 ppm is assigned  $3^1\text{-H}$ . The resonances from the propionyl side chains are found at 3.03 and 2.84 ppm. The ethyl group is seen as two multiplet at 2.32 ppm (18-  $\text{CH}_2\text{CH}_3$ ) and 0.91 ppm (18- $\text{CH}_2\text{CH}_3$ ). All PVB NMR resonances are therefore similar to those in the chromopeptide of  $\alpha$ -1 PXB from *M. laminosus* (Bishop et al., 1987), the chromophore has since been renamed PVB.

At the same, the resonances from the amino acids Ser, Lys, Cys, Val, Arg are found in the NMR spectrum. Sequences of chromophore-containing peptides were deduced from sequences around the chromophore-binding sites in holo-PecA from *Anabaena* PCC7120. The chromopeptide is SKC(PVB)VR.

### 3.1.7 Discussion

The studies described here documented successful reconstitution of the predicted pathway for the biosynthesis of the phycoerythrocyanin holo- $\alpha$ -subunit (Fig.3-1) in *E. coli*. The results of experiments also support the conclusions reached by Tooley et al.(2002, *in vivo*), Zhao et al. (2000, *in vitro*) and Storf et al. (2001, *in vitro*) that the heterodimeric lyase/isomerase (PecE/PecF) catalyzes both the covalent attachment of PCB and the concurrent isomerization of the molecule to PVB.

Jung et al. (1995) established that in *Anabaena* PCC7120 interposon mutagenesis of *pecE*, *pecF*, or *pecE* and *pecF* eliminates the formation of holo-PecA. They showed

that ~30% of the wild-type level of PecB was present in the phycobilisomes of all these mutants. In contrast, holo-PecA was barely detectable in the *pecE* and *pecF* mutants, but it was present in a modified form in the *pecEF* deletion mutant in a 1:1 ratio with the PecB. Instead of PVB, the chromoprotein contained PCB, as identified by isolation of the subunit and amino-terminal sequencing.

PecA forms a complex with both lyase subunits, PecE and PecF (in section 3.1.2). The identities of all three components in the holo-HT-PecA–PecE–PecF ternary complexes were established unambiguously by protein and tryptic peptide analyses performed by matrix-assisted laser desorption ionization–time of flight mass spectrometry (Tooley et al. 2002). Probably, complex formation of in the single subunit mutants with the respective complementary subunit prevents addition of PCB, possibly by another lyase. This inhibition would be relieved in the double mutant. PecA and PecE form a weak complex that is stabilized by PCB. It has been suggested that the first reaction step involves a conformational change and/or protonation of PCB, and that PecE has a chaperone-like function on the chromoprotein (Boehm et al. 2007).

Zhao et al. (2002) studied the cofactor requirements and enzyme kinetics of the novel, dual-action enzyme, the isomerizing phycoviolobilin phycoerythrocyanin- $\alpha$ 84-cystein-lyase (PVB-PEC-lyase) from *M. laminosus*, which catalyses both the covalent attachment of phycocyanobilin to PecA, the apo- $\alpha$ -subunit of phycoerythrocyanin, and its isomerization to phycoviolobilin. Mercaptoethanol and the divalent metals,  $Mg^{2+}$  or  $Mn^{2+}$ , were required, and the reaction was aided by the detergent, Triton X-100. Phosphate buffer inhibits precipitation of the proteins present in the reconstitution mixture, but at the same time binds the required metal. Kinetic constants were obtained for both substrates, the chromophore ( $K_m = 12\text{--}16 \mu\text{M}$ , depending on [PecA],  $k_{cat} = 1.2 \cdot 10^{-4} \text{ s}^{-1}$ ) and the apoprotein ( $K_m = 2.4 \mu\text{M}$  at  $14 \mu\text{M}$  PCB,  $k_{cat} = 0.8 \cdot 10^{-4} \text{ s}^{-1}$ ).

A multi-plasmid system was established for reconstitution of holo-PecA in *E. coli*. HPLC, FPLC, affinity chromatography and SDS–PAGE separations followed by absorbance, fluorescence, circular dichroism, MS and NMR detections were used for spectroscopic and structural characterization of reconstitution product or the chromopeptides obtained from enzymatic digestion. This also established a methodology to analyze of other phycobiliproteins and fluorescent proteins in general.

After cloning of apophycobiliprotein genes, phycobilin biosynthesis genes and lyase genes from several cyanobacteria, various phycobiliproteins could be biosynthesized in the heterologous *E. coli* system using dual plasmids containing their respective genes. BL21(DE3) cells could be transformed to express up to eight proteins in the desired combination. This heterologous system in *E. coli* is more advantageous than reconstitution *in vitro* in the following two respects: (1) On reconstitution *in vitro*, where the respective genes were first overproduced in *E. coli*, and then reconstituted *in vitro*, both some lyases and some apoproteins were difficult to dissolve and refold, so reconstitution yields *in vitro* were often low and poorly reproducible. An example is the phycoerythrin reconstitution: apo-phycoerythrin is insoluble when expressed in *E. coli*, and phycoerythrin biosynthesis is therefore very difficult to study *in vitro*. Using the heterologous system in *E. coli*, both  $\alpha$ - and  $\beta$ -phycoerythrin could be correctly chromophorylated with PEB at C84 sites (consensus sequence) (Zhao et al., 2007a). (2) *In vitro* reconstitution is complicated by the fact that most apo-phycobiliproteins bind phycobilins spontaneously, but with low fidelity and often with low yield. This results in unwanted products and mixtures that are difficult to analyze and handle, and complicate enzymatic studies. By using the heterologous system in *E. coli*, the spontaneous phycobilin binding is generally inhibited, and properly chromophorylated subunits of phycoerythrocyanin, phycocyanin and allophycocyanin were successfully prepared by this way (Zhao et al., 2006, 2007a, 2007b)

In extending this methodology to other system, the expression in prokaryotic or eukaryotic cells of an appropriate selection of genes encoding enzymes and apophycobiliprotein subunit-containing fusion proteins could lead to the intracellular production of constructs carrying specific bilins at unique locations, with broad utility in addressing a variety of questions in cell biology.

The ability to express in heterologous hosts phycobiliprotein subunits with distinctive spectroscopic properties, such as holo-PecA ( $\lambda_{\text{max}}^{\text{abs}} = 561 \text{ nm}$  and a  $\lambda_{\text{max}}^{\text{F}} = 582 \text{ nm}$ ), provides the good potential for use as fluorescence probes in single-molecule detection and single-cell analysis.

## 3.2 Structure analysis of reconstituted holo-CpcA

### 3.2.1 Reconstitution principle of holo-CpcA

PCB is biosynthesized from heme by the action of two enzymes, heme oxygenase and a BV-reductase. Using endogenous heme as substrate, Tooley et al. (2001) introduced five genes into *E. coli* to produce holo-HT-CpcA from *Synechocystis* PCC6803 with absorption and fluorescence properties characteristic of the native holo subunit. Besides the genes for the apoprotein (*cpcA*) and the lyase (*cpcE/F*), these included the two respective genes for PCB synthesis, viz. *ho1* and *pcyA*, from the same organism (Fig. 3-10).

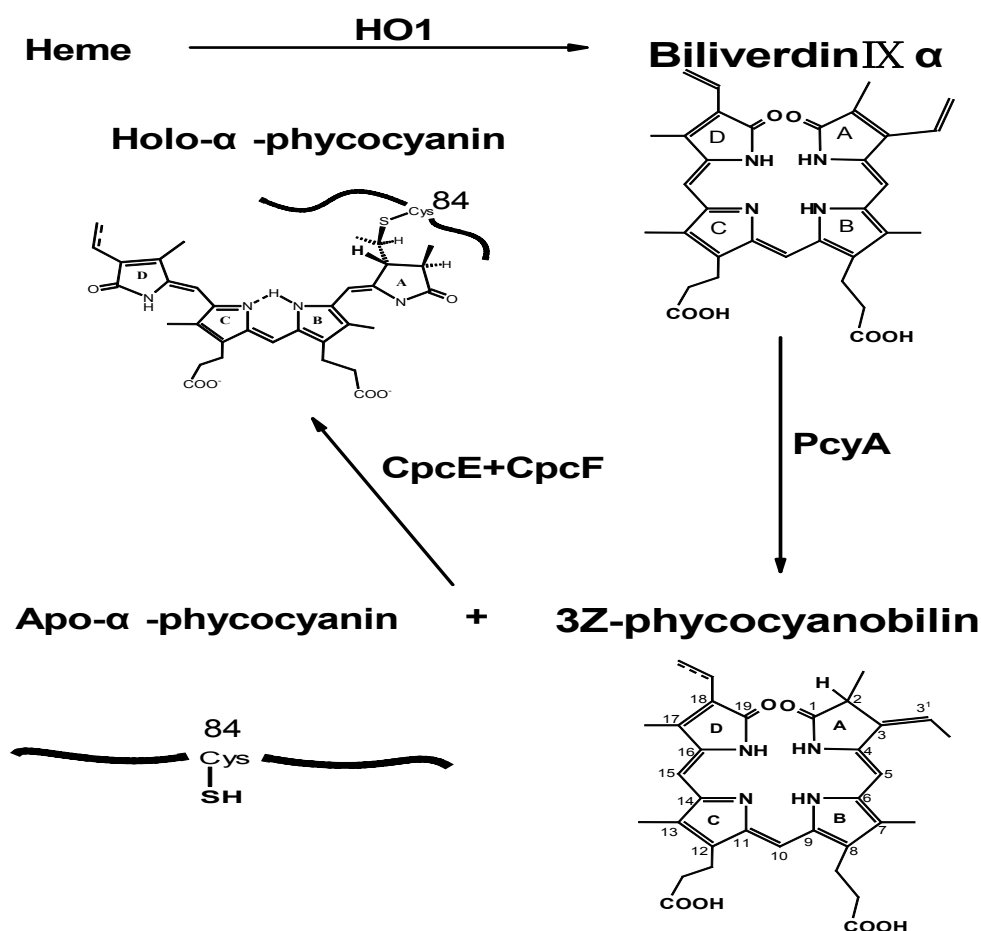


**Fig. 3-10: Minimal biosynthetic pathway for the production of phycocyanobilin from heme and its addition to the C-phycocyanin apo- $\alpha$ - subunit, CpcA.**

### 3.2.2 Expression and Purification of the holo-CpcA

A similar pathway was established for CpcA from *M. lamosus* and *Anabaena* PCC7120. Expressing pCOLADuet-*cpcE-cpcF*, pACYCDuet-*ho1-pcyA* and pETDuet-*cpcA* plasmids in strain *E. coli* BL21(DE3), upon induction with IPTG, the culture acquired a pronounced blue tint. The His-tagged – holoprotein (holo-HT-CpcA) was purified by immobilized Ni<sup>2+</sup> affinity chromatography, and its spectroscopic properties were determined after dialysis against 50 mM K-phosphate (pH 7.0). The absorbance spectrum of holo-HT-CpcA had a  $\lambda_{\max}$  = 618 nm and a ratio of  $Q_{\text{Vis/UV}} = A_{618} \text{ nm}/A_{367} \text{ nm}$  of 5.41 (Fig. 3-11). The corresponding values for *Synechococcus* PCC7002 holo-CpcA are 620 nm and 4.22 (Fairchild and Glazer, 1994), for *Synechocystis* PCC6803 holo-HT-CpcA are 625 nm and 4.14 (Tooley et al., 2001) or 623 nm and 6.41 (Guan et al., 2007). The absorbance properties of native holo-CpcA preparations from other cyanobacteria are similar (Sidler, 1994). The differences are due to the different species, and to a large extent also to the different measurement conditions. In particular  $Q_{\text{Vis/UV}}$  depends on pH and ionic strength (Kupka et al., 2008), compare e.g. the two values for the holoprotein from *Synechocystis* PCC6803. For external comparison, other methods are therefore required. It should be mentioned that the value of  $Q_{\text{Vis/UV}} = 5.41$  is in the upper range and indicates complete chromophorylation of CpcA. The fluorescence emission maximum of the holo-HT-CpcA produced in *E. coli* was at  $\lambda_{\max} = 639$  nm (Fig. 3-11), as compared with 642 nm for *Synechococcus* PCC7002 holo-CpcA (Nakamura et al., 1998), 641 nm (Tooley et al., 2001) or 648 nm (Guan et al., 2007) for *Synechocystis* PCC6803 holo-HT-CpcA. The variations are again due to species and experimental differences.

Extinction coefficient  $\epsilon$  and fluorescence yield  $\Phi_F$  of reconstituted holo-CpcA have been determined by the methods given in section 2.2.4.3 and 2.2.4.4. The values for *in vivo* reconstituted holo-HT-CpcA ( $\epsilon_{618} = 1.35(\pm 0.01) \times 10^5 \text{ M}^{-1}\text{cm}^{-1}$  and  $\Phi_F = 0.22$ ) were similar to those of reconstituted holo-HT-CpcA in *E. coli* from *Synechocystis* PCC6803 ( $\epsilon_M = 127600 \text{ M}^{-1}\text{cm}^{-1}$ ,  $\Phi_F = 0.31$ ) (Tooley et al., 2001), but more different from those of native holo-CpcA from *M. lamosus* ( $\epsilon_{618} = 1.08 \times 10^5 \text{ M}^{-1}\text{cm}^{-1}$ ,  $\Phi_F = 0.65$ ) (Mimuro et al., 1986). These differences may relate to the different condition used in the measurements, they may furthermore also be influenced by the His-tag present in the reconstituted chromoprotein, and by the presence of the residual Ni<sup>++</sup>. Heavy

atoms are known to complex with bile pigments like PCB (Falk, 1989) and quench their fluorescence. A more detailed characterization of the reconstitution products was therefore desirable.

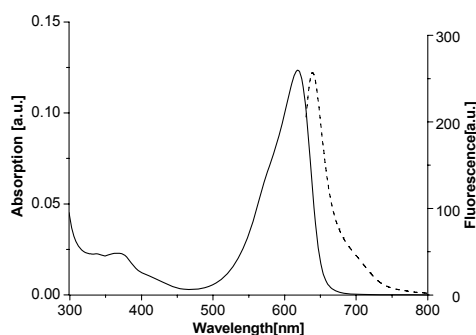


**FIG. 3-11: Spectroscopic properties of *Anabaena* PCC7120 holo-CpcA expressed and assembled in *E. coli*.** Absorption (solid) ( $\lambda_{\text{max}}=618$  nm) and fluorescence emission spectra (dashed) ( $\lambda_{\text{max}}=639$  nm) of the chromoprotein purified by affinity chromatography.

Analysis of Coomassie brilliant blue-stained gels after SDS-PAGE of the purified protein showed only one distinct band of 19.5 kDa (Fig.3-12, lane A) corresponding to the calculated molecular mass of holo-HT-CpcA (19.5 kDa). Covalent binding of the chromophore was confirmed upon exposure to  $\text{Zn}^{2+}$  and UV illumination, which results in an orange fluorescence (Fig.3-12, lane a).

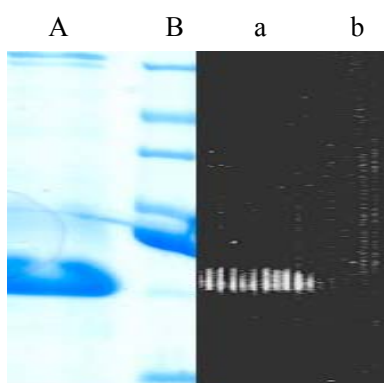


**FIG. 3-12: SDS-PAGE analysis of *Anabaena* PCC7120 HT-CpcA expressed and assembled in *E. coli*, and purified by affinity chromatography.** Proteins were visualized by Coomassie brilliant blue staining (left panel) and by the UV excited fluorescence of bilin-bearing polypeptides in the presence of  $\text{Zn}^{2+}$  (right panel). Lanes A;a, HT-CpcA expressed and assembled in *E. coli* strain; lanes B;b, molecular mass standards (from the top, 45, 36, 29, 24, 20 and 14 kDa).

### 3.2.3 Circular Dichroism Spectroscopy

The biosynthesized holo-CpcA CD spectrum was similar to that of the native  $\alpha$  subunit of C-phycoerythrin of *M. lamosus* (Mimuro et al., 1986), it shows a strong positive Vis band at 618 nm (Mimuro:618 nm) and a negative near-UV band at 342 nm (Mimuro: about 342 nm) (Fig. 3-13). The far-UV CD spectra are typical for  $\alpha$ -helical proteins. This confirms native conformations of both the chromophore and the protein.

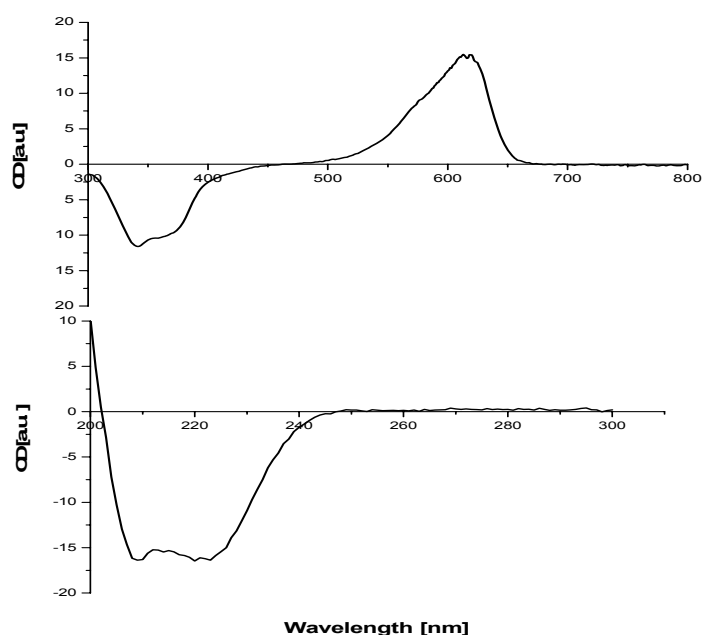


**FIG. 3-13: CD spectra of reconstituted holo-CpcA**

Vis- CD (top) and far-UV CD spectra (bottom) of *Anabaena* PCC7120 holo-CpcA reconstituted and assembled *in E. coli* and purified by immobilized  $\text{Ni}^{2+}$  affinity chromatography.

### 3.2.4 HPLC–ESI-MS analysis of chromopeptides from holo-CpcA

RP-HPLC separation of the tryptic digest (Fig. 3-14) on a C18 column gave two main colored peaks. Peak 1 ( $t_r=16.4$  min) had an absorption maximum at 637 nm that is typical for PCB-containing peptides. Peak 2 ( $t_r= 29.1$  min) corresponds to free PCB according to its retention time and the absorption maximum at 684 nm.

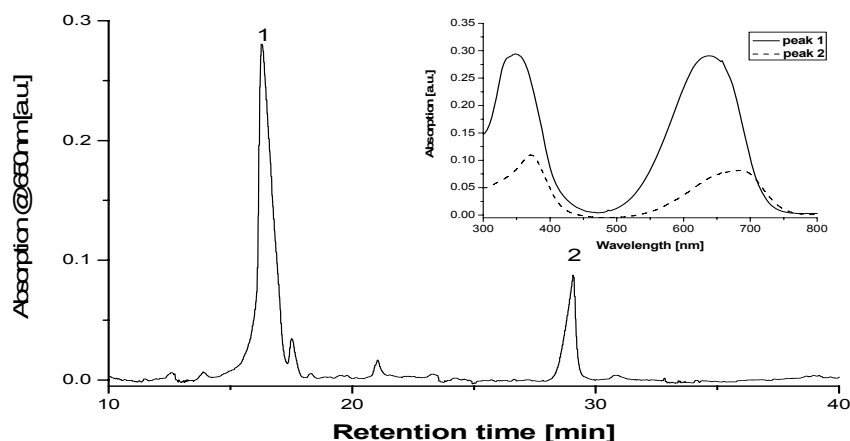


**FIG. 3-14: HPLC and in situ absorption spectra of the tryptic digest of reconstituted holo-PecA.** C18-column, gradient (80:20 to 60:40) of aqueous formic acid (0.1%, pH 2) and acetonitrile containing 0.1% formic acid.

The molecular weight of the PCB containing peptide ( $t_r=16.4$  min) was determined by ESI mass spectrometry. Sequences of chromophore-containing peptides were deduced from sequences around the chromophore-binding sites in holo-CpcA from *Anabaena* PCC7120. In the native  $\alpha$ -subunit of C-phycoerythrin, PCB is bound to cysteine residues 84 of the alpha subunit. There is excellent agreement between the measured peptide  $M_r$  and the values calculated from sequences of alpha subunits of holo-CPC from *Anabaena* PCC7120 (Table 3-3, Fig 3-15), which proves correct binding to the correct site in the *E. coli* system. The major peaks at 468 and 935 m/z represent doubly and singly charge chromopeptide C(PCB)AR respectively. The chromopeptide sequence C(PCB)AR confirms chromophore covalent binding to Cys-84 of the apo-protein. Peak of 587 m/z corresponds to the free chromophore that is partially lost during MS.

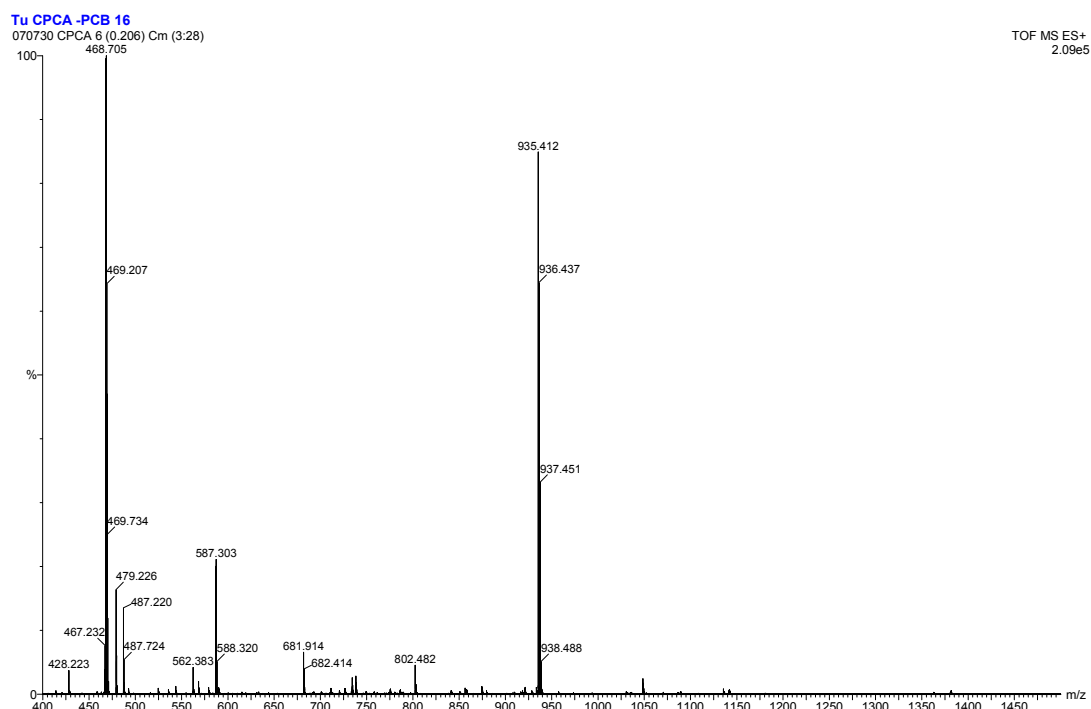


**FIG. 3-15: Negative ion mass spectrum by ESI-MS of chromopeptide from reconstituted holo-CpcA.** The main peaks 468 m/z and 935m/z represent the doubly and singly charged chromopeptide C(PCB)AR, respectively.

**Table 3-3 Major mass peaks of chromopeptide from tryptic digestion of holo-CpcA**

Chromopeptide sequence		Peptide mass	
		Calc.	Expt.
C(PCB)AR	$[M+2H]^{2+}$	467.86	468.18
C(PCB)AR	$[M+2H]^+$	935.71	935.41
PCB	$[M+2H]^+$	587.29	587.30

### 3.2.5 NMR analysis of peptic chromopeptides from holo-CpcA

For NMR spectroscopy, again peptic chromopeptides were used. RP-HPLC separation of pepsin digest (Fig. 3-16) was achieved on a C18 column. Peptides having retention times at 5.4 and 6.2 min show absorption maxima at 639 nm and 638nm respectively (inset of Fig.3-16) that are typical for PCB-containing peptides. Samples of the 5.4 min fraction were used for NMR spectroscopy.

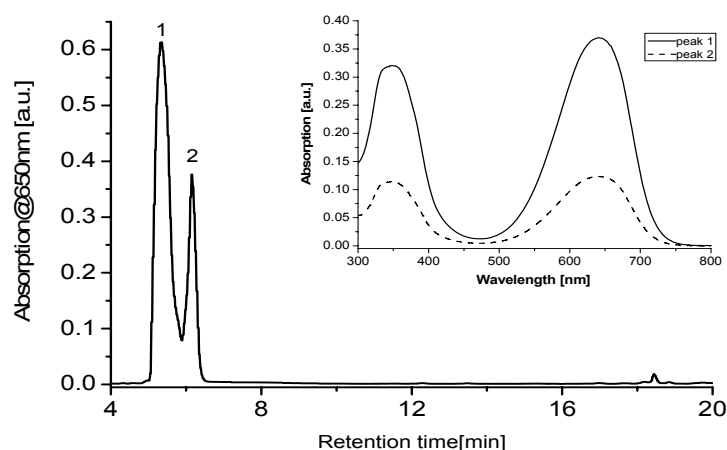


**FIG. 3-16:** HPLC ( $\lambda_{\text{detect}}=650$  nm) and absorption of the chromopeptides obtained from peptic digestion of reconstituted holo-CpcA. HPLC conditions as in Fig. 3-14. Absorption spectra of peak 1 (solid line,  $\lambda_{\text{max}}=639$  nm) and of the peak 2 (dashed line  $\lambda_{\text{max}}=638$  nm)

The  $^1\text{H-NMR}$  spectrum of this chromopeptide is shown in Fig.3-17. All assignments refer to the A-ring linkage numbering scheme (see Fig 3-10) and are summarized in Table 3-4.

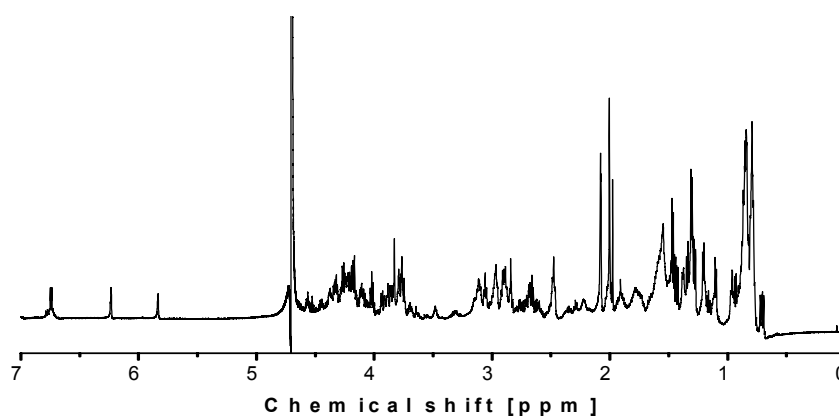


**FIG. 3-17:** 1-D  $^1\text{H-NMR}$  spectra of chromopeptide SKC(PCB)AR from reconstituted holo-CpcA in 10 mM TFA/ $\text{D}_2\text{O}$

The NMR-spectrum results from a combination of the chromophore and peptide signals. In the downfield region of the spectrum, there are three vinylic 10-H, 15-H and 5-H resonances at 7.42, 6.23 and 5.84 ppm, respectively, these peaks are

characteristic for the A-ring-linked  $\alpha$ -1 PCB chromophore (Bishop et al., 1986). The  $3^1$ -H multiplet at 3.48 ppm is downfield shifted due to its proximity to the sulfur atom, confirming the attachment at this site. The  $3^1$ -H is coupled to the  $3^2$ -CH<sub>3</sub> group, yielding a doublet at 1.27 ppm. Similarly the 2-CH<sub>3</sub> signal (1.10 ppm) is coupled to the 2-H proton (2.66 ppm). The 3-H proton (multiplet at 3.06) is coupled to both the 2-H and  $3^1$ -H. All these signals are again characteristic of a PCB bound to cysteine at C-3<sup>1</sup>.

**Table 3-4: <sup>1</sup>H NMR(600-MHz) assignments for peptide SKC(PCB)AR of reconstituted CpcA-PCB ( 10 mM TFA/D<sub>2</sub>O)**

Chemical shift	Multiplicity (J <sub>H-H</sub> ,[Hz])	Number of H's	Assignment
7.42	s	1	10-H
6.23	s	1	15-H
5.84	s	1	5-H
3.47	m	1	3 <sup>1</sup> -H
3.06	m	1	3-H
2.84	m	4	8,12-CH <sub>2</sub> CH <sub>2</sub> COOH
2.66	d (6.50)	1	2-H
2.48	m	4	8,12-CH <sub>2</sub> CH <sub>2</sub> COOH
2.08	s	9	7,13,17-CH <sub>3</sub>
2.00	s		
1.98	s		
1.93	m	2	18-CH <sub>2</sub> CH <sub>3</sub>
1.27	d (7.11)	3	3 <sup>2</sup> -CH <sub>3</sub>
1.10	d (6.41)	3	2-CH <sub>3</sub>
0.96	m	3	18-CH <sub>2</sub> CH <sub>3</sub>
4.33	m	1	Cys $\alpha$ -CH
2.89	m	2	Cys $\beta$ -CH <sub>2</sub>
4.45	dd (6.63, 14.06)	1	Ala $\alpha$ -CH
1.21	d (7.12)	3	Ala $\beta$ -CH <sub>3</sub>
4.26	dd (6.46, 13.65)	1	Arg $\alpha$ -CH
1.47	d (4.65)	2	Arg $\beta$ -CH <sub>2</sub>
3.11	m	2	Arg $\gamma$ -CH <sub>2</sub>
2.97	m	2	Arg $\delta$ -CH <sub>2</sub>
4.52	t	1	Lys $\alpha$ -CH
1.31	d (7.19)	4	Lys $\beta,\delta$ -CH <sub>2</sub>
1.35	d (7.11)	2	Lys $\gamma$ -CH <sub>2</sub>
4.56	m	1	Ser $\alpha$ -CH
3.79	m	2	Ser $\beta$ -CH <sub>2</sub>

The resonances attributed to the aromatic methyls at C-7, -13, and -17, the ethyl group at C-18, and the propionic acid methylenes at C-8 and -12 are salient features of the spectra of bile pigments. The three aromatic methyls at C-7, -13, and -17 singlets resonate at 2.08, 2.00 and 1.98 ppm. The ethyl group at C-18 is seen as two multiplets at 1.93 ppm (18-CH<sub>2</sub>CH<sub>3</sub>) and 0.96 ppm (18-CH<sub>2</sub>CH<sub>3</sub>). The multiplet resonances from methylene group of the propionic acid side chains at C-8 and C-12 were found at 2.84 and 2.48 ppm. These results correspond well with the A-ring-linked  $\alpha$ -1 PCB from *Synechococcus* PCC6801 C-PC (Bishop et al., 1986)

In addition to the chromophore signals, resonances from the following amino acid Ser, Lys, Cys, Ala, Arg are found in the NMR spectrum. Sequence SKC(PCB)AR was deduced from sequences around the chromophore-binding sites in holo-CpcA from *Anabaena* sp. strain PCC7120.

### 3.2.6 Discussion

The studies described here documented successful reconstitution of the predicted pathway for the biosynthesis of the phycocyanin holo- $\alpha$  subunit (Fig.3-10) in *E. coli*. The results of the experiments support and extend the conclusion reached by Tooley et al. (2001, *in vivo*), Guan et al. (2007, *in vivo*), Zhao et al. (2006, *in vitro*) and Fairchild et al. (1992, *in vitro*) that the heterodimeric lyase/isomerase (CpcE/CpcF) catalyzes the covalent attachment of PCB. They unambiguously identify the correct binding site. The lack of split NMR signals, which is particularly clear in the low-field region, establishes that no isomers are formed in the process, and the coincidence with chromophore signals of a PCB peptide from holo-CpcA of *Synechocystis* PCC6803 also verify the correct stereochemistry of the product.

SDS-PAGE gel (Fig. 3-12) showed that there is a single band (holo-HT-CpcA) at 19.5 kDa, while Tooley's work yielded two separate bands for holo and apo-HT-CpcA (Tooley et al., 2001), probably due to incomplete chromophore attachment. Complete chromophorylation in the current reconstitution is also supported by the Q<sub>A</sub> value.

The evidence that CpcE and CpcF are needed for the correct addition of PCB to apo-CpcA, *in vivo* in various cyanobacteria (Zhou et al., 1992; Swanson et al., 1992; Cai et al., 1997; Tooley et al., 2001) as well as *in vitro* (Fairchild et al., 1992,

Zhao et al., 2006), is very strong. *In vitro*, nonenzymic addition of PCB to CpcA leads to the formation of product mixtures containing an unnatural, oxidized adduct, mesobiliverdin-CpcA, with distinctive spectroscopic properties (Arciero et al., 1988); however, normal holo-CpcA is produced in the presence of CpcE and CpcF (Fairchild et al., 1992). *In vivo* nonenzymic addition of PCB to CpcA leads to the formation of very little of the natural product (0.2%) (Chen, 2006).

*In vitro*, CpcE and CpcF overproduced in *E. coli* catalyze the attachment of PCB to the  $\alpha$  subunit of apophycocyanin at the appropriate site,  $\alpha$ -Cys-84, to form the correct adduct. CpcE and CpcF also efficiently catalyze the reverse reaction, in which the bilin from holo- $\alpha$  subunit is transferred either to the apo- $\alpha$  subunit of the same CPC or to the apo- $\alpha$  subunit of a heterologous CPC. The forward and reverse reactions each require both CpcE and CpcF and are specific for the  $\alpha$ -Cys-84 position (Fairchild et al., 1992).

CpcE and CpcF form an enzymatically active 1:1 complex (CpcEF), stable to size exclusion chromatography. CpcEF causes a reduction in  $\alpha$ -PC fluorescence and strongly affects its absorption spectrum but has no effect on the  $\beta$  subunit. CpcEF also catalyzes the addition of PEB to apo-alpha PC; PEB is thought to be on the biosynthetic pathway of PCB. CpcEF shows a preference for PCB relative to PEB, both in binding affinity and in the rate of catalysis, sufficient to account for selective attachment of PCB to apo- $\alpha$  C-PC (Fairchild and Glazer 1994).

The CpcE/F bound PCB could be transferred to CpcA to yield holo-CpcA. The PCB transfer capacity correlates with the activity of the lyase, indicating that PCB bound to CpcE/F is an intermediate of the enzymatic reaction. A catalytic mechanism has been proposed, in which a CpcE/F complex binds PCB and adjusts via a salt bridge the conformation of PCB, which is then transferred to CpcA (Zhao et al., 2006b). In summary, these results show that in *E. coli* the presence of CpcE and CpcF is necessary and sufficient to correctly chromophorylate CpcA with PCB, and that autocatalytic or spontaneous chromophylation is negligible. The latter is in contrast to reconstitution *in vitro*.

### 3.3 Structure analysis of reconstituted subunits of allophycocyanin

#### 3.3.1 Reconstitution principle of subunits of allophycocyanin

Phycocyanobilin(PCB) is biosynthesized from heme by the action of two enzymes, heme oxygenase and BV-reductase. PCB is then attached to the apoprotein of allophycocyanin by a lyase, CpcS (alr0617) (Zhao et al. 2007). Using endogenous heme as substrate, Zhao et al.(2007) introduced four genes into *E. coli* to produce holo-subunits of allophycocyanins from *Anabaena* PCC7120 with spectroscopic properties characteristic of the native holo subunits. Besides the genes for the apoproteins (*apcA1*, *apcB*, *apcA2*, *apcD*, *apcF*) and the lyase (*cpcS*), these included the two respective genes for PCB synthesis, viz. *ho1* and *pcyA*, from the same organism(Fig.3-18)

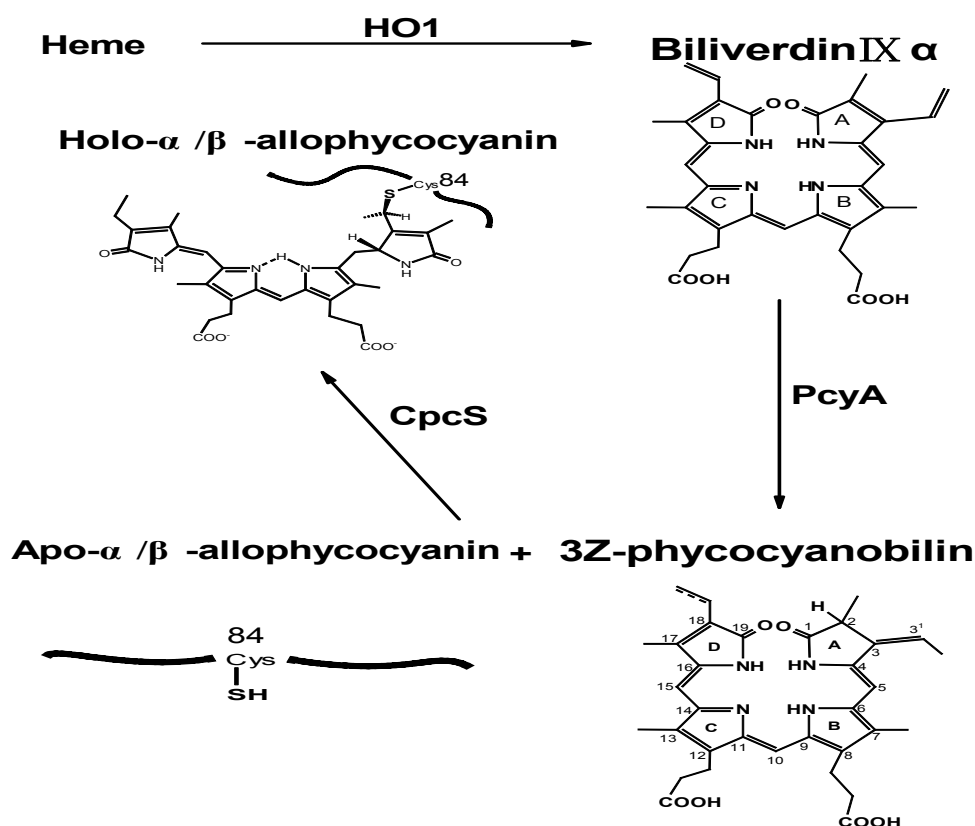
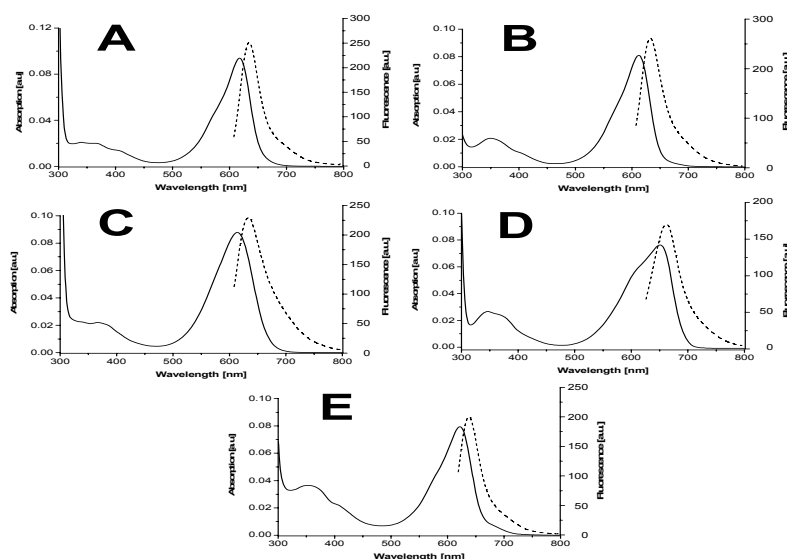


Fig. 3-18: Minimal biosynthetic pathway for the production of PCB from heme, and addition to the allophycocyanin apo- subunits.

### 3.3.2 Expression and Purification of the subunits of allophycocyanin

Plasmids pCDFDuet-cpcS, pACYCDuet-ho1-pcyA and pET-apcA1 (or apcB, apcA2, apcD, apcF) were expressed in the *E. coli* strain BL21(DE3). Upon induction with IPTG, the culture acquired a pronounced blue tint. The various His-tagged subunits of APC were purified by affinity chromatography. The absorption and fluorescence emission properties of the dialyzed chromoproteins are shown in Fig. 3-19 and Tab. 3-5.



**FIG. 3-19:** Absorption(solid) and fluorescence emission(dashed) properties of *Anabaena* PCC7120 PCB-ApcA1(A), PCB -ApcB(B), PCB -ApcA2(C), PCB -ApcD(D) and PCB -ApcF(E) expressed in *E. coli*.

**Table 3-5:** Quantitative absorption and fluorescence data of the biosynthesized and purified PCB-ApcA1, PCB-ApcB, PCB-ApcA2, PCB-ApcD, and PCB-ApcF.

Biliprotein	Absorption		Fluorescence	
	$\lambda_{\max}$ [nm] ( $Q_{\text{vis/uv}}$ )	$\epsilon_{\text{vis}}$ [ $\text{M}^{-1}\cdot\text{cm}^{-1}$ ]	$\lambda_{\max}$ [nm]	$\Phi_{\text{F}}$
PCB-ApcA1	338/618 (4.3)	111,000	641	0.37
PCB-ApcB	344/613 (2.4)	86,700	640	0.20
PCB-ApcA2	365/622 (3.2)	71,800	641	0.18
PCB-ApcD	346/650 (2.3)	62000	663	0.074
PCB-ApcF	355/622 (2.4)	96,400	645	0.19

The absorption and fluorescence emission data for PCB-ApcA1 and PCB-ApcB agree, qualitatively and quantitatively, with those of the isolated APC subunits,  $\alpha$ -APC and  $\beta$ -APC, respectively, from several cyanobacteria (MacColl, 2004; Rübelen et al., 1987; Canaani et al., 1980). The corresponding values for *Synechocystis* PCC6803 ApcA reconstituted by CpcE/CpcF catalysis are 626 nm and 640 nm (Yang et al., 2008). The differences are in part due to the different species and lyases, and to a large extent also to the different measurement conditions. All products showed the correct chromopeptide sequences for APC isolated from *Anabaena* PCC7120 (Fig. 3-21). The absorption and fluorescence of autocatalytic reconstituted ApcA from *Spirulina* sp. are 610 nm and 642 nm respectively (Hu et al., 2006), which is rather different spectroscopically, maybe is not properly attached.

The heterologous reconstitution product PCB-ApcA2 had similar absorption and fluorescence spectra as PCB-ApcA1. The strong fluorescence ( $\Phi_F=0.18$ ) and the large intensity ratio of the Vis- and UV-absorptions ( $Q_A=3.2$ ) are characteristic of a native biliprotein. ApcA2 is highly homologous to ApcA1, but to our knowledge it has never been isolated, and may be an allophycocyanin-like protein (Montgomery et al., 2004).

The absorption (622 nm) and fluorescence maxima (645 nm) of PCB-ApcF are very similar to the values reported for the native 16.2 kDa  $\beta$ -subunit of *Mastigocladus* PCC7603 (Rübelen et al., 1987).

The strong absorption (650 nm) and the relatively weak fluorescence (663 nm) of PCB-ApcD agree well with those of the native  $\alpha$ -subunit of APB from *Synechococcus* 6301 (Lundell and Glazer, 1981,  $\lambda_{abs}=648$  nm). This maximum is significantly blue shifted from that found for the intact trimer containing the  $\alpha^B$  subunit, which has a broad band from 671 to 679 nm. The spectral differences between APC trimers and isolated subunits are well known, but their origins are unclear. There are several possible reasons, excitonic coupling, modified interactions with the protein, and linker proteins. The  $\alpha^B$  subunit attains its complete trimeric spectrum by engaging in strong coupling with the chromophore on the allophycocyanin  $\beta$  subunit. The full red shift for the trimer containing the  $\alpha^B$  subunit would consist of two parts; one part provided by

the  $\alpha^B$  subunit itself, and the second part coming from another strongly coupled chromophore. In support of this possibility, the amino acid sequence of the  $\alpha^B$  subunit shows a significant homology with the  $\alpha$  subunit of allophycocyanin(ApcA), and it might readily replace the allophycocyanin a subunit in a similar type of strong coupling (MacColl, 2004).

It is concluded that in the *E. coli* system a single lyase, CpcS, attaches PCB to Cysteine-84 (consensus sequence) of ApcA1, ApcB, ApcA2, ApcD and ApcF to form holo-APC units with optical spectra like those of the respective native chromoproteins.

### 3.3.3 Circular Dichroism Spectroscopy

CD spectra are very sensitive to the conformation of protein and chromophore: they were therefore measured for reconstituted and FPLC-purified PCB-ApcA1, PCB-ApcB, PCB-ApcA2, PCB-ApcD and PCB-ApcF (Fig. 3-20 and in Tab. 3-6).

The CD spectrum of PCB-ApcA1 (614(+)/340(-) nm), PCB-ApcB (614(+)/341(-) nm), PCB-ApcA2 (384(+)/630(-) nm), PCB-ApcD (588(+)/666(-) nm) and PCB-ApcF (617(+)/343(-) nm) are typical for PCB-containing biliproteins. However, the CD signals of ApcA2 and ApcD are of opposite sign, indicating a different chromophore conformation. Spectrum of ApcD also shows a broad positive band, indicating a heterogeneity. The far-UV CD spectra of PCB-ApcA1, PCB-ApcB, PCB-ApcD and PCB-ApcF are typical for  $\alpha$ -helical proteins. This confirms native conformations of both the chromophore and the protein for ApcA1, ApcB, and ApcF. The far-UV CD spectrum of PCB-ApcA2 is typical for a  $\beta$ -strand protein, no such case has been reported so far for biliproteins, it may therefore be due to misfolding; this protein has never been isolated from *Anabaena* PCC 7120.

**Table 3-6: CD bands of biliproteins**

Biliprotein	Visible CD ( $\lambda_{\max}$ [nm])		UV CD ( $\lambda_{\min}$ [nm])
PCB-ApcA1	614 (+)	340 (-)	210/221
PCB-ApcB	614 (+)	341 (-)	211/221
PCB-ApcA2	630 (-)	384 (+)	212
PCB-ApcD	666 (-)	588 (+)	210/222
PCB-ApcF	617 (+)	343 (-)	210/222

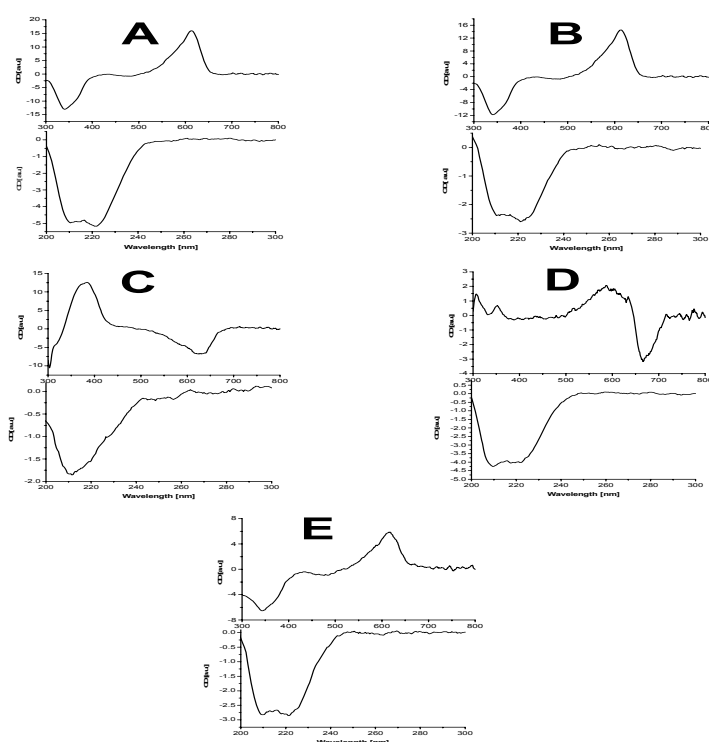


**FIG. 3-20: CD spectra of reconstituted and FPLC-purified PCB-ApcA1(A), PCB-ApcB(B), PCB-ApcA2(C), PCB-ApcD(D) and PCB-ApcF(E)**

CD spectra, Vis- CD (top) and far-UV CD spectra (bottom) of *Anabaena* PCC7120 subunits of allophycocyanin reconstituted with PCB *in E. coli* and FPLC-purified, in KPB(20 mM, pH 7.0) containing NaCl (500 mM)

### 3.3.4 Chromophore analyses of reconstitution products

After denaturation in acidic urea solution (8 M, pH 2.0), the purified reconstituted chromoproteins (PCB-ApcA1, -ApcB, -ApcA2, -ApcD and -ApcF) gave nearly identical spectra with maximal absorption at 661 - 664 nm. The spectrum of denatured ApcB is

shown as an example in Fig.3-21. This is evidence for an intact, cysteine-bound PCB and the absence of significant amounts of mesobiliverdin, which absorbs at longer wavelengths (Arciero et al., 1988a, b). Purified PCB-ApcA1 and PCB-ApcB were digested with pepsin under acidic conditions, chromopeptides enriched by chromatography on Bio-Gel under acidic conditions, and then analyzed by HPLC (Storf, 2003). The chromopeptides absorb maximally at 656 nm (in dilute HCl) (Fig.3-21), which is characteristic for PCB-chromopeptides (Arciero et al., 1988b; Zhao et al., 2006). HPLC analyses gave in both cases one major and several minor peaks (Fig. 3-21), which were at identical positions to the respective ones arising from APC isolated from the parent cyanobacterium, *Anabaena* PCC7120. In summary, therefore, we conclude that CpcS catalyzes correct attachment of PCB to both ApcA1 and ApcB to form holo- $\alpha$ -APC and  $\beta$ -APC, respectively.

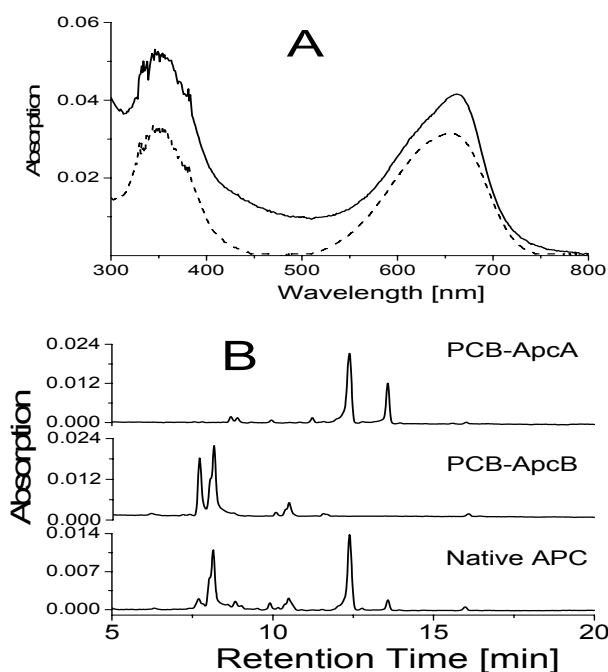


**FIG. 3-21: A: Absorption (solid line,  $\lambda_{\max}$  = 662 nm) of the purified chromoprotein, ApcB in acidic urea (8 M, pH 2.0), and of the purified peptide obtained by pepsin digestion, in diluted HCl (pH 2.5, dashed line,  $\lambda_{\max}$  = 656 nm); PCB-ApcA1 produced similar results. B: HPLC ( $\lambda_{\text{detect}}$  = 650 nm) of the chromopeptides obtained from peptic digestion of the reconstituted PCB-ApcA1 (top), of the reconstituted PCB-ApcB (middle), and of native APC from *Anabaena* PCC7120 (bottom). Reconstitutions were heterologously done in *E. coli* with genes from *Anabaena* PCC7120.**

### 3.3.5 HPLC–ESI-MS analysis of chromopeptides from reconstituted subunits of allophycocyanin

RP-HPLC separation of trypsin digests (Fig.3-22) on a C18 column, gave two types of colored components. Component 1 (A:  $t_r$ =24.6 min and  $t_r$ =27.7 min ; B:  $t_r$ =26.7 min and  $t_r$ =27.1 min; C:  $t_r$ =27.7 min ; D:  $t_r$ =28.2 min; E:  $t_r$ =20.6 min and  $t_r$ =23.8 min) had an absorption maximum around 640 nm (Fig.3-23) that is typical for PCB-containing peptides; component 2 (A:  $t_r$ =39.3 min ; B:  $t_r$ =40.7 min; C:  $t_r$ =39.1 min ; D:  $t_r$ =39.2 min;) corresponds to free PCB according to its retention time and the absorption maximum about at 685 nm (Fig.3- 23). The underlined fractions were used for MS.

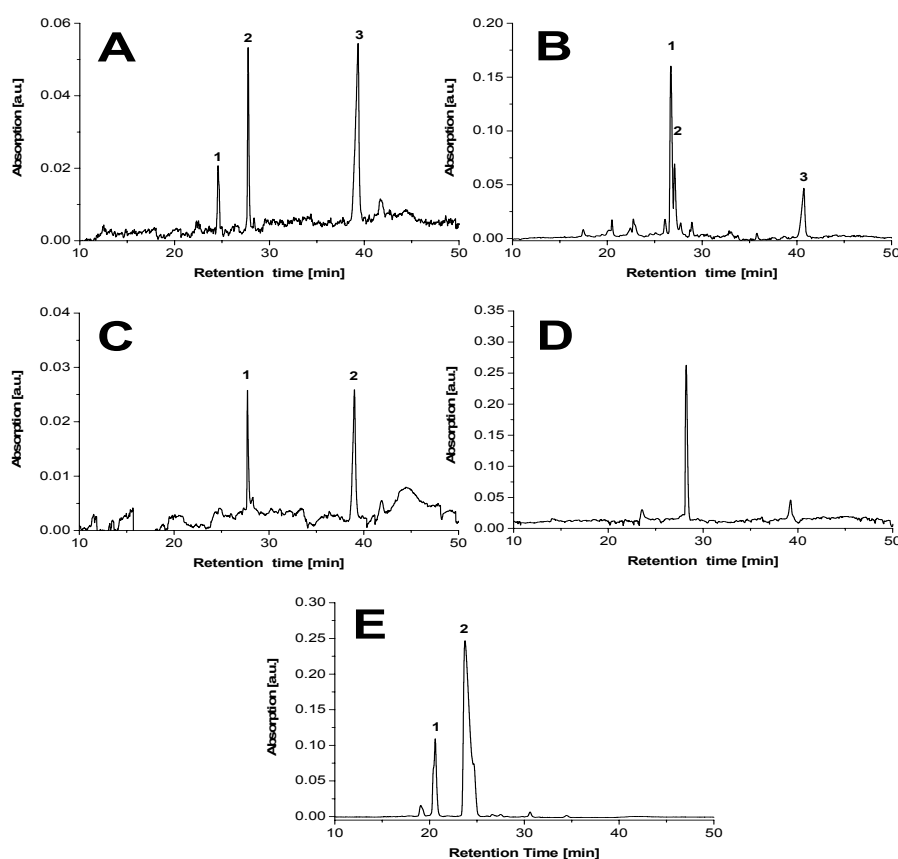


**FIG. 3-22: HPLC of chromopeptides obtained from tryptic digestion of the reconstituted holo-subunit of allophycocyanin(PCB-ApcA1(A), PCB-ApcB(B), PCB-ApcA2(C), PCB-ApcD(D) and PCB-ApcF(E)). HPLC were eluted using a gradient (80:20 to 60:40) of formic acid (0.1%, pH 2) and acetonitrile containing 0.1% formic acid.**

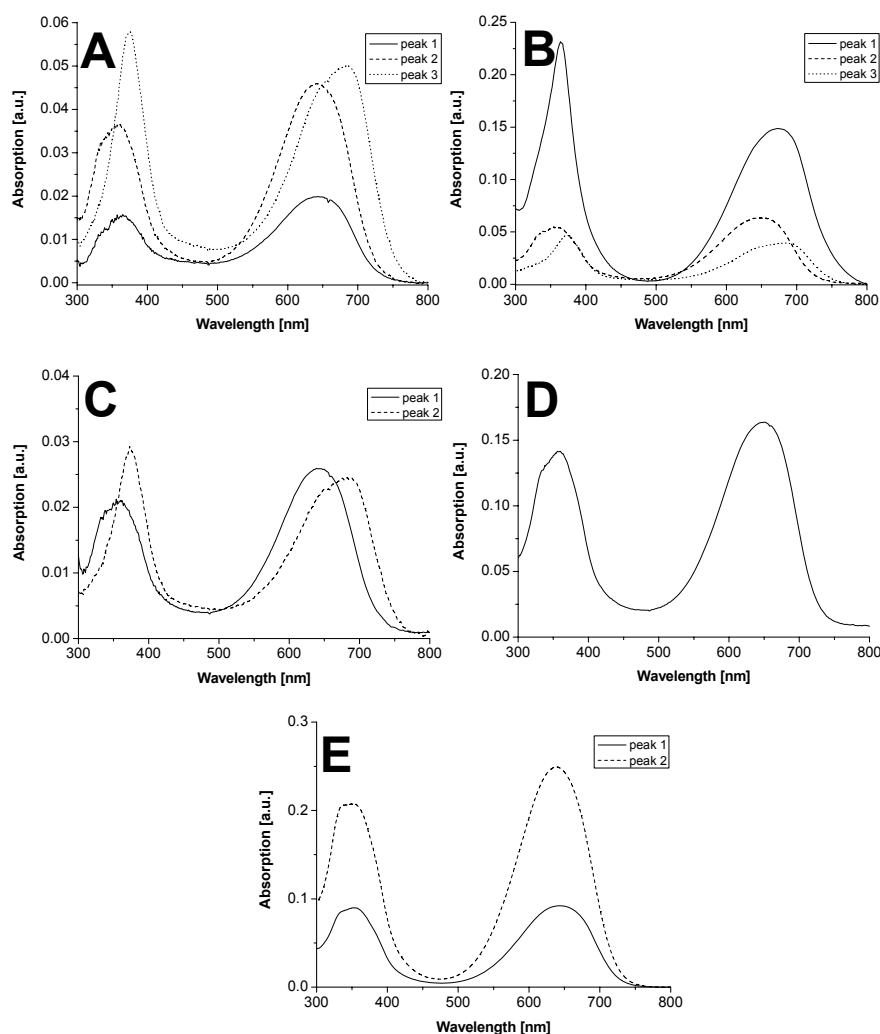


**FIG. 3-23: Absorption spectra of the chromopeptides obtained from tryptic digestion of the reconstituted holo-subunit of allophycocyanin (PCB-ApcA1(A), PCB-ApcB(B), PCB-ApcA2(C), PCB-ApcD(D) and PCB-ApcF(E)).**

Sequences of potential chromophore-containing peptides were deduced from sequences around the chromophore-binding sites in subunits of allophycocyanin from *Anabaena* PCC7120. In native APC subunits, PCB is bound to cysteine residues 81 of the  $\alpha$ -subunit and 82 of the  $\beta$ -subunit. There is excellent agreement between the measured peptide  $M_r$  values and peptide  $M_r$  values calculated from sequences of alpha subunits and beta subunits of allophycocyanin from *Anabaena* PCC7120 (Table 3-7). The chromopeptide sequences confirm the attachment of PCB to the known binding sites (C84, consensus sequence) of ApcA1 or ApcB, ApcD and ApcF also to the consensus site of Apc A2.

**Table 3-7: Mass of chromopeptides from tryptic digestion**

Biliprotein	Chromopeptide		Peptide peak (m/z)	
			Calc.	Expt.
PCB-ApcA1	R(62)PDVVSPGGNAYG QEMTATC(PCB)LR	$[M+4H]^{4+}$	727.47	727.86
PCB-ApcA2	R(62)PDIVSPGGNAYGQ DMTATC(PCB)LR	$[M+3H]^{3+}$	969.96	970.09
PCB-ApcB	Y(79)AAC(PCB)IR	$[M+2H]^{2+}$	641.56	641.78
PCB-ApcD	A(79)LC(PCB)IR	$[M+2H]^{2+}$	581.02	581.28
PCB-ApcF	L(79)AAC(PCB)LR	$[M+2H]^{2+}$	616.56	616.78

### 3.3.6 NMR analysis of peptic chromopeptides from reconstituted subunits of allophycocyanin

RP-HPLC separation of pepsin digests (Fig.3-24) on a C18 column, gave one type of colored components, including A:  $t_r=25.5$  min and  $t_r=26.6$  min ; B:  $t_r=17.9$ , 18.7, 19.6 and 23.9 min; C:  $t_r=25.2$  min ; D:  $t_r=18.7$ , 19.8 and 23.1 min; E:  $t_r=19.9$ , 26.9 and 27.9 min, had an absorption maximum about at 640 nm (Fig.3-25) that is typical for PCB-containing peptides. The underlined fractions were used to measure NMR spectra.

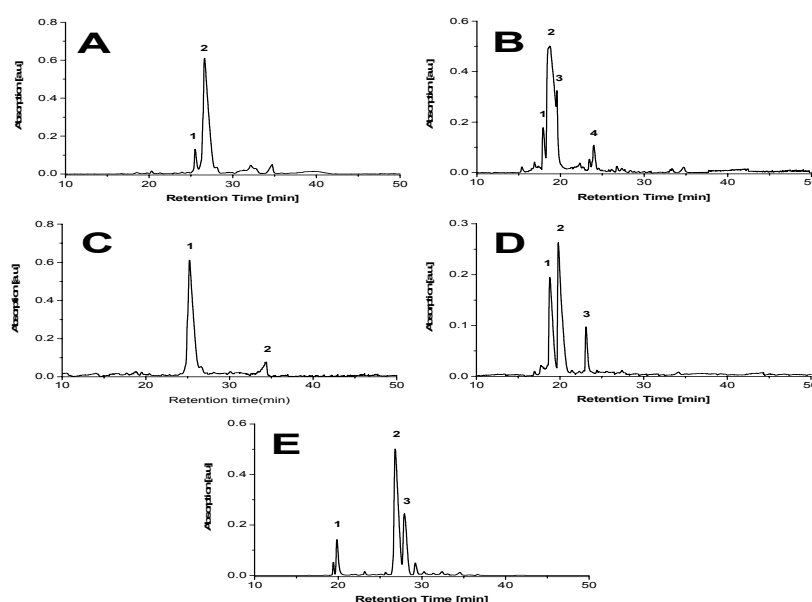


**FIG. 3-24: HPLC of chromopeptides obtained from peptic digestion of the reconstituted holo-subunit of allophycocyanin(PCB-ApcA1(A), PCB-ApcB(B), PCB-ApcA2(C), PCB-ApcD(D) and PCB-ApcF(E)).**

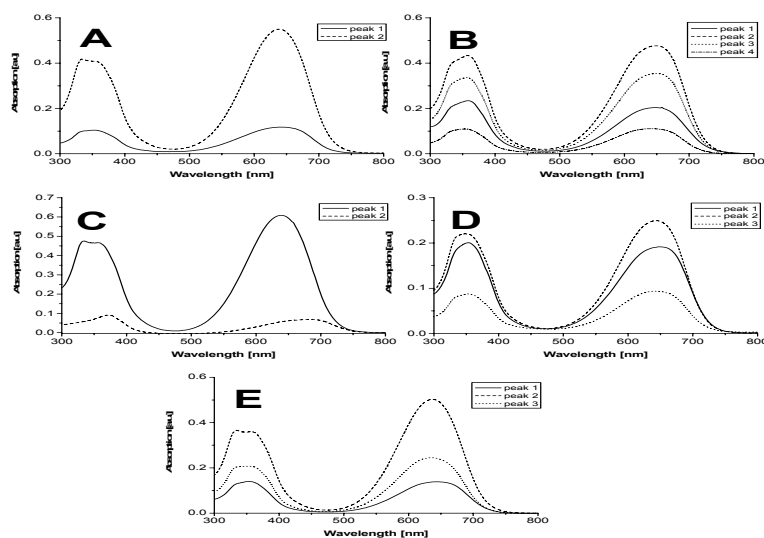


**FIG. 3-25:** Absorption spectra of the chromopeptides obtained from peptic digestion of the reconstituted holo-subunit of allophycocyanin(PCB-ApcA1(A), PCB-ApcB(B), PCB-ApcA2(C), PCB-ApcD(D) and PCB-ApcF(E)).

In order to determine the chromophore structure and mode of linkage to the peptide, the 600-MHz  $^1\text{H}$  NMR spectra of the chromopeptide of holo subunit of allophycocyanin (PCB-ApcA1, PCB-ApcB, PCB-ApcA2 and PCB-ApcF) in 10 mM TFA/D<sub>2</sub>O, were compared (Table 3-8,9,10 and Fig. 3-26) .

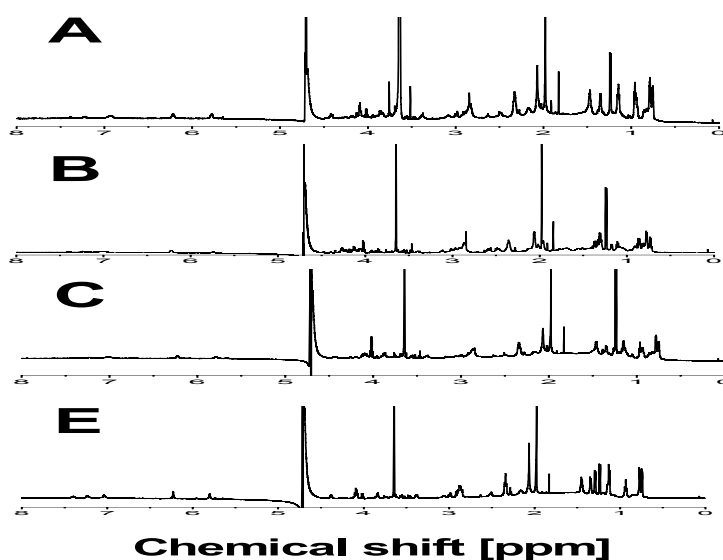


**FIG. 3-26:** 1-D  $^1\text{H}$  NMR spectra of chromopeptides from holo subunit of allophycocyanin(PCB-ApcA1(A), PCB-ApcB(B), PCB-ApcA2(C) and PCB-ApcF(E)) in 10 mM TFA/D<sub>2</sub>O at 25 °C

**Table 3-8:  $^1\text{H}$  NMR(600-MHz) assignments for chromophore protons in APC chromopeptides of reconstituted ApcA1-PCB (A), ApcB-PCB(B), ApcA2-PCB(C), ApcF-PCB(E) (10 mM TFA/D<sub>2</sub>O).**

Chemical shift (ppm)				Multiplicity (J <sub>H-H<sub>L</sub></sub> [Hz])	Number of H's	Assignment
A	B	C	E			
6.92	6.98	7.01	7.03	s	1	10-H
6.22	6.23	6.23	6.23	s	1	15-H
5.78	5.74	5.79	5.80	s	1	5-H
3.47	3.46	3.46	3.46	m	1	3'-H
2.92	3.02	2.92	2.99	m	1	3-H
2.85	2.85	2.86	2.88	m	4	8,12-CH <sub>2</sub> CH <sub>2</sub> COOH
2.47	2.46	2.51	2.48	m	1	2-H
2.32	2.35	2.34	2.34	m	4	8,12-CH <sub>2</sub> CH <sub>2</sub> COOH
2.07	2.06	2.07	2.06	s	9	7,13,17-CH <sub>3</sub>
1.98	1.98	1.98	1.98	s		
1.83	1.84	1.83	1.83	s		
1.96	1.96	1.96	1.95	m	2	18- CH <sub>2</sub> CH <sub>3</sub>
1.35	1.38	1.34	1.34	d (6.73)	3	3'- CH <sub>3</sub>
1.15	1.17	1.15	1.12	d (6.94)	3	2-CH <sub>3</sub>
0.95	1.11	0.95	0.94	t (7.54)	3	18- CH <sub>2</sub> CH <sub>3</sub>

Parallel analysis of the NMR spectra of holo subunit of allophycocyanin (PCB-ApcA1, PCB-ApcB, PCB-ApcA2 and PCB-ApcF) chromopeptide reveals the expected similarity of the resonant frequencies of the chromophore (Table 3-8), the assignment of almost all resonances to the phycocyanobilin (PCB) prosthetic group can be made. The  $^1\text{H}$  NMR spectral assignments of the bilin moiety of chromopeptides show great similarity with those reported for the blue pigment (=PCB-peptide) (Bishop et al., 1986). In particular, the resonances attributed to the aromatic methyls of C-7, -13, and -17, the three vinylic of C-5, -10, and -15, the ethyl group of C-18, and the propionic acid methylenes at C-8 and -12 are salient features of the spectra of both pigments.

Parallel analysis of the NMR spectra of PCB-ApcA1 and PCB-ApcA2 chromopeptide reveals the expected similarity of the resonant frequencies of the amino acid residues expected for binding at Cysteines-81 (Table 3-9). These two  $\alpha$ -apoproteins are highly homologous (86% similar, 70% identical). All amino acid  $\alpha$  protons appear between 3.7 and 4.7 ppm. The chemical shifts of the hydrogens of these same amino acids (Ala, Cys, Gly, Gln, Met and Thr) in the PCB-ApcA1 chromopeptide are displaced within 0.04 ppm upfield from those in PCB-ApcA2 chromopeptide. However, these

chemical shifts are not observed in some of the resonances of the  $\gamma$  protons of Gln, Glu and Met of chromopeptides. Minor differences in the spectra of the two chromopeptides are evident in the resonances attributed to the Glu and Asp residues. Based on the sequences around the chromophore-binding sites in PCB-ApcA1 and PCB-ApcA2 from *Anabaena* PCC7120, chromopeptides sequence GQEMTATC(PCB) of PCB-ApcA1 and GQDMTATC(PCB) of PCB-ApcA2 were deduced.

**Table 3-9:  $^1\text{H}$  NMR(600-MHz) assignments for peptides of reconstituted ApcA1-PCB and ApcA2-PCB ( 10 mM TFA/D<sub>2</sub>O).**

Chemical shift		Multiplicity (J <sub>H-H</sub> ,[Hz])	Number of H's	Assignment
ApcA1-PCB	ApcA2-PCB			
3.75	3.75	s	2	Gly $\alpha$ - CH <sub>2</sub>
4.17	4.19	d (7.28)	1	Gln $\alpha$ - CH
2.28	2.27	m	2	Gln $\beta$ - CH <sub>2</sub>
/	/	/	2	Gln $\gamma$ - CH <sub>2</sub>
3.94	3.95	t (6.55)	1	Met $\alpha$ - CH
2.17	2.14	m	2	Met $\beta$ - CH <sub>2</sub>
/	/	/	2	Met $\gamma$ - CH <sub>2</sub>
4.42	4.43	m	1	Cys $\alpha$ - CH
2.99	3.03	m	2	Cys $\beta$ - CH <sub>2</sub>
4.08,3.85	4.12,3.87	m	2	Thr $\alpha$ - CH
3.52	3.56	d (6.93)	2	Thr $\beta$ - CH
1.24	1.23	d (6.94)	6	Thr $\gamma$ - CH <sub>3</sub>
4.01	4.01	q (6.95)	1	Ala $\alpha$ - CH
1.24	1.23	d (6.93)	3	Ala $\beta$ - CH <sub>3</sub>
4.12	/	d (4.19)	1	Glu $\alpha$ - CH
2.33	/	m	2	Glu $\beta$ - CH <sub>2</sub>
/	/	/	2	Glu $\gamma$ - CH <sub>2</sub>
/	4.61	m	1	Asp $\alpha$ - CH
/	2.86	m	2	Asp $\beta$ - CH <sub>2</sub>

Parallel analysis of the NMR spectra of PCB-ApcB and PCB-ApcF chromopeptides reveals the expected similarity of the resonant frequencies of the corresponding amino acid residues (Table 3-10). They are  $\beta$  subunits of allophycocyanin, but their homology is relatively low (72% similar, 51% identical). All amino acid  $\alpha$  protons appear between 3.8 and 4.6 ppm. The chemical shifts of the  $\alpha$  hydrogens of like amino acids (Ala, Cys) in PCB-ApcB chromopeptide are displaced within 0.04 ppm upfield from the respective ones in the PCB-ApcF chromopeptides. Minor differences (0.1-0.2 ppm) in the spectra of the two chromopeptides are evident in the resonances

attributed to the Thr and Arg residues, and chemical shifts are not observed for some of the resonances of the  $\beta$  and  $\delta$  protons of Arg. Major differences in the spectra of the two chromopeptides are evident in the resonances attributed to the Asp, Ile, Leu and Tyr residues. Based on the sequences around the chromophore-binding sites in PCB-ApcB and PCB-ApcF from *Anabaena* PCC7120, chromopeptides sequence TTRRYAAC(PCB)IRD of PCB- ApcB and TTRRLAAC(PCB) of PCB-ApcF were deduced.

**Table 3-10:  $^1\text{H}$  NMR(600-MHz) assignments for peptides of reconstituted ApcB-PCB and ApcF-PCB (10 mM TFA/D<sub>2</sub>O).**

Chemical shift		Multiplicity ( $J_{\text{H-H}}$ [Hz])	Number of H's	Assignment
ApcB-PCB	ApcF-PCB			
4.18, 4.27	3.83, 4.08	m	1	Thr $\alpha$ - CH
3.47	3.54	m	1	Thr $\beta$ - CH
1.24, 1.31	1.24, 1.29	d (6.92)	3	Thr $\gamma$ - CH <sub>3</sub>
4.02, 4.22, 4.27	4.08	m	1	Arg $\alpha$ - CH
/	/	/	2	Arg $\beta$ - CH <sub>2</sub>
1.31	1.35	d (6.95)	2	Arg $\gamma$ - CH <sub>2</sub>
/	/	/	2	Arg $\delta$ - CH <sub>2</sub>
4.39	4.38	t (7.05)	1	Cys $\alpha$ - CH
3.11	3.06	m	2	Cys $\beta$ - CH <sub>2</sub>
4.56	/	d (8.23)	1	Asp $\alpha$ - CH
2.85	/	m	2	Asp $\beta$ - CH <sub>2</sub>
/	4.08	m	1	Leu $\alpha$ - CH
/	1.45	m	2	Leu $\beta$ - CH <sub>2</sub>
/	0.78	d (5.91)	1	Leu $\gamma$ - CH
/	0.75	d (6.23)	3	Leu $\delta$ - CH <sub>3</sub>
3.84, 4.02	3.83, 4.01	q (7.04)	1	Ala $\alpha$ - CH
1.24, 1.31	1.24,1.29	d (6.92)	3	Ala $\beta$ - CH <sub>3</sub>
4.48	/	t (6.72)	1	Tyr $\alpha$ - CH
2.85	/	m	2	Tyr $\beta$ - CH <sub>2</sub>
4.35	/	d (4.96)	1	Ile $\alpha$ - CH
0.86	/	m	1	Ile $\beta$ - CH
1.31	/	d (6.95)	2	Ile $\gamma$ - CH <sub>2</sub>
0.78	/	m	3	Ile $\delta$ - CH <sub>3</sub>

### 3.3.7 Discussion

The studies described here document the successful reconstitution of the predicted

pathway for the biosynthesis of the subunits of allophycocyanin (Fig.3-18) in *E. coli*, and identify CpcS not only as a lyase for Cys-84 of the  $\beta$  subunits of phycocyanin and phycoerythrocyanin in *Anabaena* PCC 7120 (Zhao et al., 2006a), but also for all APC subunits. They unambiguously identify the correct binding site. The lack of split signals in the NMR spectra, which is particularly clear in the low-field region, establishes that no isomers are formed in the process, and the coincidence with chromophore signals of PCB peptides from subunits of allophycocyanin of *Anabaena* PCC7120 also verify the correct stereochemistry of the product. Taken together, these results demonstrate, in the *E. coli* system, a remarkable substrate spectrum of CpcS: besides the already known  $\beta$ -subunits of CPC and PEC (Zhao et al., 2006; 3.4 and 3.5), it covers all APC-subunits known, and an additional  $\alpha$ -subunit that has not been described before. The enzyme has, on the other hand, a high site-specificity: in CpcB and PecB, PCB is attached exclusively to the Cys-84 binding site, which is homologous to the Cys-84 (consensus sequence) binding site of the APC subunits.

Allophycocyanin is a biliprotein located in the core of the phycobilisome. The biliprotein is isolated and purified as a trimer ( $\alpha_3\beta_3$ ), where a monomer has  $\alpha\beta$  structure. Each  $\alpha$  and  $\beta$  subunit have a single PCB chromophore. The trimer of allophycocyanin has an unusual absorption maximum at 650 nm with a shoulder at 620 nm, while the monomer has an absorption maximum at 615 nm. There are three other core proteins with PCB chromophores, namely,  $L_{CM}$  (ApcF),  $\beta^{16}$  (ApcF), and  $\alpha^B$  (ApcD) (MacColl, 2004). Ashby and Mullineaux (1999) suggest that both ApcD and ApcF are involved in the energy transfer from phycobilisome to PS II and PS I. In both cases, the energy transfer to the reaction centers may be eventually via the chromophore of ApcE (the  $L_{cm}$  or anchor polypeptide). However, the major route of energy transfer to both kinds of reaction centre appears to involve ApcF rather than ApcD. When both ApcF and ApcD are absent, the phycobilisomes are unable to transfer energy to either reaction centre.

The report of Shen et al. (2006) on the CpcSTUV-family opened a new horizon in biliprotein biosynthesis. It indicated that these were lyases with a much broader specificity than that of the known E/F-type, extending to APC, and that the substrate specificity was controlled by the relative amounts of the different lyases present. Their suggestions have been substantiated, but also modified for one member, CpcS, by the present study. The substrate specificity is even broader; it can not only attach

PCB to all APCs but also PEB to both subunits of CPE (Zhao et al., 2007). Together with its already established action on the  $\beta$ -subunits of CPC and PEC (Zhao et al., 2006), CpcS is therefore capable of attaching chromophores to members of all groups of biliproteins. Particularly unexpected was the chromophorylation of CpeA at cysteine-84, because an E/F-type lyase had been suggested to work on this protein (Kahn et al., 1997). At the same time, the specificity is high with regard to the binding site, which is always cysteine-84 (consensus sequence). In APC proteins, this is the only binding site, but the selectivity holds also for the proteins with multiple binding sites. A similar specificity had already been shown for the CPC and PEC subunits, CpcB and PecB, which both carry two binding sites (Zhao et al., 2006a). CpcS therefore seems to be a (nearly) universal lyase with respect to the protein, but is at the same time highly specific for a single binding site, cysteine-84. Similar results were more recently reported by Shen *et al.* (2008) and Saunee et al. (2008) for CpcS-I and CpcU. However, in this case CpcS-I and CpcU form a heterodimeric lyase that attaches PCB to Cys-82 on  $\beta$ -PC and to Cys-81 of the  $\alpha$  and  $\beta$  subunits of AP from *Synechocystis* sp. PCC 6803 and *Synechococcus* sp. PCC 7002.

Homologs of the CpcS and CpeS proteins can be classified into five groups. Two of them, groups A and B, only include strains that can synthesize one or more PEs. This observation, and the further observation that these genes are usually clustered with other genes known to play a role in PE biosynthesis or assembly, suggests that these proteins denoted CpeS and CpeU, respectively, probably play roles in phycoerythrobilin (PEB) attachment to PE subunits. All of the other groups contain at least some members that only synthesize proteins with PCB chromophores, and thus these proteins cannot be involved in PE synthesis, at least in some organisms. The largest of these groups, Group C, can be further divided into three clades, which Saunee et al. (2008) have denoted CpcS-I, CpcS-II, and CpcS-III. *Synechococcus* sp. PCC 7002 has a protein within the CpcS-I clade. CpcS-I and CpcU together form a heterodimeric PCB lyase for  $\beta$ -PC and AP subunits. Clade III of Group C includes the *Anabaena* sp. PCC 7120 open reading frame *alr0617*, the product of which has been shown by this work (Zhao et al., 2006a, 2007a) to ligate PCB to Cys-82 of CpcB, PecB, ApcA, ApcB, ApcD, and ApcF. With the exception of *N. punctiforme*, no organism with a CpcS-III protein also has a protein in Group D (CpcU). The CpcS-II clade includes a variety of marine *Synechococcus* sp., some of which produce PC with PEB

chromophores. Finally, Group E includes several divergent sequences, and the organisms that produce the members of this clade do not have an obvious PBP pigmentation pattern. *Synechococcus* sp. PCC 7002 produces one of the members of this clade; we have provisionally designated these proteins as CpcV (Shen *et al.*, 2008).

There is one notable exception for the protein specificity. CpcA and PecA both have a cysteine-84 binding site, but here CpcS is inactive (Zhao *et al.*, 2006), and the sites are rather served by the site and protein-specific EF-type lyases (Schluchter *et al.*, 1999; Zhao *et al.*, 2000). This exception, and the presence of specialized enzymes for only these subunits, indicates some special status of the latter. One might argue that in the case of PecA, the EF-type lyase has a second function by which the chromophore is isomerized (Arciero *et al.*, 1988). However, such a function is not required for CpcA. Here, is attached by homologous E/F-type lyases in the conventional fashion by addition to the  $\Delta 3,3^1$ -double bond, and with stereochemistries and conformations that are very similar to those of PCB bound to cysteine-84 of the CPC and PEC  $\beta$ -subunits (Fairchild *et al.*, 1994; Zhao *et al.*, 2005; Dammeyer *et al.*, 2006). This indicates a structural difference which, among the cysteine-84 binding sites, sets aside the ones of CpcA and PecA from those of the other biliproteins. Such a difference is supported by a sequence analysis (Zhao *et al.*, 2007a).

It is tempting to speculate on a functional difference of these two groups of biliproteins that goes beyond the lyase specificity. The  $\alpha$ -84 sites of all cyanobacterial and red algal biliproteins are at the contact surface to the  $\beta$ -subunits in the trimers, and show similar geometries and stereochemistries. While this argues against a structural or photosynthetic function, the difference may be relevant to phycobilisome degradation. The  $\alpha$ -subunit of EF-type lyases share homologies to proteins involved in phycobilisomes degradation (Dolganov *et al.*, 1999; Balabas *et al.*, 2003). They are also capable of chromophore detachment (Schirmer *et al.*, 1987), while no such activity has been found for CpcS (Zhao *et al.*, 2006a). There is, moreover, another protein interaction that is specific for these subunits: complex formation of  $\alpha$ -CPC and  $\alpha$ -PEC has been observed with NbIA, which is implicated in biliprotein degradation (Luque *et al.*, 2003; Bienert *et al.*, 2006).

## 3.4 Structure analysis of reconstitution $\beta$ -subunit of C-phycoerythrin

### 3.4.1 Reconstitution principle of $\beta$ -subunit of C-phycoerythrin

Phycocyanobilin (PCB) is biosynthesized from heme by the action of two enzymes, heme oxygenase and BV-reductase. PCB is then attached to the  $\beta$  subunit apoprotein of C-phycoerythrin by a lyase, CpcS (Zhao et al. 2006; Shen et al., 2008) or CpcT (Zhao et al. 2007; Shen et al. 2006). Using endogenous heme as substrate, Zhao et al. (2006, 2007) introduced four genes into *E. coli* to produce single chromophore  $\beta$ -subunit of C-phycoerythrin from *M. lamosus* with spectroscopic properties characteristic of the native single chromophore  $\beta$ -subunit. Besides the genes for the apoprotein (*cpcB*, *cpcB(C84S)*, *cpcB(C155I)*) and the lyase (*CpcS* or *cpcT*) from *Anabaena* PCC7120, these included the two respective genes for PCB synthesis, viz. *ho1* and *pcyA*, from *Anabaena* PCC7120 (Fig.3-27)

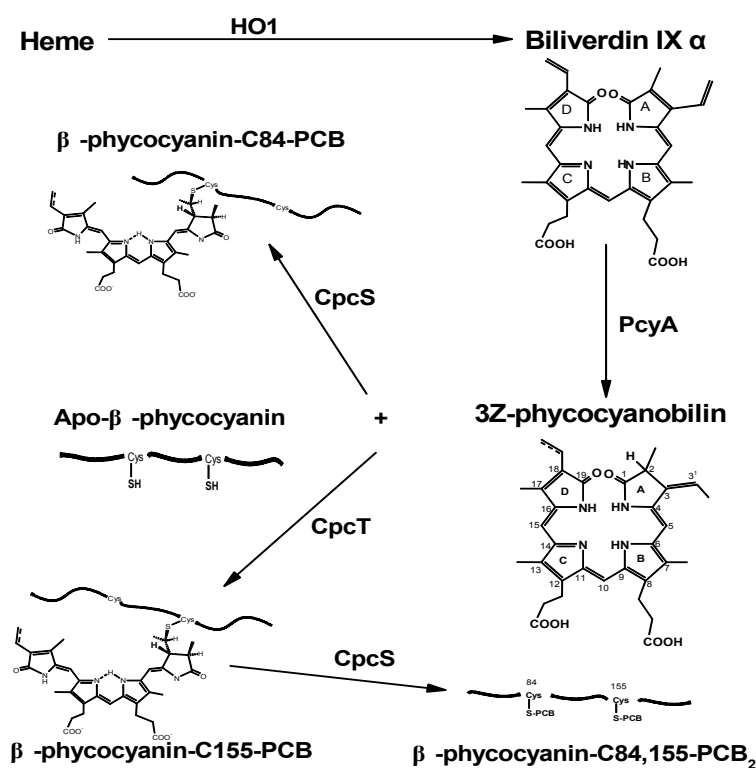
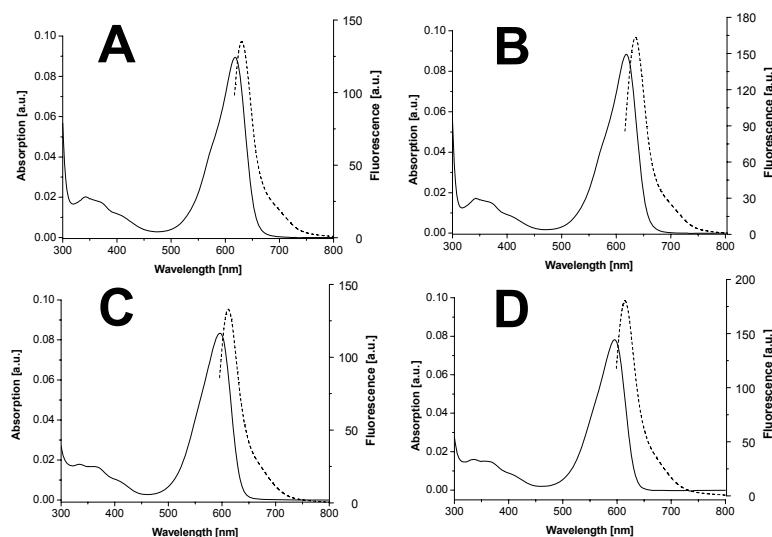


Fig. 3-27: Minimal biosynthetic pathway for the production of PCB from heme and addition to individual binding sites of the C-phycoerythrin apo- $\beta$  subunit.

### 3.4.2 Expression and Purification of the $\beta$ -subunits of C-phycoerythrin

The plasmids pCDFDuet-*cpcS* or pETDuet-*cpcT*, pACYCDuet-*ho1-pcyA* and pET-*cpcB* (or *cpcB(C84S)*, *cpcB(C155I)*) were introduced in the *E. coli* strain BL21(DE3). Upon induction with IPTG, the culture acquired a pronounced blue tint. The various His-tagged subunits of C-phycoerythrin were purified by affinity chromatography. The absorption and fluorescence emission properties of the dialyzed chromoproteins are shown in Fig. 3-28 and Tab. 3-11.



**FIG. 3-28: Absorption (solid) and fluorescence emission (dashed) spectra of *M. lamosus* CpcB-C84-PCB(A), CpcB(C155I)-C84-PCB(B), CpcB-C155-PCB(C) and CpcB(C84S)-C155-PCB(D) expressed in *E. coli*.**

The absorption spectrum of HT-CpcB-C84-PCB had a  $\lambda_{\max}$  at 619 nm and the bright red fluorescence had a  $\lambda_{\max}$  at 643 nm (Fig. 3-28A). Identical results were obtained with a mutant lacking the  $\beta$ -155 binding site, namely CpcB(C155I) (Fig. 3-28B). When pHO1-PcyA and pETDuet-CpcT(All5339) were co-transformed into *E. coli* BL21(DE3), together with pET-CpcB(C84S) or pET-CpcB, the biosynthesized and purified

phycobiliprotein had an absorption maximum at 595 nm and a fluorescence maximum at 625 nm (Fig.3-28C,D). The affinity-purified products obtained with CpcS have the intense visible absorption and fluorescence typical of native phycobiliproteins (see Table 3-11,  $\epsilon_{\text{Vis}}$ ,  $Q_{\text{Vis/uv}}$  and  $\Phi_{\text{F}}$ ), with the position of the bands red-shifted compared with holo- $\beta$ -CPC, peaking in the range associated with the cysteine- $\beta$ 84 chromophore (CpcS). The products obtained with CpcT had. *Vive versa*, blue-shifted maxima as compared to holo- $\beta$ -CPC, peaking in the range associated with the cysteine- $\beta$ 155 chromophore of CPC (Debreczeny et al., 1995; Sauer and Scheer 1988). We therefore conclude that CpcS catalyses the site-selective attachment of PCB to cysteine- $\beta$ 84 in CpcB; and CpcT catalyses the site-selective attachment of PCB to cysteine- $\beta$ 155 in CpcB.

**Table 3-11: Quantitative absorption and fluorescence data of the biosynthesized and purified CpcB-C84-PCB, CpcB(C155I)-C84-PCB, CpcB-C155-PCB and CpcB(C84S)-C155-PCB.**

Biliprotein	Absorption		Fluorescence	
	$\lambda_{\text{max}}$ [nm] ( $Q_{\text{Vis/uv}}$ )	$\epsilon_{\text{Vis}}$ [ $\text{M}^{-1}\cdot\text{cm}^{-1}$ ]	$\lambda_{\text{max}}$ [nm]	$\Phi_{\text{F}}$
CpcB-C84-PCB	338/619 (2.6)	132000	644	0.11
CpcB(C155I)-C84-PCB	338/619 (2.5)	122000	644	0.23
CpcB-C155-PCB	338/595 (3.3)	113000	625	0.40
CpcB(C84S)-C155-PCB	337/596 (5.2)	106000	626	0.34

### 3.4.3 Circular Dichroism Spectroscopy

CD spectra of reconstituted and DEAE column purified CpcB-C84-PCB, CpcB(C155I)-C84-PCB, CpcB-C155-PCB and CpcB(C84S)-C155-PCB are summarized in Fig. 3-29 and in Tab. 3-12

The CD spectra of all four chromoproteins indicated that the pattern (+ for red band, - for blue band) and intensities are typical for PCB chromophores in their native conformations, and the maxima of the red bands show the same red shifts for C84-PCB compared to C155-PCB as the absorption spectra. However, there are two bands at 330 nm (+) and 370 nm (-) of the C155-PCB in the near uv, which is different from C84-PCB. In x-ray structures, C155-PCB has a different overall conformation and C3<sup>1</sup> stereochemistry than C84-PCB on both subunits (Düring et al., 1991; Adir et al., 2001). The spectrum then probably reflects the unusual stereochemistry, these

are the first CD spectra of individual C155-PCB in the native state, which do reflect the stereochemistry. The far-UV CD spectra of all four chromoproteins are typical for  $\alpha$ -helical proteins. This confirms native conformations of the protein.

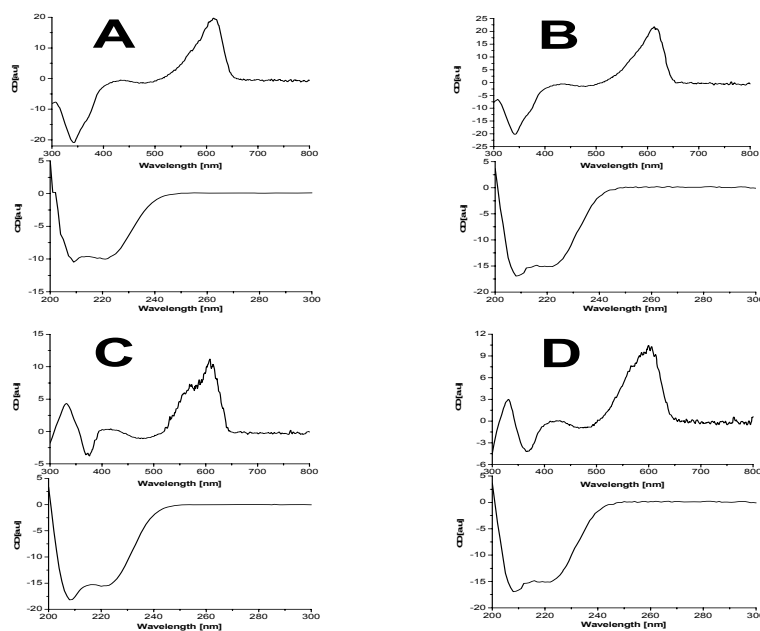


**FIG. 3-29: CD spectra of reconstituted and DEAE column purified CpcB-C84-PCB(A), CpcB(C155I)-C84-PCB(B), CpcB-C155-PCB(C) and CpcB(C84S)-C155-PCB(D)**

CD spectra, Vis- CD (top) and far-UV CD spectra (bottom) of *M. laminosus*  $\beta$  subunit of C-phycoerythrin reconstituted *in E. coli*, affinity chromatography and DEAE column purified.

**Table 3-12: CD bands of CpcB-biliproteins**

Biliprotein	Visible CD ( $\lambda_{max}$ [nm])		UV CD ( $\lambda_{min}$ [nm])
CpcB-C84-PCB	615 (+)	344 (-)	208/221
CpcB(C155I)-C84-PCB	614 (+)	342 (-)	208/222
CpcB-C155-PCB	607 (+)	377 (-)	208/221
CpcB(C84S)-C155-PCB	606 (+)	368 (-)	208/222

### 3.4.4 Chromophore analyses of reconstitution products

After denaturation in acidic urea solution (8 M, pH 2.0), the purified reconstituted chromoproteins (CpcB-C84-PCB, CpcB(C155I)-C84-PCB, CpcB-C155-PCB and CpcB(C84S)-C155-PCB) gave nearly identical spectra with maximal absorption

around 660 nm. This is evidence for an intact, cysteine-bound PCB and the absence of significant amounts of mesobiliverdin, which absorbs at longer wavelengths (Arciero et al., 1988a,b). Purified PCB-C84-CpcB(C155I) and PCB-C155-CpcB(C84S) were digested with pepsin under acidic conditions, chromopeptides enriched by chromatography on Bio-Gel under acidic conditions, and then analyzed by HPLC (Storf, 2003). The chromopeptides absorb maximally around 660 nm (in acid condition) (Fig.3-31), which is characteristic for PCB-chromopeptides (Arciero et al., 1988; Zhao et al., 2006). HPLC analyses gave in both cases one major and several minor peaks (Fig. 3-30), which were at identical positions to the respective ones arising from CpcB isolated from the parent cyanobacterium, *M. laminosus*. This further supports that CpcS catalyses the site-selective attachment of PCB to cysteine- $\beta$ 84 in CpcB; and CpcT catalyses the site-selective attachment of PCB to cysteine- $\beta$ 155 in CpcB.

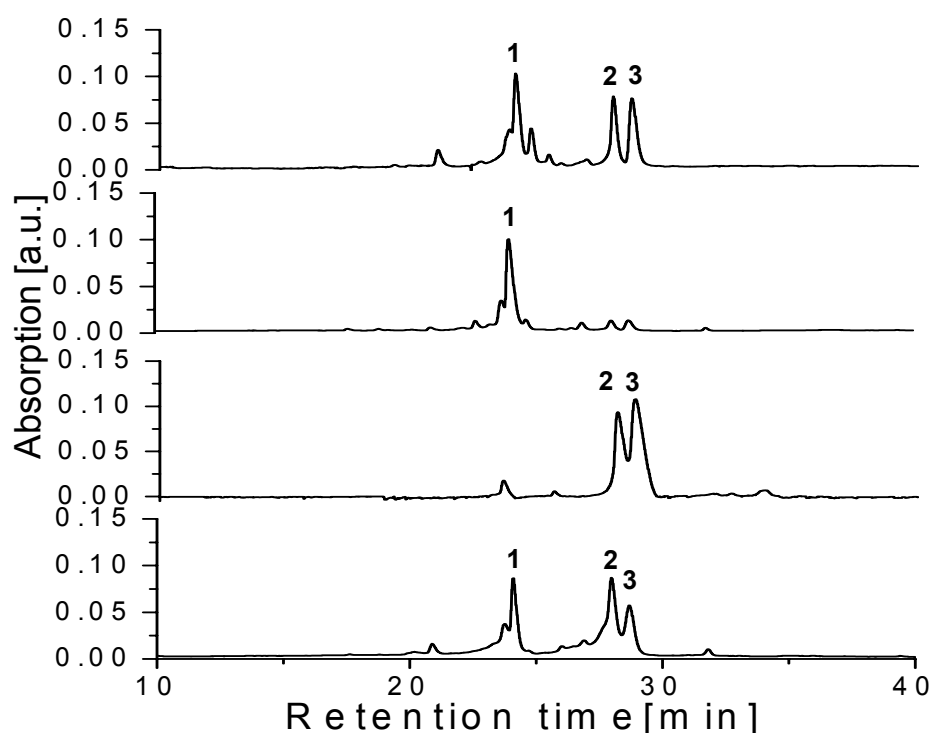


**FIG. 3-30:** HPLC ( $\lambda_{\text{detect}} = 650 \text{ nm}$ ) of the chromopeptides obtained from peptic digestion of the sequentially reconstituted CpcB-C84,C155-PCB<sub>2</sub> (data from Zhao et al., 2007b) (top), CpcB(C84S)-C155-PCB(second), CpcB(C155I)-C84-PCB (third) and  $\beta$ -CPC (bottom). HPLC were eluted using a gradient (80:20 to 60:40) of formic acid (0.1%, pH 2) and acetonitrile containing 0.1% formic acid. CpcB from *M. laminosus*.

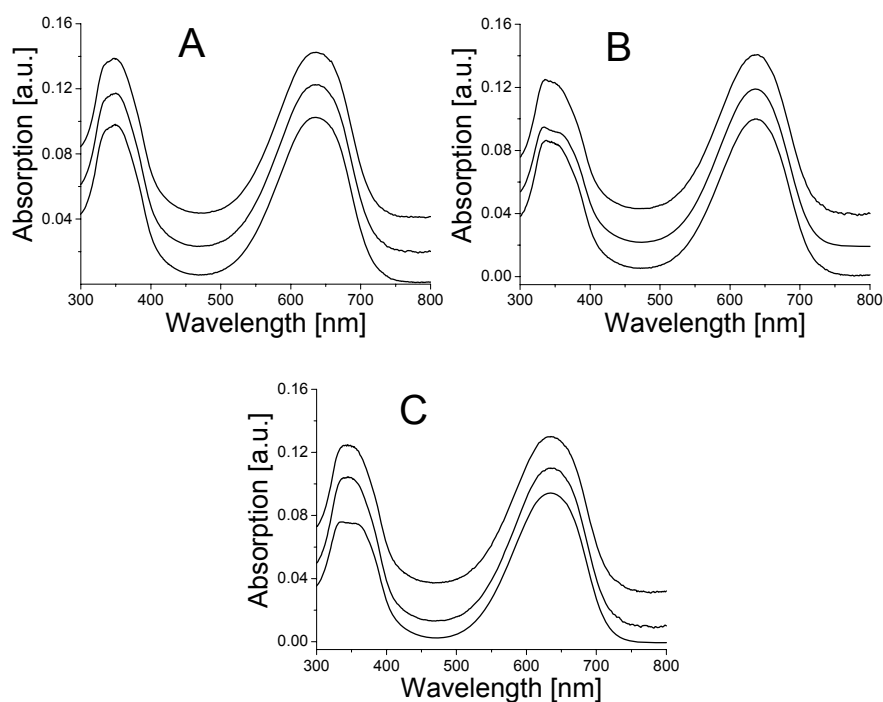


**FIG. 3-31: Absorption spectra of major peptic chromopeptide peaks in the chromatograms shown in Fig. 3-30. A:** Peak 1 derived from the sequentially reconstituted CpcB-C84,155-PCB<sub>2</sub> (Fig.3-31, top), from singly-chromophorylated CpcB(C1551) (Fig. 3-31, second), and  $\beta$ -CPC (Fig. 3-31, bottom). **B:** Peak 2 derived from the sequentially-reconstituted CpcB-C84,155-PCB<sub>2</sub> (Fig.3-31, top), from singly chromophorylated CpcB(C84S) (Fig. 3-31, third), and  $\beta$ -CPC (Fig. 3-31, bottom). **C:** sequentially reconstituted CpcB-C84,155-PCB<sub>2</sub> (Fig.3-31, top), from singly chromophorylated CpcB(C84S) (Fig. 3-31, third), and  $\beta$ -CPC (Fig. 3-31, bottom).

### 3.4.5 HPLC–ESI-MS analysis of chromopeptides from reconstituted $\beta$ -subunits of C-phycoerythrin

RP-HPLC separation of trypsin digests (Fig.3-32) on a C18 column, gave two types of colored components. Component 1 (A:  $t_r=17.7$  min ; B:  $t_r=17.7$  min; C:  $t_r=20.9$  min; D:  $t_r=20.9$  min) had an absorption maximum around 640nm (Fig.3-33) that is typical for PCB-containing peptides; component 2 (A:  $t_r=29.2$  min ; B:  $t_r=29.6$  min) corresponds to free PCB according to its retention time and the absorption maximum about at 685 nm (Fig.3-33). We found an interesting phenomenon that there is no free PCB in the C155-PCB samples, maybe due to PCB tighter binding of PCB to C155 than to C84.

The underlined fractions were used for MS.

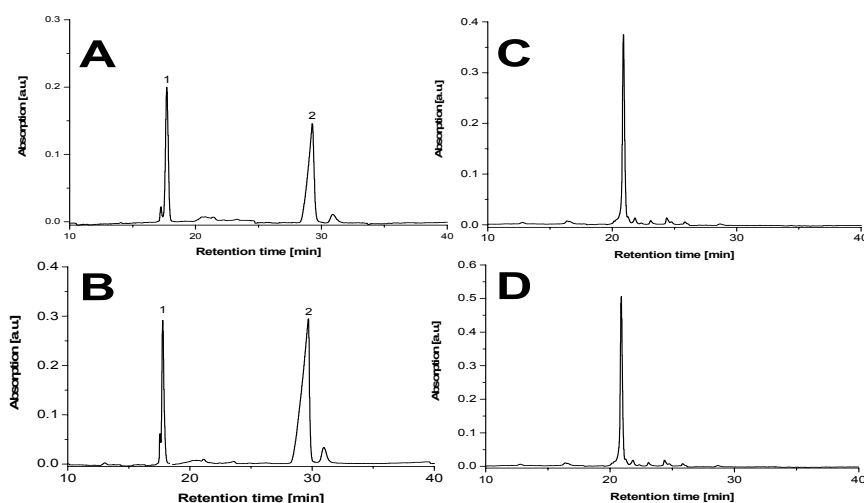


**FIG. 3-32:** HPLC ( $\lambda_{\text{detect}} = 650 \text{ nm}$ ) of the chromopeptides obtained from tryptic digestion of the reconstituted  $\beta$ -subunit of C-phycoerythrin (CpcB-C84-PCB(A), CpcB(C155I)-C84-PCB(B), CpcB-C155-PCB(C) and CpcB(C84S)-C155-PCB(D)). Spectra of individual peaks of the chromatograms are shown in Fig. 3-33. HPLC were eluted using a gradient (80:20 to 60:40) of formic acid (0.1%, pH 2) and acetonitrile containing 0.1% formic acid.

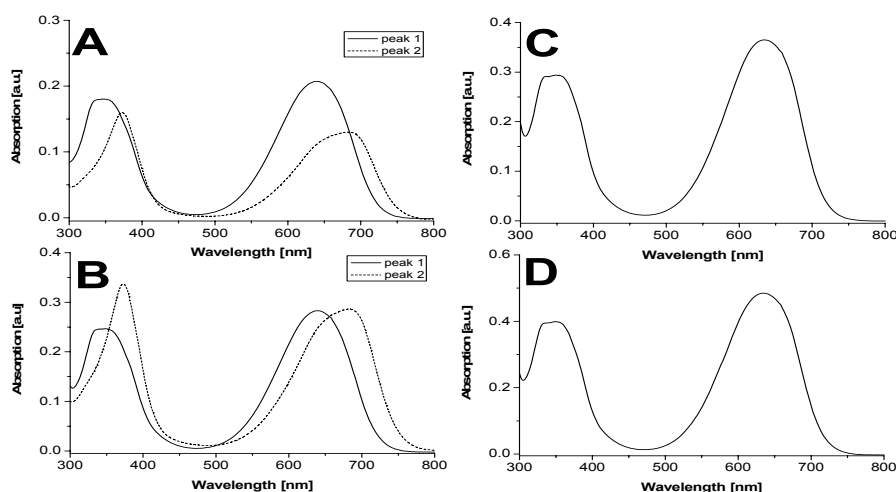


**FIG. 3-33:** Absorption spectra of the chromopeptides obtained from tryptic digestion of the reconstituted  $\beta$  subunit of C-phycoerythrin (CpcB-C84-PCB(A), CpcB(C155I)-C84-PCB(B), CpcB-C155-PCB(C) and CpcB(C84S)-C155-PCB(D))..

Sequences of chromophore-containing peptides were deduced from sequences around the chromophore-binding sites in  $\beta$ -subunits of phycocyanin from *M. laminosus*. In native CPC subunits, PCB is bound to cysteine residues 82 and 153 of the beta subunit. There is excellent agreement between the measured peptide Mr values and those calculated from sequences of  $\beta$ -subunits of phycocyanin from *M. laminosus* (Tab. 3-13). The chromopeptide sequences confirm the attachment of PCB to the known binding sites (C84 and C155, consensus sequence) of CpcB.

**Table 3-13: Mass of chromopeptides from tryptic digestion**

Biliprotein	Chromopeptide		Peptide peak (m/z)	
			Calc.	Expt.
CpcB-C84-PCB	M(79)AAC(PCB)LR	[M+2H] <sup>2+</sup>	625.57	625.80
CpcB(C155I)-C84-PCB	M(79)AAC(PCB)LR	[M+2H] <sup>2+</sup>	625.57	625.74
CpcB-C155-PCB	G(151)DC(PCB)SAL	[M+2H] <sup>2+</sup>	575.95	576.19
CpcB(C84S)-C155-PCB	G(151)DC(PCB)SAL	[M+2H] <sup>2+</sup>	575.95	576.19

### 3.4.6 NMR analysis of peptic chromopeptides from reconstituted $\beta$ subunits of C-phycocyanin

RP-HPLC separation of pepsin digests (Fig.3-34) on a C18 column, gave one type of colored components, including A:  $t_r$ =18.5, 22.9, 23.6 min; B:  $t_r$  =18.4, 22.9, 23.6 min; C:  $t_r$  =20.3 min and 22.7 min; D:  $t_r$  =20.4 min and 22.8 min, had an absorption maximum about at 640nm that is typical for PCB-containing peptides. The underlined fractions were used to measure NMR spectroscopy.

In order to determine the chromophore structure and mode of linkage to the peptide, the 600-MHz <sup>1</sup>H NMR spectra of the chromopeptide of  $\beta$  subunit of phycocyanin (CpcB-C84-PCB and CpcB-C155-PCB) in 10 mM TFA/D<sub>2</sub>O, were compared (Tab. 3-14 and Fig. 3-36).

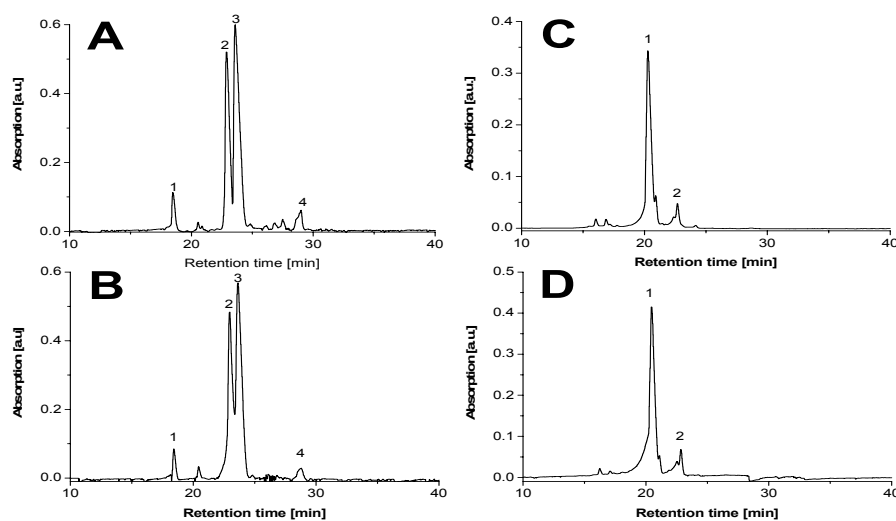


FIG. 3-34: HPLC ( $\lambda_{\text{detect}} = 650 \text{ nm}$ ) of the chromopeptides obtained from peptic digestion of the reconstituted  $\beta$ -subunit of C-phycoerythrin (CpcB-C84-PCB(A), CpcB(C155I)-C84-PCB(B), CpcB-C155-PCB(C) and CpcB(C84S)-C155-PCB(D)).

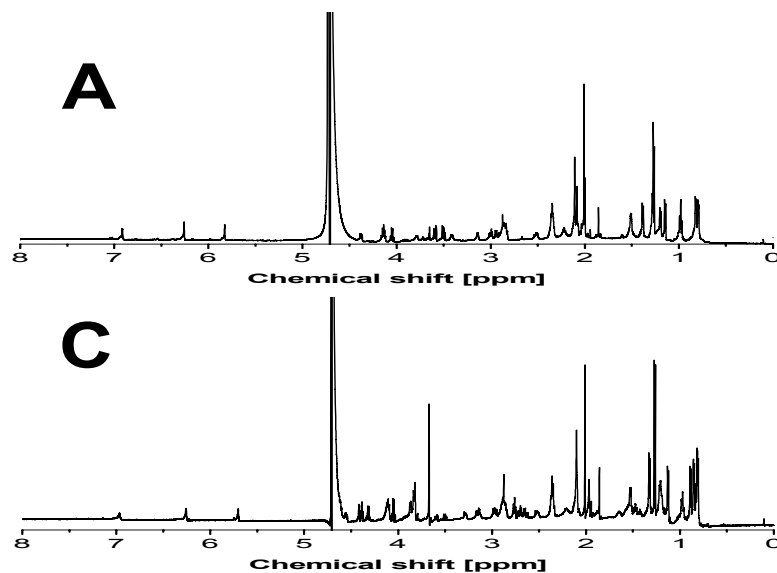


FIG. 3-36: 1-D  $^1\text{H}$  NMR spectra of peptic chromopeptides from the  $\beta$  subunit of C-phycoerythrin (CpcB-C84-PCB(A), CpcB-C155-PCB(C)) in 10 mM TFA/ $\text{D}_2\text{O}$  at 25 °C

The NMR-spectrum results from a combination of the chromophore and peptide signals. Parallel analysis of the NMR spectra of  $\beta$  subunit of C-phycoerythrin

CpcB-C84-PCB and CpcB-C155-PCB chromopeptides reveals the expected resonance frequencies of the chromophore (Tab. 3-14). The  $^1\text{H}$  NMR spectral assignments of the bilin moiety of chromopeptides show great similarity with those reported for the blue pigment (Bishop et al., 1986, chapter 3.2 and 3.3). The assignment of the remaining resonances to protein can be made.

In the downfield region of the spectrum, the three vinylic 10-H, 15-H and 5-H resonances at 6.91(6.97), 6.26(6.26) and 5.83(5.70) ppm, respectively. The  $3^1\text{-H}$  multiplet at 3.49(3.50) ppm is downfield shifted due to its proximity to the sulfur atom, confirming the attachment at this site. The  $3^1\text{-H}$  is coupled to the  $3^2\text{-CH}_3$  group, yielding a doublet at 1.38(1.32) ppm. Similarly the 2-  $\text{CH}_3$  signal (1.14(1.13) ppm) is coupled to the 2-H proton (2.52(2.53) ppm). The 3-H proton (multiplet at 2.94(2.97) ppm) is coupled to both the 2-H and  $3^1\text{-H}$ . All these signals are again characteristic of a PCB bound to cysteine at C- $3^1$ . We found that there are only very small differences between the signals of the C84-PCB and C155-PCB chromopeptides, in spite of the different stereochemistry at C- $3^1$ . The only distinct difference is for the 5-H, which may be diagnostic.

The resonances attributed to the aromatic methyls at C-7, -13, and -17, the ethyl group at C- 18, and the propionic acid methylenes at C-8 and -12 are salient features of the spectra of bile pigments. The three aromatic methyls at C-7, -13, and -17 give singlets at 2.11(2.10), 2.08(2.01) and 1.99(1.97) ppm. The ethyl group at C-18, is seen as two multiplets at 1.96(1.95) ppm (18-  $\text{CH}_2\text{CH}_3$ ) and 0.98(0.97) ppm (18- $\text{CH}_2\text{CH}_3$ ). The multiplet resonances from methylene group of the propionic acid side chains at C-8 and C-12 were found around 2.85(2.87) and 2.35(2.36) ppm. These results correspond well with the A-ring-linked PCB structure (chapter 3.2 and 3.3).

Analysis of the NMR spectra of CpcB-C84-PCB and CpcB-C155-PCB chromopeptides reveals in both cases the resonances of the expected amino acid residues (Table 3-14). All amino acid  $\alpha$  protons appear between 3.8 and 4.6 ppm. The chemical shifts of the  $\alpha$  hydrogens of these same amino acids (Ala, Cys, Thr) in CpcB-C84-PCB chromopeptide are displaced within 0.03 ppm upfield from those in the CpcB-C155-PCB chromopeptide. Chemical shifts are not observed for some of the resonances of the  $\delta$  protons of Lys and Arg; and the  $\gamma$  proton of Met of

chromopeptide. Major differences in the spectra of the two chromopeptides are evident in the resonances attributed to the Arg, Asn, Asp, Gly, Leu, Lys, Met and Ser residues. Based on the sequences around the chromophore-binding sites in CpcB-C84-PCB and CpcB-C155-PCB from *M. lamosus*, chromopeptides sequence TNRRMAAC(PCB) of CpcB-C84-PCB and TKGDC(PCB)SAL of CpcB-C155-PCB were deduced. These confirm the attachment of PCB to correct site of CpcB by CpcS and CpcT lyase catalysis.

**Table 3-14:  $^1\text{H}$  NMR (600-MHz) assignments for peptide TNRRMAAC(PCB) of reconstituted CpcB-C84-PCB and peptide TKGDC(PCB)SAL of reconstituted CpcB-C155-PCB ( 10 mM TFA/D<sub>2</sub>O)**

Chemical shift		Multiplicity (J <sub>H-H</sub> ,[Hz])	Number of H's	Assignment
CpcB-C84-PCB	CpcB-C155-PCB			
6.91	6.97	s	1	10-H
6.26	6.26	s	1	15-H
5.83	5.70	s	1	5-H
3.49	3.50	m	1	3'-H
2.94	2.97	m	1	3-H
2.85	2.87	m	4	8,12-CH <sub>2</sub> CH <sub>2</sub> COOH
2.52	2.53	m	1	2-H
2.35	2.36	m	4	8,12-CH <sub>2</sub> CH <sub>2</sub> COOH
2.11	2.10	s	9	7,13,17-CH <sub>3</sub>
2.08	2.01	s		
1.99	1.97	s		
1.96	1.95	m	2	18- CH <sub>2</sub> CH <sub>3</sub>
1.38	1.32	d	3	3'- CH <sub>3</sub>
1.14	1.13	d	3	2-CH <sub>3</sub>
0.98	0.97	m	3	18- CH <sub>2</sub> CH <sub>3</sub>
4.05, 4.14	4.04	q	1	Ala $\alpha$ - CH
1.20	1.27	d	3	Ala $\beta$ - CH <sub>3</sub>
4,12, 4.05	/	m	1	Arg $\alpha$ - CH
1.51	/	d	2	Arg $\beta$ - CH <sub>2</sub>
1.27	/	m	2	Arg $\gamma$ - CH <sub>2</sub>
/	/	/	2	Arg $\delta$ - CH <sub>2</sub>
4.36	/	m	1	Asn $\alpha$ - CH
2.86	/	m	2	Asn $\beta$ - CH <sub>2</sub>
/	/	/	1	Asp $\alpha$ - CH
/	2.87	m	2	Asp $\beta$ - CH <sub>2</sub>
4.38	4.38	m	1	Cys $\alpha$ - CH
3.00	3.15	m	2	Cys $\beta$ - CH <sub>2</sub>
/	3.87	d	1	Gly $\alpha$ - CH

/	4.42	d	1	Leu $\alpha$ - CH
/	/	/	2	Leu $\beta$ - CH <sub>2</sub>
/	0.89	d	1	Leu $\gamma$ - CH
/	0.85	d	2	Leu $\delta$ -CH <sub>2</sub>
/	4.55	m	1	Lys $\alpha$ - CH
/	1.53	d	2	Lys $\beta$ - CH <sub>2</sub>
/	1.47	m	2	Lys $\gamma$ - CH <sub>2</sub>
	/	/	2	Lys $\delta$ - CH <sub>2</sub>
4.16	/	m	1	Met $\alpha$ - CH
2.18	/	m	2	Met $\beta$ - CH <sub>2</sub>
/	/	/	2	Met $\gamma$ - CH <sub>2</sub>
/	4.32	m	1	Ser $\alpha$ - CH
/	3.83	m	2	Ser $\beta$ - CH <sub>2</sub>
4.14	4.11	t	1	Thr $\alpha$ - CH
3.58	3.59	d	2	Thr $\beta$ - CH <sub>2</sub>
1.27	1.27	d	3	Thr $\gamma$ - CH <sub>3</sub>

### 3.4.7 Discussion

The studies described here documented successful reconstitution of PCB to  $\beta$ -subunit of CPC, CpcB, and thereby the proposed pathway for the biosynthesis of the phycocyanin  $\beta$  subunit (Fig.3-27) in *E. coli*. The results of experiments support and extend the conclusion reached by Shen et al. (2006, 2008), Saunee et al. (2008) and Zhao et al. (2006a, 2007b) that the lyases CpcS and CpcT catalyse the site-selective attachment of PCB to cysteine- $\beta$ 84 and 155, respectively, in CpcB.

Compared with enzymatic chromophore attachment to the  $\alpha$ -subunits, relatively little has been known, until recently, about the catalytic chromophore attachment to the  $\beta$ -subunits of phycobiliproteins, where the process is complicated by the presence of two or even more binding sites (Glazer, 1994; Grossman et al., 1993; Zhao et al., 2007; Sidler, 1994). Nonenzymatic attachment of PCB to CpcB from *M. lamosus* indicated that both binding sites can bind the chromophore spontaneously, and that the site-specificity can be influenced by the reaction medium: binding of C155 is favored under the influence of the detergent, Triton X- 100, and binding to C84 in its absence (Zhao et al., 2004). The spontaneous reaction, however, is unspecific. Moreover, experiments with multiply transformed *E. coli* indicate that a spontaneous addition to either site is very low *in vivo*, at least in *E. coli* (Zhao et al., 2006, 2007b).

The identification of a set of four genes (*cpcS*, *T*, *U* and *V*) from *Synechococcus* sp. PCC7002 that catalyze the addition of PCB to phycobiliprotein  $\beta$ -subunits (Shen *et al.*, 2004) initiated a better understanding of the process. Distinct specificities for the two binding sites of  $\beta$ -CPC recently became obvious for these proteins. Under catalysis of CpcS-I-CpcU, from *Synechococcus* PCC7002, PCB is attached regioselectively to cysteine- $\beta$ 84 (Shen *et al.*, 2008; Saunee *et al.*, 2008). Conversely, CpcT from *Synechococcus* PCC7002 catalyzed the attachment to cysteine-155 of CpcB (Shen *et al.*, 2006). The site specificity of CpcS and CpcT are fully supported by our finding that the homologous CpcS and CpcT from *Anabaena* PCC7120, catalyzes the attachment of PCB to cysteine- $\beta$ 84 and cysteine- $\beta$ 155 of CpcB. It is noteworthy that most of the work reported here was done with CpcB from *M. laminosus*; and the lyase was from *Anabaena* PCC7120 CpcT catalyzes equally well the PCB attachment to CpcB from *Anabaena* PCC7120 (Zhao *et al.*, 2007b). A similar cross-reactivity was shown for the cysteine-84 lyase, CpcS (Zhao *et al.*, 2006a). Taken together, chromophore attachment to the  $\beta$ -subunit of CpcB is catalyzed by enzymes that are specific for the two binding sites, Cys- $\beta$ 84 and Cys- $\beta$ 155, but both lyases have a broader specificity to their substrate proteins than the  $\alpha$ 84 lyases, CpcE/F and PecE/F.

The lyase CpcS (CpcT) catalyses the site-selective attachment of PCB to cysteine- $\beta$ 84(155) in CpcB, resulting in CpcB-C84-PCB (CpcB-C155-PCB), as reported in Zhao *et al.* (2007b), they tested whether by combined catalysis of CpcT and CpcS, holo- $\beta$ -CPC could be generated in the *E. coli* system. The results showed that the purified phycobiliprotein formed had an absorption maximum at 618 nm, which is red-shifted from that of  $\beta$ -CPC isolated from *M.laminosus* ( $\lambda_{\max}$  = 609 nm). By contrast, however, the fluorescence maxima were the same for the reconstituted chromoprotein and the isolated subunit (644 nm). The PCB-C155 and PCB-C84 chromopeptide ratio of 0.7:1 was estimated of from HPLC analysis of the chromopeptides (Fig. 3-30, sequentially reconstituted CpcB-C84,155-PCB<sub>2</sub>). In  $\beta$ -CPC, PCB-C84 absorbs at longer wavelength than PCB-C155 and is the predominantly fluorescing chromophore. The data thus indicate the correct attachment of PCB to C84 when the C155-PCB is already present, but an incomplete or incorrect reconstitution of PCB to C155 when the C84-PCB is already present. In part, the failure to obtain doubly chromophorylated proteins when both lyases are present, could relate to the relatively low  $k_{\text{cat}}$  of CpcT as compared to CpcS. This is an

interesting problem which indicates that unknown regulatory factors may be present in cyanobacteria.

In contrast to *Synechococcus* PCC7002, two copies each of *cpeS*- and *cpeT*-like genes are present in *Anabaena* PCC7120. Only CpcT1 (all5339) is capable of correctly attaching PCB to cysteine-155 of CpcB, while its homologue CpcT2 is inactive *in vitro* and in *E. coli*. Similarly, only CpcS1 (alr0617) catalyzes the attachment of PCB to cysteine-84 of CpcB, while its homologue, CpcS2, is inactive. It should be noted that the kinetic constants of CpcT1 is lower than those of CpcS1 and the EF-type lyases. (Zhao et al., 2007b)

The evolution of site-specific enzymes may relate to the different binding situations of the two chromophores on the  $\beta$ -subunits. The conformation of PCB bound to cysteine- $\beta$ 155 differs from that of PCB bound to cysteines  $\beta$ 84 (and  $\alpha$ 84) (Schirmer et al., 1987), as is the stereochemistry of the asymmetric C-3<sup>1</sup> of PCB that is generated, together with the asymmetric C-3, during the addition reaction. In the high-resolution structures, C-3<sup>1</sup> is R-configured at PCB bound to cysteine-84, whereas it is S-configured in PCB bound to cysteine-155 (Ritter et al., 1999; Wang et al., 2001; Adir et al., 2002). Conceivably, this different binding requires a different conformations of the chromophore when it is presented by the lyase to the binding site, as indicated by a conformation-dependent site selectivity of the autocatalytic addition reaction (Zhao et al., 2004).

The identification and characterization of the CpcS and CpcT lyases in several organisms, and of their interactions, and also the possibility for the coexpression of the various components in *E. coli* now opens a new approach to study the assembly of phycobilisomes, the structures responsible for a major fraction of global photosynthesis.

## 3.5 Structure analysis of reconstituted $\beta$ -subunits of phycoerythrocyanin

### 3.5.1 Reconstitution principle of $\beta$ -subunit of phycoerythrocyanin

Phycocyanobilin (PCB) is biosynthesized from heme by the action of two enzymes, heme oxygenase and BV-reductase. Similar to the reaction with CpcB (section 3.4), PCB is then attached to the  $\beta$  subunit apoprotein of phycoerythrocyanin by a lyase, CpcS (Zhao et al. 2006) or CpcT (Zhao et al. 2007; Shen et al. 2006). Using endogenous heme as substrate, Zhao et al. (2006, 2007) introduced four genes into *E. coli* to produce single-chromophore  $\beta$ -subunits of phycoerythrocyanin from *M. lamosus* with spectroscopic properties characteristic of the individual chromophores in the native  $\beta$ -subunit. Besides the genes for the apoprotein (*pcb*, *pcb(C84A)*, *pcb(C155I)*) and the lyase (*CpcS* or *cpcT*) from *Anabaena* PCC7120, these included the two respective genes for PCB synthesis, viz. *ho1* and *pcyA*, from *Anabaena* PCC7120. The reconstitution principle of the  $\beta$ -subunit of phycoerythrocyanin is similar to that of  $\beta$ -CPC (see Fig. 3-27).

### 3.5.2 Expression and Purification of the $\beta$ -subunits of phycoerythrocyanin

Expression followed the principle for CpcB (section 3.4.2), using pCDFDuet-*cpcS* or pETDuet-*cpcT*, pACYCDuet-*ho1-pcyA* and pET-*pcb* (or *pcb(C84S)*, *pcb(C155I)*) plasmids in the *E. coli* strain BL21(DE3). Upon induction with IPTG, the culture acquired a pronounced blue tint. The various His-tagged subunits of phycoerythrocyanin were purified by affinity chromatography. The absorption and fluorescence emission properties of the dialyzed chromoproteins are shown in Fig. 3-37 and Tab. 3-16.

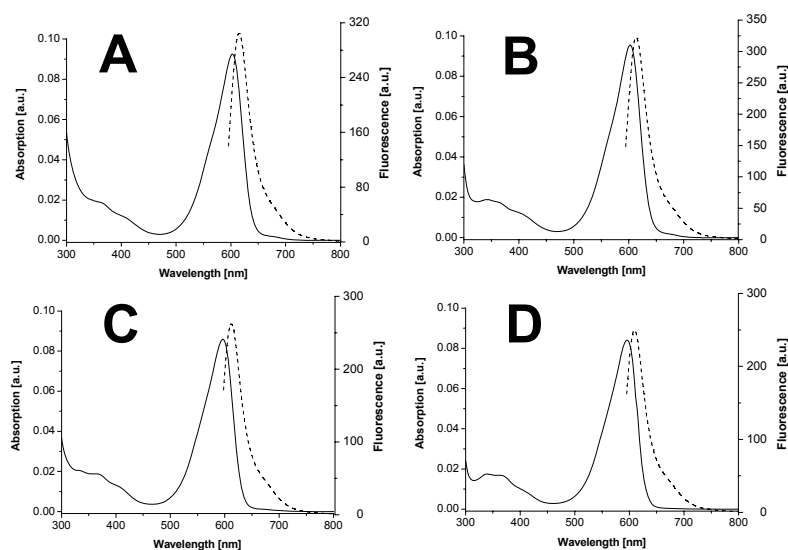


**FIG. 3-37: Absorption (solid) and fluorescence emission (dashed) spectra of *M. laminosus* PecB-C84-PCB(A), PecB(C155I)-C84-PCB(B), PecB-C155-PCB(C) and PecB(C84A)-C155-PCB(D) expressed in *E. coli*.**

The absorption spectrum of HT-PecB-C84-PCB had a  $\lambda_{\max}$  at 602 nm and the bright red fluorescence had a  $\lambda_{\max}$  at 629 nm (Fig. 3-37A). Identical results were obtained with a mutant lacking the  $\beta$ -155 binding site, namely PecB(C155I) (Fig. 3-37B).

When pHO1-PcyA and pETDuet-CpcT were co-transformed into *E. coli* BL21(DE3), together with pET-PecB(C84A) or pET-PecB, the biosynthesized and purified phycobiliprotein had an absorption at 596 nm and fluorescence at 625 nm (Fig. 3-37 C,D). The affinity-purified products obtained with CpcS have the intense visible absorption and fluorescence typical of native phycobiliproteins (see Table 3-11,  $\epsilon_{\text{vis}}$ ,  $Q_{\text{vis/uv}}$  and  $\Phi_{\text{F}}$ ), with the position of the bands red-shifted compared with holo- $\beta$ -PEC, peaking in the range associated with the cysteine- $\beta$ 84 chromophore (CpcS). The products obtained with CpcT versa, blue-shifted maxima as compared to holo- $\beta$ -PEC, peaking in the range associated with the cysteine- $\beta$ 155 chromophore of PEC from *M. laminosus* (Parbel et al., 1997). We therefore conclude that CpcS catalyses the site-selective attachment of PCB to cysteine- $\beta$ 84 in PecB; and CpcT catalyses the site-selective attachment of PCB to cysteine- $\beta$ 155 in PecB.

**Table 3-16: Quantitative absorption and fluorescence data of the biosynthesised and purified PecB-C84-PCB, PecB(C155I)-C84-PCB, PecB-C155-PCB and PecB(C84A)-C155-PCB.**

Biliprotein	Absorption		Fluorescence	
	$\lambda_{\max}$ [nm] ( $Q_{\text{vis/uv}}$ )	$\epsilon_{\text{vis}}$ [ $M^{-1}\cdot\text{cm}^{-1}$ ]	$\lambda_{\max}$ [nm]	$\Phi_{\text{F}}$
PecB-C84-PCB	337/602 (3.0)	101000	629	0.23
PecB(C155I)-C84-PCB	338/602 (2.6)	116000	629	0.51
PecB-C155-PCB	338/596 (2.9)	108000	625	0.25
PecB(C84A)-C155-PCB	338/596 (2.9)	103000	625	0.34

### 3.5.3 Circular Dichroism Spectroscopy

The CD spectra (Fig. 3-38 and in Tab. 3-17) of PecB-C84-PCB, PecB(C155I)-C84-PCB, PecB-C155-PCB and PecB(C84A)-C155-PCB are typical for PCB-containing biliproteins. But the CD signals of PecB-C155-PCB and PecB(C84A)-C155-PCB are of opposite sign, and the near uv signals of C155-PCB of PecB are different from that of CpcB, reflecting a different chromophore geometry. This is again the first time that spectra ( $\lambda_{\max}=596$  nm) for the native C155-PCB are obtained directly, they are somewhat red-shifted compared to the indirectly obtained data of Parbel et al. (1991) ( $\lambda_{\max}=583$ nm) and the theoretical spectra ( $\lambda_{\max}=585$ nm) of Scharnagl et al. (1991). The absorption maximum of the C155-PCB is red-shifted by 11 nm as compared to the CD-maximum, indicating some microheterogeneity (Scharnagl et al., 1991). The far-UV CD spectra of all four chromoproteins are typical for  $\alpha$ -helical proteins. This confirms native conformations of both the chromophore and the protein.

**Table 3-17: CD bands of PecB-biliproteins**

Biliprotein	Visible CD ( $\lambda_{\max}$ [nm])		UV CD ( $\lambda_{\min}$ [nm])
PecB-C84-PCB	600 (+)	342 (-)	209/222
PecB(C155I)-C84-PCB	599 (+)	342 (-)	209/220
PecB-C155-PCB	595 (-)	336 (+)	209/222
PecB(C84A)-C155-PCB	597 (-)	335 (+)	209/222

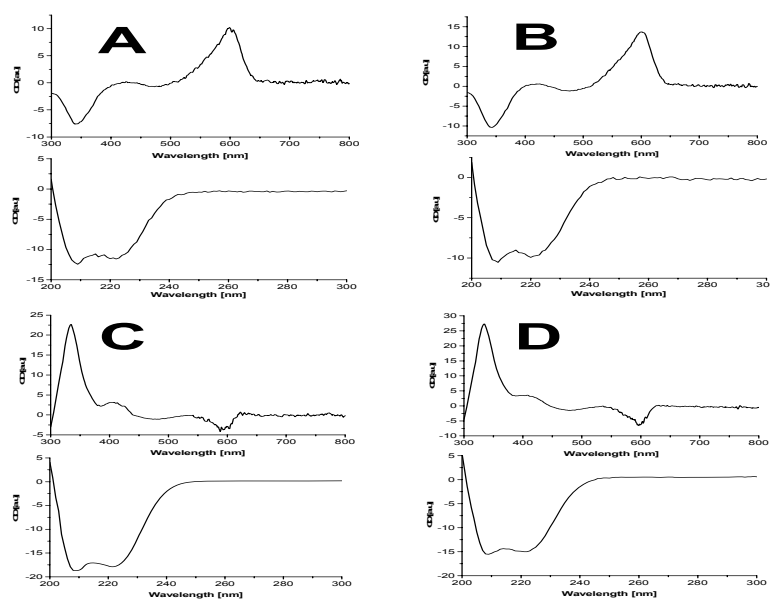


**FIG. 3-38: CD spectra of reconstituted and DEAE column purified PecB-C84-PCB(A), PecB(C155I)-C84-PCB(B), PecB-C155-PCB(C) and PecB(C84A)-C155-PCB(D)**

CD spectra, Vis- CD (top) and far-UV CD spectra (bottom) of *M. laminosus*  $\beta$  subunit of C-phycocyanin reconstituted *in E. coli*, affinity chromatography and DEAE column purified.

### 3.5.4 Chromophore analyses of reconstitution products

After denaturation in acidic urea solution (8 M, pH 2.0), the purified reconstituted chromoproteins (PecB-C84-PCB, PecB(C155I)-C84-PCB, PecB-C155-PCB and PecB(C84A)-C155-PCB) gave nearly identical spectra with maximal absorption around 660 nm. This is evidence for an intact, cysteine-bound PCB and the absence of significant amounts of mesobiliverdin, which absorbs at longer wavelengths (Arciero et al., 1988a,b). Purified PecB(C155I)-C84-PCB and PecB(C84A)-C155-PCB were digested with pepsin under acidic conditions, chromopeptides enriched by chromatography on Bio-Gel under acidic conditions, and then analyzed by HPLC (Storf, 2003). The chromopeptides absorb maximally around 660 nm (in acid condition) (Fig.3-40), which is characteristic for PCB-chromopeptides (Arciero et al., 1988b; Zhao et al., 2006). HPLC analyses gave in both cases one major and several minor peaks (Fig. 3-39), which were at identical positions to the respective ones arising from PEC isolated from the parent cyanobacterium, *M. laminosus*. In summary,

therefore, we conclude that CpcS catalyses the site-selective attachment of PCB to cysteine- $\beta$ 84 in PecB; and CpcT catalyses the site-selective attachment of PCB to cysteine- $\beta$ 155 in PecB.

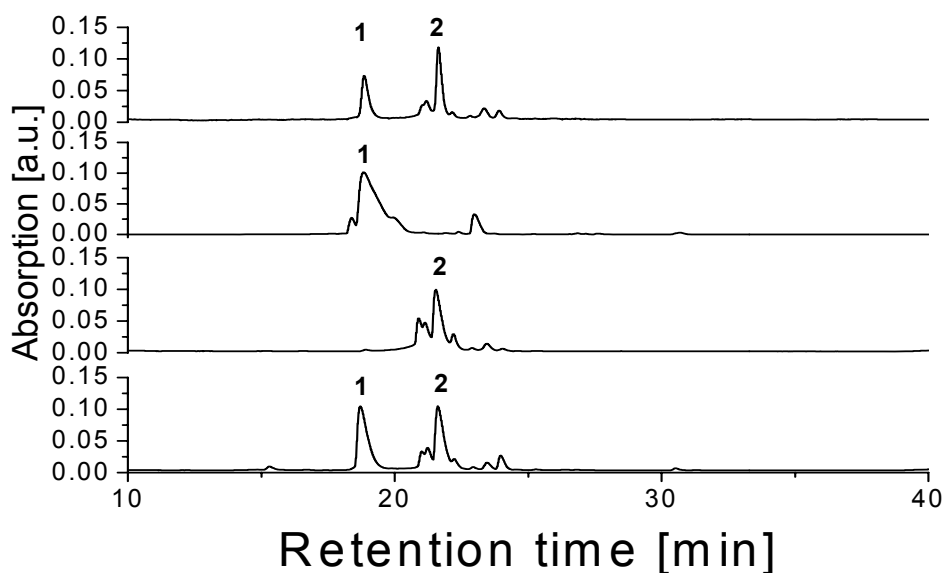


**FIG. 3-39: HPLC ( $\lambda_{\text{detect}} = 650 \text{ nm}$ ) of the chromopeptides obtained from peptic digestion of the sequentially reconstituted PecB-C84,C155-PCB<sub>2</sub> (data from Zhao et al., 2007b) (top), PecB(C155I)-C84-PCB (second), PecB(C84A)-C155-PCB (third) and  $\beta$ -PEC (bottom). HPLC were eluted using a gradient (80:20 to 60:40) of formic acid (0.1%, pH 2) and acetonitrile containing 0.1% formic acid.**

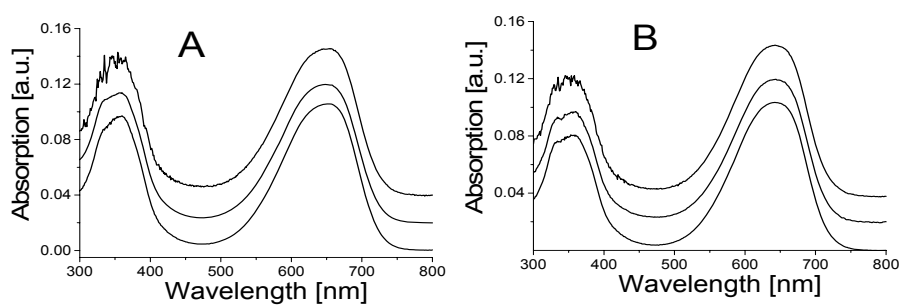


**FIG. 3-40: Absorption spectra of major peptic chromopeptide peaks in the chromatograms shown in Fig.3-39. A: Peak 1 derived from the sequentially reconstituted PecB-C84,155-PCB<sub>2</sub> (Fig.3-39, top), from singly-chromophorylated PecB(C155I) (Fig. 3-39, second), and  $\beta$ -PEC (Fig. 3-39, bottom). B: Peak 2 derived from the sequentially-reconstituted PecB-C84,155- PCB<sub>2</sub> (Fig.3-39, top), from singly chromophorylated PecB(C84A) (Fig. 3-39, third), and  $\beta$ -PEC (Fig. 3-39, bottom).**

### 3.5.5 HPLC–ESI-MS analysis of chromopeptides from reconstituted $\beta$ -subunits of phycoerythrocyanin

RP-HPLC separation of trypsin digests (Fig.3-41) on a C18 column, gave two types of colored components. Component 1 (A:  $t_r = 14.2$  min ; B:  $t_r = 14.0$  min; C:  $t_r = 19.4$ , 25.1, 26.2 and 30.8 min; D:  $t_r = 19.7$ , 25.1, 26.4, 30.9 min) had an absorption maximum around 645nm (Fig.3-23) that is typical for PCB-containing peptides; component 2 (A:  $t_r = 29.5$  min ; B:  $t_r = 28.2$  min) corresponds to free PCB according to its retention time and the absorption maximum about at 685 nm (Fig.3- 42). The underlined fractions were used for MS.

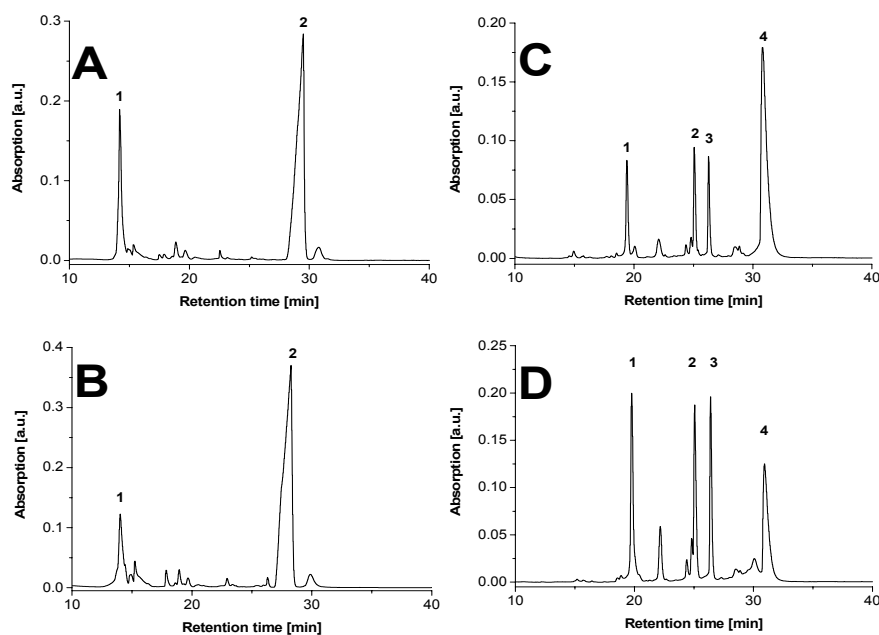


**FIG. 3-41: HPLC ( $\lambda_{\text{detect}} = 650$  nm) of the chromopeptides obtained from tryptic digestion of the reconstituted  $\beta$ -subunit of phycoerythrocyanin (PecB-C84-PCB(A), PecB(C155I)-C84-PCB(B), PecB-C155-PCB(C) and PecB(C84A)-C155-PCB(D)). Spectra of individual peaks of the chromatograms are shown in Fig. 3-43. HPLC were eluted using a gradient (80:20 to 60:40) of formic acid (0.1%, pH 2) and acetonitrile containing 0.1% formic acid.**

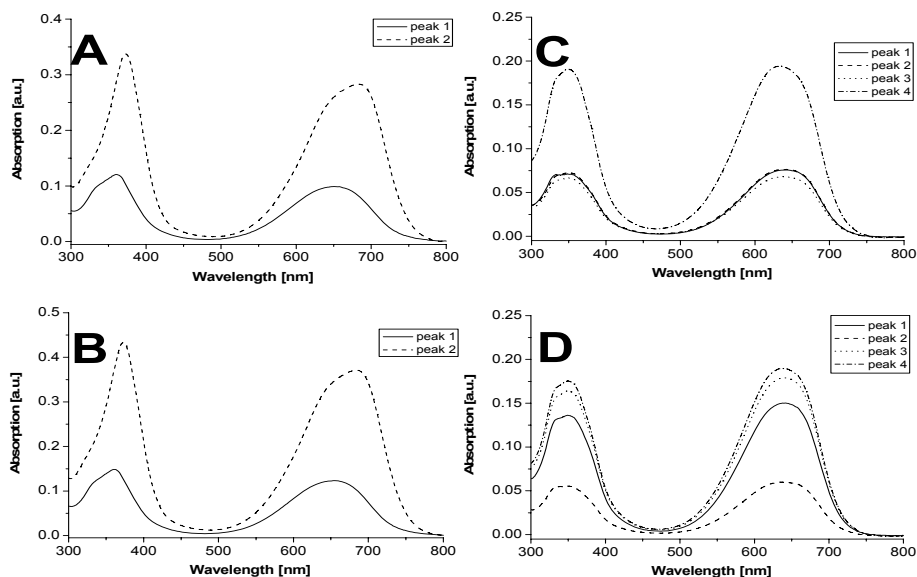


**FIG. 3-42: Absorption spectra of the chromopeptides obtained from tryptic digestion of the reconstituted  $\beta$  subunits of phycoerythrocyanin (PecB-C84-PCB(A), PecB(C155I)-C84-PCB(B), PecB-C155-PCB(C) and PecB(C84A)-C155-PCB(D)).**

Sequences of chromophore-containing peptides were deduced from sequences around the chromophore-binding sites in  $\beta$ -subunits of phycoerythrocyanin from *M. laminosus*. In native PEC subunits, PCB is bound to cysteine residues 82 and 153 of the  $\beta$ -subunit. There is excellent agreement between the measured peptide  $M_r$  values and those values calculated from sequences of beta subunits of phycoerythrocyanin from *M. laminosus* (Table 3-18). The chromopeptide sequences confirm the attachment of PCB to the known binding sites (C84 and C155, consensus sequence) of PecB.

**Table 3-18 Mass of chromopeptides from tryptic digestion**

Biliprotein	Chromopeptide		Peptide peak (m/z)	
			Calc.	Expt.
PecB-C84-PCB	N(78)QAAC(PCB)IR	$[M+2H]^{2+}$	681.09	681.26
PecB(C155I)-C84-PCB	N(78)QAAC(PCB)IR	$[M+2H]^{2+}$	681.09	681.26
PecB-C155-PCB	G(151)DC(PCB)SQLMSEL	$[M+2H]^{2+}$	834.75	834.75
PecB(C84A)-C155-PCB	G(151)DC(PCB)SQLMSELAS YFDR	$[M+2H]^{2+}$	1204.64	1204.42

### 3.5.6 NMR analysis of peptic chromopeptides from reconstituted $\beta$ -subunits of phycoerythrocyanin

RP-HPLC separation of pepsin digests (Fig.3-43) on a C18 column gave one type of colored components, including A:  $t_r=$ 17.1 min and  $t_r=$ 21.2 min ; B:  $t_r=$ 16.8 min and  $t_r=$ 21.0 min; C:  $t_r=$ 18.9min and  $t_r=$ 20.9 min ; D:  $t_r=$ 19.1min and  $t_r=$ 21.1 min, they all had an absorption maximum about at 640nm that is typical for PCB-containing peptides in the solvent system used. The underlined fractions were used to measure NMR spectroscopy.

In order to determine the chromophore structure and mode of linkage to the peptide, the 600-MHz  $^1\text{H}$  NMR spectra of the chromopeptides of PEC  $\beta$ -subunits (PecB-C84-PCB and PecB(C84A)-C155-PCB) in 10 mM TFA/ $\text{D}_2\text{O}$ , were compared (Table 3-19 and Fig. 3-45)

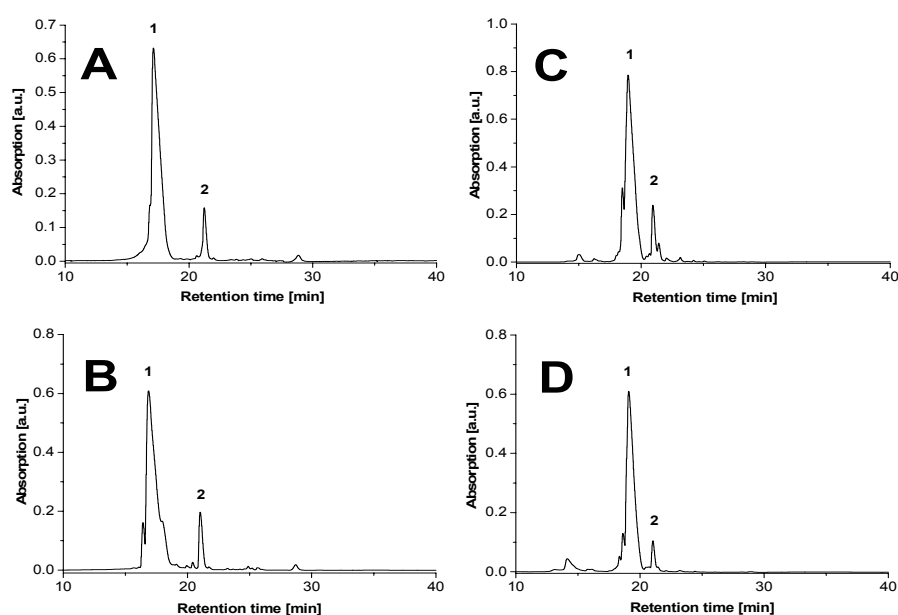


**FIG. 3-43: HPLC ( $\lambda_{\text{detect}} = 650 \text{ nm}$ ) of the chromopeptides obtained from peptic digestion of the reconstituted  $\beta$ -subunits of phycoerythrocyanin (PecB-C84-PCB(A), PecB(C155I)-C84-PCB(B), PecB-C155-PCB(C) and PecB(C84A)-C155-PCB(D)).**

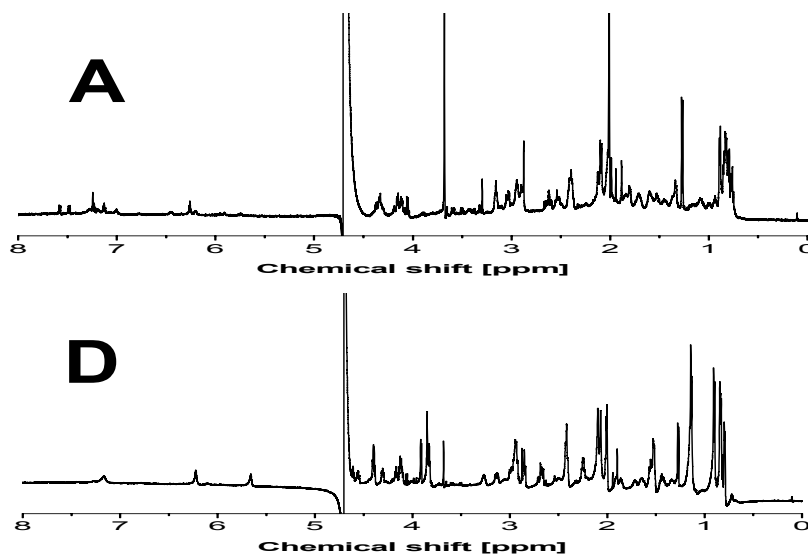


**FIG. 3-45: 1-D  $^1\text{H}$  NMR spectra of chromopeptides of PEC  $\beta$  subunits (PecB-C84-PCB(A), PecB(C84A)-C155-PCB(D)) in 10 mM TFA/D<sub>2</sub>O at 25 °C**

The NMR-spectrum results from a combination of the chromophore and peptide signals. Parallel analysis of the NMR spectra of  $\beta$  subunit of phycoerythrocyanin PecB-C84-PCB(PecB(C84A)-C155-PCB) chromopeptide reveals the expected similarities of the resonance frequencies of the chromophore (Table 3-19). The  $^1\text{H}$  NMR spectral assignments of the bilin moiety of chromopeptides show great similarity with those reported for the blue PEC-derived pigment (Bishop et al., 1986, section 3.2, 3.3 and 3.4). The assignment of the remaining resonances to protein can be made.

In the downfield region of the spectrum, there are three vinylic 10-H, 15-H and 5-H resonances at 7.01(7.16), 6.26(6.22) and 5.74(5.66) ppm, respectively. The  $3^1\text{-H}$  multiplet at 3.51(3.51) ppm is downfield shifted due to its proximity to the sulfur atom, confirming the attachment at this site. The  $3^1\text{-H}$  is coupled to the  $3^2\text{-CH}_3$  group, yielding a doublet at 1.33(1.28) ppm. Similarly the 2-  $\text{CH}_3$  proton (1.13 ppm) is coupled to the 2-H proton (2.53(2.67) ppm). The 3-H proton (multiplet at 2.96(2.98) ppm) is coupled to both the 2-H and  $3^1\text{-H}$ . All these signals are again characteristic of a PCB bound to cysteine at C- $3^1$ . We found that there are only very small differences between the signals of the C84-PCB and C155-PCB chromopeptides, in spite of the

different stereochemistry at C-3<sup>1</sup>. The only distinct difference is for the 10-H and 5-H, which may be diagnostic.

**Table 3-19: <sup>1</sup>H NMR (600-MHz) assignments for peptide HHRNQAAC(PCB)IRD of reconstituted PecB-C84-PCB and peptide TKGDC(PCB)SQL of reconstituted PecB(C84A)-C155-PCB (10 mM TFA/D<sub>2</sub>O).**

Chemical shift		Multiplicity (J <sub>H-H</sub> , [Hz])	Number of H's	Assignment
PecB-C84-PCB	PecB(C84A)-C155-PCB			
7.01	7.16	s	1	10-H
6.26	6.22	s	1	15-H
5.74	5.66	s	1	5-H
3.51	3.51	m	1	3'-H
2.96	2.98	m	1	3-H
2.87	2.93	m	4	8,12-CH <sub>2</sub> CH <sub>2</sub> COOH
2.53	2.67	m	1	2-H
2.40	2.41	m	4	8,12-CH <sub>2</sub> CH <sub>2</sub> COOH
2.10	2.09	s	9	7,13,17-CH <sub>3</sub>
2.08	2.07	s		
2.01	2.00	s		
1.98	1.94	m	2	18- CH <sub>2</sub> CH <sub>3</sub>
1.33	1.28	m	3	3'- CH <sub>3</sub>
/	1.13	/	3	2-CH <sub>3</sub>
0.89	0.90	m	3	18- CH <sub>2</sub> CH <sub>3</sub>
4.05, 3.90	/	q	1	Ala α- CH
1.27	/	d	3	Ala β- CH <sub>3</sub>
4.11, 4.05	/	m	1	Arg α- CH
1.53	/	m	2	Arg β- CH <sub>2</sub>
1.27	/	d	2	Arg γ- CH <sub>2</sub>
/	/	/	2	Arg δ- CH <sub>2</sub>
4.32	/	m	1	Asn α- CH
2.90	/	m	2	Asn β- CH <sub>2</sub>
/	4.61	/	1	Asp α- CH
2.63	2.85	m	2	Asp β- CH <sub>2</sub>
4.32	4.30	m	1	Cys α- CH
3.04	3.13	m	2	Cys β- CH <sub>2</sub>
4.15	4.16	m	1	Gln α- CH
2.39	2.25	m	2	Gln β- CH <sub>2</sub>
/	2.25	/	2	Gln γ- CH <sub>2</sub>
/	3.91	d	1	Gly α- CH
4.20, 4.15	/	m	1	His α- CH
3.16	/	m	2	His β- CH <sub>2</sub>

/	/	/	2	His $\gamma$ -CH <sub>2</sub>
4.36	/	m	1	Ile $\alpha$ -CH
0.83	/	m	1	Ile $\beta$ -CH
/	/	/	2	Ile $\gamma$ -CH <sub>2</sub>
0.83	/	m	3	Ile $\delta$ -CH <sub>3</sub>
/	4.39	q	1	Leu $\alpha$ -CH
/	1.53	m	2	Leu $\beta$ -CH <sub>2</sub>
/	0.83	d	1	Leu $\gamma$ -CH
/	0.81	d	2	Leu $\delta$ -CH <sub>2</sub>
/	4.55	m	1	Lys $\alpha$ -CH
/	1.54	m	2	Lys $\beta$ -CH <sub>2</sub>
/	1.52	d	2	Lys $\gamma$ -CH <sub>2</sub>
/	/	/	2	Lys $\delta$ -CH <sub>2</sub>
/	4.12	m	1	Ser $\alpha$ -CH
/	3.83	m	2	Ser $\beta$ -CH <sub>2</sub>
/	4.06	m	1	Thr $\alpha$ -CH
/	3.60	m	2	Thr $\beta$ -CH <sub>2</sub>
/	1.28	d	3	Thr $\gamma$ -CH <sub>3</sub>

The resonances attributed to the aromatic methyls at C-7, -13, and -17, the ethyl group at C-18, and the propionic acid methylenes at C-8 and -12 are salient features of the spectra of bile pigments. The three aromatic methyls at C-7, -13, and -17 show as singlets at 2.10(2.09), 2.08(2.07) and 2.01(2.00) ppm. The ethyl group at C-18 is seen as two multiplets at 1.98(1.94) ppm (18-CH<sub>2</sub>CH<sub>3</sub>) and 0.89(0.90) ppm (18-CH<sub>2</sub>CH<sub>3</sub>). The multiplet resonances from the methylene group of the propionic acid side chains at C-8 and C-12 were found at 2.87(2.93) and 2.40(2.41) ppm. These results correspond well with the A-ring-linked PCB structure (section 3.2, 3.3 and 3.4)

Analysis of the NMR spectra of PecB-C84-PCB and PecB(C84A)-C155-PCB chromopeptides reveals the resonances of the expected amino acid residues (Table 3-19). All amino acid  $\alpha$ -protons appear between 3.8 and 4.6 ppm. The chemical shifts of the  $\alpha$  hydrogens of Gln and Cys in PecB-C84-PCB chromopeptide are  $\leq 0.03$  ppm upfield from the respective ones in the PecB(C84A)-C155-PCB chromopeptide. No signals were observed for some of the resonances of the  $\delta$  protons of Lys and Arg;  $\gamma$  protons of Gln, His and Ile of the chromopeptide. The expected resonance of Asp  $\alpha$ -CH was hidden under the resonance of the solvent. Major differences in the spectra of the two chromopeptides are evident in the resonances attributed to the Ala, Arg, Asn, Gly, His, Ile, Leu, Lys, Ser and Thr residues. Based on the sequences around

the chromophore-binding sites in PecB-C84-PCB and PecB(C84A)-C155-PCB from *M. lamosus*, chromopeptides sequence HHRNQAAC(PCB)IRD of PecB-C84-PCB and TKGDC(PCB)SQL of PecB(C84A)-C155-PCB were deduced. These confirm the attachment of PCB to the correct site of PecB by CpcS and CpcT lyases.

### 3.5.7 Discussion

The studies described here documented the correct successful reconstitution at both binding sites of PecB in the *E. coli* system. The results of support and extend the conclusion reached by Zhao et al. (2006a, 2007 b) that the lyases CpcS and CpcT catalyses the site- and stereoselective attachment of PCB to cysteine- $\beta$ 84 and 155, respectively, in PecB.

Zhao et al. (2007b) tested whether by combined catalysis of CpcT and CpcS, holo- $\beta$ -PEC could be generated in the *E. coli* system. The results show that the purified phycobiliprotein formed, however, had an absorption maximum at 602 nm, which is red-shifted from that of  $\beta$ -PEC isolated from *M.lamosus* ( $\lambda_{\max} = 598$  nm). By contrast, however, the fluorescence maxima were the same for the reconstituted chromoprotein and the isolated subunit (629 nm). The PCB-C155 and PCB-C84 chromopeptide ratio of 0.7:1 was estimated of from HPLC analysis of the chromopeptides (Fig 3-40, the sequentially reconstituted PecB-C84,C155-PCB<sub>2</sub> ). In  $\beta$ -PEC, PCB-C84 absorbs at longer wavelength than PCB-C155 and is the predominantly fluorescing chromophore. The data thus indicate the correct attachment of PCB to C84, but an incomplete reconstitution of PCB-C155. In particular, doubly chromophorylated, nearly native  $\beta$ -PEC was again obtained only when PCB was attached first in *E. coli* to C155 of PecB with CpcT, and then the supernatant was treated with PCB and CpcS for chromophorylation at Cys- $\beta$ 84.

The two  $\beta$  subunits PecB and CpcB from *M. lamosus* are highly homologous (84% similar, 68% identical)(Fig. 3-46). This similarity seems to include the interaction sites of these subunits with both the S- and T-type lyase, because the same lyase catalyzes the attachment of PCB to PecB and CpcB, with the same site specificity. In this section and section 3.4, two type lyases were identified. CpcS catalyzes the attachment of PCB to cysteine- $\beta$ 84 of CpcB and PecB; CpcT catalyzes the

attachment of PCB to cysteine- $\beta$ 155 of CpcB and PecB.

```

PecB_3  DAFSRVVEQADKKGAYLSNDEINALQAIVADSNKRLDVVNRLTSNASSIVANAYRALVAE 62↵
        D F++VW QAD +G +LSN++++AL +V + NKRLDVVNR+TSNAS+IV NA RAL E↵
CpcB_4  DVFTKVVSQADSRGEFLSNEQLDALANVWKEGNKRLDVVNRITSNASTIVTNAARALFEE 63↵
↵
PecB_63  RPQVFNPGGPCFHHRNQAACIRDLGFILRYVTYSVLAGDTSWMDRCLNGLRETYQALGT 122↵
        +PQ+ PGG + +R AAC+RD+ ILRY+TY++LAGD S++DDRCLNGLRETYQALGT↵
CpcB_64  QPQLIAPGGNAYTNRRMAACLDMEIILRYITYAILAGDASILDDRCLNGLRETYQALGT 123↵
↵
PecB_123 PGDAVASGIKMKKEAALKIANDPNGITKGDCSQLMSELASYFDRAAAAVA 172↵
        PG +VA GI+KMKKEAA+ IANDPNGITKGDCS L+SE+ASYFDRAAAAVA↵
CpcB_124 PGSSVAVGIQKMKKEAAINIANDPNGITKGDCSALISEVASYFDRAAAAVA 173↵

```

**FIG. 3-46: Sequence alignment of the PecB and CpcB from *M. lamosus***

## 3.6 Structure analysis of imidazole-bilin adducts

### 3.6.1 Binding of PCB to CpcS

CpcS was expressed with N-terminal His-tags using the pET-30 vector to facilitate purification and PCB binding assay. The tags did not interfere with the functions of CpcS (Zhao et al. 2006a). When CpcS and PCB were mixed, the resulting absorption and CD changed remarkably within 1 min (Fig.3-48), and then remained stable. Obviously, the formation of CpcS-PCB was quick. The spectral changes indicate strong interactions between CpcS and PCB: judged from the increase and shift of the red absorption band, PCB is bound in a similar, extended conformation as in phycobiliproteins. The ratio of absorption at 634 nm to that at 370 nm, and also the inverted CD, compared to biliprotein (Fig. 3-48), are like those of PCB-ApcA2 (Fig. 3-20). The chromoprotein is only weakly fluorescent, however. The chromophore is retained during gel filtration, where the complex moved as a monomer, indicating a relatively stable CpcS-PCB complex (Fig. 3-47). During Ni<sup>2+</sup>- affinity chromatography, 60% of CpcS retained a PCB chromophore, the released PCB was removed in a wash step with 1 M NaCl. If the affinity-purified complex is denatured by acidic urea, the absorption maximum (690 nm, Fig.3-48) was that of free PCB carrying a 3-ethylidene group (Storf et al. 2001). This indicated that most of PCB was bound non-covalently with CpcS, or is bound so weakly that it is lost in the acidic solution. The complex was therefore analyzed by proteolysis with trypsin under neutral conditions, and subsequent HPLC and mass spectrometry (Fig.3-51)

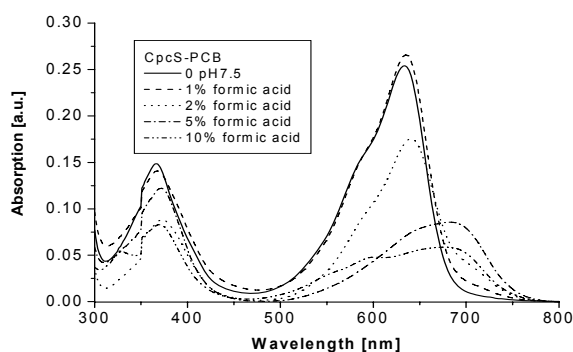


**FIG. 3-47: Absorption of CpcS-PCB in different concentration formic acid in KPB (500 mM, pH 7.5) containing NaCl (100 mM).**

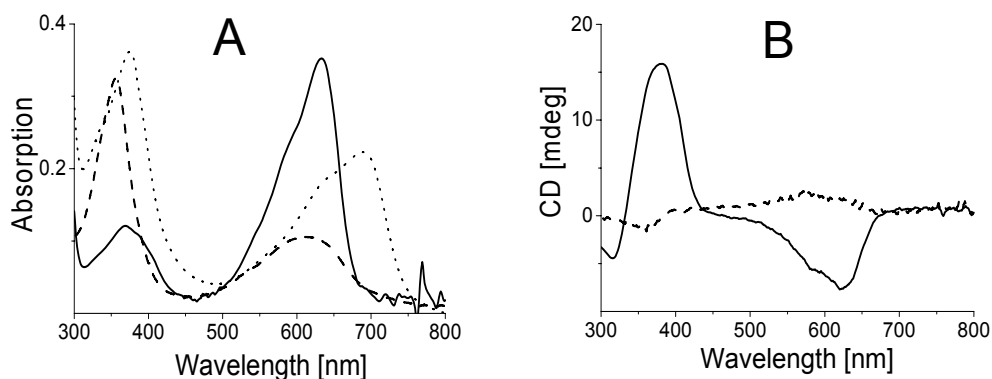


**FIG. 3-48: Binding of PCB to CpcS.** Absorption (A) and CD (B) changes on formation of CpcS-PCB. Spectra of PCB (5  $\mu$ M) in KPB (500 mM, pH 7.5) containing NaCl (100 mM) (---), plus CpcS (15  $\mu$ M) in the same buffer recorded 1 min after mixing (—), this spectrum remained unchanged for 2 hr, and absorption of the same solution after addition of acidic urea (8 M, pH 2) (••••).

### 3.6.2 Imidazole binding PCB

When CpcS, PCB and imidazole were mixed, the resulting absorption changed remarkably within 120 min (Fig.3-49), and then remained stable. The spectral changes indicate strong interactions between CpcS-PCB and imidazole, judged from the decrease and blue shift of the vis absorption band (from 634 nm to 605 nm). The formed complex was named CpcS-PCB-imidazole; it is only weakly fluorescent. The affinity-purified complex is denatured by acidic urea, the absorption maximum (660 nm, not shown) was that of PCB that is covalently attached via C-3<sup>1</sup> to a thiol, including cysteine in a protein. The CD spectrum of the complex is like that of PCB-CpcS (Fig. 3-50). CpcS-PCB-imidazole was digested with trypsin and then analyzed by HPLC with diode-array detection (Fig. 3-51). The colored bands 1 and 2 did only contain traces of several peptides that could not be identified with certainty; the major component is a IPCB-imidazole adduct according to MS (see 3.6.5). This indicated that most of PCB was bound covalently to the imidazole, and that imidazole-PCB was bound non-covalently to CpcS.

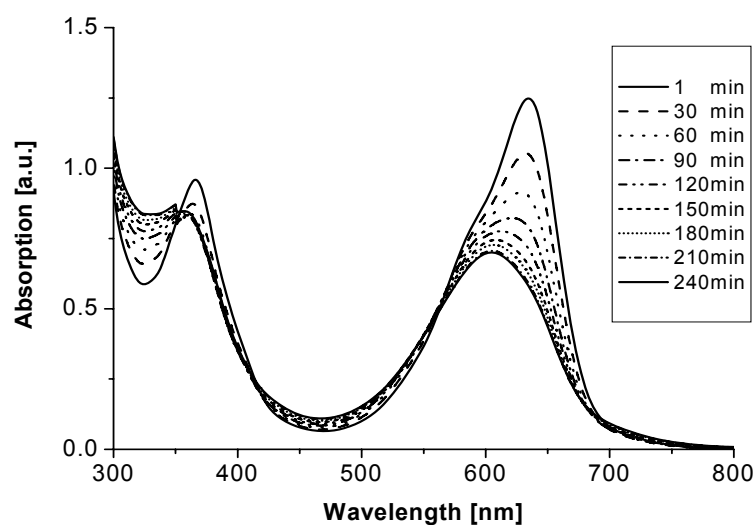


**FIG. 3-49: Binding of PCB to imidazole.** Absorption changes on formation of CpcS-PCB-imidazole after mixing PCB (5  $\mu$ M), CpcS (15  $\mu$ M) plus imidazole (500 mM) in KPb (500 mM, pH 7.5) containing NaCl (100 mM). Sample was maintained at 35  $^{\circ}$ C throughout.

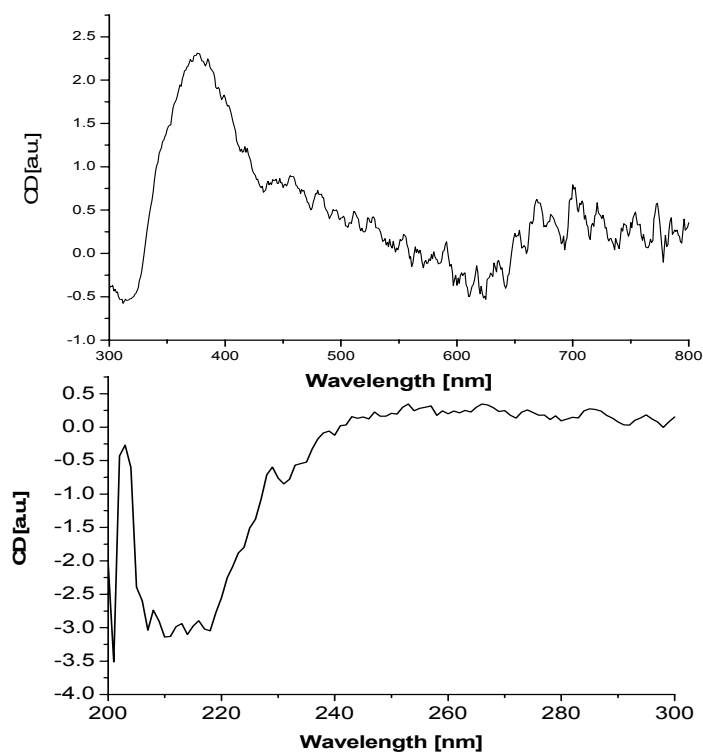


**FIG. 3-50: CD spectra of CpcS-PCB-imidazole** Vis-CD (top) and far-UV CD spectra (bottom) of complex CpcS-PCB-imidazole was purified by  $\text{Ni}^{2+}$  affinity chromatography and dialyzed against KPb (20 mM, pH 7.2)

Since imidazole is absent in CpcS untreated with PCB under the same conditions (not shown), this indicated that residual imidazole was involved and bound with high affinity during the reaction with PCB. To verify this possibility, we repeated the experiment of PCB binding in the presence of increasing concentrations of imidazole; the amounts of bands 1 and 2 containing the IPCB-imidazole adduct increased with imidazole concentration, at the expense of free PCB (Fig. 3-51). Band 1 adduct was named iPCB-imidazole 21 according to its  $t_r$  and structure (3.6.6), band 2 adduct was named iPCB-imidazole 23. To verify the difference of iPCB-imidazole 21 and iPCB-imidazole 23, we repeated the experiment of PCB binding imidazole at different temperature. The results showed increasing amounts of iPCB-imidazole 23 with increasing temperatures, at the expense of free PCB and iPCB-imidazole 21 (Fig. 3-52). Bases on the maximum absorption of iPCB-imidazole 21 ( $\lambda_{\max}$ =633 nm) and iPCB-imidazole 23 ( $\lambda_{\max}$ =648 nm), iPCB-imidazole 23 may be an iPCB-imidazole 21 oxidation product.

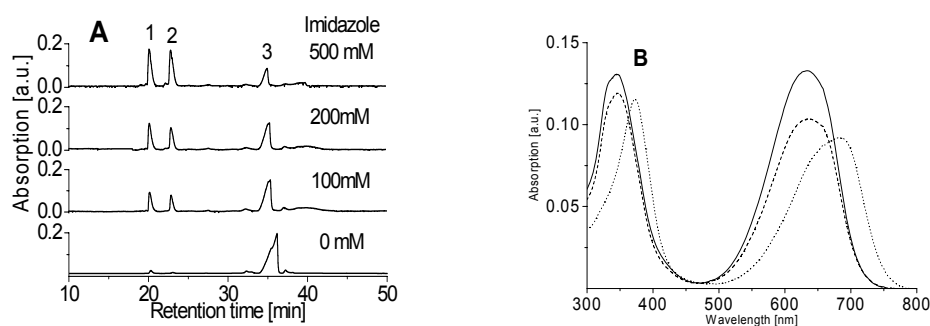


**FIG. 3-51: Dependence of colored products formed during reaction of CpcS, PCB and imidazole on imidazole concentration. HPLC of colored products from tryptic digestion of CpcS-PCB-imidazole.** CpcS (30  $\mu$ M), PCB (10  $\mu$ M) and various concentrations (0, 100, 200, 500 mM) of imidazole were incubated in KPB (500 mM, pH 7.5) containing NaCl (100 mM) at 35  $^{\circ}$ C for 3 hr. The resulting complexes were purified by  $\text{Ni}^{2+}$  affinity chromatography and dialyzed against KPB (20 mM, pH 7.2). The purified complexes (10  $\mu$ M) were then digested with trypsin (40  $\mu$ M) at 37  $^{\circ}$ C for 3 hr, and analyzed by HPLC (Zhao et al. 2007). A: HPLC traces with absorption set to 650 nm, B: absorption spectra of peak 1 (—), peak 2 (- - -) and peak 3 (••••) recorded in line by diode array detection (Tidas, J&M, Aalen).

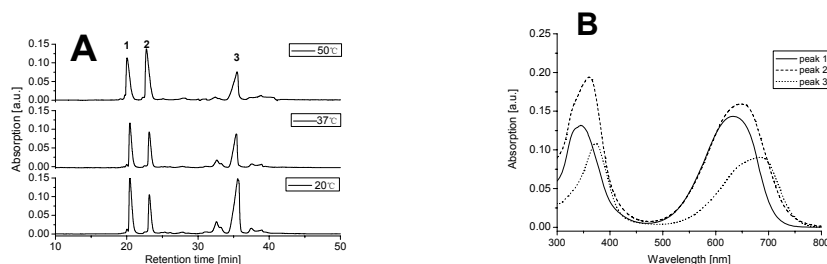


**FIG. 3-52: Temperature dependence of colored proucts formed during reaction of CpcS, PCB and imidazole. HPLC of colored products from tryptic digestion of CpcS-PCB-imidazole.** CpcS (30  $\mu$ M), PCB (10  $\mu$ M) and imidazole (500 mM) were incubated in KPB (500 mM, pH 7.5) containing NaCl (100 mM) at various temperature for 1 hr. Sample preparing methods see Fig. 3-51. A: HPLC traces with absorption set to 650 nm, B: absorption spectra of peak 1 (—), peak 2 (- - -) and peak 3 (••••) recorded in line by diode array detection (Tidas, J&M, Aalen).

### 3.6.3 Chromophore transfer from CpcS-PCB to CpcB(C155I)

The weak fluorescence of CpcS-PCB opened a way to test the chromophore transfer from CpcS-PCB to the final acceptor, CpcB(C155I), because the chromophores become highly fluorescent after correct binding to the native protein. CpcB(C155I) was used as acceptor; the second binding site at cysteine155 was removed by site-directed mutagenesis to avoid complications from unspecific binding (Fig. 3-53). As evidenced by the increase in fluorescence, and by the blue-shifted absorption, the bound PCB was transferred from CpcS-PCB to cysteine-84 of the apoproteins yielding PCB-CpcB(C155I). The spectral features of the final product were identical to those published for the respective chromoprotein (Zhao et al. 2006a). CpcS-PCB therefore seems to be an intermediate in the attachment reaction of PCB to CpcB(C155I) catalyzed by CpcS.

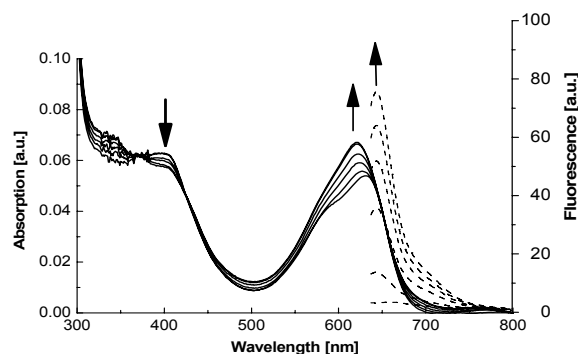


**FIG. 3-53: Chromophore transfer from CpcS-PCB to CpcB(C155I).** Absorption (—) and fluorescence (- - -) after mixing of CpcS-PCB (2  $\mu\text{M}$ ) with CpcB(C155I) (10  $\mu\text{M}$ ). The first spectrum was recorded 1 min after mixing, the subsequent ones every 20 min up to 100 min. The sample was maintained at 35  $^{\circ}\text{C}$  throughout; arrows indicate the spectral changes during the reaction.

### 3.6.4 Chromophore transfer from imidazole-bilin adducts to CpcB(C155I), CpcS or mercaptoethanol

#### 3.6.4.1 Chromophore transfer from CpcS-PCB-imidazole to CpcB(C155I)

During the transfer reaction, the absorption maximum of CpcS-PCB-imidazole shifted significantly from 605 to 618 nm (Fig. 3-54), indicating that the attachment reaction was nearly complete in 3hr. Incubation of CpcS-PCB-imidazole with CpcB(C155I) resulted in the induction of a red fluorescence of the emission maximum at 645 nm. The spectral features of product are similar that of PCB-CpcB(C155I) (Zhao et al. 2006a), indicating that PCB was transferred from CpcS-PCB-imidazole to Cys-84 of CpcB(C155I), and formed PCB-CpcB(C155I).

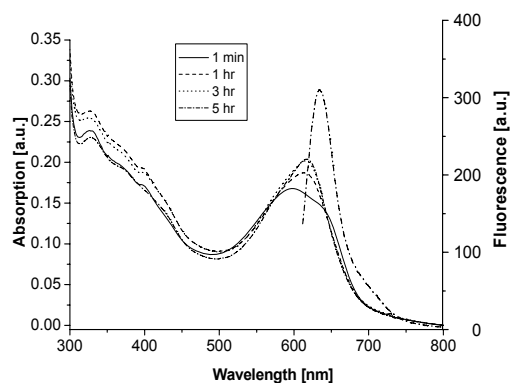


**FIG. 3-54: Chromophore transfer from CpcS-PCB-imidazole to CpcB(C155I).** Absorption (left) and fluorescence (right) after mixing of CpcS-PCB-imidazole (2  $\mu\text{M}$ ) with CpcB(C155I) (10  $\mu\text{M}$ ). The first absorption spectrum was recorded 1 min after mixing, the subsequent ones every 1~2hr up to 5hr, the fluorescence spectrum was recorded 5hr after mixing. Sample was maintained at 35  $^{\circ}\text{C}$  throughout.

### 3.6.4.2 Chromophore transfer from iPCB-imidazole to CpcS

During the transfer reaction, the absorption maximum of iPCB-imidazole shifted significantly from 600 to 634 nm (Fig. 3-55), indicating that the attachment reaction was nearly complete in 2hr. The spectral features of product are similar that of PCB-CpcS (see above), indicating that PCB was transferred from iPCB-imidazole to CpcS, and formed PCB-CpcS. Although PCB is bound non-covalently to CpcS, the equilibrium is shifted from the covalently-bound adduct, iPCB-imidazole.

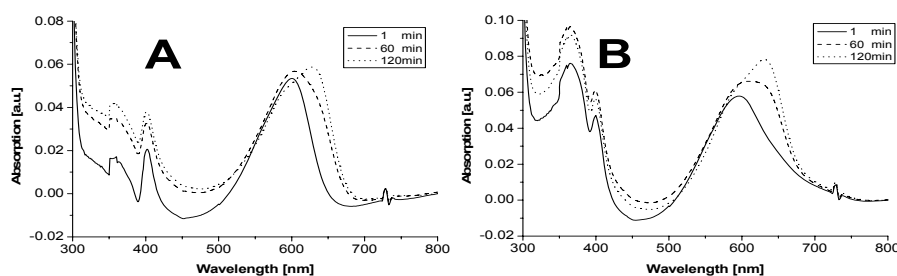


**FIG. 3-55: Chromophore transfer from iPCB-imidazole to CpcS.** Absorption after mixing of iPCB-imidazole 21(A) or iPCB-imidazole 23(B) (2  $\mu\text{M}$ ) with CpcS (10  $\mu\text{M}$ ). The first spectrum was recorded 1 min after mixing, the subsequent ones every 1hr up to 2hr. Sample was maintained at 35  $^{\circ}\text{C}$  throughout.

### 3.6.4.3 Chromophore transfer from iPCB-imidazole to CpcB(C155I)

Last, iPCB-imidazole, was incubated with both CpcS and CpcB(C155I). The ensuing spectral changes are shown in Fig. 3-56. The absorption maximum of iPCB-imidazole shifted significantly from 600 to 618 nm, indicating that the attachment reaction was nearly complete in 2hr. Incubation of iPCB-imidazole, CpcS and CpcB(C155I) also resulted in the induction of a red fluorescence of the emission maximum at 645 nm. The spectral features of final product are similar that of PCB-CpcB(C155I) (Zhao et al. 2006a), indicating that PCB was transferred from iPCB-imidazole to CpcB(C155I), and formed PCB-CpcB(C155I).

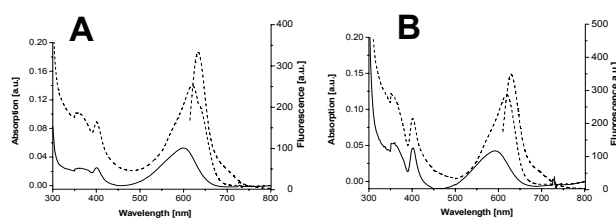


**FIG. 3-56: Chromophore transfer from iPCB-imidazole to CpcB(C155I).** Absorption (left) and fluorescence (right) after mixing of iPCB-imidazole 21(A) or iPCB-imidazole 23(B) (2  $\mu$ M), CpcS (10  $\mu$ M) with CpcB(C155I) (10  $\mu$ M). The Absorption spectrum was recorded 1 min and 2hr after mixing, the fluorescence spectrum was recorded 2hr after mixing. Sample was maintained at 35  $^{\circ}$ C throughout.

### 3.6.4.4 Chromophore transfer from iPCB-imidazole to mercaptoethanol

Imidazolides, viz. amides resulting from the reaction of imidazole with carboxylic acids, are generally very labile; we therefore also tested the reactivity of iPCB-imidazole with mercaptoethanol. When iPCB-imidazole and mercaptoethanol were mixed, the maximum absorption of the mixture did not change within 120 min (Fig. 3-57 A, B), indicating that the chromophore was not cleaved from iPCB-imidazole complex, and transferred to mercaptoethanol. To verify this stability, we reconstituted and HPLC tested the reaction product (Fig. 3-57 a, b). The figures showed that the retention time and the maximum absorption of reaction product is same of that of the initial iPCB-imidazole complex, and not reaction took place to mercaptoethanol. In view of the lability of imidazolides (Schaltiel, 1967), this indicates a different binding mode of imidazole to PCB

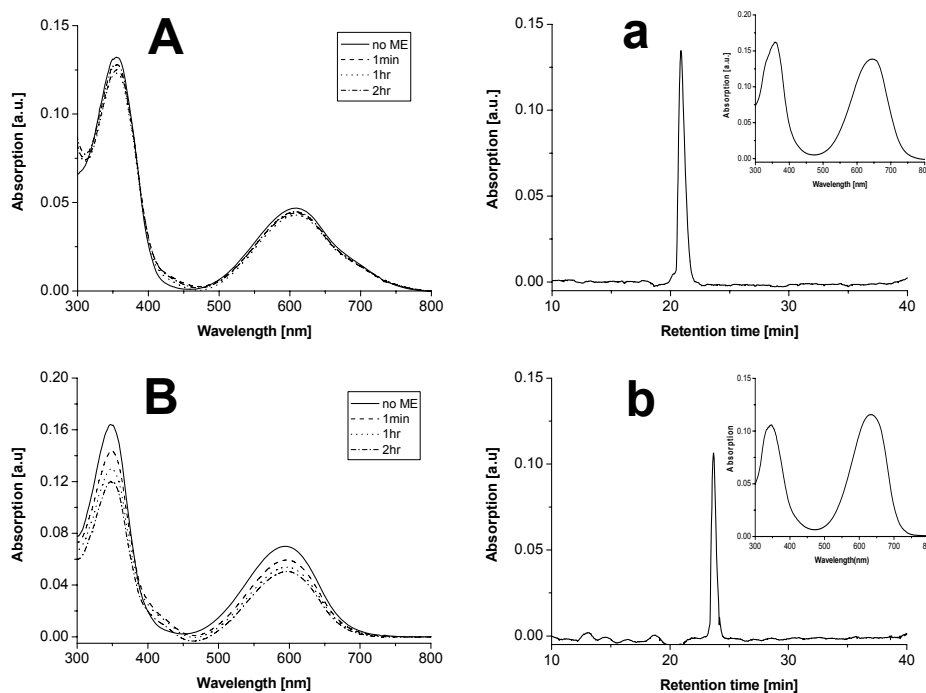


**FIG. 3-57: Absence of chromophore transfer from iPCB-imidazole to mercaptoethanol and HPLC analysis.** Absorption after mixing of iPCB-imidazole 21(A) or iPCB-imidazole 23(B) ( $2 \mu\text{M}$ ) with mercaptoethanol ( $6 \text{ mM}$ ). The first spectrum was recorded 1 min after mixing, the subsequent ones every 1hr up to 2hr. Sample was maintained at  $35 \text{ }^\circ\text{C}$  throughout. The resulting product (iPCB-imidazole 21(a) and iPCB-imidazole 23(b)) were concentrated with Sep-Pak cartridges and analyzed by HPLC (Zhao et al. 2007a)

### 3.6.5 HPLC–ESI-MS analysis of imidazole-bilin adducts

CpcS-PCB-imidazole and CpcS-PCB were digested with trypsin and then analyzed by HPLC with diode-array detection (Fig.3-51). Most of the pigments in the digest of the purified CpcS-PCB (>95%, band 3 in Fig.3-51) was free PCB, as identified by its retention time, its absorption at 690 nm and mass spectroscopy (table 3-21). Most of the colored products in the digest of the purified CpcS-PCB-imidazole (>60%, band1 and band 2 in Fig.3-51) were iPCB-imidazole adducts. The faster moving bands 1 and 2 did contain traces of several peptides that could not be identified with certainty.

**Table 3-21: Molecular masses (m/z) of colored bands in tryptic digest of CpcS-PCB-imidazole or CpcS-PCB**

Peak in Fig. 3-51	Species		Mass (m/z)	
			Calc.	Expt.(intensity)
1	iPCB-imidazole	[PCB+imidazole+H] <sup>+</sup>	655.324	655.321 (100%)
2	iPCB-imidazole	[PCB+imidazole +H] <sup>+</sup>	655.324	655.311(100%)
	Oxidation product chromophore	[PCB-imidazole-2H +H] <sup>+</sup> [PCB-2H+H] <sup>+</sup>	653.309 585.290	653.330(50%) 585.306(10%)
3	PCB	[PCB+H] <sup>+</sup>	587.290	587.301(100%)

There is excellent agreement between the measured iPCB-imidazole 21 *Mr* values and the *Mr* values calculated for a iPCB-imidazole addition product (Table 3-21), which proves PCB was bound covalently with the imidazole. It disproves at the same time the formation of an imidazolidine ( $M_{r_{cal}} = 637 m/z$ ). The major peak at 655.321 m/z represents the singly charged PCB adduct PCB-imidazole. The largest peak in band 2 had a mass of 655.311 m/z matching exactly that of band 1, this is therefore an isomeric PCB-imidazole addition product. Band 2 shows a second peak of 50% intensity that is smaller by 2 mass units (Table 3-21), possibly it relates to an oxidation product of the former. Addition products of PCB are known to oxidize readily to mesobiliverdins (Fairchild et al., 1992), the ease of this may depend on the stereochemistry. Peak 653.31 m/z was analyzed by MSMS, indicating that a chromophore of m/z = 585.31 is formed that is 2 mass units smaller than PCB, i.e. the mass of mesobiliverdin.

### 3.6.6 NMR analysis of imidazole-bilin adducts

For NMR spectroscopy, the iPCB-imidazole 21 and iPCB-imidazole 23 were purified by HPLC again. RP-HPLC separation of PCB adduct was achieved on a C18 column. The <sup>1</sup>H-NMR spectrum of iPCB-imidazole is shown in Fig. 3-58. All assignments refer to the A-ring linkage numbering scheme (see Fig. 3-59) and summarized in Table 3-22.

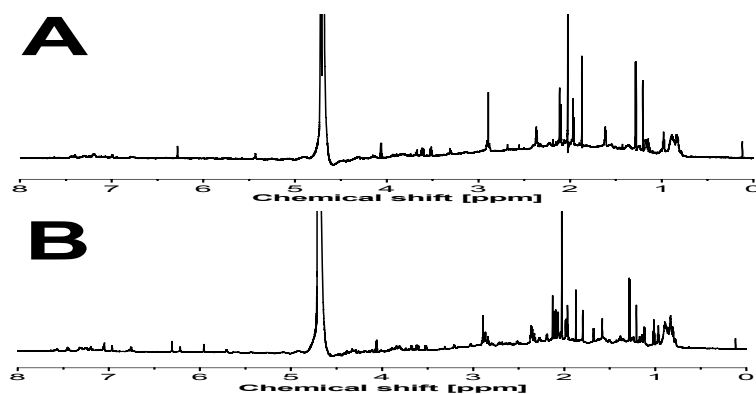


**FIG. 3-58: 1-D  $^1\text{H}$ -NMR spectra of iPCB-imidazole 21 (A) and iPCB-imidazole 23 (B) in 10 mM TFA/ $\text{D}_2\text{O}$**

The NMR-spectra (Fig. 3-58A) result from a combination of the chromophore and imidazole signals (Table 3-22). The downfield region of the spectrum shows three vinylic 10-H, 15-H and 5-H resonances at 7.00, 6.23 and 5.43 ppm, respectively, these peaks are like those of the A-ring-linked  $\alpha$ -1 PCB chromophore (Bishop et al., 1986). The  $3^1$ -H quartet at 4.06 ppm is downfield shifted due to its proximity to the imidazole nitrogen, confirming the attachment at this site. The  $3^1$ -H is coupled to the  $3^2$ - $\text{CH}_3$  group (yielding a doublet at 1.61 ppm). Similarly the 2-  $\text{CH}_3$  signal (1.15 ppm) is coupled to the 2-H proton (3.30 ppm). Remarkably, however, neither the  $3^1$ -H nor the 2-H signals couple to a second set of protons, indicating that there is no 3-H, in agreement, there is no 3-H signal in spectrum.

The resonances attributed to the aromatic methyls at C-7, -13, and -17, the ethyl group at C- 18, and the propionic acid methylenes at C-8 and -12 are salient features of the spectra of bile pigments. The three aromatic methyls at C-7, -13, and -17 singlets resonate at 2.11, 2.10 and 1.97 ppm (singlets). The ethyl group at C-18 is seen as a multiplet at 2.32 ppm (18-  $\text{CH}_2\text{CH}_3$ ) and a triplet at 0.98 ppm (18- $\text{CH}_2\text{CH}_3$ ). The multiplet resonances from methylene group of the propionic acid side chains at C-8 and C-12 were found at 2.89 and 2.37 ppm. The three vinylic 2-H, 4-H and 5-H of imidazole resonate at 7.45, 7.28 and 7.18 ppm, thus confirming, the binding via one of N-atoms. Based on this analysis of the NMR spectrum of iPCB-imidazole 21, we propose the following structure of iPCB-imidazole 21 (Fig. 3-59).

**Table 3-22:**  $^1\text{H}$  NMR(600-MHz) assignments for iPCB-imidazole 21 and iPCB-imidazole 23 (10 mM TFA/D<sub>2</sub>O).

Chemical shift (ppm)		Multiplicity (J <sub>H-H</sub> ,[Hz])	Number of H's	Assignment
iPCB-imidazole 21	iPCB-imidazole 23 (major(minor))			
7.45	7.45	br	1	Imidazole 2-H
7.28	7.31(7.27)	br	1	Imidazole 4-H
7.18	7.20	br	1	Imidazole 5-H
7.00	6.97	s	1	10-H
6.28	6.31(6.22)	s	1	15-H
5.43	5.96(5.71)	s	1	5-H
4.06	4.06	q	1	3'-H
3.30	3.30	m	1	2-H
2.89	2.89(2.83)	m	4	8,12-CH <sub>2</sub> CH <sub>2</sub> COOH
2.37	2.36(2.34)	m	4	8,12-CH <sub>2</sub> CH <sub>2</sub> COOH
2.32	2.26(2.19)	m	2	18- CH <sub>2</sub> CH <sub>3</sub>
2.11	2.12(2.11)	s	9	7,13,17-CH <sub>3</sub>
2.10	2.09(2.07)	s		
1.97	1.98(1.96)	s		
/	1.80	s	3	2- CH <sub>3</sub>
1.61	1.67	d	3	3'- CH <sub>3</sub>
1.15	1.12	d	3	2-CH <sub>3</sub>
0.98	1.02(0.97)	t	3	18- CH <sub>2</sub> CH <sub>3</sub>

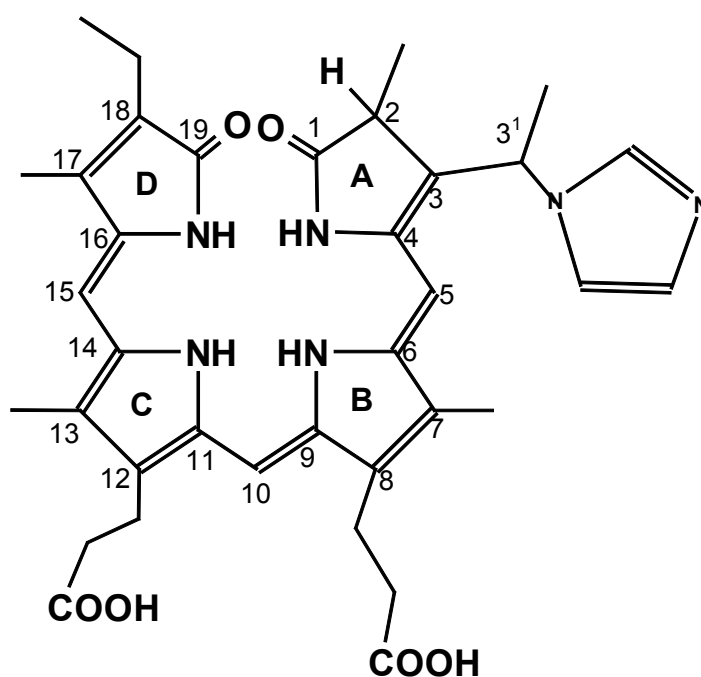


**FIG. 3-59:** Structure of iPCB-imidazole 21 (bound-2,22-DBV)

Parallel analysis of the NMR spectra of iPCB-imidazole 21 and iPCB-imidazole 23 (Table 3-22) shows, like the MS-spectrum, that iPCB-imidazole 23 is a 100:60 mixture of two compounds. The major one resembles closely that of iPCB-imidazole 21. There is in particular again no 3-H visible; however, most bands are somewhat shifted compared to iPCB-imidazole 21. The resonances attributed to the aromatic methyls of C-7, -13, and -17, the three vinylic ones of C-5, -10, and -15, the ethyl group of C-18, and the propionic acid methylenes at C-8 and -12 are salient features of the spectra of both pigments. For the minor compound, we found the 2-CH<sub>3</sub> singlet at 1.80 ppm and the 3<sup>1</sup>-H quartet at 4.06 ppm in the NMR spectrum of iPCB-imidazole 23, indicating a double bond between the C2 and C3. This indicates that the larger part of the mixture is a iPCB-imidazole adduct that is isomeric to iPCB-imidazole 21, and the minor component is the oxidation product, most likely mesobiliverdin (Fig. 3-60). It remains unclear whether the latter is formed during the addition reaction, or only later during workup and chromatography.

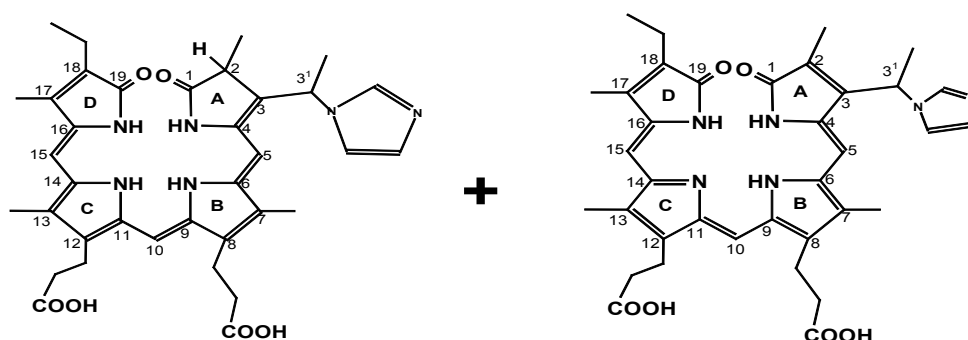


FIG. 3-60: The structure of iPCB-imidazole 23 complex

### 3.6.7 Discussion

Binding of chromophores to lyases has been observed before with both subunits of the E/F-type lyases, but there binding was relatively weak, and most of the chromophore was lost during Ni<sup>2+</sup>-affinity chromatography (Zhao et al. 2006). CpcS binds PCB strongly enough that ~60% are retained in this step during purification, and even a considerable amount (~5%) is retained during SDS-PAGE. However, also in this case most of the chromophore is lost during tryptic digestion, indicating only a weak, probably non-covalent bond compared to the thioether bond present in phycobiliproteins.

The iPCB-imidazole adducts, iPCB-imidazole 21 and iPCB-imidazole 23, were found serendipitously resulting from the presence of residual imidazole in the Ni<sup>2+</sup>-affinity purified CpcS. The structural significance of the iPCB-chromophore is discussed in the next chapter. The adduct formation indicates that CpcS can promote covalent binding of PCB to imidazole, and thereby possibly to histidine. In the phytochromes, which bind the tetrapyrrole chromophore autocatalytically, a histidine is present near the 'classical' binding site around aa 250, which is even conserved, and important for binding, in the new type of phytochromes where the binding cysteine is near the N-terminus (Lamparter et al. 2004). The CpcS-catalyzed binding of PCB to imidazole may relate to these observations, such that the imidazole of a histidine residue binds first to the chromophore, and this in turn promotes binding of the chromophore to another amino acid. Judged from the absorption and NMR spectra of iPCB-imidazole 21 and iPCB-imidazole 23, the chromophore is bound in both products via the 3-ethylidene group. It therefore appears that the ethylidene group present in free PCB can add other amino acids than cysteine, but that the resulting C-N bonds are less stable than the thioether bond resulting from addition of cysteine. There are several histidines in CpcS from *Anabaena* PCC7120, but only one near the N-terminus is conserved; there is no conserved histidine among CpcB and PecB. It is conceivable that the conserved histidine in CpcS can add to the ethylidene double-bond of PCB. Chromophorylation by CpcS might then involve a histidine-bound intermediate; this could be a model for the reaction catalysed by CpcS.

PCB binding to CpcS is fast compared to the lyase-catalyzed chromophorylation of the apoprotein. Kinetic constants for the reactions of all three types of lyases were in the range of 20 min or more (Fairchild and Glazer 1994; Zhao et al. 2006a,b), and even the binding in phytochrome (Borucki et al. 2003) is much slower than the reaction seen with CpcS, which is complete after less than one minute. This indicates that the rate limiting step in the catalytic reaction of CpcS is the transfer to the accepting apoprotein, in this case CpcB. This time (100 min) is very similar to the time constant of the full reaction of CpcS catalyzed chromophore attachment to CpcB. Protein-protein interaction has also been found rate limiting in the EF-Type lyases. Here, the rate of chromophore addition by the E-subunit was much enhanced when it was pre-incubated with the acceptor protein, PecA (Böhm et al. 2007). However, even in this case, the reaction is more than an order of magnitude slower than

chromophore binding by CpcS.

The chromophore transfer from CpcS-PCB to the acceptor apoprotein is the first solid evidence that chromophore binding to CpcS is part of the enzymatic activity. Evidence for such a transfer has also been obtained for the EF-type lyases (Zhao et al. 2006), but the reaction is much more clear-cut with CpcS. Böhm et al. (2007) have recently proposed a chaperone-like action for the E-subunit of the EF-type lyases. Covalent binding is not necessarily contradicting such a mechanism. If the lyase function involves the proper conformational control of the chromophore (Zhao et al. 2004), this may well be assisted by covalent binding to the lyase, as long as this is reversible. A native-like conformation of the chromophore bound to CpcS, is evidenced in this work by the absorption increase in the visible region, and by the CD of CpcS-PCB. A relatively loose binding is finally indicated by the weak fluorescence, and by transfer of the chromophore also to imidazole and mercaptoethanol (see Chapter 3.7)

In summary, PCB binds fast to CpcS, and the chromophore of the resulting CpcS-PCB complex is transferred much more slowly to the Cys84 of the acceptor apoprotein, CpcB. The addition of imidazole to PCB, catalyzed by CpcS, yields two isomeric iPCB-imidazole adducts that are non-covalently bound to CpcS. CpcS catalyses chromophore transfer of the two complexes, with concomitant re-isomerization to PCB, to Cys84 of the acceptor apoprotein, CpcB. The chromophore can also be transferred from the two complexes to CpcS, yielding CpcS-PCB. Based on these experimental results, we propose the following reaction schemes among the CpcS, PCB, CpcB(C155I) and imidazole (Fig. 3-61).

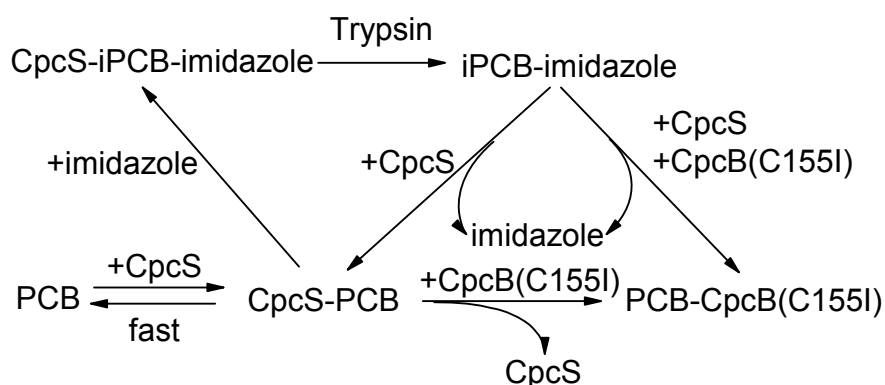


**FIG. 3-61: Reaction schemes of CpcS, PCB, CpcB(C155I) and imidazole.**

## 3.7 Structure analysis of mercaptoethanol-bilin adducts

### 3.7.1 Mercaptoethanol binding PCB catalyzed by CpcS

When CpcS, PCB and mercaptoethanol were mixed, the resulting absorption and fluorescence spectra changed remarkably within 180 min (Fig.3-62), and then remained stable. The spectral changes indicate strong interactions between CpcS, PCB and mercaptoethanol, judged from the decrease and blue shifted absorption band (from 634 nm to 597 nm) and the increase of fluorescence ( $\lambda_{\text{max}} = 630$  nm). The formed complex was named CpcS-PCB-mercaptoethanol. If the affinity-purified complex is denatured by acidic urea, the absorption maximum (660 nm, not shown) was like that of PCB attached via C-3<sup>1</sup> to a cysteine in a chromoprotein or chromopeptide. The CD spectrum of the complex (594 nm (-)/373 nm (+)) is like that of PCB-CpcS (Fig. 3-63). CpcS-PCB-mercaptoethanol was purified by Ni<sup>2+</sup> affinity chromatography and dialyzed against KPB (20 mM, pH 7.2). The purified complex was digested with trypsin and then analyzed by HPLC with diode-array detection (Fig. 3-64). The colored band 1 ( $t_r=29.1$  min) had an absorption maximum at 648 nm and band 2 ( $t_r=30.3$  min) had an absorption maximum at 633 nm that are typical for PCB-containing products. The products contained in colored band 1 and 2 adduct were named iPCB-ME 29 and iPCB-ME 31, respectively, according its retention time and structure (see section 3.7.4). The colored band 3 ( $t_r= 34.1$  min) corresponds to free PCB according to its retention time and the absorption maximum at 684 nm. iPCB-ME 29 and iPCB-ME 31 did contain traces of several peptides that could not be identified by mass spectrometry with certainty. The digestion results indicated that most of PCB was not bound covalently to CpcS (or only very weakly), but that rather some other modification had happened. As will be shown in section 3.7.4, both products are indeed addition products of PCB with ME, with the same modified iPCB chromophore as in the imidazole adducts described in the previous chapter.

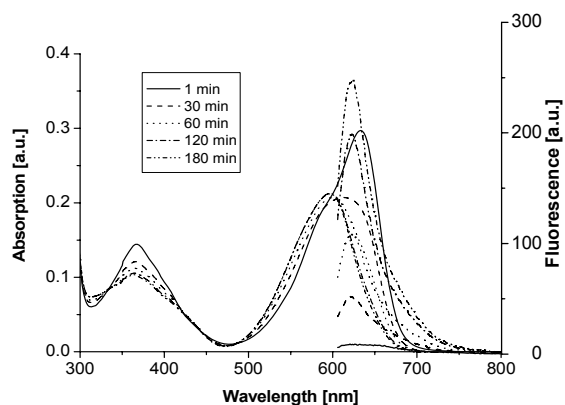


**FIG. 3-62: Binding of PCB to mercaptoethanol.** Absorption (left) and fluorescence (right) after mixing of CpcS (30  $\mu$ M), PCB (10  $\mu$ M) and mercaptoethanol (6 mM). The first spectrum was recorded 1 min after mixing, the subsequent ones every 30-60 min up to 180 min. Sample was maintained at 35  $^{\circ}$ C throughout.

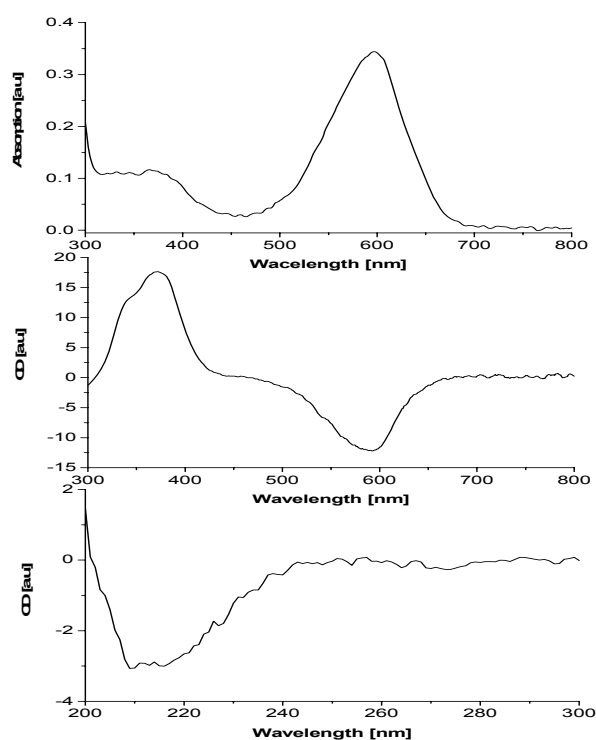


**FIG. 3-63: CD spectra of CpcS-PCB-mercaptoethanol** Absorption (top), Vis- CD (middle) and far-UV CD spectra (bottom) of complex CpcS-PCB-mercaptoethanol was purified by  $\text{Ni}^{2+}$  affinity chromatography and dialyzed against KPB (20 mM, pH 7.2)

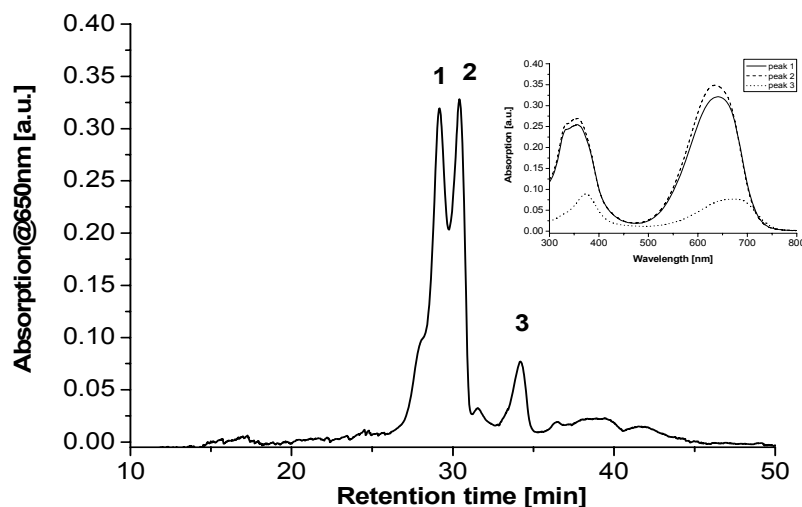
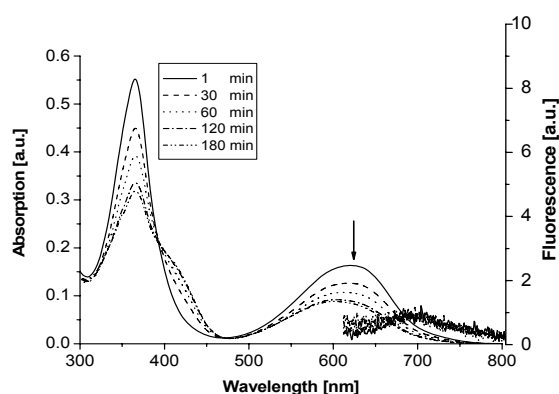


**FIG. 3-64: HPLC of colored products from tryptic digestion of CpcS-PCB-mercaptoethanol reaction mixture.** CpcS (30  $\mu\text{M}$ ), PCB (10  $\mu\text{M}$ ) and ME (60 mM) were incubated in KPB (500 mM, pH 7.5) containing NaCl (100 mM) for 3hr. The resulting complexes were purified by  $\text{Ni}^{2+}$  affinity chromatography and dialyzed against KPB (20 mM, pH 7.2). The purified complexes (10  $\mu\text{M}$ ) were then digested with trypsin (40  $\mu\text{M}$ ) at 37  $^{\circ}\text{C}$  for 3 hr, and analyzed by HPLC (Zhao et al. 2007).

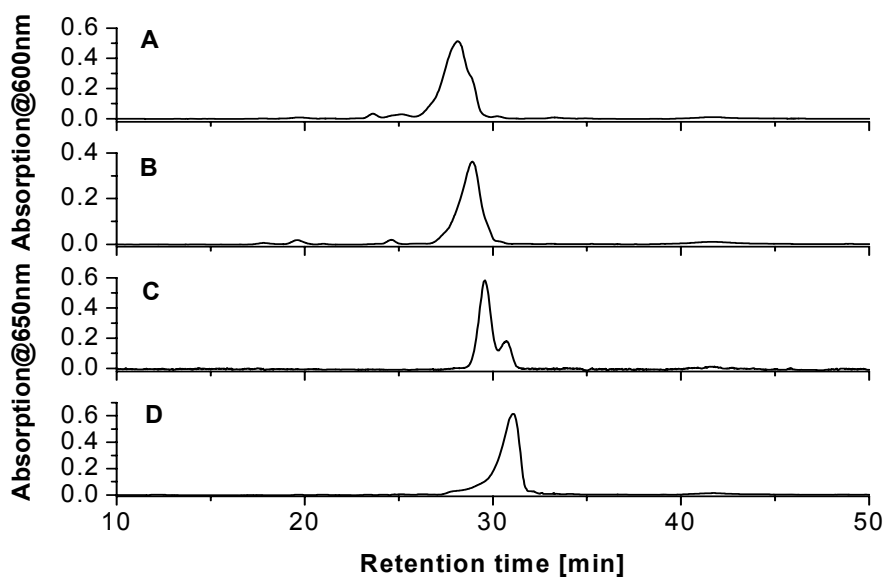
### 3.7.2 Spontaneous binding of mercaptoethanol to PCB

To test the possibility of a chemical reaction of PCB with ME, both were incubated in the absence of CpcS. When PCB and mercaptoethanol were mixed, the absorption decreased and blue shifted from 625 nm to 595 nm within 120 min (Fig.3-65), and then remained stable. The fluorescence ( $\lambda_{\text{max}} = 697$  nm) did not change and remained very weak. The formed complex was named PCB-mercaptoethanol. PCB-mercaptoethanol was concentrated by Sep-Pak cartridges and analyzed by HPLC (Zhao et al. 2007) (Fig. 3-66). It yielded four distinct colored bands, one seemed pure, the other three were mixtures judged from the band-shape that could not be further separated. The colored band A ( $t_r=27.9$  min) had an absorption maximum at 564 nm and band B ( $t_r=28.9$  min) had an absorption maximum at 584 nm both are in the range of PVB-containing products. They were named PVB-ME 27 and PVB-ME 28, respectively, according their retention times and structures (see section 3.7.4). The colored bands C and D correspond to iPCB-ME 29 and iPCB-ME 31 obtained in the reaction with ME, PCB and CpcS (Fig. 3-62) according to their

retention times and the absorption maximum. This indicated that PCB was bound covalently, in a spontaneous reaction, with the mercaptoethanol and formed 4 kinds of colored products PVB-ME 27, PVB-ME 28, iPCB-ME 29, iPCB-ME 31, but that in the presence of CpcS mainly the two iPCB-adducts were formed. The structures of all four complexes were analyzed by mass and NMR spectroscopy.



**FIG. 3-65: Binding of PCB to mercaptoethanol.** Absorption (left) and fluorescence (right) after mixing of PCB (10 $\mu$ M) and mercaptoethanol (6 mM). The first spectrum was recorded 1 min after mixing, the subsequent ones every 30-60 min up to 180 min. Sample was maintained at 35  $^{\circ}$ C throughout. The arrow indicates the spectra changes during the reaction.



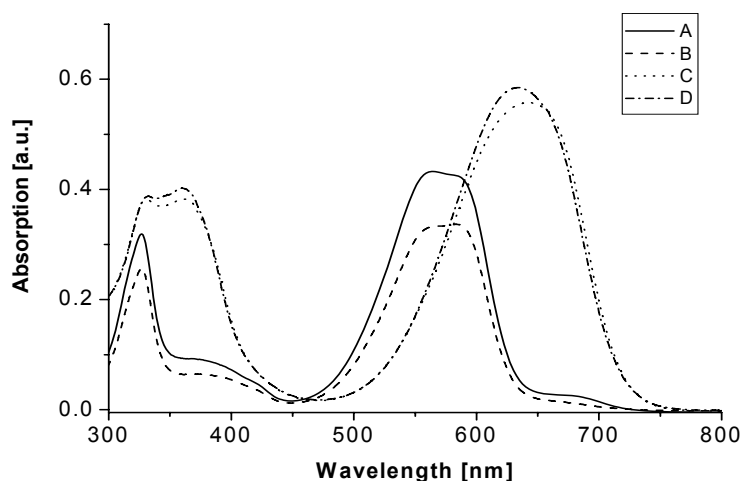


**FIG. 3-66:** HPLC and in situ absorption of PVB-ME 27(A) , PVB-ME 28 (B), iPCB-ME 29 (C) and iPCB-ME 31 (D) obtained from the reaction PCB with mercaptoethanol.

### 3.7.3 Structure analysis of mercaptoethanol-bilin adducts

All four products isolated from the reaction of PCB and ME had identical masses (Table 3-23) that are the sum of both components. They are therefore isomeric addition products.

**Table 3-23:** Molecular masses (m/z) of isolated mercaptoethanol-bilins from Fig. 3-66

Peak	Species		Mass (m/z)	
			Calc.	Expt.
A	PVB-mercaptoethanol	[PCB+ME+H] <sup>+</sup>	665.431	665.245
B	PVB-mercaptoethanol	[PCB+ME +H] <sup>+</sup>	665.431	665.226
C	iPCB-mercaptoethanol	[PCB+ME +H] <sup>+</sup>	665.431	665.236
D	iPCB-mercaptoethanol	[PCB+ME +H] <sup>+</sup>	665.431	665.264

In order to determine the chromophore structure and mode of linkage to mercaptoethanol, the 600-MHz <sup>1</sup>H NMR spectra of the ME-bilin products (PVB-ME 27, PVB-ME 28, iPCB-ME 29 and iPCB-ME 31) in 10 mM TFA/D<sub>2</sub>O, were compared (Fig. 3 -67). All assignments refer to the A-ring linkage numbering scheme (see Fig. 3-69) and are summarized in tables 3-24 and 3-25.

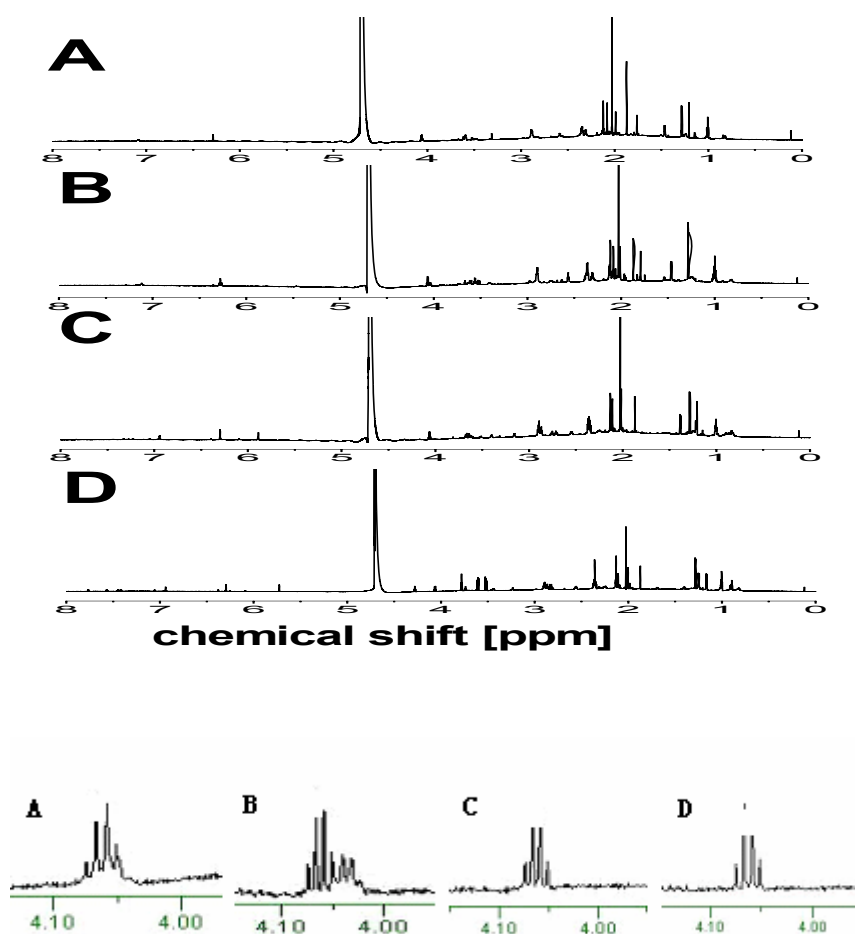


**FIG. 3-67:** 1-D  $^1\text{H}$ -NMR spectra ( up) and  $^{31}\text{H}$  spectra (bottom) of PVB-ME 27(A) , PVB-ME 28 (B) , PCB-ME 29 (C) and PCB-ME 31 (D) in 10 mM TFA/ $\text{D}_2\text{O}$

Parallel analysis of the NMR spectra of PVB-ME 27 and PVB-ME 28 reveals for both well defined resonances of the chromophore (Table 3-24), the assignment of all relevant resonances of a PVB group can be made. Analyzing the downfield region of the PVB-ME 27 (PVB-ME 28) spectrum, one observes only two vinylic 10-H and 15-H resonances at 7.08 (7.11) and 6.29 (6.28) ppm, respectively. These peaks correspond well to the 10-H and 15-H singlets previously observed in the A-ring-linked peptide  $\alpha$ -1 PVB from *Anabaena* PCC7120 (see Chapter 3.1). Noticeably absent is a third downfield vinylic resonance corresponding to 5-H. PVB lacks the methine bridge between rings A and B and, therefore, shows no such resonance, the lack of the respective signal is taken as proof of saturation between the A and B rings. Because the mass spectral data identified both PVB-adducts as addition products, another non-conjugated double bond must exist elsewhere on the PVB-tetrapyrrole moiety. The only alternative position for this unsaturation is between C-2 and C-3, which is

corroborated by the  $^1\text{H}$  NMR spectrum. There are four aromatic methyl singlets at 1.76(1.79), 1.99(2.01), 2.08(2.08) and 2.12(2.12) ppm for C-2, -7, -13, and -17, thereby proving the presence of a double bond between C-2 and C-3, as in PVB.

The doublet at 1.47(1.46) ppm is assigned to  $3^1\text{-CH}_3$  and a quartet at 4.06(4.06) ppm is assigned  $3^1\text{-H}$ . The resonances from the propionyl side chains are found at 2.89(2.90) and 2.35(2.36) ppm. The ethyl group is seen as two multiplet at 2.31(2.31) ppm (18-  $\text{CH}_2\text{CH}_3$ ) and 1.01(1.00) ppm (18- $\text{CH}_2\text{CH}_3$ ). The resonance of 4-H was hidden under the resonance of the solvent, and coupling with the two non-equivalent 5-H protons at 3.49(3.42) and 2.82(2.73) ppm is obvious. The resonance of  $\alpha\text{-CH}_2$  were found at 3.60(3.61) and  $\beta\text{-CH}_2$  at 2.59(2.56) from mercaptoethanol. There are major difference (0.07-0.08 ppm) of the two non-equivalent 5-H protons, and smaller ones ( $< 0.03$  ppm) of the other protons between PVB-ME 27 and PVB-ME 28. We propose the following structure of PVB-ME 27 and PVB-ME 28 (Fig. 3-69). They are isomeric PVB-ME addition products, with different (relative) stereochemistries at C-3 $^1$  and C-4.

**Table 3-24:  $^1\text{H}$  NMR (600-MHz) assignments for PVB-ME 27 and PVB-ME 28 (10 mM TFA/D $_2$ O).**

Chemical shift (ppm)		Multiplicity ( $J_{\text{H-H}}$ , [Hz])	Number of H's	Assignment
PVB-ME 27	PVB-ME 28			
7.08	7.11	s	1	10-H
6.29	6.28	s	1	15-H
/	/	/		4-H
4.06	4.06	q 6.98(6.95)	1	3'-H
3.60	3.61	m	2	ME $\alpha\text{-CH}_2$
3.49	3.42	m	1	5-H
2.89	2.90	m	4	8,12- $\text{CH}_2\text{CH}_2\text{COOH}$
2.82	2.73	m	2	5-H
2.59	2.56	m	1	ME $\beta\text{-CH}_2$
2.35	2.36	m	4	8,12- $\text{CH}_2\text{CH}_2\text{COOH}$
2.31	2.31	m	2	18- $\text{CH}_2\text{CH}_3$
2.12	2.12	s	3	17- $\text{CH}_3$
2.08	2.08	s	3	13- $\text{CH}_3$
1.99	2.01	s	3	7- $\text{CH}_3$
1.76	1.79	s	3	2- $\text{CH}_3$
1.47	1.46	d 6.92(7.28)	3	3'- $\text{CH}_3$
1.01	1.00	t	3	18- $\text{CH}_2\text{CH}_3$

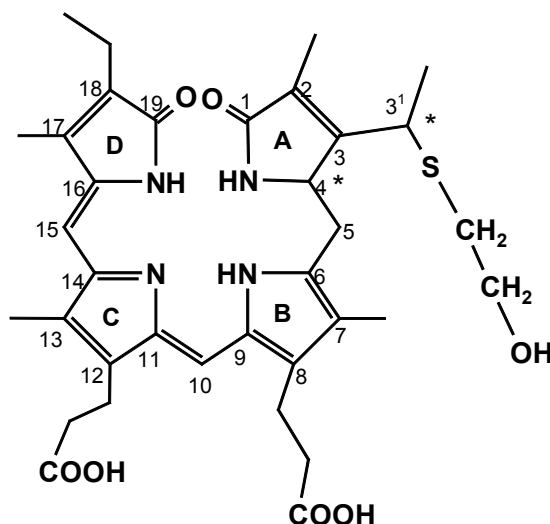


**FIG. 3-69: Structure of PVB-ME 27 and PVB-ME 28 (bound PVB), \* indicate asymmetric C-atoms**

Parallel analysis of the NMR spectra of iPCB-ME 29 and iPCB-ME 31 gives again very similar spectra for the two products (Table 3-25), which are assigned to isomers of adducts containing a novel a 2,22-DBV-ME(=iPCB) chromophore. The downfield region of the spectrum shows three vinylic 10-H, 15-H and 5-H resonances at 6.94(6.94), 6.30(6.30) and 5.89(5.73) ppm, respectively. The 3<sup>1</sup>-H quartet at 4.06 (4.06) ppm is downfield shifted due to its proximity to the thiol, confirming the attachment at this site. The 3<sup>1</sup>-H is coupled only to the 3<sup>1</sup>-CH<sub>3</sub> group (doublet at 1.38(1.25) ppm). Similarly the 2-CH<sub>3</sub> shows as a quartet (1.21(1.17) ppm) that is only coupled to the 2-H proton (3.42(3.44) ppm). Remarkably, neither the 3<sup>1</sup>-H nor the 2-H singlets therefore couple to a second set of protons, indication that there must be a double bond at C-3.

All other signals attributed to the chromophore are similar to that of a PCB adduct. The resonances attributed to the aromatic methyls at C-7, -13, and -17, the ethyl group at C-18, and the propionic acid methylenes at C-8 and -12 are salient features of the spectra of bile pigments. There are three methyls at C-7, -13, and -17 singlets resonating at 2.13(2.13), 2.11(2.11) and 2.02(2.02) ppm. The ethyl group at C-18, is seen as a multiplet at 2.24(2.24) ppm (18-CH<sub>2</sub>CH<sub>3</sub>) and a triplet at 1.01(1.01) ppm (18-CH<sub>2</sub>CH<sub>3</sub>). The multiplet resonances from the methylene groups of the propionic acid side chains at C-8 and C-12 were found at 2.90(2.90) and 2.36(2.36) ppm. The α-CH<sub>2</sub> and β-CH<sub>2</sub> of mercaptoethanol resonate at 3.64(3.64) and 2.87(2.87) ppm, thus confirming, the binding via the S-atom. There are major chemical shift difference (0.13 ppm) of the 3<sup>1</sup>-CH<sub>3</sub> protons, and several smaller differences (< 0.05 ppm) of

other respective signals between iPCB-ME 29 and iPCB-ME 31. Based on these datas, we propose the following structure of iPCB-ME 29 and iPCB-ME 31 (Fig. 3-70). They are isomeric PCB-ME addition product, with different relative stereochemistries at C-2 and C-3<sup>1</sup>.

**Table 3-25:** <sup>1</sup>H NMR (600-MHz) assignments for iPCB-ME 29 and iPCB-ME 31 (10 mM TFA/D<sub>2</sub>O).

Chemical shift (ppm)		Multiplicity (J <sub>H-H</sub> , [Hz])	Number of H's	Assignment
iPCB-ME 29	iPCB-ME 31			
6.94	6.94	s	1	10-H
6.30	6.30	s	1	15-H
5.89	5.73	s	1	5-H
4.06	4.06	q 6.92	1	3'-H
3.64	3.60	t 6.23	1	ME α-CH <sub>2</sub>
3.42	3.44	m	1	2-H
2.90	2.90	m	4	8,12-CH <sub>2</sub> CH <sub>2</sub> COOH
2.87	2.87	m	2	ME β-CH <sub>2</sub>
2.36	2.36	m	4	8,12-CH <sub>2</sub> CH <sub>2</sub> COOH
2.24	2.24	m	2	18- CH <sub>2</sub> CH <sub>3</sub>
2.13	2.13	s	3	17-CH <sub>3</sub>
2.11	2.11	s	3	13-CH <sub>3</sub>
2.02	2.01	s	3	7-CH <sub>3</sub>
1.38	1.25	d 6.98(7.47)	3	3'- CH <sub>3</sub>
1.21	1.17	d 6.91(6.96)	3	2-CH <sub>3</sub>
1.01	1.01	t	3	18- CH <sub>2</sub> CH <sub>3</sub>

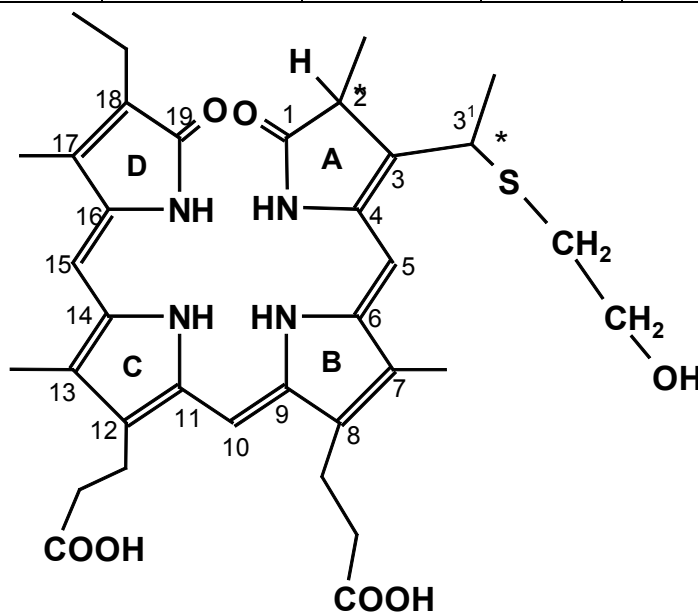


**FIG. 3-70:** Structure of iPCB-ME 29 and iPCB-ME 31 (bound 2,22-DBV) , \* indicate asymmetric C-atoms

### 3.7.4 Chromophore transfer from CpcS-PCB to ME

In order to clarify the function of CpcS in the formation of the ME products, we used the weak fluorescence of CpcS-PCB as compared to that of the CpcS-PCB adduct. When CpcS-PCB and mercaptoethanol were mixed, the ensuing absorption and fluorescence spectra (Fig.3-71) led to a final state with spectra that were nearly identical to those in Fig. 3-62. This indicates that PCB was transferred from CpcS-PCB to mercaptoethanol, and formed a CpcS-iPCB-mercaptoethanol complex (CpcS-iPCB-ME).

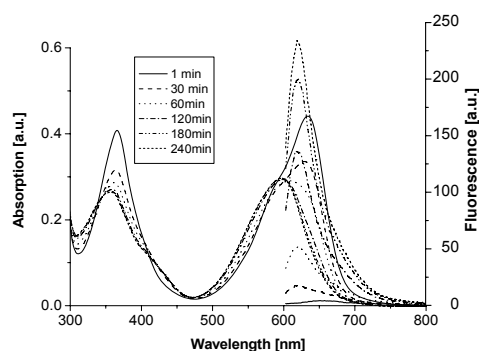


**FIG. 3-71: Chromophore transfer from CpcS-PCB to mercaptoethanol.** Absorption (left) and fluorescence (right) after mixing of CpcS-PCB (10 $\mu$ M) and mercaptoethanol (6 mM). The first spectrum was recorded 1 min after mixing, the subsequent ones every 30-60 min up to 240 min. Sample was maintained at 35 °C throughout.

### 3.7.5 Chromophore transfer from bilin adducts to CpcB(C155I)

#### 3.7.5.1 Chromophore transfer from CpcS-iPCB-ME to CpcB(C155I)

Incubation of CpcS-iPCB-ME with CpcB(C155I) resulted in an increased and red shifted absorption (from 599 to 618 nm) and fluorescence emission (from 630nm to 645 nm) (Fig. 3-72). The reaction was nearly complete in 3 hr. The spectral features of final product after 3 hr are similar that of PCB-CpcB(C155I) (Zhao et al. 2006a), indicating that iPCB was isomered and transferred from CpcS-iPCB-ME to CpcB(C155I), and formed PCB-CpcB(C155I).

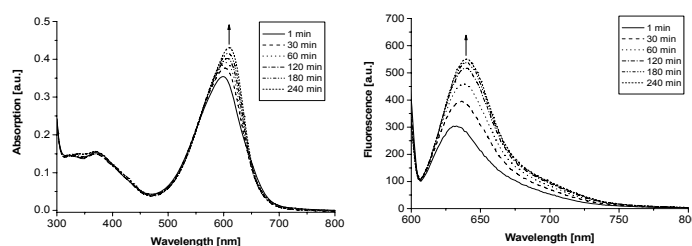


**FIG. 3-72: Chromophore transfer from CpcS-iPCB-ME to CpcB(C155I).** Absorption (left) and fluorescence (right) after mixing of CpcS-iPCB-mercaptoethanol ( $2 \mu\text{M}$ ) with CpcB(C155I) ( $10 \mu\text{M}$ ). The first absorption and fluorescence spectra were recorded 1 min after mixing, the subsequent ones every 30-60 min up to 240 min. Sample was maintained at  $35^\circ\text{C}$  throughout. Arrows indicate the spectral changes during the reaction.

### 3.7.5.2 Chromophore transfer from iPCB-ME to CpcB(C155I)

Next, we tested if the chromophores can be transferred from the isolated iPCB-ME and PVB-ME adducts to cysteine-84 of the acceptor protein, CpcB(C155I). First, iPCB-ME 29 and 31, respectively, were incubated with both CpcS and CpcB(C155I). The ensuing spectral changes are shown in Fig. 3-73. The absorption maximum of iPCB-ME increased and shifted significantly from 598 to 618 nm, the reaction was nearly complete in 3hr. Incubation of PCB-ME, CpcS and CpcB(C155I) also resulted in the induction of a red fluorescence with an emission maximum at 642 nm. The spectral features of final product are similar that of PCB-CpcB(C155I) (Zhao et al. 2006a), indicating that iPCB was transferred, with concomitant isomerization to PCB, from iPCB-ME to CpcB(C155I), and formed PCB-CpcB(C155I).

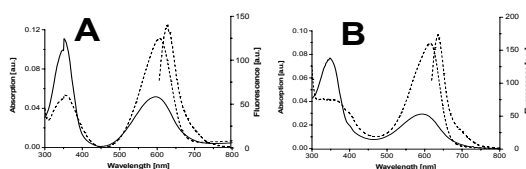


**FIG. 3-73: Chromophore transfer from iPCB-ME to CpcB(C155I).** Absorption (left) and fluorescence (right) after mixing of iPCB-ME 29(A) or iPCB-ME 31 (B) ( $2 \mu\text{M}$ ), CpcS ( $10 \mu\text{M}$ ) with CpcB(C155I) ( $10 \mu\text{M}$ ). The absorption was recorded 1 min (—) and 3hr (...) after mixing, the fluorescence spectrum was recorded 3hr after mixing. Sample was maintained at  $35^\circ\text{C}$  throughout.

### 3.7.5.3 Chromophore transfer from PVB-ME to CpcB(C155I)

Last, PVB-ME 27 and 28, were incubated individually with both CpcS and CpcB(C155I). The ensuing final spectra after 3 hr are shown in Fig. 3-74. The absorption maximum of PVB-ME increased significantly and shifted from 556 to 550 nm, and an intense fluorescence ( $\lambda_{\text{max}} = 588$  nm) arose simultaneously. The spectral features of final product were reminiscent of  $\alpha$ -PEC in the Z-form, indicating that also the PVB chromophore is transferred to the apoprotein by CpcS.

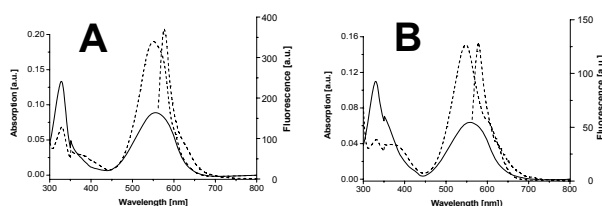


**FIG. 3-74: Chromophore transfer from PVB-ME to CpcB(C155I).** Absorption (left) and fluorescence (right) after mixing of PVB-ME 27 (A) or PVB-ME 28 (B) (2  $\mu$ M), CpcS (10  $\mu$ M) with CpcB(C155I) (10  $\mu$ M). The absorption was recorded 1 min (—) and 3hr (...) after mixing, the fluorescence spectrum was recorded 3hr after mixing. Sample was maintained at 35  $^{\circ}$ C throughout.

### 3.7.6 Discussion

PCB binds to CpcS and ME, forms CpcS-iPCB-ME complexes with the novel iPCB chromophore, which can then be transferred with concomitant re-isomerization to the acceptor apoprotein CpcB(C155I). The intermediate complex was digested with trypsin and then analyzed by HPLC; it yields two isomeric iPCB-ME addition products. CpcS catalyses transfer of the chromophore of both complexes to the acceptor apoprotein CpcB(C155I), again with concomitant re-isomerization to PCB, to yield PCB-CpcB(C155I). PCB binds to ME also auto-catalytically, in this case four products could be isolated by HPLC that contain ME. Two of them are identical to the aforementioned iPCB-ME complexes, two contain a PVB chromophore. CpcS catalyses not only transfer of the iPCB, but also of the PVB chromophore to the acceptor apoprotein CpcB(C155I), to yield PCB-CpcB(C155I) and PVB-CpcB(C155I) respectively. Based on these experimental results, we propose the following reaction

scheme among CpcS, PCB, CpcB(C155I) and ME (Fig. 3-75) .

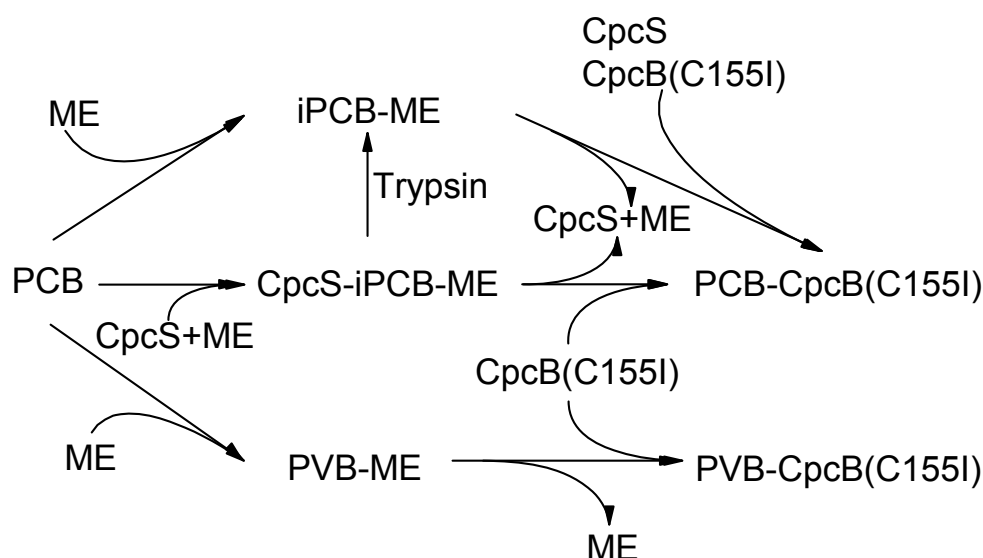


**FIG. 3-75: Reaction of the CpcS/PCB/CpcB(C155I)/ME system.**

Formation of the iPCB-ME and PVB-ME adducts is again principally an “artifact” due to the presence of mercaptoethanol in the reaction mixture. Chromophore attachment catalyzed by CpcS does not require a thiol as cofactor, unlike the catalytic activity of the  $\alpha$ 84-lyase, CpcE/F. However, their formation indicates that PCB can covalently binds to thiols without additional catalysts, and thereby possibly also to a cysteine residue of the lyase, or the acceptor protein. Moreover, none of the products is a true PCB adduct that contains the 2H,3H-PCB chromophore; instead two pairs of products are formed that contain isomerized chromophores, viz, iPCB or PVB. Autocatalytic addition to the acceptor protein is known in the classical and in the new type of phytochromes where the binding cysteine is near aa 250 and the N-terminus, respectively (Lamparter et al. 2004), and in ApcE from *Anabaena* sp. PCC 7120 (Zhao et al., 2005). In the latter cases, the bound chromophore is PCB. PecA adds autocatalytically PCB, but this reaction is of low fidelity compared to lyase-catalyzed reaction. It yields a low absorbance, low fluorescence PCB-PecA adduct, its absorption maximum is at  $\lambda=645$  nm (Boehm et al., 2007). The covalent binding of ME to PCB, yielding iPCB-ME, may relate to these observations, such that the thiol binds first to the chromophore, and this then promotes transfer of the chromophore to another amino acid, including cysteine. Judged from the absorption and NMR spectra

of iPCB-ME 29, 31, the chromophore is bound in the two products via the 3<sup>1</sup>-C, and can be transferred to Cys of apoproteins. This is an indication that such intermediary addition products may also occur during the enzymatic reaction which involves nucleophilic addition to the ethylidene group, either of cofactor, or of a suitable amino acid, including in particular imidazoles and cysteines.

The heterodimeric lyase/isomerase (PecE/PecF) catalyzes both the covalent attachment of PCB and the concurrent isomerization of the molecule to PVB, yielding PecA-PVB (see 3.1). The heterodimeric lyase/isomerase (CpcE/CpcF) catalyzes the covalent attachment of PCB, yielding CpcA-PCB (see 3.2). These two  $\alpha$ -apoproteins (CpcA and PecA) from *Anabaena* PCC7120 are highly homologous (75% similar, 58% identical). The relative lyase's homologies of CpcE and PecE (59% similar, 48% identical), CpcF and PecF (49% similar, 31% identical) are relatively low. There is a question how to explain the different roles of heterodimeric lyases, or what is the catalytic mechanism of heterodimeric lyase. Both require thiols (Fairchild et al., 1992; Zhao et al., 2000) in the *in vitro* reconstitution, and there are also thiols present in the *E. coli* cells. It is conceivable from our results that these thiols function as the nucleophiles that transiently add to the chromophore, yielding the 2,22H-adduct (iPCB). Depending on the lyases, this chromophore then isomerizes either to the PCB (=2,3H) or the PVB (=4,5H) chromophore during transfer to the apoproteins, CpcA and PecA, respectively. This idea is summarized in the following scheme (Fig. 3-76).

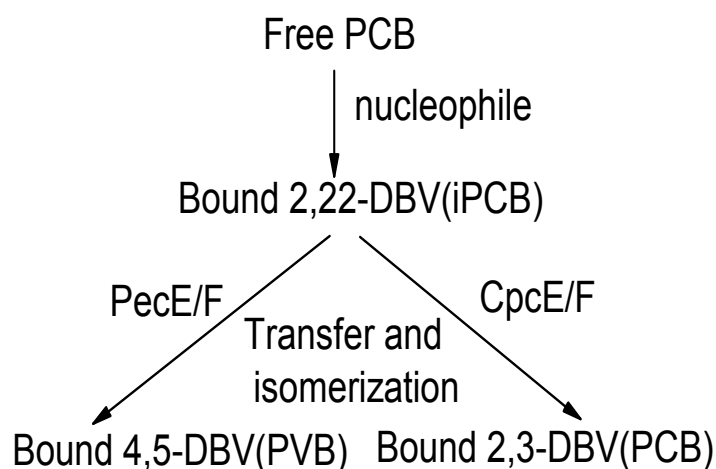


**FIG. 3-76: Minimum mechanism for chromophore transfer and isomerization**

## 3.8 Attachment of a locked chromophore, 15Za-PCB

### 3.8.1 Structure of 15Za-PCB

The locked chromophore, 15Za-PCB, was a generous gift of Prof. K. Inomata (Kanazawa University, Japan). The structure of 15Za-PCB is shown in Fig. 3-77.

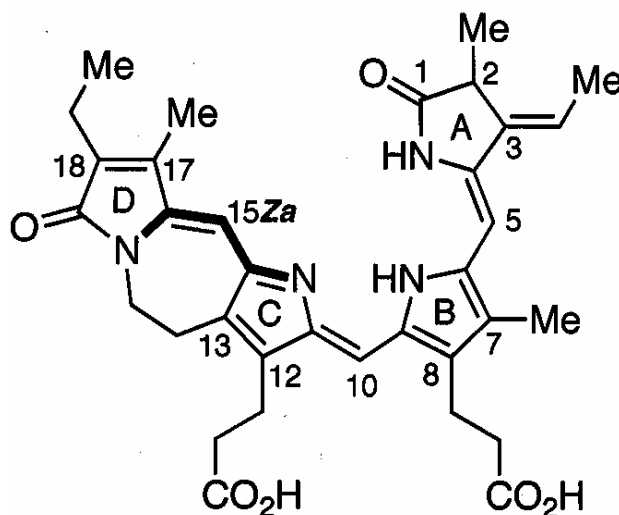
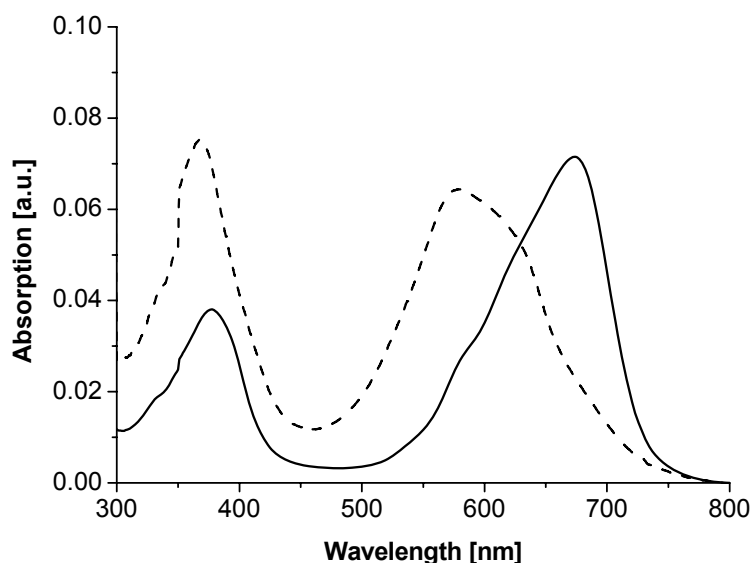


FIG. 3-77: Structure of 15Za-PCB

### 3.8.2 Absorption and extinction coefficient of 15Za-PCB

We measured absorption of 15Za-PCB under different conditions (Fig. 3-78). The spectrum of the free 15Za-PCB in KPP (pH 7.5) is structured, with the main band around 580 nm and an intense shoulder around 680 nm. In acidic MeOH, the red absorption is slightly blue-shifted ( $\lambda_{\max} \approx 680\text{nm}$ ), but has only a low extinction coefficient ( $\epsilon_{678} = 18,200 \text{ M}^{-1}\text{cm}^{-1}$ ), compared with the absorption and extinction coefficient of free PCB ( $\lambda_{\max} \approx 690\text{nm}$ ,  $\epsilon_{690} = 37,900 \text{ M}^{-1}\text{cm}^{-1}$ ) (Cole et al., 1967). This indicates that the locked conformation of 15Za-PCB is unlike the one assumed by PCB after protonation.



**FIG. 3-78:** Absorption spectra of free 15Za-PCB in acidic MeOH (—) and neutral KPP (pH=7.5, ----)

### 3.8.3 Chromophore binding assay

#### 3.8.3.1 Complex formation of 15Za-PCB with CpcS

When CpcS and 15Za-PCB were mixed, they quickly formed a complex. Already the first spectrum taken “immediately” after mixing (~1 min) had changed markedly. The absorption had shifted from 579 to 632 nm and there is a marked fluorescence at  $\lambda_{\max} \approx 680\text{nm}$  (Fig.3-79, 3-78), both then remained stable. These spectral changes indicate strong interactions between CpcS and 15Za-PCB. The complex 15Za-PCB-CpcS is only weakly fluorescent, indicating some conformational flexibility of the bound chromophore. The absorption of 15Za-PCB-CpcS is similar of the PCB-CpcS ( $\lambda_{\max} = 634\text{nm}$ ), while fluorescence spectrum had red shifted from 630nm to 680nm (section 3.6).

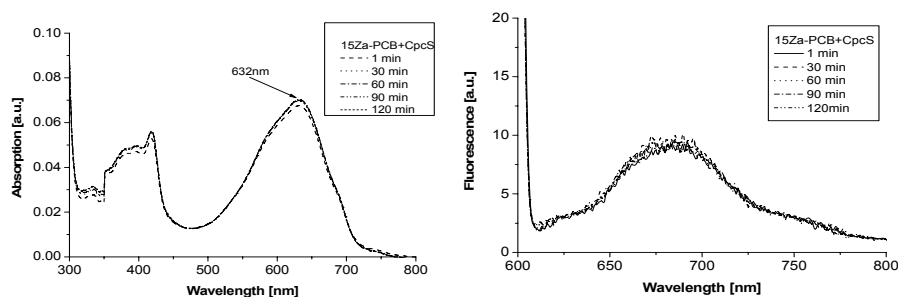


**FIG. 3-79: Binding of 15Za-PCB to CpcS.** Absorption (left) and fluorescence (right) changes on formation of 15Za-PCB-CpcS. Spectra of 15Za-PCB (5  $\mu$ M) in KPB (500 mM, pH 7.5) containing NaCl (100 mM) plus CpcS (15  $\mu$ M) recorded 1 min after mixing, this spectra remained unchanged for 2 hr.

### 3.8.3.2 Spontaneous binding of 15Za-PCB with CpcB(C155I)

When CpcB(C155I) and 15Za-PCB were mixed, the resulting absorption and fluorescence changed very fast in 1 min and slowly increase over a period of 2hr (Fig.3-80). The complex formation of 15Za-PCB-CpcB(C155I) is kinetically similar to the spontaneous formation of “aberrant” PCB-CpcB(C155I) (with incorrectly attached chromophore). The formed 15Za-PCB-CpcB(C155I) has a main absorption band around 660 nm, a weak shoulder around 700 nm and a fluorescence band around 670 nm; this is quite different from “aberrant” PCB-CpcB(C155I), which absorbs at  $\lambda_{\max} \approx 640$  nm.

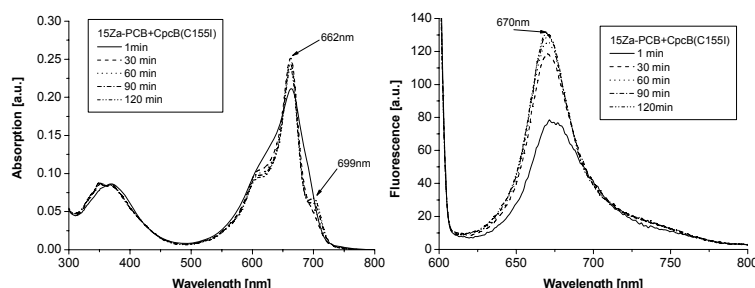


**FIG. 3-80: Binding of 15Za-PCB to CpcB(C155I).** Absorption (left) and fluorescence (right) changes on formation of 15Za-PCB-CpcB(C155I) after mixing 15Za-PCB (5  $\mu$ M) and CpcB(C155I) (15  $\mu$ M) in KPB (500 mM, pH 7.5) containing NaCl (100 mM).

### 3.8.3.3 15Za-PCB binding to CpcB(C155I) catalyzed by CpcS

When CpcB(C155I), CpcS and 15Za-PCB were mixed, the resulting absorption and fluorescence changes were like a superposition of the changes occurring with CpcS and CpcB(C155I) individually. The first spectra obtained 1 min after mixing was like that shown in Fig. 3-79, over the next two hrs the spectra then changed to those observed with CpcB(C155I). (Fig.3-81). Obviously, the reaction first produced an intermediate 15Za-PCB-CpcS (see 3.8.3.1), then the chromophore is transferred from 15Za-PCB-CpcS to CpcB(C155I), forming 15Za-PCB-CpcB(C155I). It indicates that the formation of 15Za-PCB-CpcB(C155I) is slower than the formation of 15Za-PCB-CpcS. The formation of 15Za-PCB-CpcB(C155I) has a main absorption band around 660 nm, a weak shoulder around 700 nm and a fluorescence band around 670 nm. These spectral features are the same as that of the spontaneous addition product (3.3.8.2). It indicated that the formation of 15Za-PCB-CpcB(C155I) was autocatalyzed, and did not need the CpcS lyase. This is a remarkable difference, compared with the formation of native PCB-CpcB(C155I), which absorbs at  $\lambda_{\max}$  = 619 nm (section 3.4) and has a stronger fluorescence.

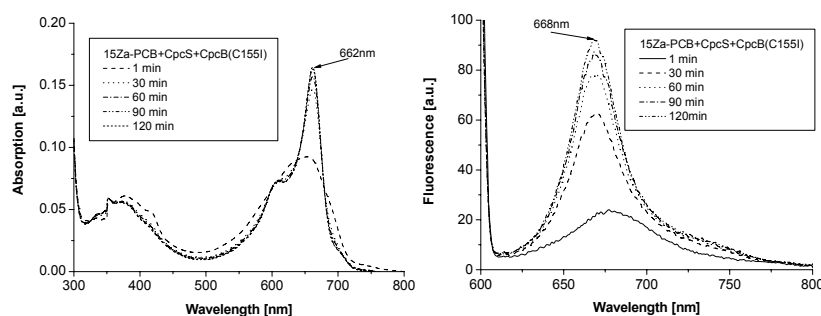


**FIG. 3-81: Binding of 15Za-PCB to CpcB(C155I) in the presence of CpcS.** Absorption (left) and fluorescence (right) changes on formation of 15Za-PCB-CpcB(C155I) after mixing 15Za-PCB (5  $\mu$ M), CpcB(C155I) (15  $\mu$ M) and CpcS (15  $\mu$ M) in KPB (500 mM, pH 7.5) containing NaCl (100 mM).

### 3.8.4 Denaturation of the 15Za-PCB addition products

When we denature the adduct 15Za-PCB-CpcS with 8 M urea, the spectra at pH 7 or pH 1.5 are identical to the respective spectra of the free chromophore (Fig. 3-82, right).

It indicates that the 15Za-PCB is not bound covalently to the lyase CpcS. If, however, the adduct 15Za-PCB-CpcB(C155I) is denatured, the spectra at pH 7 or pH 1.5 are different to the respective spectra of the free chromophore (Fig. 3-82, left). The blue-shift of ~20 nm, as compared to the free chromophore, is compatible with the loss of one conjugated double bond, this is compatible with an addition to the 3-ethylidene group of 15Za-PCB and formation of a covalent bond to the apoprotein CpcB(C155I).

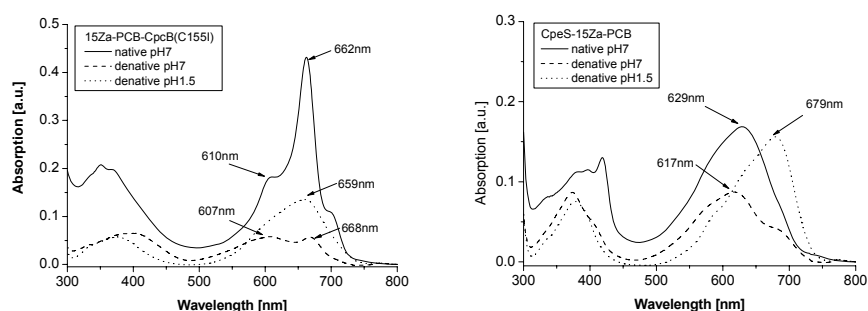


**FIG. 3-82: Absorption of the denatured 15Za-PCB-CpcB(C155I) (left) and 15Za-PCB-CpcS (right) in different conditions**

### 3.8.5 Chromophore reaction with $Zn^{2+}$

The resulting fluorescence changed markedly during the formation of chromophore addition products. These complexes were further characterized by  $Zn^{2+}$  fluorescence staining. To detect the effect of  $Zn^{2+}$ , we first tested the reaction of the free chromophore with  $Zn^{2+}$ . When 15Za-PCB and 1.5 M Zn-acetate were mixed, the absorption decreased and broadened over a period of 30 min, and a weak fluorescence nearly reached saturation within 10 min (Fig.3-83). There is already a double-peaked intermediate after 1 min that is almost as fluorescent as the final product. The results of PCB reaction with Zn-acetate showed that the absorption of the intermediate (1 min) and after 30 min is different, and the fluorescence at shorter wavelength (Fig. 3-84). It indicated that the pigment can form a Zn-complex that has a weak fluorescence. These differences probably reflect different conformations of the two chromophores.

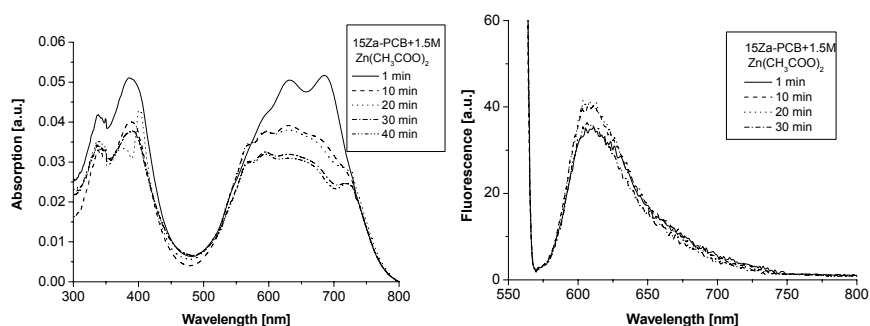


**FIG. 3-83: Binding of 15Za-PCB to  $Zn^{2+}$ .** Absorption (left) and fluorescence (right) changes on formation of 15Za-PCB- $Zn^{2+}$  after mixing 15Za-PCB ( $5 \mu M$ ) in 1.5 M Zn-acetate ( $pH=5.6$ ) Compare Fig. 3-78 for the spectra of the free chromophore.

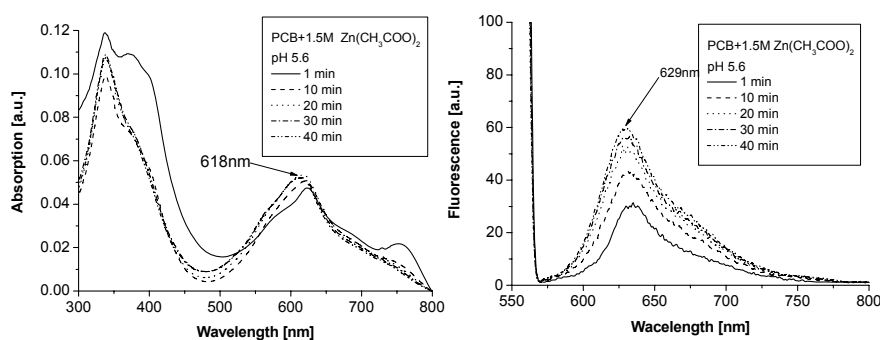


**FIG. 3-84: Binding of PCB to  $Zn^{2+}$ .** Absorption (left) and fluorescence (right) changes on formation of PCB- $Zn^{2+}$  after mixing PCB ( $5 \mu M$ ) in 1.5 M Zn-acetate ( $pH=5.6$ ).

### 3.8.6 The effect of pH on chromophore spectra

As stated in section 3.8.3.2, the CpcB(C155I) adduct with 15Za-PCB absorbs quite differently than the adduct with PCB. Since one reason might be a differential protonation, bilin spectra are strongly pH-dependent. We therefore did a pH-titration of the locked chromophore 15Za-PCB, in parallel with PCB (Fig. 3-85). It indicates that the  $pK_a$  is shifted from  $\sim 6$  (PCB) to  $\sim 5$  (15Za-PCB). The  $pK_b$  of PCB ( $\sim 10$ ) is not seen in this titration, but the changes with 15Za-PCB at high pH indicate that the  $pK_b$  is also shifted to lower pH. Maybe incomplete protonation is then reason for the low  $\epsilon$  of 15Za-PCB in acidic methanol (see section 3.8.2). Since this difference may be

relevant in the protein bound situation, one reason for different adduct spectra with CpcB(C155I) is possibly that 15Za-PCB is not protonated; PCB is protonated in all native structures (Sawatzki et al., 1990).

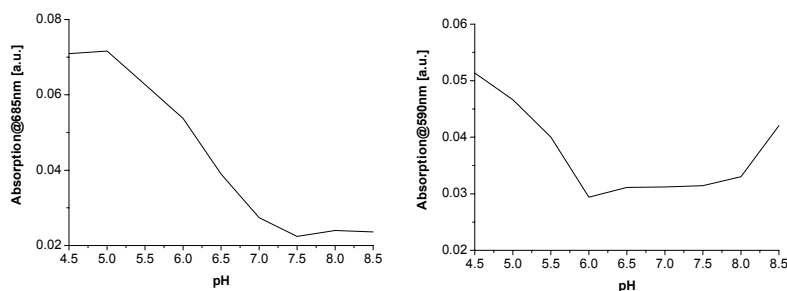


**FIG. 3-85: The effect of pH on PCB (left) and 15Za-PCB (right) absorption( 500mM KPP).**

### 3.8.7 Conclusion

PCB and the conformationally restricted 15Za-PCB have the following different characters.

There are distinct differences in the absorption, extinction coefficient in acidic methanol and pKa of the free 15Za-PCB, compared with that of free PCB.

Similar to PCB, 15Za-PCB is not bound covalently to the lyase CpcS, and bound covalently to the apoprotein CpcB(C155I), judged for their denatured absorption spectra. However, autocatalytic binding gives spectroscopically the same product as binding catalyzed by CpcS, The absorption of 15Za-PCB-CpcS is similar of that of PCB-CpcS, while fluorescence is red shifted by 50 nm.

Two pigments can form Zn-complexes, they have different absorption and fluorescence.

### 3.9 Test of a protein with Heat-like repeats, DOHH, for lyase activity

DOHH (deoxyhypusine hydroxylase) has a Heat-like repeats protein from the malaria parasite, *Plasmodium falciparum* (Kaiser et al., 2006, 2007), it completes hypusine biosynthesis through hydroxylation. These repeats are characteristic for the E/F-type biliprotein lyases. DOHH is, in particular, distantly homologous to CpcE, we therefore tested the chromophore-attaching activity using the binding assay of PCB binding to PecA in the presence of DOHH (gift of Prof. A. Kaiser (University Siegburg-Bonn, Germany)). None of the experiments (DOHH replacing PecE and PecF (Fig. 3-86), or only PecF (Fig. 3-87) or PecE (Fig. 3-88) did result in any significant changes, indicating that DOHH has no bilin lyase activity. The small changes, in particular a shoulder around 420 nm, are possibly due residual interactions, or to unspecific thiol binding to C-10 and formation of rubinoid pigment(s) with other factors in the expression system.

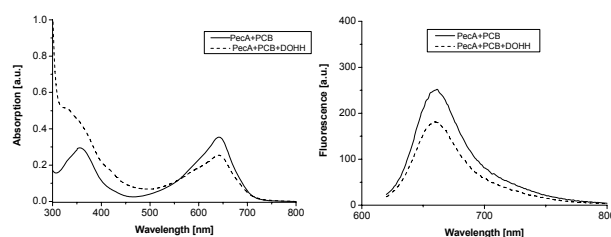


**FIG. 3-86: Effect of DOHH on binding of PCB to PecA.** Absorption (left) and fluorescence (right) of PCB-PecA after mixing PCB and PecA with, or without, DOHH in the reconstitution system (Tab. 2-1)

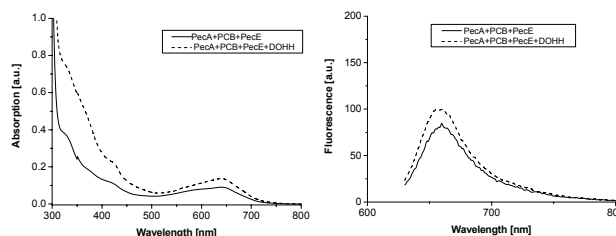


**FIG. 3-87: Effect of DOHH on binding of PCB to PecA.** Absorption (left) and fluorescence (right) of PCB-PecA after mixing PCB, PecA and PecE with, or without, DOHH in the reconstitution system (Tab. 2-1)

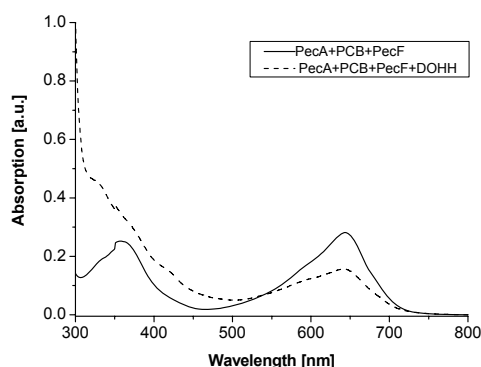


**FIG. 3-88: Effect of DOHH on binding of PCB to PecA.** Absorption of PCB-PecA after mixing PCB, PecA and PecF with, or without, DOHH in the reconstitution system (Tab. 2-1)

We therefore repeated the experiment of PCB binding to PecA in the presence of high concentration DOHH supernatant, in parallel with an “empty” cell supernatant (Fig. 3-89). The result shows that there is a difference in the 423 nm region, and DOHH and control supernatant both have this absorption band. It indicates that the difference is not due to DOHH, and since there is no change in the region >500 nm, we conclude that DOHH is inactive as bilin lyase.

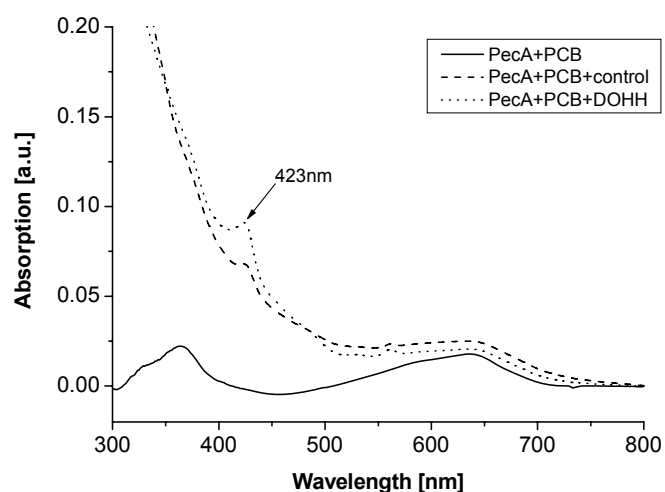


**FIG. 3-89: Effect of DOHH on binding of PCB to PecA.** Absorption of PCB-PecA after mixing PCB and PecA with, or without, DOHH/control in the reconstitution system (Tab. 2-1)

Based on above experiments, DOHH has no chromophore-attaching activity. Since Heat-like repeats are believed to be responsible for protein-protein interactions rather than for catalytic activities, it is likely that they have this function, too, in DOHH.

## 4: Concluding Discussion

### 4.1 A multi-plasmidic expression system

The first reconstitution system for a biliprotein, holo-CpcA, was developed by Tooley et al. (2001). We also established a multi-plasmidic expression system for reconstitution of phycobiliproteins in *E. coli*. After cloning of apophycobiliprotein genes, phycobilin biosynthesis genes and lyase genes from several cyanobacteria, various phycobiliproteins could be biosynthesized in the heterologous *E. coli* system using dual plasmids containing their respective genes. CpcA, PecA and subunits of allophycocyanin from *Anabaena* PCC7120 as well as C84-PCB and C155-PCB of PecB and CpcB from *M. laminosus* were successfully prepared by this way.

This heterologous system in *E. coli* is more advantageous than reconstitution *in vitro* in the following three respects: (1) On reconstitution *in vitro*, where the lyase and acceptor genes were first overexpressed in *E. coli*, and then reconstituted *in vitro* with isolated phycobilins, the lyases and/or the apoproteins were often difficult to dissolve and refold. Reconstitution yields *in vitro* were therefore often low and poorly reproducible, and even in favorable cases the system had to be optimized individually for each biliprotein. An example is the phycoerythrin reconstitution (Zhao et al., 2007a). Such problems are largely avoided with the *E. coli* system, in particular if expressions are done at low temperatures (16 – 20 °C). (2) *In vitro* reconstitution is complicated by the fact that most apo-phycobiliproteins bind phycobilins spontaneously, but with low fidelity and often with low yield. This results in unwanted products and mixtures that are difficult to analyze and handle, and complicate enzymatic studies. As shown by controls without lyase genes, spontaneous addition is, in *E. coli*, generally at or below the detection limits. (3) The system allows, at least in principle, the *in vivo* labeling of fusion products of phycobiliproteins with target proteins. A disadvantage of the system is that enzymatic and mechanistic studies are more difficult. However, for such work carefully chosen pairs of “well behaving” lyase(s) and acceptor proteins can be used as case studies. The *E. coli* reconstitution system also has some potential problems like imbalanced expressions, incompatibility of plasmids and low yields,

but this was generally no problem, and, in case, could be successfully managed.

Recently, Guan et al. (2007) successfully biosynthesized  $\alpha$ -PC in *E. coli* by using a single expression vector. The applied vector, pCDFDuet, harbored two cassettes: one cassette carried the genes *hox1* and *pcyA* required for conversion of heme to phycocyanobilin (PCB), and the other cassette carried *cpcA* encoding CpcA along with the lyase genes *cpcE* and *cpcF*. The work showed that one vector can express five genes. There were four vectors (pACYADuet, pCDFDuet, pCOLADuet, pETDuet) included in our multi-plasmidic expression system. It is expected that this multi-plasmidic expression system can principally express up to 20 genes, which may suffice for a simple phycobilisome including ApcA,B,C,D,E,F; CpcA,B; HO1, PcyA, CpcE,F, CpcS,T; L<sub>CR</sub>, L<sup>30</sup><sub>R</sub>, L<sup>8</sup><sub>R</sub>; methylase(s) (Miller et al., 2008; Shen et al., 2008b) and methionine-peptidase(s). It seems feasible that, on this basis, one could now produce in *E. coli* fully matured integral biliproteins like APC, CPC, or even simple phycobilisomes

In extending this methodology to other systems, the expression in other prokaryotic or in eukaryotic cells of an appropriate selection of genes encoding enzymes and apophycobiliprotein subunit-containing fusion proteins could lead to the intracellular production of constructs carrying specific bilins at unique locations, with broad utility in addressing a variety of questions in cell biology.

## 4.2 A multi-step analytical system

We also established a multi-step analytical system to analyze the reconstituted phycobiliproteins. The system includes the following five important steps.

- 1) Phycobiliproteins, apoprotein and lyase with His-tag were purified by using a combination of chromatographic techniques. A quick enrichment of the His<sub>6</sub>-tagged biliproteins is possible by Ni<sup>2+</sup>-affinity chromatography. For better purification, it was followed by fast Performance Liquid Chromatography (FPLC) and ion exchange (DEAE) chromatography (Zhao et al., 2002).

- 2) Quantitative absorbance, fluorescence, circular dichroism spectra of the products were recorded, and compared with those of the natural subunits of various

phycobiliproteins from several cyanobacteria. The chromophore was further characterized by using the same techniques on the denatured biliproteins. Covalent binding was established by SDS-PAGE followed by  $Zn^{2+}$  fluorescence staining (Berkelman and Lagarias, 1986; Tooley et al., 2001, 2002; Parbel et al., 1997; Nomsawai et al., 1999).

3) Proteolytic digestion of purified reconstituted phycobiliproteins with trypsin or pepsin. The digested samples were purified by P-6 DG (Bio-Rad) column and Sep-Pak C18 cartridge, and then fractionated by HPLC on reverse phase C18 column and detection of chromopeptides with diode array detection (Swanson and Glazer, 1990). This micro-preparative system without KPP is suitable for preparing samples for MS and NMR spectroscopy.

4) Tryptic chromopeptides were analyzed by mass spectrometry in positive ion mode with a nano-ESI source. Sequences of these peptides could be found when MS-MS capabilities of the instrument are employed. This method is comparable in performance to amino acid sequencing of chromophore-containing peptides (Klotz and Glazer, 1985; Hunsucker et al., 2004), but it requires far less material, and allows a better control of chromophore modification. There are indications that certain chromophore types can also be distinguished by MS-MS spectroscopy (Matthias Plösch, private communication, 2008).

5) Peptic chromopeptides were analyzed by  $^1H$ -NMR spectroscopy (Bishop et al., 1986, 1987), but the method was improved by using 2 mm diameter microtubes to minimize protein requirements.

In combination, these techniques can prove the chromophore structure and the correctness of chromophore attachment to the apoprotein in reconstituted phycobiliproteins. Most of them have been used before, but the combination and standardized protocols are necessary to fully characterize the products. This multi-step analytic system is suitable to analyze native phycobiliproteins or other reconstituted modified phycobiliproteins, and can also be extended to other fluorescent proteins.

### 4.3 E/F-type lyase catalyzed attachment

The PecA-PCB and CpcA-PCB from *Anabaena* PCC7120, were obtained by *in vivo* reconstitution. The heterodimeric lyase/isomerase (CpcE/CpcF and PecE/PecF) catalyzes the covalent attachment of PCB at Cys- $\alpha$ 84 of CpcA and PecA, respectively, and the latter the concurrent isomerization of the chromophore to PVB. Both lyase subunits are required for chromophore attachment. The reaction has been studied in some detail with the isomerizing lyase, PecE/F from *Anabaena* PCC 7120. The F-subunit alone is inactive; the E-subunit alone catalyzes only the PCB attachment without isomerization (Zhao et al., 2005, Boehm et al., 2007). We also tested the lyase activity of the deoxyhyposyl-hydroxylase (DOHH) from the malaria parasite, *Plasmodium falciparum*. This enzyme has Heat-like repeats that are characteristic for the E/F-type lyases, but it had not chromophore-attaching activity.

PUB is another example of a chromophore that had never been found in free form in cyanobacteria; in fact, it is probably the most abundant biliprotein chromophore in marine cyanobacteria: Since the same  $\Delta 5$ -to- $\Delta 2$  double-bond isomerization that generates bound PVB from PCB would generate bound PUB from PEB, it is reasonable to speculate that this reaction is again catalyzed by the action of an isomerising lyase that uses PEB as substrate. A candidate has been proposed by Six et al.(2007), but biochemical evidence for such a lyase is still lacking (Scheer and Zhao, 2008).

### 4.4 S (/U)-type lyase catalyzed attachment

In the cyanobacterium *Fremyella diplosiphon*, a *cpeCDESTR* operon was sequenced and some of the genes were shown to function in the biogenesis of phycoerythrin (PE). The function of the *cpeCDE* genes and *cpeR* gene were identified, but the roles of the *cpeS* and *cpeT* products were not identified (Cobley et al., 2002). Shen et al., (2004, 2008) analyzed the genome sequences of *Synechococcus* sp. PCC 7002 and other strains that do not synthesize PE. This revealed paralogs, whose products displayed very high sequence similarity to CpeS and CpeT. Paralogs of *cpeS* and *cpeT* were present in all phycobiliprotein containing cyanobacteria, were absent in organisms that do not synthesize phycobiliproteins, and were encoded within operons with other

phycobiliprotein-related genes including other potential lyases (CpcU and CpcV). Based on those observations, the authors suggested that these gene products were involved in phycobiliprotein synthesis, it seemed plausible that the CpeS and CpeT paralogs might be phycobiliprotein lyases for PC and/or AP. Currently, the function of CpcS from *Anabaena* PCC7120 as a phycobiliprotein lyase has been reported in several publications from our laboratory, and derived in part from this work (Zhao et al., 2007a; Zhao et al., 2006a) and of CpcS from two other cyanobacteria by the laboratories of Bryant and Schluchter (Saunée et al., 2008; Shen et al., 2008). CpcS (CpcS-III) from *Anabaena* PCC 7120 not only catalyzed PCB attachment to  $\beta$ -C82 of PecB and CpcB from *M. laminosus* and *Anabaena* PCC7120, but also catalyzed PCB attachment to all subunits of allophycocyanin from *Anabaena* PCC7120; it even attached PEB to the Cys-82 position of  $\beta$ -PE (Zhao et al., 2007a; Zhao et al., 2006a). Shen et al.(2008) and Saunée et al.(2008) reported the CpcS-I and CpcU comprise, in *Synechococcus* sp. PCC 7002 and *Synechocystis* sp PCC 6803, the heterodimeric bilin lyase that attaches phycocyanobilin to Cys-82 of  $\beta$ -phycocyanin and Cys-81 of allophycocyanin subunits.

Homologs of the CpcS and CpeS proteins were classified into five groups (Shen et al., 2008). The largest of these groups, Group C, can be further divided into three clades, which have denoted CpcS-I, CpcS-II, and CpcS-III. CpcS from *Synechococcus* sp. PCC 7002 and *Synechocystis* sp. PCC 6803 belong to clade CpcS-I, while CpcS from *Anabaena* sp. PCC 7120 belong to clade CpcS-III. Cyanobacteria can be divided into two groups on the basis of their PCB lyases for the Cys-82 position of  $\beta$ -PC. *Anabaena* sp. PCC 7120 (clade CpcS-III) apparently produces lyases that are functional as a single subunit (Zhao et al. 2006a; Zhao et al., 2007a), whereas *Synechococcus* sp. PCC 7002 and *Synechocystis* sp. PCC 6803(clade CpcS-I) produce a heterodimeric lyase composed of a CpcS-I subunit and CpcU (Shen et al., 2008).

CpcS is apparently a (nearly) universal lyase with respect to the protein but is highly specific for a single binding site, cysteine-84. It is inactive, however, for the cysteine-84-binding site of  $\alpha$ -subunits of phycocyanin (CpcA) and PEC (PecA), which is rather served by the site- and protein-specific EF-type lyase (Schluchter and Glazer, 1999; Zhao et al., 2000; section 3-1, 3-2). This probably indicates a structural difference among the cysteine-84-binding sites of CpcA and PecA from other

biliproteins. This difference was supported by a sequence analysis of the apoproteins (Zhao et al., 2007a), phylogenetic characteristics of the different types of biliproteins (Sidler, 1994), and the *N*-methylation of asparagine found only in  $\beta$ -subunits (Klotz and Glazer, 1987). The two groups of biliproteins may have different functions besides the lyase specificity. The  $\alpha$ -84 sites of all cyanobacterial and red algal biliproteins are at the contact surface to the  $\beta$ -subunits in the trimers and show similar geometric and stereochemical properties; this argues against a structural or photosynthetic function that sets CpcA and PecA apart from all other subunits. The difference may be relevant to phycobilisome degradation (Zhao et al., 2007a).

CpcS can bind PCB, as assayed by  $\text{Ni}^{2+}$  chelating affinity chromatography. Binding is rapid, probably non-covalent, but much more strongly than with E/F-type lyases. The chromophore is bound in an extended conformation similar to that in phycobiliproteins, but only poorly fluorescent. The extended conformation is supported by binding studies with a conformationally locked chromophore, 15Za-PCB, which also binds rapidly and non-covalently to CpcS and gives a product with similar spectral properties as PCB-CpcS. Upon addition of apo-biliproteins, the chromophore is transferred to the latter much slower ( $\sim 1$  hr), indicating that chromophorylated CpcS is an intermediate in the enzymatic reaction.

## 4.5 T-type lyase catalytic attachment

*Synechococcus* PCC7002 has yet another gene, *cpcT*, which is ubiquitous in cyanobacteria and codes for a third family of lyases, the T-type. Recombinant CpcT catalyzes the regiospecific PCB addition at Cys-155 of CpcB from *Synechococcus* PCC7002 (Shen et al., 2006), to Cys-155 of both  $\beta$ -CPC and  $\beta$ -PEC in *Anabaena* sp. PCC 7120 (Zhao et al., 2007), and to Cys-155 of both  $\beta$ -CPC and  $\beta$ -PEC from *M. laminosus* (this work). From these data, CpcT is a lyase with only moderate protein specificity that is combined with a high site-specificity.

Based on the above conclusion, the three lyases seem to be sufficient to attach all phycobiliprotein chromophores in *Anabaena* sp. PCC7120, and other species containing only APC, CPC, PEC in their PBS, but no PE: CpcS(/U) and CpcT attach PCB to Cys- $\beta$ 84 and Cys- $\beta$ 155, respectively, of PC and PEC, while CpcE/F and

PecE/F catalyze attachment to Cys- $\alpha$ 84 of PC and of PEC, respectively, the latter with a concomitant isomerization of PCB to PVB. Posttranslational modification is an important mechanism to modulate the structural and functional properties of proteins. Chromophore attachment is not the only post-translational modification in biliproteins. A further post-translational modification is methylation of Asparagine-71/72 of phycobiliprotein  $\beta$ -subunits (Minami et al. 1985; Klotz et al., 1986; Swanson and Glazer, 1990; Miller et al., 2008; Shen et al., 2008b). Methylation of Asn has been reported already in the 1980s in  $\beta$ -subunit of biliproteins (Minami et al. 1985; Klotz et al., 1986; Klotz and Glazer, 1987). Swanson and Glazer (1990) demonstrated that methylation of this Asn residue was catalyzed by a specific methyltransferase, such a methylase has been identified recently (Miller et al., 2008; Shen et al., 2008b). Miller et al. (2008) conclude that this post-translational modification probably occurs after chromophorylation but before trimer assembly *in vivo*. Methylated Asn-71/72 is important for efficient energy transfer in phycobilisome and reduction of photoinhibition at high light intensity (Swanson and Glazer, 1990; Shen et al., 2008b). Nothing is known, to our knowledge, on the mechanism of a third post-translational modification, that is N-terminal methionine cleavage in several biliproteins, but such enzymes have been characterized in other organisms (Schechter and Berger, 1967; Miller et al., 1987; Boufous and Vadeboncoeur, 2003).

Up to date, there are three types of lyases and one methylase identified. The general identification and characterization of a new enzyme included the following steps and methods, which may be applied to identify new enzyme in future studies. a) Using bioinformatics methods (e.g. comparative bioinformatics approach and gene neighborhood analysis) analyze the various cyanobacterial genomes that have been sequenced, find the candidate gene(s). b) Introduction of this gene into a mutant cyanobacterial cell line, or cloning it into *E.coli* using the multi-plamidic expression system together with other required genes. c) Culturing the wild-type and mutant cell of the cyanobacterium, or expressing the reconstitution system in *E. coli*. d) Isolating of PBS or collecting the *E.coli* cell. e) Protein assays and electrophoresis. f) Absorption and fluorescence spectroscopy. g) Further analysis by CD, HPLC-MS, NMR spectroscopy. h) Determining the kinetics and i) the catalytic mechanisms of new enzyme. j) Studing the activity and redulation of the enzyme in the cyanobacterium. Except for (i) and studies in the cyanobacteria, much of this has

been achieved for the three lyases.

## 4.6 Imidazole-bilin adducts

In the CpcS/PCB/imidazole reaction system, the amounts of the iPCB-imidazole and adducts with oxidized (MBV) chromophore increased with imidazole concentration, at the expense of free PCB; the amounts of the iPCB(2,22 H –bilin)-imidazole oxidation adduct increased with temperature, at the expense of free PCB and IPCB-imidazole. We have prepared the reaction products by HPLC, and determined their structures by MS and NMR spectroscopy. The results showed that CpcS can promote covalent binding of PCB to imidazole with concurrent isomerization to iPCB, and catalyses transfer of the chromophore of the iPCB-imidazole to the acceptor apoprotein CpcB(C155I). During this transfer reaction, the chromophore is re-isomerized to PCB, to yield PCB-CpcB(C155I). Chromophorylation by CpcS might then involve a histidine-bound intermediate carrying an iPCB chromophore. There is presently no direct evidence to this in cyanobacteria, but in view of the similar absorptions of PCB and iPCB-adducts, it requires testing using methods other than optical spectroscopy. Conserved histidines have been found in several lyases, plant-type phytochromes and several bacterial phytochromes (Zhao et al., 2006; Zhao et al., 2005; Wu and Lagarias, 2000; Lamparter, 2004), the reaction catalyzed by CpcS could therefore be a model for all these reactions. We proposed the following model of chromophorylation by CpcS (see Fig. 4-1).

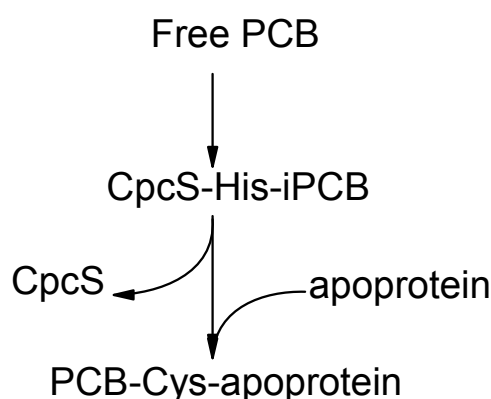


FIG. 4-1: A catalytic mechanism model of CpcS

## 4.7 Mercaptoethanol-bilin adducts

In the ME and PCB reaction system, two kinds of adducts were obtained, PVB-ME and iPCB-ME. Adducts of PCB with thiols have been described before, but characterized only by optical spectroscopy (Köst et al., 1975). Since the optical spectra of PCB and iPCB are rather similar, it is therefore not clear if these authors have been working then also with iPCB adducts. The chromophores of the both types can be transferred to CpcB(C155I), yielding CpcB(C155I)-PCB and CpcB(C155I)-PVB, respectively. Both products are remarkable. Chromophore (iPCB and PVB) can covalently bind to ME even in the absence of the lyase, as proved by MS and NMR spectrum. It indicates that the autocatalytic chromophorylation might then involve a thiol-chromophore intermediate.

Spontaneous formation of a PVB-ME adduct is intriguing, because the PVB chromophore was before only known in its bound form to the protein. Here, it is accessible for the first time in the (nearly) free form with only ME attached. Moreover, it is formed in a spontaneous reaction, and its formation is inhibited in the presence of the lyase, CpcS, indicating that one function of the lyase might be to inhibit this irreversible reaction. This isomerization from PCB to PVB is similar to the one catalyzed by PecF in the PecA biosynthesis. Up to now, the role of CpcF was not identified. The PVB-ME adduct formation might explain the role of CpcF in the holo-CpcA biosynthesis ; possibly it promotes the alternative route, that is iPCB transfer and re-isomerization (see below), and inhibit PVB formation in the holo-CpcA biosynthesis. This would also rationalize why homologous lyases are involved in the attachment of PCB, which formally does not require isomerization.

The novel 2,22H-chromophore (iPCB) has been postulated first by Grubmayr et al. (1988a,b,c), as an intermediate in a multi-step thiol addition and replacement reaction. However, in the ME and imidazole adducts it has been prepared and identified for the first time. Stereoisomers of the iPCB-ME adducts are the major products in the presence of the lyase. In line with the suggestion of Grubmayr, this chromophore is transferred in the presence of CpcS to the apoprotein, with concomitant isomerization to the 2,3H-chromophore (PCB). It might indicate that the second function of CpcF is to isomerize iPCB to PCB in holo-CpcA biosynthesis, and the lyase PecF might inhibit

the iPCB formation in the holo-PecA biosynthesis.

In a more general sense, the formation of covalent adducts of PCB with nucleophiles (ME) gave first indications for a mechanistic model for the lyases. The PVB-ME and iPCB-ME adduct formation might explain the catalytic mechanism of lyases in phycobiliprotein biosynthesis. Hugo et al. (1993) hypothesized a model reaction for biliprotein biosynthesis, which included an important intermediate, iPCB. Our identification of this chromophore conjugated to nucleophiles like imidazole or thiols lends support to this hypothesis and we suggested a unified mechanistic model of catalysis by the heterodimeric lyase CpcE/CpcF and PecE/PecF (see Fig. 3-76).

## 4.8 Some interesting observations as by-products of the experiments

During the experiments, several additional interesting observations were made that were not further explored in detail. Currently, they can not be explained well for lack of sufficient information, and it is unclear how they fit into the complete picture of biliprotein lyases. They are summarized here because they maybe relevant to future studies.

1) In the  $Zn^{2+}$  staining assay for covalent chromophore attachment, there are different fluorescence intensities for certain chromophores in the different  $Zn^{2+}$  salt solutions. For example, the fluorescence intensity of PCB in  $ZnCl_2$  solution is higher than in Zn-acetate solution, while the fluorescence intensity of PVB in  $ZnCl_2$  solution less than that in Zn-acetate solution, indicating an effect of the anion on the fluorescence.

2) The adducts CpcS-PCB and ME-PCB fluoresce only weakly. However, when CpcS-PCB and mercaptoethanol were mixed, we observed a strong fluorescence of the ternary complex, CpcS-PCB-ME. This is typical for biliproteins, in which the chromophore is held rigidly by strong interaction with the apoprotein. Biochemical evidence of a covalent bond between CpcS and PCB is still lacking. It is known, however, that such interactions can also occur in the absence of covalent binding. An example is chromophore binding in phytochrome, where in the absence of the binding cysteine adducts are formed that are spectrally very similar to native phytochrome,

and were even photoactive (Lamparter and Michael, 2005).

3) There are different adsorption characters of different chromopeptides on Sep-Pak C18 cartridge. For example, the PVB and PEB chromopeptides adsorbed to Sep-Pak C18 cartridge were eluted only with difficulties, but PCB chromopeptides were easily eluted. This is helpful for the separation of complex mixtures containing different chromophores. However, HPLC may therefore be problematic for chromophore quantification under certain conditions.

4) The PVB-PecA was digested using trypsin, and separated by HPLC. We found some products, besides the PVB-peptides, that contained the PCB, and not the PVB chromophore. We take this as evidence that the PCB to PVB isomerization is reversible. This has never been observed with the PecE/F lyases.

5) The chromopeptides of tryptic digestion were prepared by HPLC and measured MS. The HPLC results shows that MS spectra of PCB- and PEB-chromopeptides are very "clean", they gave mainly a single peak in the mass spectrum. By contrast, there are many fragment ions in the PVB- and PUB-chromopeptides. This difference indicates that the PVB and PUB chromophores are rather labile, and easily cleaved under MS conditions. Possibly, this can be used to distinguishing chromophore types by MS.

## 4.9 Future prospects

Recently, the techniques of biochemistry, molecular biology, spectroscopy, x-ray diffraction, electron microscopy and biophysics have served to improve our understanding of the structure of phycobilisomes, and their functions in photosynthesis. However, it is still largely unknown how phycobilisomes are properly assembled (and disassembled). The lyases studied here have added to our understanding of the early processes of this assembly, in particular for PC-only phycobilisomes, but leave a considerable number of open problems. In addition, also some aspects of PBS structure and function activity remain to be elucidated. In my opinion, the following problems have become obvious during this work, and can now be tackled, using in part methods developed here:

1) In order to resolve problems of imbalanced expressions, incompatibility of

plasmids and low yields, it is essential to define optimum expression conditions and plasmids forming of different phycobiliproteins. Establishing an on-line detection method of phycobiliproteins would be interesting in order to analyze the kinetics.

2) Find and determine new class phycobilin lyases that specifically attaches phycobilin to the other phycobiliproteins. Up to now, the PCB:phycobiliprotein lyases were identified, which are, at least in principle, sufficient to attach all phycobiliprotein chromophores in *Anabaena* sp. PCC7120, and other species containing only APC, CPC, PEC in their PBS. The biggest problem is currently the biosynthesis of PEs, in spite of evidence that CpcS may be part of the solution. Yet another problem is PUB, which globally is probably the most abundant bilin chromophore, but the biosynthesis is unknown.

3) Currently, E/F-type lyases (CpcE/CpcF and PecE/PecF), S-type lyases and T-type lyase were identified, but the catalytic mechanisms for these lyases are only incompletely understood; more work is needed to detail them further.

4) Biological self-assembly is remarkable in its fidelity and in the efficient production of intricate molecular machines and functional materials from a heterogeneous mixture of macromolecules. Anderson and Toole (1998) suggested a model for the assembly pathway of the cyanobacterial phycobilisome, that is still awaiting critical testing. Up to date, many cyanobacterial genomes have been sequenced, the molecular architecture of several PBS has been defined, and crystal structures are available for all major phycobiliproteins. With the identification and characterization of most of the enzymes involved in phycobiliproteins maturation, it may become feasible to study phycobilisome assemble *in vitro* using the following protocol. 1) Individual reconstitution of all subunits of the phycobilisome with chromophores in multi-plasmidic expression systems in *E. coli*. 2) Secondary modification of chromophorylated subunits *in vitro* with respective enzymes. 3) Preparation of mono- and trimers from the individual subunits *in vitro*. 4) Individual expression of all linker-proteins of the phycobilisome in *E. coli*. Finally, trimers and linker-proteins are incubated, yielding hopefully complete phycobilisome or phycobilisome fragments. Alternatively one might consider to assemble a phycobilisome in one multi-plasmidic expression system in *E. coli*. I believe, however, that this approach is presently very difficult and less likely to succeed.

## 5: Summary

Phycobilins are light harvesting pigments of cyanobacteria and red algae. In cyanobacteria, four phycobiliproteins are organized in phycobilisomes: phycocyanin (PC), allophycocyanin (APC), and often also phycoerythrocyanin (PEC) or phycoerythrin (PE). Their phycobilin chromophores, linear tetrapyrroles, are generally bound to the apoprotein at conserved positions by cysteinyl thioether linkages. A final step in phycobiliprotein biosynthesis is the post-translational phycobilin addition to the various biliproteins. *In vivo*, the correct attachment of most chromophores is catalyzed by binding-site and chromophore-specific lyases. Only two such lyases, which both belong to the E/F-type were known at the beginning of this work. Two additional types, S/(U)-type and T-type lyase, have been characterized during this work. In addition, the correct structures of the products from all three lyase types have been verified, and evidence was obtained for the reaction mechanisms.

This characterization relied on two methodological advances. The first is the use of a multi-plasmidic expression system for reconstitution of phycobiliproteins in *E. coli*. After cloning of apophycobiliprotein genes, phycobilin biosynthesis genes and (putative) lyase genes from several cyanobacteria, various phycobiliproteins could be biosynthesized in the heterologous *E. coli* system using dual plasmids containing the respective genes. This heterologous system produces higher yields than the *in vitro* reconstitution, it is nearly devoid of spontaneous binding, better reproducible, and more easily controlled. The second methodological advance is the consequent use of a combination of chromatographic, electrophoretic and spectroscopic tools that allowed a full characterization of the structure and binding sites of attached chromophores. This included, besides optical spectroscopy, in particular mass and magnetic resonance ( $^1\text{H-NMR}$ ) spectroscopy.

Using the unmodified genes coding for both subunits of PEC, as well as their cystein mutants, three lyases were identified for the three binding site. Besides the already known isomerizing lyase, PecE/PecF, for Cys-84 of  $\alpha$ -PEC, these are the two new lyases, CpcT (all5339) for Cys-153 of  $\beta$ -PEC, and CpcS (alr0617) for Cys-82 of  $\beta$ -PEC. The spectroscopic analysis proved that the chromophores (PCB and PVB)

are correctly attached to these three binding sites.

Similarly, three lyases were identified for the three binding sites of CPC. The well known heterodimeric lyase (CpcE/CpcF) catalyzes the covalent attachment of PCB to  $\alpha$ C84 of CPC, CpcS catalyses the site-selective attachment of PCB to cysteine- $\beta$ 84 in CpcB; and CpcT for cysteine- $\beta$ 155 of CpcB. CpcE/F is specific for CpcA, while CpcS and CpcT can react with both CpcB and PecB. We also tested the lyase activity of the deoxyhyposyl-hydroxylase (DOHH) from the malaria parasite, *Plasmodium falciparum*. This enzyme has Heat-like repeats that are characteristic for the E/F-type lyases, but it had not chromophore-attaching activity.

The substrate specificity of the new lyase, CpcS (coded by *alr0617*), was further tested with APC subunits; It is very unspecific with regard to the acceptor protein and attaches PCB to ApcA1, ApcB, ApcD ApcF, as well as to the product of an additional gene, *apcA2*; of unknown function that is highly homologous to *apcA1* coding for the APC  $\alpha$ -subunit. Obviously, this lyase has a much broader substrate specificity than the E/F-type lyases, but it has high site-specificity, attaching the chromophore exclusively to the Cys-84 (consensus sequence) binding site of the APC subunits.

CpcS from *Anabaena* PCC7120 is a relatively simple system, it acts as a monomer, and does not require any cofactors. CpcS binds PCB rapidly (<1s) and relatively strongly, but probably non-covalently. The chromophore is bound in an extended conformation similar to that in phycobiliproteins, but only poorly fluorescent. The extended conformation is supported by binding studies with a conformationally locked chromophore, 15Za-PCB, which also binds rapidly and non-covalently to CpcS and gives a product with similar spectral properties as PCB-CpcS. Upon addition of apo-biliproteins to the PCB-CpcS (or 15Za-PCB-CpcS) complex, the chromophore is transferred to the latter much more slowly (~1 hr), indicating that chromophorylated CpcS is an intermediate in the enzymatic reaction.

There are distinct differences in the absorption, extinction coefficient in acidic methanol and pKa of the free 15Za-PCB, compared with that of free PCB, which are probably due to a shift in the pK-values by about 1 pH unit.

Nucleophilic addition products of PCB were characterized that are formed

spontaneously or by the lyases, and gave first indications for a mechanistic model for the lyases. The first nucleophile was imidazole, which is a model for histidine. Two imidazole-PCB adducts were prepared and the structures determined by MS and NMR spectroscopy. Surprisingly, the chromophore is isomerized in this reaction to a 2,22 H –bilin termed iso-phycoerythrin (iPCB). CpcS not only can promote covalent binding of PCB to imidazole, but also catalyses the transfer of the chromophore of the formed iPCB-imidazole to the cysteine84 of acceptor apoprotein, CpcB. During this transfer reaction, the chromophore is re-isomerized to PCB, to yield CpcB-C84-PCB. It indicates that chromophorylation by CpcS might then involve a histidine-bound intermediate; this could be a model for the reaction catalyzed by CpcS.

The second nucleophile was mercaptoethanol, as a model for cysteine. In the ME and PCB reaction system, two isomers each of isomeric PVB-ME and iPCB-ME were obtained in a non-enzymatic reaction. The chromophore of the two complexes can be transferred to cysteine-84 of CpcB, yielding CpcB-C84-PCB and CpcB-C84-PVB. In the presence of the lyase, CpcS, only the iPCB adducts are formed. It indicates autocatalytical chromophorylation might then involve a thiol-chromophore intermediate; this could be a model for the chromophorylation reaction. At the same, we propose a possible generalized catalytic mechanism for the non-isomerizing heterodimeric lyase, CpcE/CpcF, and its isomerizing homolog, PecE/PecF.

## 6: References

- Adir N. (2005) Elucidation of the molecular structures of components of the phycobilisome : reconstructing a giant. *Photosynth. Res.* **85**:15-32
- Adir N, Dobrovetsky Y, Lerner N. (2001) Structure of c-phycoerythrin from the thermophilic cyanobacterium *Synechococcus vulcanus* at 2.5 Å: structural implications for thermal stability in phycobilisome assembly. *J. Mol. Biol.* **313**:71-81.
- Adir N, Vainer R, Lerner N. (2002) Refined structure of c-phycoerythrin from the cyanobacterium *Synechococcus vulcanus* at 1.6 Å: insights into the role of solvent molecules in thermal stability and co-factor structure. *Biochim. Biophys. Acta.* **1556**:168-174.
- Ajlani G. and Vernotte C. (1998) Deletion of the PB-loop in the L<sub>CM</sub> subunit does not affect phycobilisome assembly or energy transfer functions in the cyanobacterium *Synechocystis* sp. PCC6714. *Eur. J. Biochem.* **257**: 154-159
- Ajlani G, Vernotte C. (1998) Construction and characterization of a phycobiliprotein-less mutant of *Synechocystis* sp. PCC 6803. *Plant Mol. Biol.* **37**:577-580.
- Alvey RM, Karty JA, Roos E, Reilly JP, Kehoe DM. (2003) Lesions in phycoerythrin chromophore biosynthesis in *Fremyella diplosiphon* reveal coordinated light regulation of apoprotein and pigment biosynthetic enzyme gene expression. *Plant Cell* **15**:2448-2463.
- Ammerman JW, Glover WB (2000) Continuous underway measurement of microbial ectoenzyme activities in aquatic. Ecosystems. *Mar Ecol Prog Ser* **201**:1–12
- Anderson LK and Toole CM (1998) A model for early events in the assembly pathway of cyanobacterial phycobilisomes. *Mol. Microbiol.* **30**:467-474
- Apt KE, Grossman AR. (1993) Characterization and transcript analysis of the major phycobiliprotein subunit genes from *Aglaothamnion neglectum* (Rhodophyta). *Plant Mol Biol.* **21**:27-38.
- Apt KE, Collier JL, Grossman AR. (1995) Evolution of the phycobiliproteins. *J. Mol. Biol.* **248**: 79-96.
- Apt KE, Hoffman NE, Grossman AR. (1993) The gamma subunit of R-phycoerythrin and its possible mode of transport into the plastid of red algae. *J Biol Chem.* **268**:16208-16215.
- Araoz R, Lebert M, Hader DP. (1998) Electrophoretic applications of phycobiliproteins.

*Electrophoresis*. **19**:215-219.

Araoz R, Shelton M, Lebert M, Hader DP. (1998) Differential behaviour of two cyanobacterium species to UV radiation. Artificial UV radiation induces phycoerythrin synthesis. *J Photochem Photobiol B*. **44**:175-183.

Arciero DM, Bryant DA, Glazer AN. (1988a) *In vitro* attachment of bilins to apophycocyanin. I. Specific covalent adduct formation at cysteinyl residues involved in phycocyanobilin binding in C- phycocyanin. *J. Biol. Chem*. **263**:18343-18349.

Arciero DM, Dallas JL, Glazer AN.(1988b) *In vitro* attachment of bilins to apophycocyanin. II. Determination of the structures of tryptic bilin peptides derived from the phycocyanobilin adduct. *J. Biol. Chem*. **263**:18350-18357.

Ashby MK, Mullineaux CW. (1999) The role of ApcD and ApcF in energy transfer from phycobilisomes to PS I and PS II in a cyanobacterium. *Photosynthe Res*. **61**:169-179.

Balabas BE, Montgomery BL, Ong LE, and Kehoe DM. (2003) CotB is essential for complete activation of green light-induced genes during complementary chromatic adaptation in *Fremyella diplosiphon*. *Mol Microbiol*. **50**: 781–793.

Barber J, Morris EP, da Fonseca PC. (2003) Interaction of the allophycocyanin core complex with photosystem II. *Photochem Photobiol Sci*. **2** :536-541.

Batard P, Szollosi J, Luescher I, Cerottini JC, MacDonald R, Romero P. (2002) Use of phycoerythrin and allophycocyanin for fluorescence resonance energy transfer analyzed by flow cytometry: advantages and limitations. *Cytometry*. **48**:97-105.

Beale SI, Cornejo J. (1991) Biosynthesis of phycobilins. 3(Z)-phycoerythrobilin and 3(Z)-phycocyanobilin are intermediates in the formation of 3(E)-phycocyanobilin from biliverdin IX alpha. *J Biol Chem*. **266**:22333-22340.

Beale SI, Cornejo J.(1991) Biosynthesis of phycobilins. 15,16-Dihydrobiliverdin IX alpha is a partially reduced intermediate in the formation of phycobilins from biliverdin IX alpha. *J Biol Chem*. **266**:22341-22345.

Becker w.(2004) Microalgae in human and animal nutrition, p312-351. In Richmond, A. (ed), Handbook of microalgae culture, Blackwell, Oxford.

Berkelman TR, Lagarias JC. (1986). Visualization of bilin-linked peptides and proteins in polyacrylamide gels. *Anal. Biochem*. **156**:194–201.

Benjamin Q. Wolfgang G. (2004) Chromophore selectivity in bacterial phytochromes: dissecting the process of chromophore attachment. *Eur. J. Biochem*. **271**:1117-1126.

Bermejo R, Fernandez E, Alvarez-Pez JM, Talavera EM. (2002) Labeling of cytosine residues with biliproteins for use as fluorescent DNA probes. *J. Luminescence* **99**:113–124.

Bhalerao RP, Lind LK, Gustafsson P. (1994) Cloning of the *cpcE* and *cpcF* genes from *Synechococcus* sp. PCC 6301 and their inactivation in *Synechococcus* sp. PCC 7942. *Plant Mol Biol.* **26**:313-326.

Bhat VB, Madyastha KM. (2000) C-phycoerythrin: a potent peroxyl radical scavenger *in vivo* and *in vitro*. *Biochem Biophys Res Commun* ;**275**:20-25.

Bhoo SH, Davis SJ, Walker J, Karniol B, Vierstra RD. (2001) Bacteriophytochromes are photochromic histidine kinases using a biliverdin chromophore. *Nature* **414**:776-779.

Bhoo SH, Hirano T, Jeong H, Lee J, Furuya M, Song P. (1997) Phytochrome photochromism probed by site-directed mutations and chromophore esterification. *J Am Chem Soc* **119**: 11717–11718.

Bienert R, Baier K, Volkmer R, Lockau W. & Heinemann U. (2006) Crystal structure of NblA from *Anabaena* sp. PCC 7120, a small protein playing a key role in phycobilisome degradation. *J. Biol. Chem.* **281**: 5216-5223.

Bishop JE, Lagarias JC, Nagy JO, Schoenleber RW, Rapoport H, Klotz AV & Glazer AN. (1986) Phycobiliprotein-bilin linkage diversity. I. Structural studies on A- and D-ring-linked phycocyanobilins. *J. Biol. Chem.* **261**: 6790-6796

Bishop JE, Rapoport H, Klotz AV, Chan CF, Glazer AN, Flüglistaller P & Zuber H. (1987) Chromopeptides from phycoerythrocyanin: Structure and linkage of the three bilin groups. *J. Am. Chem. Soc.* **109**: 857-881.

Björn G.S & Björn L.O. (1976) Photochromic pigments from blue-green algae: phycochromes a, b and c. *Physiol. Plant* **36**: 297-300.

Boehm S (2006)  $\alpha$ -Phycoerythrocyanin: Dynamics of Reversible Photochromism and Lyase-catalyzed Holoprotein Assembly. Ph.D. thesis, University of Munich, Germany

Boehm S, Endres S, Scheer H, Zhao KH. (2007) Biliprotein Chromophore Attachment: Chaperone-like function of the PecE subunit of  $\alpha$ -phycoerythrocyanin lyase. *J. Biol. Chem* **282**:25357-25366.

Borucki B, Otto H, Rottwinkel G, Hughes J, Heyn MP, Lamparter T. (2003) Mechanism of Cph1 phytochrome assembly from stopped-flow kinetics and circular dichroism. *Biochemistry* **42**:13684-13697.

Boufous H, and Vadeboncoeur C. (2003) Purification and characterization of the

- Streptococcus salivarius methionine aminopeptidase (MetAP). *Biochimie* (Paris) **85**:993–997
- Brejc K, Ficner R, Huber R, Steinbacher S. (1995) Isolation, crystallization, crystal structure analysis and refinement of allophycocyanin from the cyanobacterium *Spirulina platensis* at 2.3 Å resolution. *J Mol Biol.* **249**:424–440.
- Bryant DA. (1982) Phycoerythrocyanin and phycoerythrin: properties and occurrence in cyanobacteria. *J. Gen. Microbiol.* **128**:835–844.
- Bryant DA. (1986) The cyanobacterial photosynthetic apparatus: comparisons to those of higher plants and photosynthetic bacteria. *Can Bull Fish Aquat Sci* **214**: 423–500
- Bryant DA. (1987) The cyanobacterial photosynthetic apparatus: comparisons to those of higher plants and photosynthetic bacteria. In Platt T and Li WKW (Eds.): *Photosynthetic Picoplankton*. Ottawa, Canada. **214**: 423–500
- Bryant, DA. (1991) Cyanobacterial phycobilisomes: Progress toward complete structural and functional analysis via molecular genetics. In: *Cell Culture and Somatic Cell Genetics of Plants*. Bogorad, L. & Vasil, I. K. (Eds.). pp. 257–300. Academic Press Inc., New York.
- Bryant, DA. (Ed.) (1994) *Advances in photosynthesis: The molecular biology of cyanobacteria*. Kluwer Academic Publisher, Dordrecht.
- Bryant DA, Glazer AN and Eiserling FA. (1976) Characterization and structural properties of the major biliproteins of *Anabaena* sp. *Arch. Microbiol.* **110**:60–75.
- Bryant DA, de Lorimier R, Guglielmi G, Stevens SE Jr. (1990) Structural and compositional analyses of the phycobilisomes of *Synechococcus* sp. PCC 7002. Analyses of the wild-type strain and a phycocyanin-less mutant constructed by interposon mutagenesis. *Arch Microbiol.* **153**:550–560.
- Bryant DA, Stirewalt VL, Glauser M, Frank G, Sidler W & Zuber H. (1991) A small multigene family encodes the rod-core linker polypeptides of *Anabaena* sp. PCC 7120 phycobilisomes. *Gene* **107**: 91–99.
- Cai YA, Murphy JT, Wedemayer GJ, Glazer AN. (2001) Recombinant phycobiliproteins. Recombinant C-phycocyanins equipped with affinity tags, oligomerization, and biospecific recognition domains. *Anal Biochem.* **290**:186–204.
- Cai, YA, Schwartz SH & Glazer AN. (1997) Transposon insertion in genes coding for the biosynthesis of structural components of the *Anabaena* sp. phycobilisome. *Photosynth. Res.* **53**:109–120.

Canaani OD, Gantt E (1980) Circular dichroism and polarized fluorescence characteristics of blue-green algal allophycocyanins. *Biochemistry* **19**:2950–2956.

Capuano V, Braux AS, Tandeau de Marsac N, Houmard J. (1991) The "anchor polypeptide" of cyanobacterial phycobilisomes. Molecular characterization of the *Synechococcus* sp. PCC 6301 apce gene. *J Biol Chem.* **266**:7239-7247.

Chang WR, Jiang T, Wan ZL, Zhang JP, Yang ZX, Liang DC. (1996) Crystal structure of R-phycoerythrin from *Polysiphonia urceolata* at 2.8 Å resolution. *J Mol Biol.* **262**:721-731.

Chen Fang (2006) Master thesis, HuaZhong University of Science and Technology, Wuhan, China.

Cobley JG, Clark AC, Weerasurya S, Quesada FA, Xiao JY, Bandrapali N, D'Silva I, Thounaojam M, Oda JF, Sumiyoshi T, Chu MH.(2002)CpeR is an activator required for expression of the phycoerythrin operon (cpeBA) in the cyanobacterium *Fremyella diplosiphon* and is encoded in the phycoerythrin linker-polypeptide operon (cpeCDEST). *Mol Microbiol.* **44**:1517-1531.

Cole, WJ, Chapman DJ & Siegelman HW. (1967) Structure of Phycocyanobilin. *J. Am. Chem. Soc.* **89**: 3643-3645.

Collier JL, Grossman AR. (1992) Chlorosis induced by nutrient deprivation in *Synechococcus* sp. strain PCC 7942: not all bleaching is the same. *J Bacteriol.* **174**:4718-4726.

Colyer CL, Kinkade CS, Viskari PJ, Landers JP. (2005) Analysis of cyanobacterial pigments and proteins by electrophoretic and chromatographic methods. *Anal. Bioanal. Chem.* **382**:559-569

Cornejo J, Beale SI, Terry MJ, Lagarias JC. (1992) Phytochrome assembly. The structure and biological activity of 2(R),3(E)-phytochromobilin derived from phycobiliproteins. *J Biol Chem.* **267**:14790-14798.

Dammeyer T, Frankenberg-Dinkel N. (2006) Insights into Phycoerythrobilin Biosynthesis Point toward Metabolic Channeling. *J Biol Chem.* **281**:27081-27089.

Dammeyer T, Bagby SC, Sullivan MB, Chisholm SW, Frankenberg-Dinkel, N. (2008) Efficient phagemediated pigment biosynthesis in oceanic cyanobacteria. *Curr Biol* **18**:442-448.

de Lorimier R, Wilbanks SM, Glazer AN. (1993) Genes of the R-phycoyanin II locus of marine *Synechococcus* spp., and comparison of protein-chromophore interactions in phycocyanins differing in bilin composition. *Plant Mol Biol.* **21**:225-237.

- Demidov AA, Mimuro M. (1995) Deconvolution of C-phycoyanin beta-84 and beta-155 chromophore absorption and fluorescence spectra of cyanobacterium *Mastigocladus laminosus*. *J Biophys.* **68**:1500-1506.
- Debreczeny MP, Sauer K, Zhou J, and Bryant D A. (1995) Comparison of calculated and experimentally resolved rate constants for excitation energy transfer in C-phycoyanin.2.Trimers *J. Phys. Chem.* **99**:8420–8431
- Dolganov N, Grossman AR. (1999) A polypeptide with similarity to phycoyanin alpha-subunit phycoyanobilin lyase involved in degradation of phycobilisomes. *J Bacteriol.* **181**:610-617.
- Ducret A, Muller SA, Goldie KN, Hefti A, Sidler WA, Zuber H, Engel A. (1998) Reconstitution, characterisation and mass analysis of the pentacylindrical allophycoyanin core complex from the cyanobacterium *Anabaena* sp. PCC 7120. *J Mol Biol.* **278**:369-388.
- Ducret A, Sidler W, Wehrli E, Frank G, Zuber H. (1996) Isolation, characterization and electron microscopy analysis of a hemidisoidal phycobilisome type from the cyanobacterium *Anabaena* sp. PCC 7120. *Eur J Biochem.* **236**:1010-1024.
- Duerring M, Huber R, Bode W, Ruemeli R, Zuber H. (1990) Refined three-dimensional structure of phycoerythrocyanin from the cyanobacterium *Mastigocladus laminosus* at 2.7 Å. *J Mol Biol.* **211**:633-644.
- Duerring M, Schmidt GB, Huber R. (1991) Isolation, crystallization, crystal structure analysis and refinement of constitutive C-phycoyanin from the chromatically adapting cyanobacterium *Fremyella diplosiphon* at 1.66 Å resolution. *J Mol Biol.* **217**:577-592.
- Eberlein M, Kufer W. (1990) Genes encoding both subunits of phycoerythrocyanin, a light-harvesting biliprotein from the cyanobacterium *Mastigocladus laminosus*. *Gene.* **94**:133-136.
- Elmorjani K, Thomas JC, Sebban P. (1986) Phycobilisomes of wild type and pigment mutants of the cyanobacterium *Synechocystis* PCC 6803. *Arch Microbiol.* **146**:186-191.
- Fairchild CD, Glazer AN. (1994a) Oligomeric structure, enzyme kinetics, and substrate specificity of the phycoyanin alpha subunit phycoyanobilin lyase. *J Biol Chem.* **269**:8686-8694.
- Fairchild CD, Glazer AN. (1994b) Nonenzymatic bilin addition to the alpha subunit of an apophycoerythrin. *J Biol Chem.* **269**:28988-28996.

- Fairchild CD, Zhao J, Zhou J, Colson SE, Bryant DA, Glazer AN. (1992) Phycocyanin alpha-subunit phycocyanobilin lyase. *Proc Natl Acad Sci USA*. **89**:7017-7021
- Falk H. (1989) The Chemistry of Linear Oligopyrroles and Bile Pigments. Wien, New York: Springer.
- Falk H. & Müller N. (1982) Force field calculations on linear polypryrrole systems. *Tetrahedron* **39**: 1875-1885.
- Ficner R, Lobeck K, Schmidt G, Huber R. (1992) Isolation, crystallization, crystal structure analysis and refinement of B-phycoerythrin from the red alga *Porphyridium sordidum* at 2.2 Å resolution. *J Mol Biol*. **228**:935-950.
- Foerstendorf H, Parbel A, Scheer H, Siebert F. Z,E (1997) isomerization of the alpha-84 phycoviolobilin chromophore of phycoerythrocyanin from *Mastigocladus laminosus* investigated by Fourier-transform infrared difference spectroscopy. *FEBS Lett*. **402**:173-176.
- Frank G, Sidler W, Widmer H. & Zuber H. (1978) The complete amino acid sequence of both subunits of C-phycocyanin from the cyanobacterium *Mastigocladus laminosus*. *Hoppe Seylers Z. Physiol. Chem*. **359**: 1491-1507.
- Frankenberg N, Lagarias JC. (2003) Phycocyanobilin:ferredoxin oxidoreductase of *Anabaena* sp. PCC 7120. Biochemical and spectroscopic characterization. *J Biol Chem*. **278**:9219-9226.
- Füglister P, Suter F. & Zuber H. (1983) The complete amino-acid sequence of both subunits of phycoerythrocyanin from the thermophilic cyanobacterium *Mastigocladus laminosus*. *Hoppe Seylers Z. Physiol. Chem*. **364**: 691-712.
- Gambetta GA, Lagarias JC. (2001) Genetic engineering of phytochrome biosynthesis in bacteria. *Proc Natl Acad Sci USA* . **98**:10566-10571.
- Gantt E. (1975) Phycobilisomes: Light-harvesting pigment complexes. *BioScience* **25**: 781-788.
- Gantt E. (1980) Structure and function of phycobilisomes: light harvesting pigment complexes in red and blue-green algae. *Int. Rev. Cyt*. **66**: 45-80.
- Gantt E. (1986) Phycobilisomes. In: Photosynthesis III. Staehelin, L. A. & Arntzen, C. J.(Eds.). pp.327-337. Springer-Verlag, Berlin.
- Gantt E. (1988) Phycobilisomes: assessment of core structure and thylakoid interaction. In: *Light-Energy Transduction in Photosynthesis: Higher Plants and Bacterial Models*.

Stevens, S. E. & Bryant, D. A. (Eds.), pp. 91-101. American Society of Plant Physiologists, Rockville, USA.

Gindt YM, Zhou J, Bryant DA and Sauer K. (1992) Core mutations of *Synechococcus* sp. PCC 7002 phycobilisomes: a spectroscopic study. *J Photochem Photobiol B* **15**: 75–89.

Gindt YM, Zhou J, Bryant DA, Sauer K. (1994) Spectroscopic studies of phycobilisome subcore preparations lacking key core chromophores: assignment of excited state energies to the Lcm, beta 18 and alpha AP-B chromophores. *Biochim. Biophys. Acta.* **1186**:153-162.

Glazer AN. (1985) Light harvesting by phycobilisomes. *Annu Rev Bioph Biom.*, **14**: 47-77

Glazer AN. (1987) Phycobilisomes: assembly and attachment. In: The Cyanobacteria. Fay, P. & Van Baalen, C. (Eds.), pp. 69-88. Elsevier Biomedical, Amsterdam.

Glazer AN. (1988) Phycobilisomes. *Meth. Enzymol.* **167**: 304-312.

Glazer AN. (1989) Light guides. Directional energy transfer in a photosynthetic antenna. *J. Biol. Chem.* **264**: 1-4

Glazer AN. (1994) Adaptive variations in phycobilisome structure. *Adv. Mol. Cell Biol.* **10**:119-149

Glazer A, Fang S & Brown D. (1973) Spectroscopic properties of C-phycocyanin and of its  $\alpha$  and  $\beta$  subunits. *J. Biol. Chem.* **248**: 5679-5685.

Glazer, A. N. & Fang, S. (1973) Chromophore content of blue-green algal phycobiliproteins. *J. Biol. Chem.* **248**: 663-671.

Glazer AN and Stryer L. (1983) Fluorescent tandem phycobiliprotein conjugates. Emission wavelength shifting by energy transfer. *Biophys J* **43**: 383–386.

.Glauser M, Bryant DA, Frank G, Wehrli E, Rusconi SS, Sidler W, Zuber H. (1992) Phycobilisome structure in the cyanobacteria *Mastigocladus laminosus* and *Anabaena* sp. PCC 7120. *Eur J Biochem.* **205**:907-915.

Gottschalk L, Lottspeich F, Scheer H. (1994) Reconstitution of an allophycocyanin trimer complex containing the C-terminal 21-23 kDa domain of the core-membrane linker polypeptide Lcm. *Z Naturforsch [C]*. **49**:331-336.

Grossman AR, Schaefer MR, Chiang GG and Collier JL. (1993) Environmental effects on the light-harvesting complex of cyanobacteria. *Microbiol. Rev.* **57**:725-749

Grubmayr K, Wagner UG. (1988a) Intramolecular nucleophilic addition of 2,3-dihydrodipyrin-1-(10H)-ones. *Monatsh Chem.* **119**:813-831

Grubmayr K, Wagner UG. (1988b) Mechanism of the nucleophilic addition to 2,3-dihydrodipyrin-1-(10H)-ones. *Monatsh Chem* **119**:793-812.

Grubmayr K., Wagner UG. (1988c) Addition of thiols to 3-ethylidene-2,3-dihydrodipyrin-1(10H)-ones - a model study on the covalent chromophore-protein bond in biliproteins. *Monatsh Chem.* **119**:965-983

Guan XY, Qin S, Su ZL, Zhao FQ, Ge BS, Li FC, Tang XX. (2007) Combinational biosynthesis of a fluorescent cyanobacterial holo- $\alpha$  - phycocyanin in *Escherichia coli* by using one expression vector. *Appl. Biochem. Biotech.* **142**:52-59.

Hagiwara Y, Sugishima M, Takahashi Y & Fukuyama K. (2006) Crystal structure of phycocyanobilin:ferredoxin oxidoreductase in complex with biliverdin IXalpha, a key enzyme in the biosynthesis of phycocyanobilin. *Proc. Natl. Acad. Sci. USA* **103**: 27-32.

He JA., Hu YZ, Jiang LJ.(1996) Photochemistry of phycobiliproteins: first observation of reactive oxygen species generated from phycobiliproteins on photosensitization. *J Am Chem Soc.* **118**:8957-8959

Houmard J, Capuano V, Colombano MV, Coursin T, (1990)Tandean de Marsac N. Molecular characterization of the terminal energy acceptor of cyanobacterial phycobilisomes. *Proc Natl Acad Sci U S A.* **87**:2152-2156.

Hu IC, Lee TR, Lin HF, Chiueh ChCh, and Lyu PCh (2006) Biosynthesis of Fluorescent Allophycocyanin R-Subunits by Autocatalytic Bilin Attachment, *Biochemistry*, **45**:7092-7099

Huang B, Wang GC, Zeng CK, Li ZG. (2002)The experimental research of R-phycoerythrin subunits on cancer treatment: a new photosensitizer in PDT. *Cancer Biother Radiopharm.* **17**:35-42.

Huang F, Parmryd I, Nilsson F, Persson AL, Pakrasi HB, Andersson B, Norling B. (2002) Proteomics of *Synechocystis* sp. strain PCC 6803: identification of plasma membrane proteins. *Mol Cell Proteom* **1**:956–996

Hunsucker SW, Klage K, Slaughter SM, Potts M, Helm RF(2004) *Biochem Biophys Res Commun* **317**:1121–1127

Imashimizu M, Fujiwara S, Tanigawa R, Tanaka K, Hirokawa T, Nakajima Y, Higo J, Tsuzuki M. (2003)Thymine at -5 is crucial for cpc promoter activity of *Synechocystis* sp. strain PCC 6714. *J Bacteriol.* **185**:6477-6480.

Inomata K, Noack S, Hammam MA, Khawn H, Kinoshita H, Murata Y, *et al.* (2006) Assembly of synthetic locked chromophores with *Agrobacterium* phytochromes Agp1 and Agp2. *J Biol Chem* **281**: 28162–28173.

Isailovic D, Li H-W, Yeung E.S.(2004) Isolation and characterization of R-phycoerythrin subunits and enzymatic digests. *J Chromatogr A*. **1051**:119-130

Jiang T, Zhang JP, Chang WR, Liang DC. (2001) Crystal structure of R-phycoerythrin and possible energy transfer pathways in the phycobilisome. *Biophys J*. **81**:1171-1179.

Jorissen HJ, Quest B, Remberg A, Coursin T, Braslavsky SE, Schaffner K, de Marsac NT, Gartner W. (2002) Two independent, light-sensing two-component systems in a filamentous cyanobacterium. *Eur J Biochem*. **269**:2662-26671.

Jung LJ, Chan CF, Glazer AN. (1995) Candidate genes for the phycoerythrocyanin alpha subunit lyase. Biochemical analysis of pecE and pecF interposon mutants. *J Biol Chem*. **270**:12877-12884.

Kahn K, Mazel D, Houmard J, Tandeau de Marsac N, Schaefer MR. (1997) A role for cpeYZ in cyanobacterial phycoerythrin biosynthesis. *J Bacteriol*. **179**(4):998-1006.

Kahn K, Schaefer MR. (1997) rpbA controls transcription of the constitutive phycocyanin gene set in *Fremyella diplosiphon*. *J Bacteriol*. **179**:7695-704.

Kaiser A, Hammels I, Gottwald A N, Assar M, Zaghloul MS, Motaal BA, Hauber J, Hoerauf A. (2007) Modification of eukaryotic initiation factor 5A from *Plasmodium vivax* by a truncated deoxyhypusine synthase from *Plasmodium falciparum*: An enzyme with dual enzymatic properties. *Bioorganic & Med. Chem*. **15**:6200-6207.

Kaiser A, Ulmer D, Goebel T, Holzgrabe U, Saefte M, Hoerauf A. (2006) Inhibition of hypusine biosynthesis in *Plasmodium*: a possible, new strategy in prevention and therapy of malaria. *Mini-Rev. Med. Chem*. **6**:1231-1241

Klotz AV. & Glazer AN. (1985) Characterization of the bilin attachment sites in R-phycoerythrin. *J Biol Chem* **260**: 4856-4863.

Klotz AV, and Glazer AN. (1987) Gamma-N-methylasparagine in phycobiliproteins. Occurrence, location and biosynthesis. *J. Biol. Chem*. **262**:17350–17355.

Klotz AV, Leary JA and Glazer AN (1986) Post-translational methylation of asparaginy residues. Identification of  $\beta$ -71  $\gamma$ -N-methylasparagine in allophycocyanin. *J. Biol. Chem*. **261**:15891–15894.

Klotz AV, Thomas BA, Glazer AN and Blacher RW. (1990). Detection of methylated

- asparagines and glutamine residues in polypeptides. *Anal.Biochem.* **18**:95–100.
- Kohchi T, Kataoka H, Linley PJ. (2005) Biosynthesis of chromophores for phytochrome and related photoreceptors. *Plant Biotech* (Tokyo, Japan) **22**:409-413.
- Kohchi T, Mukougawa K, Frankenberg N, Masuda M, Yokota A and Lagarias JC. (2001) The *Arabidopsis* HY2 gene encodes phytochromobilin synthase, a ferredoxindependent biliverdin reductase. *Plant Cell* **13**: 425–436.
- Köst HP, Rüdiger W and Chapman DJ. (1975) Über die Bindung zwischen Chromophor und Protein in Biliproteiden. 1. Abbaueversuche und Spektraluntersuchungen. *Liebig's Ann Chem* **1975**: 1582–1593.
- Kufer W & Björn GS. (1989) Photochromism of the cyanobacterial light harvesting biliprotein phycoerythrocyanin. *Physiol. Plant* **75**: 389-394.
- Kupka M, Scheer H. (2008) Unfolding of C- phycoyanin followed by loss of non-covalent chromophore-protein interactions 1. Equilibrium experiments. *Biochim. Biophys. Acta.* **1777**:94-103.
- Lagarias JC, Glazer AN, Rapoport H. (1979) Chromopeptides from C-phycoyanin. structure and linkage of a phycocyanobilin bound to the  $\beta$  subunit. *J. Am. Chem. Soc.* **101**: 5030-5037.
- Lagarias JC, Klotz AV, Dallas JL, Glazer AN, Bishop JE, Connel JF, Rapoport H.(1988) Exclusive A-ring Linkage for singly attached phycocyaninbilins and phycoerythrobilins in phycobiliproteins. *J Biol Chem* **263**:12977-12985
- Lamparter T. (2004) Evolution of cyanobacterial and plant phytochromes. *FEBS Lett* **573**: 1–5.
- Lamparter T and Michael N. (2005) *Agrobacterium* phytochrome as an enzyme for the production of ZZE bilins. *Biochemistry* **44**: 8461–8469.
- Lamparter T, Michael N, Mittmann F, Esteban B. (2002) Phytochrome from *Agrobacterium tumefaciens* has unusual spectral properties and reveals an N-terminal chromophore attachment site. *Proc Natl Acad Sci USA.* **99**:11628-11633.
- Lamparter T, Carrascal M, Michael N, Martinez E, Rottwinkel G, Abian J.(2004) The Biliverdin Chromophore Binds Covalently to a Conserved Cysteine Residue in the N-Terminus of *Agrobacterium* Phytochrome Agp1. *Biochemistry.* **43**:3659-3669.
- Li H, Sherman LA. (2002) Characterization of *Synechocystis* sp. strain PCC 6803 and  $\Delta$ tanbl mutants under nitrogen-deficient conditions. *Arch Microbiol.* **178**:256-266.

- Li L, Lagarias JC. (1994) Phytochrome assembly in living cells of the yeast *Saccharomyces cerevisiae*. *Proc Natl Acad Sci USA*. **91**:12535-12539.
- Liu JY, Jiang T, Zhang JP, Liang DC. (1999) Crystal structure of allophycocyanin from red algae *Porphyra yezoensis* at 2.2-Å resolution. *J Biol Chem*. **274**:16945-16952.
- Lundell DJ, Glazer AN. (1981) Allophycocyanin B. A common  $\beta$  subunit in *Synechococcus* allophycocyanin B ( $\lambda_{\max}$  670 nm) and allophycocyanin ( $\lambda_{\max}$  650 nm), *J. Biol. Chem.* **256**: 12600-12606.
- Luque I, Ochoa De Alda JA, Richaud C, Zabulon G, Thomas JC, Houmard J. (2003) The NblAI protein from the filamentous cyanobacterium *Tolypothrix* PCC 7601: regulation of its expression and interactions with phycobilisome components. *Mol Microbiol.* **50**:1043-54.
- Ma Y, Xie J, Zhang C and Zhao J. (2007) Three-stage refolding/unfolding of the dual-color b-subunit in R-phycocyanin from *Polysiphonia urceolata*. *Biochem Biophys Res Commun* **352**: 787-793.
- MacColl R. (1998) Cyanobacterial phycobilisomes *J Struct Biol.* **124**:311-334.
- MacColl R. (2004) Allophycocyanin and energy transfer. *Biochim. Biophys. Acta.* **1657**:73-81.
- MacColl R, Lam I, Choi CY, Kim J. (1994) Exciton splitting in phycoerythrin 545. *J Biol Chem.* **269**:25465-25469.
- MacColl R, Malak H, Gryczynski I, Eisele LE, Mizejewski GJ, Franklin E, Sheikh H, Montellese D, Hopkins S, MacColl LC. (1998) Phycoerythrin 545: monomers, energy migration, bilin topography, and monomer/dimer equilibrium. *Biochemistry.* **37**:417-423.
- Migita CT, Zhang X, Yoshida T. (2003) Expression and characterization of cyanobacterium heme oxygenase, a key enzyme in the phycobilin synthesis. Properties of the heme complex of recombinant active enzyme. *Eur J Biochem.* **270**:687-698.
- Miller CA, Leonard HS, Pinsky IG, Turner BM, Williams SR, Jr LH, Fletcher AF, Shen G, Bryant DA, Schluchter WM. (2008) Biogenesis of Phycobiliproteins III. CpcM is the asparagine methyltransferase for phycobiliprotein  $\beta$ -subunit in cyanobacteria. *J Biol Chem* **283**:19293-19300
- Miller CG, Strauch KL, Kukral AM, Miller JL, Wingfield PT, Mazzei GJ, Werlen RC, Graber P, and Movva NR. (1987) N-terminal methionine-specific peptidase in *Salmonella typhimurium*. *Proc. Natl. Acad. Sci. USA.* **84**:2718-2722

- Mimuro M, Fueglistaller P, Ruemбели R, Zuber H. (1986) Functional assignment of chromophores and energy transfer in C phycocyanin isolated from the thermophilic cyanobacterium *Mastigocladus laminosus*. *Biochim. Biophys. Acta.* **848**: 155-166
- Minami Y, Yamada F, Hase T, Matsubara H, Murakami A, Fujita Y, Takao T. and Shimonishi Y. (1985) Amino acid sequences of allophycocyanin  $\alpha$ - and  $\beta$ -subunits isolated from *Anabaena cylindrica*: presence of an unknown derivative of aspartic acid in the  $\beta$ -subunit. *FEBS Lett.* **191**:216–220.
- Montgomery BL, Casey ES, Grossman AR, Kehoe DM (2004) Apla, a Member of a New Class of Phycobiliproteins Lacking a Traditional Role in Photosynthetic Light Harvesting. *J Bacteriol* **186**:7420–7428.
- Muramoto T, Tsurui N, Terry MJ, Yokota A, Kohchi T. (2002) Expression and biochemical properties of a ferredoxin-dependent heme oxygenase required for phytochrome chromophore synthesis. *Plant Physiol.* **130**:1958-1966.
- Nagy JO, Bishop JE, Klotz AV, Glazer AN & Rapoport H. (1985) Bilin attachment sites in the alpha, beta, and gamma subunits of R-phycoerythrin. Structural studies on singly and doubly linked phycourobilins. *J. Biol. Chem.* **260**: 4864-4868.
- Nakajima M, Sakamoto T, Wada K. (2002) The complete purification and characterization of three forms of ferredoxin-NADP(+) oxidoreductase from a thermophilic cyanobacterium *Synechococcus elongatus*. *Plant Cell Physiol.* **43**:484-493.
- Nakamura Y, Kaneko T, Hirosawa M, Miyajima N & Tabata S. (1998) Extension of CyanoBase. CyanoMutants: repository of mutant information on *Synechocystis* sp. strain PCC6803 *Nucleic Acids Res.* **26**:63–67.
- Nanni B, Balestreri E, Dainese E, Cozzani I, Felicioli R. (2001) Characterisation of a specific phycocyanin-hydrolysing protease purified from *Spirulina platensis*. *Microbiol Res.* **156**:259-266.
- Nomsawai P, Tandeau de Marsac N, Thomas JC, Tanticharoen M, Cheevadhanarak S (1999) Light regulation of phycobilisome structure and gene expression in *Spirulina platensis* C1 (*Arthrospira* sp. PCC 9438). *Plant Cell Physiol* **40**:1194–1202
- Noubir S, Luque I, Ochoa de Alda JA, Perewoska I, Tandeau de Marsac N, Copley JG, Houmard J. (2002) Co-ordinated expression of phycobiliprotein operons in the chromatically adapting cyanobacterium *Calothrix* PCC 7601: a role for RcaD and RcaG. *Mol Microbiol.* **43**:749-762.
- Ong LJ, Glazer AN. (1987) R-phycocyanin II, a new phycocyanin occurring in marine *Synechococcus* species. Identification of the terminal energy acceptor bilin in phycocyanins.

*J. Biol. Chem.* **262**: 6323-6327.

Ong LJ, Glazer AN. (1991) Phycoerythrins of marine unicellular cyanobacteria. I. Bilin types and locations and energy transfer pathways in *Synechococcus* spp. phycoerythrins. *J Biol Chem.* **266**:9515-9527.

Padyana AK, Bhat VB, Madyastha KM, Rajashankar KR, Ramakumar S. (2001) Crystal structure of a light-harvesting protein C-phycoyanin from *Spirulina platensis*. *Biochem Biophys Res Commun.* **282**:893-898.

Papenbrock J, Grimm B. (2001) Regulatory network of tetrapyrrole biosynthesis--studies of intracellular signalling involved in metabolic and developmental control of plastids. *Planta.* **213**:667-681.

Parbel A, Zhao KH, Breton J, Scheer H. (1997) Chromophore assignment in phycoerythrocyanin from *Mastigocladus laminosus*. *Photosynth. Res.* **54**: 25-34.

Piven Irina (2006) Characterisation of mechanisms and components of protein phosphorylation in photosynthetic membranes of *Synechocystis* sp. PCC 6803. Ph.D. thesis, University of Munich, Germany

Pizarro SA, Sauer K. (2001) Spectroscopic study of the light-harvesting protein C-phycoyanin associated with colorless linker peptides. *Photochem Photobiol.* **73**:556-563.

Pueyo JJ, Go' mez-Moreno C (1991) Purification of ferredoxin-NADP<sup>+</sup> reductase, ferredoxin and flavodoxin from a single batch of the cyanobacterium *Anabaena* PCC7119. *Prep Biochem* **21**:191-204

Quest B, Gartner W. (2004) Chromophore selectivity in bacterial phytochromes: dissecting the process of chromophore attachment. *Eur J Biochem.* **271**:1117-1126.

Reuter W, Nickel-Reuter C (1993) Molecular assembly of the phycobilisomes from the cyanobacterium *Mastigocladus laminosus*. *J Photochem Photobiol B Biol* **18**:51-66

Reuter W, Westermann M, Brass S, Ernst A, Boger P, Wehrmeyer W. (1994) Structure, composition, and assembly of paracrystalline phycobiliproteins in *Synechocystis* sp. strain BO 8402 and of phycobilisomes in the derivative strain BO 9201. *J Bacteriol.* **176**:896-904.

Reuter W, Wiegand G, Huber R, Than ME. (1999) Structural analysis at 2.2 Å of orthorhombic crystals presents the asymmetry of the allophycoyanin-linker complex, APLC7.8, from phycobilisomes of *Mastigocladus laminosus*. *Proc Natl Acad Sci USA.* **96**:1363-1368.

- Rhie G, Beale SI. (1995) Phycobilin biosynthesis: reductant requirements and product identification for heme oxygenase from *Cyanidium caldarium*. *Arch Biochem Biophys.* **320**:182-194.
- Ritter S, Hiller RG, Wrench PM, Welte W, Diederichs K. (1999) Crystal structure of a phycourobilin-containing phycoerythrin at 1.90-Å resolution. *J Struct Biol.* **126**:86-97.
- Rommán RB, Álvarez-Pez, JM, Acín Fernández, F.G. and Molina Grima, E. (2002) Recovery of pure B-phycoerythrin from the microalga *Porphyridium cruentum*. *J. Biotechnol.* **93**: 73-85
- Ruembeli R, Wirth M, Suter F, Zuber H (1987) The phycobiliprotein beta 16.2 of the allophycocyanin core from the cyanobacterium *Mastigocladus laminosus*. Characterization and complete amino-acid sequence *Biol Chem Hoppe–Seyler* **368**:1–9.
- Sauer, Kenneth and Scheer, Hugo (1988) Excitation transfer in C-phycoyanin. Förster transfer rate and exciton calculations based on new crystal structure data for C-phycoyanins from *Agmenellum quadruplicatum* and *Mastigocladus laminosus*. *Biochim. Biophys. Acta.* **936**: 157-170.
- Saunée NA, Williams SR, Bryant DA, and Schluchter WM. (2008) Biogenesis of Phycobiliproteins II. CpcS-I and CpcU comprise the heterodimeric bilin lyase that attaches phycocyanobilin to Cys-82 of  $\beta$ -phycoyanin and Cys-81 of allophycocyanin subunits in *synechococcus* sp. PCC 7002. *J. Biol. Chem.* **283**:7513-7522
- Sawatzki J, Fischer R, Scheer H., Siebert F. (1990) Fourier transform Raman spectroscopy applied to biological systems. *Proc. Natl. Acad. Sci. USA* **87**:5903-5906
- Sawaki H, Sugiyama T, Omata T. (1998) Promoters of the phycocyanin gene clusters of the cyanobacterium *Synechococcus* sp. strain PCC 7942. *Plant Cell Physiol.* **39**:756-61.
- Scharnagl C, Schneider S. (1991) UV visible absorption and circular dichroism spectra of the subunits of C- phycoyanin. I: Quantitative assessment of the effect of chromophore-protein interaction in the  $\beta$  -subunit. *J Photochem. Photobiol.B: Bio.*, **3**:603-614.
- Scharnagl C, Schneider S. (1991) UV-visible absorption and circular dichroism spectra of the subunits of C- phycoyanin. II: a quantitative discussion of the chromophore-protein and chromophore-chromophore interactions in the  $\beta$ -subunit. *J Photochem. Photobiol. B:Bio.*, **8**:129-157.
- Schechter I, Berger A. (1967) On the size of the active site in proteases. I. Papain. *Biochem. Biophys. Res. Commun.* **27**:157–162

Scheer H. (1982) Phycobiliproteins: Molecular aspects of photosynthetic antenna systems. In Light Reaction Path of Photosynthesis. Fong, F.K. (ed). Berlin: Springer, pp. 7-45.

Scheer H, and Zhao KH. (2008) Biliprotein maturation: the chromophore attachment. *Mol. Microbiol.* **68**:263-276.

Schirmer T, Bode W and Huber R. (1987) Refined three-dimensional structures of two cyanobacterial C-phycoyanins at 2.1. and 2.5 Å resolution – a common principle of phycobilin–protein interaction. *J Mol Biol* **196**:677–695

Schluchter WM, Bryant DA. (1992) Molecular characterization of ferredoxin-NADP+ oxidoreductase in cyanobacteria: cloning and sequence of the petH gene of *Synechococcus* sp. PCC 7002 and studies on the gene product. *Biochemistry*. **31**:3092-3102.

Schluchter WM and Bryant DA. (2002) Analysis and reconstitution of phycobiliproteins. methods for the characterization of bilin attachment reactions. In *Heme, Chlorophyll, and Bilins*. Smith, A.G., and Witty, M. (eds). Totowa, NJ: Humana Press, pp. 311–334.

Schluchter WM and Glazer AN. (1999) Biosynthesis of phycobiliproteins in cyanobacteria. In *The Phototrophic Prokaryotes*. Peschek, G.A., Löffelhardt, W., and Schmetterer, G. (eds). New York: Kluwer/Plenum Press, pp.83–95.

Schmidt M, Krasselt A & Reuter W. (2006) Local protein flexibility as a prerequisite for reversible chromophore isomerization in alpha-phycoerythrocyanin. *Biochim. Biophys. Acta*. **1764**: 55-62.

Shen G, Leonard HS, Schluchter WM, Bryant DA. (2008b) CpcM Posttranslationally Methylates Asparagine-71/72 of Phycobiliprotein Beta Subunits in *Synechococcus* sp. Strain PCC 7002 and *Synechocystis* sp. Strain PCC 6803. *J. Bacteriol.* **190**: 4808-4817

Shen G, Saunee NA, Gallo E, Begovic Z, Schluchter WM & Bryant DA. (2004) Identification of novel phycobiliprotein lyases in cyanobacteria. In: Photosynthesis 2004 lightharvesting systems workshop. Niederman, R. A., Blankenship, R. E., Frank, H., Robert, B. & van Grondelle, R. (Eds.). pp.14-15. Saint Adele, Québec, Canada.

Shen G, Saunee N A, Williams SR, Gallo EF, Schluchter WM & Bryant DA. (2006) Identification and characterization of a new class of bilin lyase: the cpcT gene encodes a bilin lyase responsible for attachment of phycocyanobilin to Cys-153 on the beta subunit of phycocyanin in *Synechococcus* sp. PCC 7002. *J. Biol. Chem.* **281**: 17768-17778.

Shen G, Schluchter WM and Bryant DA. (2008) Biogenesis of Phycobiliproteins I. *cpcS-I* and *cpcU* mutants of the cyanobacterium *synechococcus* sp. PCC 7002 define a heterodimeric phycocyanobilin lyase specific for β-phycocyanin and allophycocyanin subunits. *J. Biol. Chem.* **283**:7503–7512

Sidler WA. (1994). Phycobilisome and phycobiliprotein structures. In Bryant D. A. (Ed), *The Molecular Biology of Cyanobacteria*. Dordrecht, Netherlands: Kluwer Academic Publishers.

Sidler W, Gysi J, Isker E & Zuber H. (1981) The complete amino acid sequence of both subunits of allophycocyanin, a light harvesting protein-pigment complex from the cyanobacterium *Mastigocladus laminosus*. *Hoppe Seylers Z. Physiol. Chem.* **362**: 611-628.

Sidler W, Kumpf B, Rüdiger W & Zuber H. (1986) The complete amino-acid sequence of C-phycoerythrin from the cyanobacterium *Fremyella diplosiphon*. *Biol. Chem. Hoppe Seyler* **367**: 627-642.

Siebzehnriibl S. (1990) Chromophorzuordnung und reversible Photochemie von C-Phycocyanin und Phycoerythrocyaninen. Dissertation, LMU München.

Six C, Thomas JC, Thion L, Lemoine Y, Zal F & Partensky F. (2005) Two novel phycoerythrin-associated linker proteins in the marine cyanobacterium *Synechococcus* sp. strain WH8102. *J. Bacteriol.* **187**: 1685-1694.

Spolare P, Joannis CC, Duran E, Isambert A. (2006) commercial applications of microalgae. *J Biosci. Bioeng.* **101**:87-96

Storf M, Parbel A, Meyer M, Strohmam B, Scheer H, Deng MG, Zheng M, Zhou M, Zhao KH. (2001) Chromophore Attachment to Biliproteins : Specificity of PecE/PecF, a Lyase -Isomerase for the Photoactive 3<sup>1</sup>-Cys- 84-phycoviolobilin Chromophore of Phycoerythrocyanin. *Biochemistry.* **40**: 12444-12456.

Storf M. (2003) Chromophorbinding und Photochemie der -Untereinheit des Phycoerythrocyanins aus *Mastigocladus laminosus*. Dissertation, LMU München.

Studier FW & Moffat BA. (1986) Use of bacteriophage T7 RNA polymerase to direct selective high-level expression of cloned genes. *J. Mol. Biol.* **189**: 113-130.

Stumpe H, Mueller N, Grubmayr K. (1993) Addition of methyl-2-mercaptoacetate to phycocyanobilin dimethyl ester: a model reaction for biliprotein biosynthesis? *Tetrahedron Lett*, **34**:4165-4168.

Sun L, Wang S (2003) Allophycocyanin complexes from the phycobilisome of a thermophilic blue-green alga *Myxosarcina concinna* Printz. *J Photochem Photobiol B Biol* **72**:45-53.

Swanson RV, Glazer AN. (1990) Separation of phycobiliprotein subunits by reverse-phase high pressure liquid chromatography. *Anal Biochem* **188**:295-299.

Swanson RV, Glazer AN. (1990) Phycobiliprotein methylation: effect of the  $\gamma$ -N-methylasparagine residue on energy transfer in phycocyanin and the phycobilisome. *J.*

*Mol. Biol.* **214**:787–796.

Swanson RV, Ong LJ, Wilbanks SM, Glazer AN. (1991)Phycocerythrins of marine unicellular cyanobacteria. II. Characterization of phycobiliproteins with unusually high phycocourobilin content. *J Biol Chem.* **266**:9528-9534.

Swanson RV, Zhou J, Leary JA, Williams T, de Lorimier R, Bryant DA, Glazer AN. (1992)Characterization of phycocyanin produced by *cpcE* and *cpcF* mutants and identification of an intergenic suppressor of the defect in bilin attachment. *J Biol Chem.* **267**:16146-16154.

Toole CM, Plank TL, Grossman AR, Anderson LK. (1998)Bilin deletions and subunit stability in cyanobacterial light-harvesting proteins. *Mol Microbiol.* **30**:475-486.

Tooley AJ, Cai YA, Glazer AN. (2001)Biosynthesis of a fluorescent cyanobacterial C-phycocyanin holo-alpha subunit in a heterologous host. *Proc Natl Acad Sci USA.* **98**:10560-10565.

Tooley AJ, Glazer AN. (2002)Biosynthesis of the cyanobacterial light-harvesting polypeptide phycocerythrocyanin holo-alpha subunit in a heterologous host. *J Bacteriol.* **184**:4666-4671.

Tu JM, Kupka M, Böhm S, Plösch M, Eichacker L, Zhao KH and Scheer H.(2008) Intermediate binding of phycocyanobilin to the lyase, CpeS1, and transfer to apoprotein. *Photosynth. Res.* **95**: 163-168.

Tu Sh-L, Sughrue W, David BR, and Lagarias JC. (2006) A Conserved Histidine-Aspartate Pair Is Required for Exovinyl Reduction of Biliverdin by a Cyanobacterial Phycocyanobilin:Ferredoxin Oxidoreductase, *J. Biol. Chem.*, **281**: 3127-3136

Viskari PJ, Colyer CL (2002) Separation and quantitation of phycobiliproteins using phytic acid in capillary electrophoresis with laser-induced fluorescence detection. *J Chromatogr A* **972**:269–276

Viskari PJ, Kinkade CS, Colyer CL (2001) The determination of phycobiliproteins by capillary electrophoresis with laser-induced fluorescence detection. *Electrophoresis* **22**:2327–2335

Wagner JR, Brunzelle JS, Forest KT & Vierstra RD. (2005) A light-sensing knot revealed by the structure of the chromophore-binding domain of phytochrome. *Nature* **438**:325-331.

Walter NG, Huang CY, Manzo AJ, Sobhy MA. (2008)Do-it-yourself guide: how to use the modern single-molecule toolkit.*Nat. Method* **5**:475-489

- Wang XQ, Li LN, Chang WR, Zhang JP, Gui LL, Guo BJ and Liang DC. (2001) Structure of C-phycoyanin from *Spirulina platensis* at 2.2 Angstrom resolution: a novel monoclinic crystal form for phycobiliproteins in phycobilisomes. *Acta Cryst D Biol Cryst* **57**: 784–792.
- Wiegand G, Parbel A, Seifert MH, Holak TA, Reuter W. (2002) Purification, crystallization, NMR spectroscopy and biochemical analyses of alpha-phycoerythrocyanin peptides. *Eur J Biochem.* **269**:5046-5055.
- Wu Shu-Hsing, Lagarias JC. (2000) Defining the Bilin Lyase Domain: Lessons from the Extended Phytochrome Superfamily. *Biochemistry.* **39**:13487-13495.
- Yang Yu, Ge BS, Guan XY, Zhang WJ, Qin S. (2008) Combinational biosynthesis of a fluorescent cyanobacterial holo- $\alpha$ -allophycoyanin in *Escherichia coli*. *Biotech. Lett.* **30**:1001-1004.
- Zehetmayer P, Hellerer T, Parbel A, Scheer H, Zumbusch A. (2002) Spectroscopy of single phycoerythrocyanin monomers: dark state identification and observation of energy transfer heterogeneities. *Biophys J.* **83**:407-415.
- Zehetmayer P, Kupka M, Scheer H, Zumbusch A. (2004) Energy transfer in monomeric phycoerythrocyanin. *Biochim. Biophys. Acta.* **1608**:35-44.
- Zhang SP, Qian SP, Zhao JQ, Yao SD, Jiang LJ. (1999) Characterization of the transient species generated by the photoexcitation of C-phycoyanin from *Spirulina platensis*: a laser photolysis and pulse radiolysis study. *Biochim. Biophys. Acta.* **1472**:270-278.
- Zhang S, Xie J, Zhang J, Zhao J, Jiang L. (1999) Electron spin resonance studies on photosensitized formation of hydroxyl radical by C-phycoyanin from *Spirulina platensis*. *Biochim. Biophys. Acta.* **1426**:205-211.
- Zhang SP, Zhao JQ, Jiang LJ. (2000) Photosensitized formation of singlet oxygen by phycobiliproteins in neutral aqueous solutions. *Free Radic Res.* **33**:489-496.
- Zhao FQ and Qin S (2006) Evolutionary Analysis of Phycobiliproteins: Implications for Their Structural and Functional Relationships. *J. Mol. Evol.*, **63**:330–340
- Zhao J, Shen G, Bryant DA. (2001) Photosystem stoichiometry and state transitions in a mutant of the cyanobacterium *Synechococcus* sp. PCC 7002 lacking phycoyanin. *Biochim. Biophys. Acta.* **1505**:248-257.
- Zhao KH, Haessner R, Cmiel E, and Scheer H. (1995) Type I reversible of phycoerythrocyanin involves Z/E-isomerization of  $\alpha$ -84 phycoviolobilin chromophore. *Biochim. Biophys. Acta.* **1228**: 235-243.

Zhao KH & Scheer H. (1999) Intermediates of reversible photochemistry of phycoerythrocyanin  $\alpha$ -subunit from *Mastigocladus laminosus* probed by low temperature absorption and circular dichroism spectroscopy. *Int. J. Photoenergy* **1**: 25-30.

Zhao KH, Deng MG, Zheng M, Zhou M, Parbel A, Storf M, Meyer M, Strohmann B & Scheer H. (2000) Novel activity of a phycobiliprotein lyase: both the attachment of phycocyanobilin and the isomerization to phycoviolobilin are catalyzed by PecE and PecF. *FEBS Lett.* **469**: 9-13.

Zhao KH, Ran Y, Li M, Sun YN, Zhou M, Storf M, Kupka M, Böhm S, Bubenzer C and Scheer H. (2004a) Photochromic biliproteins from the cyanobacterium *Anabaena sp.* PCC 7120: lyase activities, chromophore exchange and photochromism in phytochrome and phycoerythrocyanin. *Biochemistry* **43**: 11576-11588.

Zhao KH, Su P, Böhm S, Song B, Zhou M, Bubenzer C & Scheer H. (2005a) Reconstitution of phycobilisome core-membrane linker, Lcm, by autocatalytic chromophore binding to ApcE. *Biochim. Biophys. Acta.* **1706**: 81-87.

Zhao KH, Su P, Li J, Tu JM, Zhou M, Bubenzer C & Scheer H. (2006a) Chromophore attachment to phycobiliprotein beta-subunits: phycocyanobilin: cysteine-beta84 phycobiliprotein lyase activity of CpeS-like protein from *Anabaena sp.* PCC7120. *J. Biol. Chem.* **281**: 8573-8581.

Zhao KH, Su P, Tu JM, Wang X, Liu H, Plösch M, Eichacker L, Yang B, Zhou M and Scheer H (2007a) Phycobilin:cysteine-84 biliprotein lyase, a near-universal lyase for cysteine-84-binding sites in cyanobacterial phycobiliproteins. *Proc Natl Acad Sci USA*, **104**:14300-14305.

Zhao KH, Wu D, Zhou M, Zhang L, Böhm S, Bubenzer C & Scheer H. (2005b) Amino acid residues associated with enzymatic activity of the isomerizing phycoviolobilin lyase PecE/F. *Biochemistry* **44**: 8126-8137.

Zhao KH, Wu D, Wang L, Zhou M, Storf M, Bubenzer C, Strohmann B & Scheer H. (2002) Characterization of Phycoviolobilin Phycocyanin- $\alpha$ 84-cysteine-lyase-(isomerizing) from *Mastigocladus laminosus*. *Eur. J. Biochem.* **269**: 4542-4550.

Zhao KH, Wu D, Zhang L, Zhou M, Böhm S, Bubenzer C & Scheer H. (2006b) Chromophore attachment in phycocyanin. Functional amino acids of phycocyanobilin:  $\alpha$ - phycocyanin lyase and evidence for chromophore binding. *FEBS J.* **273**: 1262-1274.

Zhao KH, Zhang J, Tu JM, Böhm S, Plösch M, Eichacker L, Bubenzer C, Scheer H, Wang X, and Zhou M. (2007b) Lyase activities of CpcS and CpcT-like proteins from *Nostoc sp.* PCC7120, and sequential reconstitution of binding sites of phycoerythrocyanin and phycocyanin  $\beta$ -subunits. *J. Biol. Chem.* **282**: 34093-34103.

Zhao KH, Zhu JP, Deng MG, Zhou M, Storf M, Parbel A & Scheer H. (2003) Photochromic chromopeptides derived from phycoerythrocyanin: biophysical and biochemical characterization. *Photochem. Photobiol. Sci.* **2**: 741-748.

Zhao KH, Zhu JP, Song B, Zhou M, Storf M, Böhm S, Bubenzer C & Scheer H.(2004b) Non-enzymatic chromophore attachment in biliproteins: Conformational control by the detergent Triton X-100. *Biochim. Biophys. Acta* **1657**: 131-145.

Zhou J, Gasparich GE, Stirewalt VL, de Lorimier R & Bryant DA. (1992) The *cpcE* and *cpcF* genes of *Synechococcus* sp. PCC 7002. *J. Biol. Chem.* **23**: 16138-16145.

Zolla L, Bianchetti M (2001) High-performance liquid chromatography coupled on-line with electrospray ionization mass spectrometry for the simultaneous separation and identification of the *Synechocystis* PCC 6803 phycobilisome proteins. *J Chromatogr A* **912**:269–279

Zuber H. (1987) The structure of light-harvesting pigment-protein complexes. In: *The Light Reactions*. Barber, J. (Eds.).pp..157-259. Elsevier Biomedical, Amsterdam.

---

# Curriculum Vitae

## Personal data

Family name: Tu  
First name: Jun-Ming  
Data of birth: 10.02.1972  
Place of birth: Hubei, P.R. China  
Family status: married

## Education

2006- 2008 Post-graduate study in the Ludwig-Maximilians-University, Department of Biology I, Botanic, Munich, Germany

2005- 2006 Post-graduate study in the Huazhong University of Science and Technology, College of Environmental Science and Engineering, Wuhan, P.R. China.

1998-2000 Master study in Jiangnan University, School of Biotechnology, Wuxi, P.R. China

1989- 1993 Bachelor of Fermentation Engineering, Hubei University of Technology, Wuhan, P.R. China

1983-1989 Secondary School, Ezhou, P.R. China

---

### **Eidesstattliche Erklärung**

Hiermit bestätige ich, dass ich die vorliegende Arbeit selbständig verfasst und keine anderen als die hier angegebenen Quellen und Hilfsmittel verwendet habe. Ich versichere ferner, dass ich die vorliegende Arbeit nicht schon als Doktor-, Magister oder Diplomarbeit bei einer anderen Hochschule eingereicht habe.

---

Ort, Datum

---

Unterschrift